

CHRISTOFOROS PAPPAS

**MODELING TERRESTRIAL
CARBON AND WATER DYNAMICS**

A CRITICAL APPRAISAL AND WAYS FORWARD

DISS. ETH NO. 22152

MODELING TERRESTRIAL CARBON AND WATER
DYNAMICS: A CRITICAL APPRAISAL AND WAYS
FORWARD

A thesis submitted to attain the degree of
DOCTOR OF SCIENCES OF ETH ZURICH
(Dr. sc. ETH Zurich)

presented by

CHRISTOFOROS PAPPAS

DIPL. CIVIL ENG. NATIONAL TECHNICAL UNIVERSITY OF ATHENS

born 30 January 1988

citizen of GREECE

accepted on the recommendation of

PROF. DR. PAOLO BURLANDO, EXAMINER

PROF. DR. VALERIY IVANOV, CO-EXAMINER

DR. SIMONE FATICHI, CO-EXAMINER

2014

Christoforos Pappas: *Modeling terrestrial carbon and water dynamics: a critical appraisal and ways forward*, A thesis submitted to attain the degree of Doctor of Sciences of ETH Zurich, 2014

*Dedicated to the memory
of my beloved mother.*

ACKNOWLEDGMENTS

I would like to thank all those people that helped me during the period of my studies at ETH Zurich and made my time in Switzerland a very nice experience. I am grateful to my advisor, Paolo Burlando for his trust in offering me this PhD position and for his guidance and support during my research. Many thanks go to Simone Fatichi for his support during the last three years of my research, for all the fruitful discussions and ideas, but mostly for our disagreements that made me improve my argumentation. I would like to acknowledge the external examiner of my thesis, Valeriy Ivanov, who accepted my invitation to review my work and provided thoughtful comments on my thesis.

I wish also to thank former and current members of the HWRM group of the Institute of Environmental Engineering for the nice time we had. Special thanks go to Grigoris Anagnostopoulos for his generous support during my first months in Zurich, Marco Carenzo for the nice time inside and outside of the ETH campus, Stefan Rimkus for helping me with the ‘Zusammenfassung’, and the Silvan Ragetti, Álvaro Ayala and Simone Schauwecker for all the brainstorming at KuBaA! I am grateful to Martin Heynen ([http://martinheynen.com](http://martinheyнен.com)) for designing the artwork of my thesis cover.

I would like to express my sincere gratitude to Demetris Koutsoyiannis, my diploma thesis advisor at National Technical University of Athens, for introducing me to the fascinating world of probability theory and stochastics and for his support to conduct my doctoral studies abroad. Special thanks go to my friend, and diploma thesis co-advisor, Simon-Michael Papalexiou for the numerous challenging discussions (scientific and non-scientific) and for his continuous encouragement.

Last but not least, I would like to thank my family, my friends in Greece, and Anna for all our amazing non-PhD-related moments and for their continuous support and encouragement.

Funding: This study was funded by the Swiss National Science Foundation under the NRP 61 project HydroServ (Vulnerability of hydrological ecosystem services: Integrative analysis under changes of climate and socio-economy with an emphasis on adaptation; project no. 4061-125926).

ABSTRACT

Terrestrial carbon and water balances and their variability under changing climatic conditions and anthropogenic disturbances are topics of great societal and scientific importance. The role of vegetation in shaping carbon and water dynamics is of paramount significance. Many numerical models, reflecting different degrees of complexity and abstraction, have therefore been developed to mimic plant function. The aim of this thesis is to (i) shed light on how vegetation functioning is simulated in state-of-the-art terrestrial ecosystem models, (ii) provide a critical appraisal of model strengths and weaknesses, and (iii) present ways forward to remove some of the identified model limitations.

The first part of the thesis provides a thorough evaluation of a state-of-the-art, process-based, dynamic vegetation model, LPJ-GUESS, by means of a global sensitivity analysis. The rationale is that since process-based models embed physical causalities, the sensitivity of the simulated processes should also reflect measurable and observed sensitivities. Having scrutinized the structural and parameterization issues underlying LPJ-GUESS, reflecting also that of other, structurally similar dynamic vegetation models, the subsequent parts of the thesis are devoted to two major model limitations, namely (1) the lack of spatial representation and simplified soil water hydrology, and (2) the lack of ecological realism due to simplified representation of plant trait variability.

The former limitation is analyzed with a novel ecohydrological scheme, D-LPJ, which is based on an iterative coupling between a spatially explicit, process-based hydrological model (TOPKAPI-ETH) and a well-established dynamic vegetation model (LPJ). The advantages of D-LPJ over the original, aspatial approaches of LPJ and LPJ-GUESS are illustrated for a topographically-complex area located in the central Switzerland. The aggregation-induced biases due to smoothing of spatial heterogeneities through coarse-grained aspatial representations are also explicitly quantified.

The second limitation is investigated with an innovative Monte Carlo approach that is applied to simulate the diversity of plant traits. This approach revises the broad vegetation categories, based on a discrete and static parameterization (named Plant Functional Types), often incorporated in terrestrial ecosystem models. Proxy plant species are generated using observed multivariate distributions of coordinated plant traits. Their performance is assessed with a mechanistic ecohydrological model (T&C) across continuous, naturally occurring, meteorological gradients in the European Alps. The significant importance of trait-induced variability in simulating water and carbon dynamics is quantified and

an alternative, probabilistic approach is presented, enhancing the ecological realism within models.

The last part of the thesis provides a synthesis of the aforementioned findings together with a critique of commonly applied approaches for modeling terrestrial carbon and water dynamics. Directions for future model improvements are highlighted, combining deterministic with probabilistic concepts, aiming towards a predictive framework of terrestrial ecosystem functioning.

ZUSAMMENFASSUNG

Terrestrische Kohlenstoff- und Wasserkreisläufe und ihre Variabilität unter sich ändernden Klimaverhältnissen und unter anthropogener Einwirkung sind von grosser sozialer als auch wissenschaftlicher Bedeutung. Die Vegetation spielt in diesen Kreisläufen eine entscheidende Rolle. Viele numerische Modelle mit unterschiedlicher Abstraktion und Komplexität wurden bis heute entwickelt um Vegetationsfunktionen abzubilden. Die Ziele dieser Arbeit sind, (i) zu untersuchen, wie Vegetationsfunktionen in modernen Modellen terrestrischer Ökosysteme abgebildet sind, (ii) die Schwächen und Stärken der Modelle kritisch zu beleuchten, und (iii) Ansätze zu präsentieren, um Limitationen der Modellanwendung zu lösen.

Der erste Teil dieser Dissertation präsentiert eine gründliche Evaluation des modernen, prozessbasierten dynamischen Vegetationsmodells LPJ-GUESS durch eine globale Sensitivitätsanalyse. Diese Methode wurde gewählt in der Annahme, dass in Methoden welche physikalische Kausalitäten abbilden, die Sensitivitäten der Prozesse denen in der gemessenen und observierten Welt entsprechen sollten. Nach eingehender Prüfung der Struktur und Parameter von LPJ-GUESS, welche auch Schlüsse zu strukturell ähnlichen Modellen erlaubt, werden die weiteren Teile dieser Arbeit zwei Limitationen behandeln: (1) jene bedingt durch grobe räumliche Auflösung und die Vereinfachungen der Bodenwasserhydrologie, und (2) die Limitationen durch den Mangel an Realismus in den simplifizierten Ansätzen zur Abbildung der Variabilität von pflanzlichen Eigenschaften.

Die erste Limitation wird mit Hilfe eines neuen öko-hydrologischen Modells D-LPJ analysiert. Dieses ist eine iterative Koppelung des räumlich expliziten, prozessbasierten hydrologischen Modells TOPKAPI-ETH und des etablierten dynamischen Vegetationsmodells LPJ. Die Vorteile von D-LPJ gegenüber den nicht räumlich expliziten Ansätzen von LPJ und LPJ-GUESS werden anhand eines topografisch sehr heterogenen Einzugsgebietes in der Zentralschweiz demonstriert. Die Abweichungen, welche aus der Homogenisierung der räumlichen Variabilität entstehen, werden quantifiziert.

Die zweite Limitation wird mit einem innovativen Ansatz der Monte-Carlo Methode untersucht, welcher die Pflanzendiversität simuliert. Dieser ermöglicht die Revision der groben Vegetationskategorien, welche durch diskrete und statische Parameter definiert sind und häufig Anwendung in terrestrischen Ökosystemmodellen finden. Mit Hilfe von observierten multivariaten Verteilungen von pflanzlichen Eigenschaften werden Proxy-Pflanzentypen generiert. Das Verhalten dieser Pflanzentypen entlang von kontinuierlichen, meteorologischen

Gradienten typisch für die Europäischen Alpen wird mit dem mechanischen öko-hydrologischen Modell T&C untersucht. Die Signifikanz von pflanzlichen Eigenschaften für die Simulation von Wasser- und Kohlenstoffdynamiken wird quantifiziert. Ein alternativer probabilistischer Ansatz wird präsentiert, welcher den ökologischen Realismus in Modellen verbessert.

Abschliessend werden die Resultate gebündelt und die etablierten Ansätze für Kohlenstoff- und Wasserdynamiken in terrestrischen Modellen kritisch diskutiert. Mögliche Modellverbesserungen werden aufgezeigt, welche deterministische und probabilistische Konzepte vereinen, um ein verbessertes Vorhersagesystem für die Funktionalität von terrestrischen Ökosystemen zu erreichen.

Στα χερσαία οικοσυστήματα, το ισοζύγιο του νερού και του άνθρακα, καθώς επίσης και η διακύμανσή τους λόγω μεταβαλλόμενων κλιματικών συνθηκών και ανθρωπογενών επεμβάσεων, κεντρίζουν ιδιαίτερο επιστημονικό και κοινωνικό ενδιαφέρον. Η συνεισφορά της βλάστησης στη διαμόρφωση του ισοζυγίου του άνθρακα και του νερού είναι ουσιαστική. Πληθώρα υπολογιστικών μοντέλων έχουν προταθεί με στόχο την προσομοίωση των βασικών της λειτουργιών. Σκοπός της παρούσας εργασίας είναι: (i) να διερευνήσει πως οι βασικές λειτουργίες της βλάστησης προσομοιώνονται στα σύγχρονα μοντέλα χερσαίων οικοσυστημάτων, (ii) να παρέχει μια κριτική ανασκόπηση των πλεονεκτημάτων και μειονεκτημάτων των διαφόρων μεθόδων προσομοίωσης της δυναμικής της βλάστησης, και (iii) να παρουσιάσει καινοτόμες αριθμητικές μεθόδους μοντελοποίησης οικοσυστημάτων, βελτιώνοντας έτσι μερικά από τα υπάρχοντα μειονεκτήματα.

Το πρώτο μέρος της εργασίας παρουσιάζει μια λεπτομερή αξιολόγηση ενός ευρέως χρησιμοποιούμενου μηχανιστικού μοντέλου δυναμικής της βλάστησης (LPJ-GUESS), διεξάγοντας μια καθολική ανάλυση ευαισθησίας του μοντέλου στη διακύμανση των διαφόρων παραμέτρων του. Η λογική αυτής της αξιολόγησης μπορεί να συνοψισθεί ως εξής: καθώς τα μηχανιστικά μοντέλα εμπεριέχουν αιτιατές σχέσεις βασιζόμενες σε φυσικούς νόμους, η ευαισθησία των διεργασιών που προσομοιώνονται πρέπει να αντικατοπτρίζει την ευαισθησία της βλάστησης όπως αυτή παρατηρείται στο φυσικό περιβάλλον. Έχοντας λοιπόν διερευνήσει τα ασθενή σημεία του LPJ-GUESS (που αποτελεί αντιπροσωπευτικό παράδειγμα από μια πληθώρα μηχανιστικών μοντέλων δυναμικής της βλάστησης), που σχετίζονται με τη δομή του μοντέλου (δηλ. σχέσεις αιτίου-αιτιατού) αλλά και με την παραμετροποίηση της βλάστησης, τα επόμενα κεφάλαια της παρούσας εργασίας διερευνούν και βελτιώνουν τα εξής μειονεκτήματα: (1) έλλειψη λεπτομερούς χωρικής διακριτοποίησης και απλοποιημένη προσομοίωση των υδρολογικών διεργασιών, και (2) έλλειψη ρεαλιστικής προσομοίωσης της ετερογένειας της βλάστησης και των λειτουργικών χαρακτηριστικών των φυτών.

Προκειμένου να αναλυθεί το πρώτο μειονέκτημα, αναπτύχθηκε, στα πλαίσια της εργασίας, ένα καινούριο οικο-υδρολογικό μοντέλο (D-LPJ). Το D-LPJ βασίζεται στο συνδυασμό ενός χωρικά διακριτού υδρολογικού μοντέλου (TOPKAPI-ETH) με ένα ευρέως διαδεδομένο μηχανιστικό μοντέλο δυναμικής της βλάστησης (LPJ), μέσω μίας συγκλίνουσας επαναληπτικής διαδικασίας. Τα πλεονεκτήματα του D-LPJ έναντι των χωρικά μη διακριτοποιημένων LPJ και LPJ-GUESS εξετάζονται σε μια λεκάνη απορροής της κεντρικής Ελβετίας με πλούσιο τοπογραφικό ανάγλυφο. Επιπρόσθετα, εξετάζονται και ποσοτικοποιούνται σφάλματα που προκύπτουν στις εκτιμήσεις του ισοζυγίου του άνθρακα και του νερού με μοντέλα χωρίς χωρική διακριτοποίηση.

Το δεύτερο μειονέκτημα διερευνάται εφαρμόζοντας μια πρωτοπόρα μεθοδολογία **Monte-Carlo** για την προσομοίωση της ετερογένειας της βλάστησης και των λειτουργικών της χαρακτηριστικών. Αυτή η μεθοδολογία αναθεωρεί τις μέχρι τώρα παγιωμένες πρακτικές μοντελοποίησης της βλάστησης που βασίζονται σε μια διακριτή και χρονικά αμετάβλητη παραμετροποίηση των χαρακτηριστικών της (λειτουργικοί τύποι φυτών, PFTs). Υποκατάστατα είδη βλάστησης προσομοιώνονται χρησιμοποιώντας εμπειρικές πολυμεταβλητές κατανομές των αλληλεξαρτώμενων λειτουργικών της χαρακτηριστικών. Η συμπεριφορά τους εξετάζεται σε διάφορες κλιματικές συνθήκες, αντιπροσωπευτικές εκείνων που επικρατούν στις κεντρικές Άλπεις, χρησιμοποιώντας ένα μηχανιστικό οικο-υδρολογικό μοντέλο (T&C). Με αυτόν τον τρόπο ποσοτικοποιείται ο καθοριστικός ρόλος των λειτουργικών χαρακτηριστικών της βλάστησης και της ετερογένειάς τους για την προσομοίωση των ισοζυγίων του άνθρακα και του νερού. Επίσης, παρουσιάζονται εναλλακτικές, πιθανοτικές μέθοδοι, βελτιώνοντας έτσι τη μοντελοποίηση της ετερογένειας της βλάστησης και του δυναμικού της (χωρικά και χρονικά) χαρακτηριστήρα.

Το τελευταίο μέρος της εργασίας αποτελεί μια σύνθεση των προηγούμενων κεφαλαίων και μια κριτική ανασκόπηση των ευρέως χρησιμοποιούμενων μεθοδολογιών για την αριθμητική μοντελοποίηση του κύκλου του άνθρακα και του νερού στα χερσαία οικοσυστήματα. Παρουσιάζονται επίσης κατευθυντήριες γραμμές για περεταίρω βελτιώσεις των αριθμητικών μοντέλων δυναμικής της βλάστησης, συνδυάζοντας ντετερμινιστικές με πιθανοτικές προσεγγίσεις, στοχεύοντας έτσι σε ένα καλύτερο μεθοδολογικό πλαίσιο εκτίμησης της δυναμικής των χερσαίων οικοσυστημάτων.

CONTENTS

| | |
|---|-------|
| Acknowledgments | v |
| Abstract | vii |
| Zusammenfassung | ix |
| Περίληψη | xi |
| List of Figures | xvii |
| List of Tables | xxvii |
| | |
| 1 INTRODUCTION | 1 |
| 1.1 Motivation and research aims | 1 |
| 1.2 State of the art and directions of previous research | 4 |
| 1.3 Thesis methodological approach and structure | 6 |
| 2 SENSITIVITY ANALYSIS OF AN ECOSYSTEM MODEL | 9 |
| 2.1 Introduction | 9 |
| 2.2 Methodology | 12 |
| 2.2.1 The Lund-Potsdam-Jena General Ecosystem Simulator (LPJ-GUESS) | 12 |
| 2.2.2 Climate data | 14 |
| 2.2.3 Sensitivity analysis | 15 |
| 2.3 Results | 23 |
| 2.3.1 Screening results | 23 |
| 2.3.2 Results of variance-based sensitivity analyses | 24 |
| 2.4 Discussion | 35 |
| 2.4.1 Sensitivity to photosynthesis and plant growth | 36 |
| 2.4.2 Photosynthesis in the LPJ model family | 37 |
| 2.4.3 Sensitivity to soil moisture | 38 |
| 2.4.4 Sensitivity to stand composition | 39 |
| 2.5 Conclusions | 40 |
| 3 HETEROGENEITIES AND ECOSYSTEM MODELING | 43 |
| 3.1 Introduction | 43 |
| 3.2 Methodology | 45 |
| 3.2.1 Models | 45 |
| 3.2.2 Case study | 48 |
| 3.2.3 Input data | 49 |
| 3.2.4 Confirmation datasets | 51 |
| 3.2.5 Experimental design | 53 |
| 3.3 Results | 54 |
| 3.3.1 Regionalizing the parameterization of vegetation | 54 |
| 3.3.2 Confirming the hydrological consistency | 55 |
| 3.3.3 Bird's-eye view on vegetation indices | 55 |

| | | |
|-------|--|----|
| 3.3.4 | Ant's-eye view on carbon stocks | 59 |
| 3.4 | Discussion | 62 |
| 3.4.1 | Aggregating landscape heterogeneity: DGVMs, gap-models, and ecohydrological schemes | 62 |
| 3.4.2 | Equilibrium vegetation and the rate of carbon sequestration | 65 |
| 3.4.3 | Vegetation carbon fluxes and stocks: towards a better model-data integration | 66 |
| 3.4.4 | Broader implications and ways forward | 67 |
| 3.5 | Conclusions | 67 |
| 4 | PLANT DIVERSITY AND ECOSYSTEM FUNCTIONING | 69 |
| 4.1 | Introduction | 69 |
| 4.2 | Materials and Methods | 72 |
| 4.2.1 | Modeling ecosystem functioning | 72 |
| 4.2.2 | Meteorological forcing across climatic gradients | 74 |
| 4.2.3 | Mimicking plant diversity | 74 |
| 4.2.4 | Variance partitioning | 76 |
| 4.2.5 | Data | 77 |
| 4.3 | Results | 78 |
| 4.3.1 | Species variability and long-term vegetation dynamics | 78 |
| 4.3.2 | Species variability and water fluxes | 79 |
| 4.3.3 | Species variability and aggregation-induced biases | 83 |
| 4.3.4 | Partitioning the output variance between climate- and species-induced variability | 84 |
| 4.3.5 | Leaf traits and their contribution to simulated plant responses | 84 |
| 4.4 | Discussion | 85 |
| 4.4.1 | Converging and diverging ecosystem responses to species-induced variability | 86 |
| 4.4.2 | Variety versus evenness: the fallacy of averages and the emerging aggregation biases | 88 |
| 4.4.3 | Species variability outweighs environmental heterogeneity | 89 |
| 4.4.4 | Broader implications and ways forward | 89 |
| 4.4.5 | Uncertainties and limitation | 91 |
| 4.5 | Conclusions | 92 |
| 5 | CONCLUSIONS AND OUTLOOKS | 93 |
| 5.1 | Major conclusions | 93 |
| 5.1.1 | On a comprehensive model evaluation | 93 |
| 5.1.2 | On the spatial heterogeneities and boundary conditions | 94 |
| 5.1.3 | On the ecological realism and species variability | 94 |
| 5.2 | Outlook for further research | 95 |
| 5.2.1 | Towards better resource allocation schemes | 95 |
| 5.2.2 | Towards better up-scaling approaches | 96 |
| 5.2.3 | Towards a predictive framework of terrestrial ecosystem responses | 97 |

| | | |
|-------|---|-----|
| A | APPENDIX: SENSITIVITY ANALYSIS OF AN ECOSYSTEM MODEL | 99 |
| A.1 | Screening exercise: Elementary Effects | 99 |
| A.2 | Variance-based sensitivity analysis | 100 |
| A.3 | Parameter sampling | 104 |
| A.4 | Convergence test of sensitivity indices | 107 |
| B | APPENDIX: HETEROGENEITIES AND ECOSYSTEM MODELING | 109 |
| B.1 | D-LPJ ecohydrological scheme: convergence test | 109 |
| B.2 | Distributed meteorological variables | 109 |
| B.2.1 | Precipitation | 109 |
| B.2.2 | Temperature | 110 |
| B.2.3 | Cloud transmissivity and shortwave radiation | 110 |
| B.3 | Vegetation carbon fluxes | 110 |
| B.4 | MODIS pre-processing | 111 |
| B.5 | Swiss national forest inventory: data details | 114 |
| B.6 | Confirming the hydrological consistency | 115 |
| B.7 | Temporal dynamics of GPP and LAI over the Kleine Emme catchment | 116 |
| B.8 | Disentangling the role of land cover initialization | 116 |
| B.9 | Downscaling dynamic vegetation models | 119 |
| C | APPENDIX: PLANT DIVERSITY AND ECOSYSTEM FUNCTIONING | 123 |
| C.1 | Climatic forcings | 123 |
| C.1.1 | Generating the climatic gradients: methodology | 123 |
| C.1.2 | Climatic gradients: validation | 125 |
| C.1.3 | Climatic gradients: long-term dynamics | 126 |
| C.2 | Methodological details on the generation of proxy plant species | 127 |
| C.2.1 | Separating plant-life forms | 128 |
| C.2.2 | Parameterizing plant drought tolerance | 130 |
| C.2.3 | Sampling proxy species with coordinated leaf traits | 132 |
| C.2.4 | Converting values of photosynthetic capacity (A_{mass}) to maximum Rubisco capacity at 25 °C (V_{cmax}) | 135 |
| C.3 | Data description | 140 |
| C.3.1 | Eddy flux tower data | 140 |
| C.3.2 | MODIS data | 141 |
| C.3.3 | Swiss National Forest Inventory | 141 |
| | REFERENCES | 143 |
| | CURRICULUM VITAE | 191 |

LIST OF FIGURES

- Figure 1.1 A description of major model families, and the scientific disciplines from which they are originated. Models that simulate major processes of the terrestrial water and energy balance are included in the present classification and throughout this thesis they will be referred as *terrestrial ecosystem models*. 3
- Figure 1.2 A schematic representation of the thesis structure. Chapter 2 provides a thorough evaluation of a state-of-the-art terrestrial ecosystem model (LPJ-GUESS), and the following chapters improve the identified model limitations, namely, the lack of spatial representation, reflecting topographic variations, and mechanistic soil water dynamics (D-LPJ ecohydrological scheme; Chapter 3) and the lack of inter- and intra-specific plant trait variability (proxy plant species from a multivariate plant-trait distribution; Chapter 4). 7
- Figure 2.1 (a) The 200 analyzed meteorological stations in Switzerland with the 3 selected stations, representative of dry, normal, and wet conditions. (b) Annual statistics, i.e., mean, standard deviation, and percentage of dry days for the investigated stations. The selected stations are highlighted. 16
- Figure 2.2 Qualitative results of the screening analysis for the total NPP (i.e., vegetation carbon fluxes). The sensitivity metric ϵ under different climate conditions is illustrated. The 11 parameters selected for the detailed analysis are highlighted with bold italic characters. 25
- Figure 2.3 Qualitative results of the screening analysis for the total vegetation biomass (i.e., vegetation carbon pools). The sensitivity metric ϵ under different climate conditions is illustrated. The 11 parameters selected for the detailed analysis are highlighted with bold italic characters. 25

- Figure 2.4 Distribution of LAI, NPP, and carbon fluxes for different climatic forcings (from wet to dry conditions and from low to high elevations), when the 11 selected parameters were varied simultaneously (6656 model evaluations). LAI (a), annual NPP (b) as well as carbon fluxes (c) for the different ecosystem components are presented. Boxes are extended from 25% lower quartile ($q_{0.25}$) to 75% upper quartile ($q_{0.75}$) while whiskers represent the range of $[q_{0.5} - 1.5\text{IQR}, q_{0.5} + 1.5\text{IQR}]$, where $q_{0.5}$ is the median and IQR is the interquartile range ($q_{0.75} - q_{0.25}$). 26
- Figure 2.5 First and total Sobol' sensitivity indices of the 11 investigated parameters with their 95% confidence intervals (vertical lines), for total vegetation NPP under different climate forcings (from wet to dry conditions and from low to high elevations). 28
- Figure 2.6 First and total Sobol' sensitivity indices of the 11 investigated parameters for the NPP of needle-leaved trees under different climate forcings (from wet to dry conditions and from low to high elevations). The 95% confidence intervals are also plotted (vertical lines). Constrained by the ascribed bioclimatic limits, needle-leaved vegetation occurs only between 800 m and 1400 m a.s.l. elevation. 29
- Figure 2.7 First and total Sobol' sensitivity indices of the 11 investigated parameters for the NPP of broad-leaved trees under different climate forcings (from wet to dry conditions and from low to high elevations). The 95% confidence intervals are also plotted (vertical lines). Constrained by the ascribed bioclimatic limits, broad-leaved vegetation occurs only between 200 m and 800 m a.s.l. elevation. 30
- Figure 2.8 First and total Sobol' sensitivity indices of the 11 investigated parameters for the NPP of grass, under different climate forcings (from wet to dry conditions and from low to high elevations). The 95% confidence intervals are also plotted (vertical lines). 31
- Figure 2.9 First and total Sobol' sensitivity indices of the 11 investigated parameters with their 95% confidence intervals (vertical lines) for the vegetation carbon pools (sum of the carbon allocated in leaves, sapwood, heartwood and fine roots) under different climate forcings. 32

- Figure 2.10 Distribution of LAI, NPP, and carbon fluxes for different climatic forcings, when the 8 remaining parameters, after removing photosynthesis parameterization from the GSA, were varied simultaneously (5120 model evaluations). LAI (a), annual NPP (b), as well as carbon fluxes (c) for the different ecosystem components are presented. Boxes are extended from 25% lower quartile ($q_{0.25}$) to 75% upper quartile ($q_{0.75}$) while whiskers represent the range of $[q_{0.5} - 1.5IQR, q_{0.5} + 1.5IQR]$, where $q_{0.5}$ is the median and IQR is the interquartile range ($q_{0.75} - q_{0.25}$). 33
- Figure 2.11 Coxcomb plots of the total effect sensitivity indices for vegetation carbon fluxes, subplots (a) and (b), and vegetation carbon pools, subplots (c) and (d). Total effect sensitivity indices are reported for the three different elevation bands where each of the simulated PFT is the dominant (TBS at 200 m a.s.l., NE at 1400 m a.s.l., and GRS at 2000 m a.s.l.) under normal precipitation conditions, subplots (a) and (c), as well as for the elevation band where all the PFTs co-exist (800 m a.s.l.), subplots (b) and (d). 34
- Figure 2.12 Coxcomb plots of the total effect sensitivity indices for NPP, subplots (a) and (b), and LAI, subplots (c) and (d). Total effect sensitivity indices of NPP and LAI are reported for the three different elevation bands where each of the simulated PFT is the dominant (TBS at 200 m a.s.l., NE at 1400 m a.s.l., and GRS at 2000 m a.s.l.) under normal precipitation conditions, subplots (a) and (c), and for the elevation band where all the PFTs co-exist (800 m a.s.l.), subplots (b) and (d). 35
- Figure 2.13 Total order sensitivity index of the subset of 8 examined parameters with the different GSA experiments, including (photosynthesis on) and excluding (photosynthesis off) parameters related to the Farquhar photosynthesis parameterization (ALPHA_C3, ALPHA_A and THETA). The median of Sobol' total order sensitivity indices over the 15 examined climatic forcings is plotted. 39
- Figure 3.1 Representation of the D-LPJ ecohydrological scheme. D-LPJ is based on an iterative coupling of the LPJ ecosystem model with the TOPKAPI-ETH hydrological model. LPJ provides an estimate of evapotranspiration fluxes (ETA; soil evaporation, evaporation from interception, and plant transpiration) to TOPKAPI-ETH which then feeds back to LPJ an estimate of the soil water content (SWC), snow pack (SP), and snow melt (SM). Several iterations of the exchange variables (ETA and SWC, SP, SM) are performed until convergence of estimated fluxes over the simulated area is achieved. 47

- Figure 3.2 The Kleine Emme catchment is located in the central part of Switzerland. Three stream gauges operate in the main river network (blue circles) and three meteorological stations (red circles) with high quality temperature and radiation measurements are located close to the catchment boundaries. 49
- Figure 3.3 Spatial distribution ($100\text{ m} \times 100\text{ m}$ resolution) of mean daily (a) precipitation, (b) temperature, and (c) radiation, averaged over the examined period (January 2000 to December 2009) for the Kleine Emme catchment. Inner plots illustrate the areal probability density function with the areal mean denoted by a continuous red line. D-LPJ simulations are driven with spatially explicit meteorological forcings while area-averaged values are used for the simulations with LPJ and LPJ-GUESS. 50
- Figure 3.4 Landscape-level information, in a $100\text{ m} \times 100\text{ m}$ regular grid, used for the D-LPJ simulations over the Kleine Emme area: (a) digital elevation model, (b) effective saturation, averaged over the period January 2000 to December 2009, for the first soil layer, and (c) land cover map imposed on the D-LPJ simulations. Inner plots illustrate the areal probability density function with the areal mean denoted by a continuous red line. 51
- Figure 3.5 (a) Total vegetation carbon as simulated with D-LPJ, LPJ, and LPJ-GUESS for the spin-up (500 years) and the historical period (10 years; shaded area). (b) Distribution of vegetation types over the catchment area, at the end of the simulation period, as estimated by D-LPJ (based on the current land cover map; Figure 3.4c). Long-term vegetation-carbon dynamics over the Kleine Emme catchment, as obtained through the spin up period, for simulations with (c) D-LPJ, (d) LPJ, and (e) LPJ-GUESS. Different plant types are grouped in major plant life forms, i.e., evergreen, deciduous, grass, and shrubs. 56
- Figure 3.6 Spatial patterns of mean Gross Primary Production (GPP) for the period 2000 through 2009, over the Kleine Emme catchment, as estimated by: (a) MODIS, (b) D-LPJ, (c) LPJ, and (d) LPJ-GUESS as well as (e) a comparison of the spatial distribution among the four different estimates. The mean of the distributions are denoted by dashed lines. Note that since LPJ and LPJ-GUESS are not spatially explicit, a single value, representative for the entire catchment, is provided. 57

- Figure 3.7 Spatial patterns of mean Leaf Area Index (LAI) for the period 2000 through 2009, over the Kleine Emme catchment, as estimated by: (a) MODIS, (b) D-LPJ, (c) LPJ, and (d) LPJ-GUESS as well as (e) a comparison of the spatial distribution among the four different estimates. The mean of the distributions are denoted by dashed lines. Note that since LPJ and LPJ-GUESS are not spatially explicit, a single value, representative for the entire catchment, is provided. 58
- Figure 3.8 Seasonal dynamics of normalized Gross Primary Production (GPP) and normalized Leaf Area Index (LAI), averaged over the Kleine Emme catchment, for the period 2000 to 2009, based on MODIS and D-LPJ. 60
- Figure 3.9 (a) Spatial patterns of the rate of long-term changes in vegetation carbon stocks (denoted as $\Delta C_{veg}/\Delta t$) of forested areas in Kleine Emme as estimated by D-LPJ, and by the National Forest Inventories (NFI; black dots; filled symbols are used for increase while open circles are used for decrease in total vegetation carbon). (b) Box-plot of $\Delta C_{veg}/\Delta t$ values over the Kleine Emme region, based on LPJ-GUESS, LPJ, D-LPJ, and NFI. Grey dots correspond to $\Delta C_{veg}/\Delta t$ values either in each simulated grid-cell (case of D-LPJ), or in each of the forest inventory plots (case of NFI). The areal mean is indicated with red circles. 61
- Figure 4.1 Variation of the mean annual values of major environmental variables across the examined precipitation (wet, dry), and elevation gradients over the 30 yr of simulated climate. Boxes extend from the 25th to the 75th percentile, while whiskers extend to 1.5 times the interquartile range of the lower and upper quartiles respectively. PAR [$W\ m^{-2}$] stands for Photosynthetically Active Radiation. 75
- Figure 4.2 Covariation among the examined leaf-traits for the 100 generated proxy species per plant-life form (evergreen: red, deciduous: green, grass: blue). Scatter- (e, i, g, m, n, o), probability density- (a, f, k, p) as well as contour-plots (b, c, d, g, h, l) of the generated leaf-traits are shown. 77

- Figure 4.3 Vegetation activity of proxy plant species across different elevation and precipitation gradients. Box-plots illustrate the long-term variability (25 yr) of 100 generated proxy plant species per plant-life form (deciduous, evergreen, and grass) and per drought tolerance (low, medium, and high) for the case of photosynthetic activity (GPP; a, b, c), leaf area dynamics (LAI; d, e, f) and changes in woody aboveground biomass (Δ AGB; g, h, note that grass consists only of fine roots and leaves, no wood components, thus it is not included in the comparison). Red and blue box-plots illustrate the dry and wet precipitation gradients respectively. Boxes extend from the 25th to the 75th percentile, while whiskers extend to 1.5 times the interquartile range of the lower and upper quartiles respectively. Bar-plots, included within each box-plot, depict the response of proxy plant species, grouped according to their drought tolerance. Light red, green, and blue fill colors correspond to low, medium, and high drought tolerance respectively. Bar-plots cover the 25th to 75th percentile of the distribution. Dashed red and blue lines highlight the mean model response across the elevation gradient ($\overline{f(x = X)}$, i.e., mean of the box-plots) as obtained using all the simulated proxy species ($x = X$), while continuous lines illustrate the obtained model response ($f(x = \bar{X})$) when only mean values of the empirical distribution of plant trait are used ($x = \bar{X}$), for dry and wet precipitation gradients respectively. Vertical lines with points in the middle, denoted in black, represented estimates of GPP (mean \pm standard deviation), as obtained from eddy covariance measurements for several locations in the European Alps with similar plant types and elevation (a, b, c). Continuous black lines and shaded areas represent the mean and the range of variation (mean \pm standard deviation) of vegetation variables across the elevation gradient based on MODIS estimates from European Alps (a, b, c, for the case of GPP; and d, e, f, for the case of LAI) and Swiss National Forest Inventory estimates (NFI; g, h, for the case of Δ AGB). 81

Figure 4.4 Biotic (transpiration) and abiotic (total evaporation i.e., sum of ground evaporation, evaporation and sublimation from the snowpack at the ground, evaporation from intercepted water and snow) water fluxes and soil water dynamics (soil water content available to plants, SWC) across different elevation and precipitation gradients, simulated using different proxy plant species. Box-plots illustrate the long-term variability (25 yr) of 100 generated proxy plant species per plant-life form (deciduous, evergreen, and grass) and per drought tolerance (low, medium, and high) for the case of plant transpiration (a, b, c), total evaporation (d, e, f) and soil water content (SWC, g, h, i). Red and blue box-plots illustrate the dry and wet precipitation gradients respectively. Boxes extend from the 25th to the 75th percentile, while whiskers extend to 1.5 times the interquartile range of the lower and upper quartiles respectively. Bar-plots, included within each box-plot, depict the response of proxy plant species, grouped according to their drought tolerance. Light red, green, and blue fill colors correspond to low, medium, and high drought tolerance respectively. Bar-plots cover the 25th to 75th percentile of the distribution. Dashed red and blue lines highlight the mean model response across the elevation gradient ($f(x = \bar{X})$, i.e., mean of the box-plots) as obtained using all the simulated proxy species ($x = X$), while continuous colored lines illustrate the obtained model response ($f(x = \bar{X})$) when only mean values of the empirical distribution of plant trait are used ($x = \bar{X}$), for dry and wet precipitation gradients respectively. 83

Figure 4.5 Partitioning of total variance in annual Gross Primary Productivity (GPP), Leaf Area Index (LAI), changes in woody aboveground biomass (ΔAGB), transpiration, total evaporation, and Soil Water Content available to plants (SWC) due to environmentally induced variability (i.e., elevation and precipitation gradients; depicted in orange) and trait variability (i.e., variability in leaf-traits and drought strategies; depicted in green) for deciduous (a), evergreen (b), and grass (c) plant-life forms. 85

- Figure 4.6 Surface-plots of the long-term response (25 yr) of photosynthetic activity (GPP) to environmental variability (summarized by elevation; vertical axis) and to major leaf-traits (specific leaf area, SLA, carbon-nitrogen mass ratio for the foliage N_f , maximum Rubisco capacity, V_{cmax} , and critical age for leaf shed, A_{cr} ; horizontal axis). The reported annual GPP corresponds to mean values over the precipitation gradients (wet, dry) and drought tolerances (low, medium, high). 86
- Figure 4.7 Surface-plots of the long-term response (25 yr) of plant-water fluxes (transpiration) to environmental variability (summarized by elevation; vertical axis) and to major leaf-traits (plant specific leaf area, SLA, carbon-nitrogen mass ratio for the foliage N_f , maximum Rubisco capacity, V_{cmax} , and critical age for leaf shed, A_{cr} ; horizontal axis). The reported annual transpiration corresponds to mean values over the precipitation gradients (wet, dry) and drought tolerances (low, medium, high). 87
- Figure A.1 Scatter plots and histograms for the case of LP_τ sequences and (pseudo) random numbers scaled in $[0,1]$ interval, for different sample sizes. LP_τ sequences fill out the space in an evenly dispersed manner such that the new points fill in the previous gaps. 106
- Figure A.2 Convergence test for the estimators of the first and the total order effects with their uncertainty bounds, for vegetation carbon fluxes under normal precipitation conditions at 1400 m a.s.l. The sample size corresponds to the number of rows of the sample and re-sample matrices **A** and **B**, respectively. A sample size of 512, highlighted in the plots, is found to be sufficient for the convergence of the estimators, with relatively narrow uncertainty bounds. 108
- Figure B.1 Convergence test of the density functions of the exchange variables of D-LPJ ecohydrological scheme. Four iterations are enough for achieving a convergence over the simulated area of (a) evapotranspiration (soil evaporation, evaporation from interception, and plant transpiration) as well as of (b) the effective saturation. 109
- Figure B.2 Monthly gross Primary Productivity (GPP) in five Swiss FLUXNET sites estimated by Eddy-Covariance measurements (black lines) as well as with LPJ with the original parameterization (green lines), and LPJ with the adjusted plant physiological parameters (red lines). 112

- Figure B.3 (a) Seasonality and (b) scatter plots of Gross Primary Productivity (GPP) in five Swiss FLUXNET sites estimated by Eddy-Covariance measurements (black lines) as well as with LPJ with the adjusted plant physiological parameters (the mean response over the simulated period is depicted with the red lines, while the light red areas illustrate the variation among the different years of the simulated period). 113
- Figure B.4 (a) Seasonality and (b) scatter plots of river discharge, for the period 2000 through 2009, in three locations over the Kleine Emme catchment. 115
- Figure B.5 Seasonality plots of (a, b) Gross Primary Productivity (GPP) and (c, d) Leaf Area Index (LAI) over the Kleine Emme catchment as estimated by D-LPJ, LPJ, and LPJ-GUESS over the 2000-2009 period. 116
- Figure B.6 (a) Spatial patterns of mean Gross Primary Production (GPP) for the period 2000 to 2009, over the Kleine Emme catchment, as estimated by D-LPJ and LPJ with mean climatic conditions but with prescribed land cover (based on the current land use map, as in D-LPJ simulations). (b) Distribution of GPP over the catchment as estimated by the spatially explicit D-LPJ and the LPJ simulations with mean climate forcing but prescribed land cover. Solid lines depict the estimates based on LPJ and LPJ-GUESS, while dashed lines highlight the mean of the distributions. 117
- Figure B.7 (a) Spatial patterns of mean Leaf Area Index (LAI) for the period 2000 to 2009, over the Kleine Emme catchment, as estimated by D-LPJ and LPJ with mean climatic conditions but with prescribed land cover (based on the current land use map, as in D-LPJ simulations). (b) Distribution of LAI over the catchment as estimated by the spatially explicit D-LPJ and the LPJ simulations with mean climate forcing but prescribed land cover. Solid lines depict the estimates based on LPJ and LPJ-GUESS, while dashed lines highlight the mean of the distributions. 118
- Figure B.8 Spatial patterns of mean soil water content for the period 2000 to 2009, over the Kleine Emme catchment, as estimated by (a) LPJ using exactly the same inputs as D-LPJ (i.e., fine resolution meteorological forcing and local land use information) and (b) D-LPJ (i.e., fine resolution meteorological forcing, local land use map, and in addition, detailed hydrological representation of vertical and lateral fluxes using TOPKAPI-ETH distributed hydrological model). 120
- Figure B.9 Same as Figure B.8, but for evapotranspiration (ETA). 120

- Figure B.10 Same as Figure B.8, but for annual net primary production (NPP). 121
- Figure B.11 Same as Figure B.8, but for Leaf Area Index (LAI). 121
- Figure C.1 (a) Map of mean annual precipitation [mm yr^{-1}] in the South-West of Switzerland. Red and blue lines depicted the selected meteorological stations for generating the dry and wet gradients respectively. (b) Mean annual precipitation vs elevation in Switzerland based on data from the MeteoSwiss network. 124
- Figure C.2 Mean climate gradients for the examined meteorological variables, as simulated with the weather generator (blue and red points correspond to wet and dry precipitation regimes respectively) as well as the observed mean climatic variables based on the station data (black diamonds). 126
- Figure C.3 Hourly standard deviations of the climate gradients for the examined meteorological variables, as simulated with the weather generator (blue and red points correspond to wet and dry precipitation regimes respectively) as well as of the observed climatic variables based on the station data (black diamonds). 126
- Figure C.4 Seasonal precipitation as simulated with the weather generator (blue and red points correspond to wet and dry precipitation regimes respectively) as well as the observed seasonality based on the station data (black diamonds). 127
- Figure C.5 Variation of the mean annual values (averaged over 30 yr) of major environmental variables across the examined precipitation (wet, dry), and elevation gradients. Boxes extend from the 25th to the 75th percentile, while whiskers extend to 1.5 times the interquartile range of the lower and upper quartiles respectively. 127
- Figure C.6 Quantile-quantile plots for the three analyzed plant-life forms (evergreen, E, deciduous, D, and grass, G), for the examined leaf traits (plotted in the logarithmic scale; Acr [mo]: leaf lifespan; LMA [gDM m^{-2}]: Leaf Mass per Area; Nf [%]: leaf N per leaf dry mass; A_{mass} [$\text{nmol C gDM}^{-1} \text{s}^{-1}$]: photosynthetic capacity), as obtained from the GLOPNET dataset. Units are indicated prior to \log_{10} transformation. 134

| | |
|-------------|---|
| Figure C.7 | Major plant functional traits (Acr [mo]: leaf lifespan; LMA [gDM m ⁻²]: Leaf Mass per Area; Nf [%]: leaf N per leaf dry mass; A _{mass} [nmol C gDM ⁻¹ s ⁻¹]: photosynthetic capacity) for evergreen trees as obtained by the GLOPNET database (http://bio.mq.edu.au/~iwright/glopian.htm), denoted in red, as well as the 100 generated plant strategies (denoted in blue) based on the GLOPNET statistics (mean, variance, and covariances of the examined traits). Units are indicated prior to log ₁₀ transformation. In order to avoid rare/extreme values of plant traits, only values in the 5 to 95% quantile of the probability density function are included in the analysis. 136 |
| Figure C.8 | Same as Figure C.7, but for deciduous trees. 137 |
| Figure C.9 | Same as Figure C.7, but for grass. 138 |
| Figure C.10 | Conversion function between photosynthetic capacity and maximum Rubisco capacity as obtained by a mechanistic biochemical model of photosynthesis. (a) Density of the yielded V _{cmax} , (b) theoretical curve as derived from the photosynthesis model, and (c) density of the originally sampled A _{mass} values for the three examined plant-life forms. 140 |

LIST OF TABLES

| | |
|-----------|---|
| Table 2.1 | Plant Functional Types (PFTs) used for the analysis, abbreviations and bioclimatic limits. 14 |
| Table 2.2 | Climatic forcings used for the sensitivity analysis based on observations from 200 Swiss meteorological stations. The temperature-based elevation bands are created according to the meteorological station of Chaumont. 15 |
| Table 2.3 | Detailed description of the 34 investigated parameters and the processes in which they are involved. Their standard values as well as their uncertainty ranges, based on the literature, are shown. 18 |
| Table 2.4 | The 11 parameters selected through the screening test, categorized in terms of simulated processes. 24 |
| Table 3.1 | Summary of the model configurations used for the numerical experiments. Model settings are assigned based on typical practices, i.e., coarse resolution for LPJ and LPJ-GUESS and a spatially explicit representation for D-LPJ. 48 |

| | |
|-----------|--|
| Table 4.1 | Description of the parameters used for generating proxy plant species as well as the main processes where they play a role (P: photosynthesis, R: respiration, T: transpiration, TT: tissue turnover, VS: vegetation structure). 76 |
| Table C.1 | Selected stations (with mean values of different meteorological variables) used for generating the dry and wet climatic gradients across the different elevation bands. 125 |
| Table C.2 | T&C parameters used for generating proxy plant species for the three examined plant life forms (E: evergreen, D: deciduous, G: grass). More information, and justification of the selected values can be found in <i>Fatichi et al.</i> [2012a, 2014]. 129 |
| Table C.3 | Description of the parameters used for mimicking different plant strategies for drought tolerance (L: low, M: medium, H: high). 131 |
| Table C.4 | A description of leaf-traits used for generating proxy plant species with coordinated properties. The empirical covariances from the GLOPNET dataset are conserved among the leaf traits. The ranges from the multivariate normal sampling are reported as minimum (Min.) and maximum (Max.) values, while in parentheses are the ranges from the original GLOPNET dataset. E, D, G, correspond to the three investigated plant life forms, i.e., evergreen, deciduous, and grass, respectively. 133 |
| Table C.5 | Sample size of the examined sub-sets from the GLOPNET dataset as well as the obtained p-values of the implemented statistical test for assessing the normality of the sampled data for the three examined plant life forms (E: evergreen, D: deciduous, G: grass). 135 |
| Table C.6 | Sites (location and tower characteristics) with eddy covariance measurements used for the gross primary productivity (GPP) comparisons. 141 |

INTRODUCTION

1.1 MOTIVATION AND RESEARCH AIMS

$$P = E + T + Q + \frac{dS}{dt} \quad (1.1)$$

$$R_N = H + \lambda(E + T) + G \quad (1.2)$$

Equation 1.1 and 1.2 summarize the major¹ physical laws underlying our current mechanistic model representations of terrestrial carbon and water dynamics, namely the conservation of mass (Equation 1.1; summarizing the terrestrial water balance, but can be also written for the case of carbon) and energy (Equation 1.2).

The conservation of mass (Equation 1.1; i.e., matter can neither be created nor destroyed, but can only change state and location) implies that water falling on the simulation domain (P ; precipitation in liquid or solid phase over the land surface) is partitioned to water losses in the system through evaporation (E ; representing conversion of solid or liquid water into water vapor by physical processes such as ground evaporation, evaporation from intercepted water and snow, evaporation and sublimation from snow and ice), transpiration (T ; represents the phase conversion to water vapor in leaf interior), surface and subsurface runoff and deep drainage (Q), and change in water storage (dS/dt).

The conservation of energy (Equation 1.2; i.e., in a given system energy can neither be created nor destroyed, but can only be absorbed, released or change form) can be also respected in models, although due to computational constraints it is not a common practice in many modeling approaches. State-of-the-art physically-based numerical tools partition the incoming energy to the system (net radiative flux, i.e., the balance between incoming and outgoing shortwave and longwave radiation; R_N) into sensible heat flux (H), latent heat flux ($\lambda(E+T)$; where λ is the latent heat of vaporization or sublimation, converting the mass fluxes to equivalent energy needed for the state transition), and soil heat flux (G).

¹ Conservation of momentum in lateral water fluxes can be also preserved in numerical models, when routing approximations are used, e.g., dynamic wave approach solving explicitly the 1-D Saint Venant flow equations or its approximation using the kinematic wave approach [Miller, 1984].

Energy is also needed for several plant metabolic processes (e.g., photosynthesis and respiration) but is negligible in comparison to the previously mentioned terms of the energy balance. As Equation 1.1 and 1.2 demonstrate, water and energy balances are intrinsically coupled since state-changes of water require significant amount of energy (e.g., for converting 1 g of liquid water at 20 °C to water vapour, about 2450 J are needed). More details on the coupled nature of water and energy fluxes over land are provided in reviews by *Pielke* [2001], *Seneviratne et al.* [2010], and *Wang and Dickinson* [2012], while the recent review by *Katul et al.* [2012] offers insights on the evapotranspiration process across various spatiotemporal scales.

This thesis focuses on numerical models that simulate major processes involved in Equation 1.1 and 1.2 at the regional, catchment, and plot scales. Numerical models are used here as virtual labs for a better understanding of physical mechanism controlling the interplay between water and energy cycles, and the intrinsically coupled carbon dynamics. While Earth observations offer an overview of terrestrial ecosystem functioning across scales, they have to be combined with manipulation experiments and controlled numerical simulations for getting a better understanding of the underlying mechanisms and feedbacks [e.g., *Raupach et al.*, 2005; *Kirchner*, 2006; *Dietze et al.*, 2013]. The term *terrestrial ecosystem models* will be often used to refer to process-based models that simulate major processes involved in the conservation of mass and energy in terrestrial ecosystems, with emphasis on hydrological processes (e.g., vertical and lateral water fluxes) and short- and long-term vegetation dynamics (e.g., plant establishment, growth, and mortality). Figure 1.1 summarizes the major model types included under the umbrella term *terrestrial ecosystem models*, grouped based on the scientific disciplines from which they are originated.

Uncertainties are ubiquitous in every single term of the aforementioned equations and are reflected in both observation- and simulation-based inferences. Model inputs are uncertain due to limitations of monitoring instruments together with high spatiotemporal variability of natural phenomena (particularly *P*, as well as other meteorological variables affecting the energy and water balance). The stochastic nature of physical phenomena cannot be ignored, especially when future model projections are envisioned. However, throughout this thesis the driving force of the model (hydrometeorological variables; input to the model, and to the water and energy balance) is treated as given, focusing on a better examination and understanding of processes partitioning the inputs (water and energy). The partitioning of available water and energy to different components (summarized in the right-hand side of Equations 1.1 and 1.2) is also uncertain.

Data-based estimates of the global water and energy budgets over land highlight the uncertainties and the importance of each component involved in the water and energy balance. More specifically, in a recent update of the global annual mean energy budget by *Stephens et al.* [2012] at the Earth's surface, com-

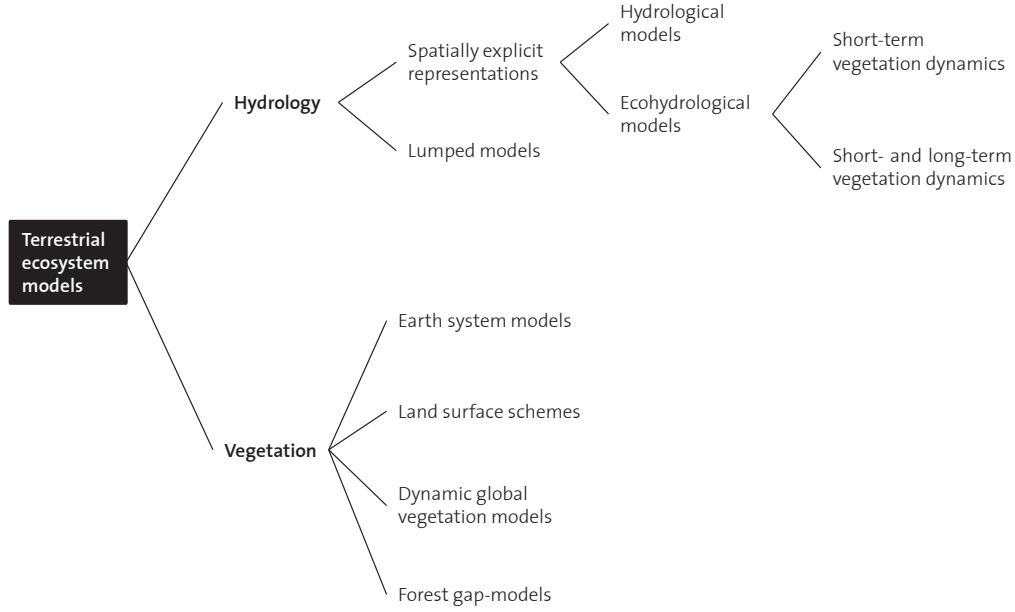


Figure 1.1: A description of major model families, and the scientific disciplines from which they are originated. Models that simulate major processes of the terrestrial water and energy balance are included in the present classification and throughout this thesis they will be referred as *terrestrial ecosystem models*.

piling up-to-date surface and satellite data for an approximate period 2000 to 2010, indicates that the net radiative flux is $R_N = 112.6 \pm 7 \text{ W m}^{-2}$ ($188 \pm 6 \text{ W m}^{-2}$ incoming shortwave, $23 \pm 3 \text{ W m}^{-2}$ outgoing shortwave, $345.6 \pm 9 \text{ W m}^{-2}$ incoming longwave and $398 \pm 5 \text{ W m}^{-2}$ outgoing longwave) and is converted to $24.7 \pm 7 \text{ W m}^{-2}$ sensible heat flux, H , i.e., 22% of R_N , and $88 \pm 10 \text{ W m}^{-2}$ latent heat flux, $\lambda(E+T)$, i.e., 80% of R_N . The fundamental role of latent heat flux (evapotranspiration) is also highlighted when the global water cycle is analyzed. Data-based estimates from *Okai and Kanae [2006]* show that out of the $111 \times 10^3 \text{ km}^3 \text{ yr}^{-1}$ precipitated water over land, $65.5 \times 10^3 \text{ km}^3 \text{ yr}^{-1}$, i.e., about 60%, returns back to the atmosphere through evapotranspiration. A large fraction of terrestrial evapotranspiration is attributed to plant activity. More than half of the water that goes back to the atmosphere passes through plants via the transpiration process [*Dirmeyer et al., 2006; Lawrence et al., 2007; Miralles et al., 2011; Jasechko et al., 2013; Schlaepfer et al., 2014; Coenders-Gerrits et al., 2014; Schlesinger and Jasechko, 2014*].

Plant functioning is of utmost importance in shaping water and energy cycles over land, not only through direct, short-term biophysical and biochemical processes (e.g., photosynthesis, transpiration) but also through carry-over effects due to environmentally-induced limitations (e.g., water-stress conditions), therefore affecting the long-term carbon and water dynamics. Droughts are an illustrative example: water-induced stress apart from changes in short-term plant responses (e.g., reduction in transpiration and downregulation of photosynthe-

sis), affects also plant mortality rates as well as species competition [see *van der Molen et al., 2011*, for a recent review]. The critical role of vegetation is particularly important when projections of ecosystem states and dynamics under non-stationary conditions are envisioned, as for example the carbon source or sink dynamics of forested ecosystems under changing environmental conditions, the resilience of ecosystems and species distributions under climate-induced variability or the assessment of the impact of land use and climate change to hydrological ecosystem services. Models therefore have to provide accurate approximations of plant activity, so that terrestrial water- as well as the intrinsically coupled energy-, carbon-, and nutrient-cycle are realistically represented and the fate of terrestrial ecosystems under future, hypothetical scenarios is robustly assessed.

Motivated by the importance of transpiration, and thus plant activity, in shaping terrestrial water and energy dynamics, this study is geared toward a better understanding of the interactions between terrestrial water cycle and short- and long-term vegetation dynamics, combining state-of-the-art methodologies from hydrology and vegetation science. More specifically, this thesis aims to (i) shed light on how plant activity is represented in state-of-the-art numerical tools; (ii) assess the strengths and weaknesses of our current model representation of vegetation functioning; (iii) quantify the importance of spatiotemporal heterogeneities in abiotic (e.g., meteorological forcing, boundary conditions) and biotic (e.g., plant attributes) characteristics when ecosystem responses at regional, catchment and plot scales are simulated; and finally (iv) provide tractable ways towards a better predictive framework for terrestrial ecosystem modeling.

1.2 STATE OF THE ART AND DIRECTIONS OF PREVIOUS RESEARCH

Terrestrial ecosystem modeling is a highly interdisciplinary topic. Several modeling tools have been developed for mimicking terrestrial water and energy dynamics (see Figure 1.1 for an overview). Depending on the scientific discipline from which they are originated, different levels of abstraction are employed. Two distinct modeling families have been emerged, namely (i) hydrological and (ii) vegetation models. Each of them has its own strengths and weaknesses, reflecting biased perspectives from their developers. Hydrologists focus on abiotic processes (e.g., rainfall-runoff mechanisms and vertical and horizontal water fluxes), with simplistic representation of biophysical processes (e.g., plant transpiration). Models originated from vegetation science simulate explicitly biophysical, biochemical, and demographic processes but simplistic approximations are made for soil water dynamics.

Hydrologists have a long tradition in modeling terrestrial water cycle. During the recent years, so called process-based, distributed hydrological models were developed, recognizing the importance of topography and water routing, in

shaping the hydrological response [*Freeze and Harlan, 1969; Abbott et al., 1986a, b; Grayson et al., 1992; Todini, 1996; Beven, 2001, 2002; Liu and Todini, 2002; Reed et al., 2004; Ebel et al., 2008*]. Such tools nowadays provide continuous, quantitative, spatially-explicit simulations of water fluxes at the local and regional scales. Detailed reviews of the classification and the evolution of hydrological models throughout years, e.g., from empirical, lumped representations, to spatially explicit process-based models, are provided by *Rafsgaard [1996]* and recently by *Solomatine and Wagener [2011]*. Contrary to their detailed representation of abiotic water dynamics, terrestrial surface boundary layer is typically simplistically approximated. Plant activity is not explicitly simulated, with the exception of plant transpiration for which empirical modules are often employed. Vegetation therefore is treated as a passive component, affecting mainly water losses through transpiration and surface roughness. Transpiration is crudely represented with empirical and static parameterizations, ignoring direct feedbacks to stomatal activity through e.g., photosynthesis, or other biophysical, biochemical, and demographic processes affecting plant activity.

Vegetation community has provided also several process-based models simulating terrestrial water-, energy-, carbon-, and recently also nutrient-cycle across different spatiotemporal scales (from the stand-level to regional and global scale analyses, and from short- to long-term responses). Biophysical, biochemical, and demographic processes occurring over land, are therefore mechanistically simulated. Extensive reviews and classifications of vegetation models and their properties can be found in *Bugmann et al. [1996]; Le Roux et al. [2001]; Perry and Enright [2006]; Prentice et al. [2007]; Jeltsch et al. [2008]; Medlyn et al. [2011]*, and thus only a short description, highlighting major model classes and attributes is provided here. Land surface schemes, originally developed from the climate modeling community for a better description of the coupling between biosphere and atmosphere [e.g., *Sellers et al., 1986; Pitman, 2003; Arora, 2002*] provide detailed simulation of biophysical processes occurring in the land surface boundary layer, respecting the conservation of mass and energy. Dynamic vegetation models [often called in literature as Dynamic Global Vegetation Models; DGVMs; *Prentice et al., 1993; Sitch et al., 2003; Prentice et al., 2007; Sitch et al., 2008; Friedlingstein and Prentice, 2010; Levis, 2010*] are also widely applied for understanding the carbon cycle (i.e., changes in carbon fluxes and stocks related to forest dynamics) as well as the dynamic transitions between different vegetation types under non-stationary climatic conditions. Forest gap-models are also developed for a better representation of landscape heterogeneities simulating explicitly demographic processes, e.g., plant establishment, competition and disturbances [*Bugmann et al., 1996; Reynolds et al., 2001*]. Earth System Models coupling state-of-the-art climate and vegetation models have also recently been developed [e.g., *Cox et al., 2000; Prinn, 2012*]. Vegetation models provide therefore a detailed, process-based framework, covering a wide range of vegetation-related processes occurring in terrestrial ecosystems, with soil hydrological pro-

cesses being an exception. Simplified representations of hydrological processes are unfortunately a common practice in vegetation models. Vertical water fluxes in soil are crudely represented using simplistic approaches [e.g., “bucket” hydrology *Gerten et al., 2004*] while lateral water fluxes and topographic effects are often not at all represented.

The intrinsic coupling of terrestrial biosphere and atmosphere with the hydrological cycle has led over the last years to the development of a new interdisciplinary scientific field called ecohydrology [*Rodriguez-Iturbe, 2000; Rodriguez-Iturbe et al., 2001; Eagleson, 2002; Nuttle, 2002; Porporato and Rodriguez-Iturbe, 2002; Boone et al., 2004; D’Odorico et al., 2010; Asbjornsen et al., 2011; Thompson et al., 2011; Porporato and Rodriguez-Iturbe, 2013; Dolman et al., 2014*]. Ecohydrology can be defined as “the science, which seeks to describe the hydrologic mechanisms that underlie ecologic patterns and processes” [*Rodriguez-Iturbe, 2000*], and combines process understanding from both hydrological and vegetation communities. The innovation of ecohydrological models in comparison to the classical distributed hydrological models is that, instead of simulating the contribution of the vegetation component to water balance empirically, they explicitly account for biophysical mechanisms (e.g., vegetation structure and the coupling of photosynthesis with stomatal regulation, and thus transpiration rates). Ecohydrological models are thus process-oriented hydrological models, which explicitly account for the intrinsic coupling of hydrological response and plant physiological processes and dynamics. Such numerical tools aim to improve the realism regarding the simulated biophysical processes, but account mostly for short-term vegetation dynamics (e.g., phenological cycles of a forest preserved always in a mature state), ignoring soil biogeochemistry and forest stand demography that shape forest growth dynamics in the long-term. Examples of hydrological models with a mechanistic representation of vegetation component are becoming more abundant [e.g., *Arora, 2002; Wattenbach et al., 2005; Ivanov et al., 2008a; Fatichi et al., 2012a; Maxwell et al., 2014*]. Few examples of ecohydrological models that encapsulate also long-term ecological processes exist [e.g., *Tague and Band, 2004*].

1.3 THESIS METHODOLOGICAL APPROACH AND STRUCTURE

In order to accomplish the aims of this study, summarized in four key points in Section 1.1, state-of-the-art numerical tools are evaluated, revised and applied, together with advanced statistical techniques and multiple Earth observations. The main research points addressed in this thesis are summarized in Figure 1.2.

Specifically, two well-established dynamic vegetation models (LPJ [*Sitch et al., 2003*] and LPJ-GUESS [*Smith et al., 2001*]) are first selected as representative models for simulating biophysical, biochemical, and demographic processes across a wide range of spatiotemporal scales (from local, to regional, and global, and from

short- to long-term vegetation dynamics). A critical evaluation of LPJ-GUESS is performed by means of a global sensitivity analysis (Chapter 2). The rationale behind this analysis is that since process-based tools embed physical causalities, the sensitivity of the simulated processes should reflect the observed, real-world sensitivities. Having scrutinized structural and parameterization issues underlying LPJ-GUESS (reflecting also that of other, structurally similar models) the rest of the thesis focuses on two major limitations identified by the sensitivity analysis, namely (i) lack of spatial representation and simplified soil water hydrology, and (ii) lack of ecological realism due to a simplified representation of species variability.

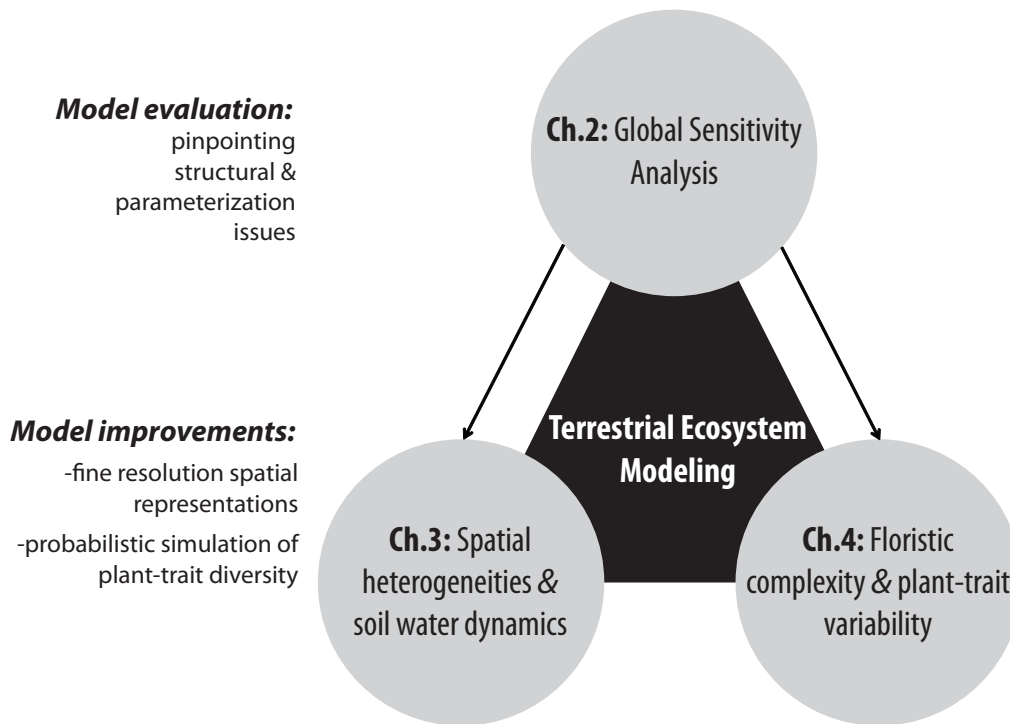


Figure 1.2: A schematic representation of the thesis structure. Chapter 2 provides a thorough evaluation of a state-of-the-art terrestrial ecosystem model (LPJ-GUESS), and the following chapters improve the identified model limitations, namely, the lack of spatial representation, reflecting topographic variations, and mechanistic soil water dynamics (D-LPJ ecohydrological scheme; Chapter 3) and the lack of inter- and intra-specific plant trait variability (proxy plant species from a multivariate plant-trait distribution; Chapter 4).

In order to further investigate the role of local scale heterogeneities in terrestrial ecosystem functioning, a spatially explicit version of LPJ is developed, D-LPJ, where “D” stands for distributed in space (Chapter 3). In D-LPJ, the simplified soil hydrological modules of the original LPJ are substituted with a distributed hydrological model (TOPKAPI-ETH) and detailed information of local scale attributes (e.g., meteorological forcing, soil properties) is prescribed using a fine resolution grid. In addition, local scale information of dominant vegetation types is also prescribed in D-LPJ simulations, moving beyond the paradigm of

potential natural vegetation, embedded in most of the DGVM applications. The performance of the new, spatially explicit dynamic vegetation model (D-LPJ) is assessed in a topographically-complex area located in central Switzerland using multivariate datasets. The advantages of D-LPJ over the original, non-spatially explicit, approaches of LPJ and LPJ-GUESS are further demonstrated.

The role of species diversity in simulated terrestrial water and carbon dynamics, highlighted by the global sensitivity analysis as a key model limitation, is further analyzed in Chapter 4. A state-of-the-art ecohydrological model, T&C [Fatichi *et al.*, 2012a], is used for this purpose. Ecohydrological tools are developed for local and regional scale applications and therefore provide a more detailed representation of the soil-plant-atmosphere continuum when compared to dynamic vegetation models (such as LPJ and LPJ-GUESS), that due to the larger simulation domains and the computational burden, heuristic approximations are often made. T&C is selected due to its realism in preserving the water and energy budget as well as mechanistic representation of environmental controls on plant functioning. The importance of species-induced variability in simulating water and carbon dynamics is evaluated across naturally occurring meteorological gradients in the European Alps. Proxy-plant species are generated, with observed coordinated plant traits, and their performance is simulated using the T&C model. The analysis reveals the important role of plant diversity when terrestrial carbon and water dynamics are simulated. It further demonstrates that species-induced heterogeneities can be encapsulated in modeling schemes through probabilistic approaches. The use of empirical multivariate distributions of coordinated plant-traits can enhance species representation and thus the robustness of terrestrial ecosystem models.

The last part of the thesis (Chapter 5) provides a synthesis of the findings presented in Chapter 2, 3, and 4 together with a critique of current, commonly applied approaches for modeling terrestrial carbon- and water-cycles. Building upon the presented results and the identified model strengths and weaknesses, directions of future model improvements are highlighted, combining deterministic with probabilistic concepts, aiming towards a predictive framework of terrestrial ecosystem functioning and the intrinsically coupled water and carbon dynamics.

SENSITIVITY ANALYSIS OF A PROCESS-BASED ECOSYSTEM MODEL: PINPOINTING PARAMETERIZATION AND STRUCTURAL ISSUES

ABSTRACT

Dynamic vegetation models have been widely used for analyzing ecosystem dynamics and their interactions with climate. Their performance has been tested extensively against observations and by model intercomparison studies. In the present analysis, LPJ-GUESS, a state-of-the-art ecosystem model, was evaluated by performing a global sensitivity analysis. The study aims at examining potential model limitations, particularly with regard to long-term applications. A detailed sensitivity analysis based on the variance decomposition is presented to investigate the structural model assumptions and to highlight processes and parameters that cause the highest variability in the output. First and total order sensitivity indices were calculated for selected parameters using Sobol's methodology. In order to elucidate the role of climate on model sensitivity, different climate forcings were used based on observations from Switzerland. The results clearly indicate a very high sensitivity of LPJ-GUESS to photosynthetic parameters. Intrinsic quantum efficiency alone is able to explain about 60% of the variability in vegetation carbon fluxes and pools for a wide range of climate forcings. Processes related to light harvesting were also found to be important together with parameters affecting forest structure (growth, establishment, and mortality). The model shows minor sensitivity to hydrological and soil texture parameters, questioning its skills in representing spatial vegetation heterogeneity at regional or watershed scales. In the light of these results, we discuss the deficiencies of LPJ-GUESS and possibly that of other, structurally similar, dynamic vegetation models and we highlight potential directions for further model improvements.

2.1 INTRODUCTION

Understanding and simulating the terrestrial carbon cycle continues to be a great challenge [Pitman *et al.*, 1990; Bonan *et al.*, 1992; Cox *et al.*, 2000; Cramer *et al.*,

Pappas, C., S. Fatichi, S. Leuzinger, A. Wolf, and P. Burlando, Sensitivity analysis of a process-based ecosystem model: Pinpointing parameterization and structural issues, *Journal of Geophysical Research: Biogeosciences*, 118(2), 505–528, doi: 10.1002/jgrg.20035, 2013

2001; *Melillo et al.*, 2002; *Moorcroft*, 2006; *Heimann and Reichstein*, 2008; *Purves and Pacala*, 2008a]. The role of vegetation is of paramount importance since it regulates the transport of water, carbon, energy, and momentum at the land surface, via many non-linear biophysical and biochemical processes [*Pitman*, 2003; *Bonan*, 2008b; *Heimann and Reichstein*, 2008; *Arnell et al.*, 2010; *Anderson et al.*, 2011; *Fatichi et al.*, 2012a]. Many numerical models, reflecting different degrees of complexity and abstraction, were developed mimicking terrestrial ecosystem structure and dynamics. The need for a better understanding and representation of the biosphere, as well as an increasing interest in investigating the terrestrial carbon cycle contributed to the development of process-based terrestrial ecosystem models [*Foley*, 1994; *Liu et al.*, 1997; *Purves and Pacala*, 2008a; *Levis*, 2010; *McMahon et al.*, 2011]. Process-based models are very often used as reliable tools for investigating the effect of climate and anthropogenic intervention on short and long term vegetation dynamics [*Melillo et al.*, 1993; *Cox et al.*, 2000; *Moorcroft*, 2003; *Evans*, 2012]. In the present study, we are focusing on Dynamic Global Vegetation Models (DGVMs) [*Peng*, 2000; *Ostle et al.*, 2009; *Levis*, 2010; *Quillet et al.*, 2010]. DGVMs have been extensively used for simulating the terrestrial carbon balance and for assessing changes and feedbacks in vegetation structure and productivity due to climate variability [e.g., *Cramer et al.*, 2001; *Bachelet et al.*, 2003; *Morales et al.*, 2007; *Zaehle et al.*, 2007; *Le Quéré et al.*, 2009].

Testing model performance against observations as well as model intercomparisons are important steps for model evaluation [*Hurt et al.*, 1998; *Moorcroft*, 2006; *Quillet et al.*, 2010]. Although absolute verification and validation of numerical models is basically impossible as natural systems are never closed [*Oreskes et al.*, 1994], model confirmation in relative terms can be obtained by comparing model output with observed variables. The recent increase in data quantity and quality especially due to eddy-flux tower networks [*Baldocchi et al.*, 2001; *Baldocchi*, 2008], remote sensing products [*Myneni et al.*, 2002; *Kerr and Ostrovsky*, 2003], and forest inventories [*Freyer and Furnival*, 1999; *Lischke and Löffler*, 2006], offers a great chance for assessing model performance against multiple variables and datasets. The use of these datasets led to numerous model applications assessing the skill of terrestrial biosphere models in reproducing current ecosystem variables [e.g., *Kucharik et al.*, 2000; *Cramer et al.*, 2001; *Bachelet et al.*, 2003; *Hickler et al.*, 2004; *Krinner et al.*, 2005; *Kucharik et al.*, 2006; *Beer et al.*, 2010; *Medvigy and Moorcroft*, 2012]. There are also many intercomparison studies among different terrestrial ecosystem models, testing the consensus of a variety of model structures and parameterizations [*Cramer et al.*, 1999, 2001; *House et al.*, 2003; *Morales et al.*, 2005; *Friedlingstein et al.*, 2006; *Ito and Sasai*, 2006; *Luo et al.*, 2008; *Sitch et al.*, 2008; *Schwalm et al.*, 2010; *Dietze et al.*, 2011; *Haddeland et al.*, 2011; *Wang et al.*, 2011; *Wolf et al.*, 2011; *Keenan et al.*, 2012].

While many intercomparison studies showed substantial differences among the results of process-based models, few mechanistic explanations on the reasons of their poor agreement are usually provided [*Cramer et al.*, 1999; *Roxburgh et al.*,

2004; *Ito and Sasai, 2006; Jung et al., 2007b, a*]. Discrepancies among DGVMs raise doubts about their robustness and reliability [*Morales et al., 2005*], illustrating that a predictive modeling framework of the biosphere is still problematic [*Moorcroft, 2006; Heimann and Reichstein, 2008; Fisher et al., 2010; Richardson et al., 2011; Evans et al., 2012*]. Therefore, a better process representation and a more accurate parameterization of terrestrial ecosystem models are required.

Model development and improvements of their performance based only on model intercomparison studies or model evaluation against observations can be difficult due to the high complexity and dimensionality of model structures. In fact, intrinsic structural model uncertainties can often be compensated through parameter adjustments [*Chen et al., 2011; Bonan et al., 2011*], leading to satisfactory model performance and realistic results, without providing a holistic understanding of the system [*Medlyn et al., 2005; Beven, 2006; Keenan et al., 2011a*]. In addition, while model evaluation against observed variables and model intercomparison studies are fundamental for describing the overall structural model uncertainty and discrepancies, they provide only partial information about the sources of bias and uncertainties, especially when metrics summarizing many processes are used in the comparison.

Sensitivity analysis, i.e., the study of how the uncertainty in model realizations is apportioned to the different sources of uncertainty in the model inputs, is considered one of the major steps for model evaluation as well as a very elegant test highlighting model limitations and directions of further improvements [*Sheng et al., 1993; Saltelli and Scott, 1997; Saltelli et al., 2000b; Medlyn et al., 2005; Jakeman et al., 2006; Cariboni et al., 2007*]. The need for well designed, rigorous Global Sensitivity Analysis (GSA) is reinforced due to: (i) the intrinsic complexity of terrestrial ecosystems that is typically translated in the DGVMs' framework through non-linear relationships among processes (e.g., photosynthesis, respiration, stomatal regulation) and environmental variables (e.g., air temperature, radiation, CO₂ concentration) [*Jarvis, 1995; Baldocchi et al., 2002; Cox et al., 2006; Kimmins et al., 2008*], (ii) the large number of parameters (i.e., many degrees of freedom) that this type of models include [*Manson, 2001; Lawrie and Hearne, 2007; Tang and Bartlein, 2008*], (iii) the physically-based framework of DGVMs, implying that the sensitivity of the implemented components should also reflect the sensitivity of the real processes. Therefore, sensitivity analysis can be seen as an important step for model evaluation. Advanced statistical techniques are strongly recommended for performing a thorough GSA, accounting not only for first order parameter effects, but also assessing the effect of interactions among different parameters and processes [*Saltelli et al., 2000a, 2004, 2008*].

Surprisingly, the variety of terrestrial ecosystem models, their increasing degree of sophistication, and their numerous applications, are usually followed by a scarcity of proper sensitivity analyses, ignoring European [*EC, 2009*] and American [*EPA, 2009*] guidelines about best modeling practices. Despite the vast amount of GSA methodologies and literature covering this topic [e.g., *Hamby,*

1994; Saltelli *et al.*, 2000a; Frey and Patil, 2002; Saltelli *et al.*, 2004; Cariboni *et al.*, 2007; Saltelli *et al.*, 2008, 2006], practitioners and modelers very often choose simplistic approaches for investigating parameter uncertainty and sensitivity, that are prone to numerous problems [Saltelli, 1999; Saltelli and Annoni, 2010].

Taking into account that sensitivity analysis is an essential step for model development, improvement and evaluation, we performed a detailed GSA, based on a state-of-the-art methodology, for a well established DGVM: the LPJ-GUESS terrestrial ecosystem model [Smith *et al.*, 2001; Sitch *et al.*, 2003; Gerten *et al.*, 2004]. Many studies have been published demonstrating the skill of LPJ, and LPJ-GUESS in predicting potential vegetation and productivity at global and regional scales [e.g., Morales *et al.*, 2005; Hély *et al.*, 2006; Koca *et al.*, 2006; Morales *et al.*, 2007; Hickler *et al.*, 2012]. The uncertainty in LPJ and LPJ-GUESS results was also assessed, under different perspectives, by Zaehle *et al.* [2005] and Wramneby *et al.* [2008] respectively.

The present study conducts for the first time a variance-based GSA of a representative DGVM. Parameters covering the entire spectrum of simulated processes are included in the analysis. In order to elucidate the role of climate on model sensitivity, different climatic forcings, based on meteorological data from Switzerland, are selected. This study allows not only for identification of the most influential parameters (which is the typical objective of many published sensitivity analyses), but goes a step further. Specifically, the following questions are posed: (i) does the sensitivity (or the lack of sensitivity) of the implemented components reflect the sensitivity of the real processes? (ii) Is there any dominant process (characterized by a group of parameters) that controls model response?

On the basis of the GSA analysis, structural and conceptual deficiencies underlying LPJ-GUESS are therefore highlighted and suggestions for potential improvements of DGVMs are discussed. While differences may exist in the way specific components are parameterized in different DGVMs (e.g., photosynthesis, transpiration, soil biogeochemistry), the general model structure and the environmental controls are mostly similar [Levis, 2010; Quillet *et al.*, 2010]. Therefore, we argue that many of our conclusions are not limited to the LPJ family of models but are relevant for many other terrestrial ecosystem models.

2.2 METHODOLOGY

2.2.1 The Lund-Potsdam-Jena General Ecosystem Simulator (LPJ-GUESS)

LPJ-GUESS is a state-of-the-art terrestrial biogeochemical model of forest growth which combines LPJ-DGVM [Lund-Potsdam-Jena Dynamic Global Vegetation Model; Sitch *et al.*, 2003] with a more detailed representation of vegetation

dynamics GUESS [General Ecosystem Simulator; *Smith et al.*, 2001]. A short overview of the features and assumptions of LPJ-GUESS is provided here. A more detailed model description can be found elsewhere [*Smith et al.*, 2001; *Sitch et al.*, 2003; *Gerten et al.*, 2004], as well as numerous model applications in different locations worldwide [*Badeck et al.*; *Hickler et al.*, 2004; *Morales et al.*, 2005; *Hély et al.*, 2006; *Koca et al.*, 2006; *Morales et al.*, 2007; *Wolf et al.*, 2008; *Hickler et al.*, 2012].

LPJ-GUESS has a process-based representation of land-atmosphere carbon and water exchange and embeds a mechanistic approach for mimicking terrestrial vegetation dynamics. Key ecosystem processes such as photosynthesis, respiration, stomatal regulation, plant phenology and soil biogeochemistry as well as soil hydrological processes are simulated daily. Processes related to forest successional dynamics such as plant growth, establishment, and mortality are computed annually. Vegetation properties are assigned using plant functional types (PFTs), a classification that groups plants based on their major functional traits [*Bonan et al.*, 2002]. Each PFT has predefined physiological and bioclimatic attributes (Table 2.1) which determine whether the prevailing climate conditions are favorable or not for its establishment and growth, i.e., different PFTs occur in different climates. The model version used in this study includes the hydrological improvements presented by *Gerten et al.* [2004]. While LPJ and LPJ-GUESS apply identical modules for simulating land-atmosphere coupling and plant-level carbon dynamics, their main difference, which optimizes LPJ-GUESS for regional applications, lies in the representation of vegetation dynamics [*Smith et al.*, 2001]. LPJ-GUESS, similarly to other individual-based models [e.g., *Moorcroft et al.*, 2001; *Sato et al.*, 2007; *Medvigy et al.*, 2009], uses a mechanistic approach based on forest dynamic models [*gap models* e.g., *Prentice et al.*, 1993], for mimicking vegetation heterogeneity at the local scale. Forest structure is represented by simulating 100 replicated patches of potential PFTs with different age classes (cohorts). The use of several replicated patches accommodates for the variability due to stochastic processes such as plant establishment and mortality. In the present study, three PFTs were used: two woody PFTs (needle-leaved evergreen, NE, and broad-leaved summergreen, TBS) and one generic herbaceous (C_3 grass, GRS). The parameterization of PFTs is based on previous works of *Sitch et al.* [2003], *Hickler et al.* [2004], and *Miller et al.* [2008]. Fire disturbances were not used in the current study. Only a generic background mortality represented by stochastic disturbances (e.g., storms, diseases) was considered for the sensitivity analysis experiment. Simulation starts with no vegetation (i.e., bare ground), therefore for each parameter set a period of 1000 years (constructed by repeating randomly years of the observed climate), with preindustrial CO_2 levels, was used to spin-up the model and define the initial states of carbon pools and vegetation cover in equilibrium with the climate forcing (spin-up simulation period). Starting from the steady state obtained after the spin-up, the model was successively driven with daily data (Section 2.2.2) based on the historical Swiss

meteorological records (historical simulation period). The sensitivity analysis was carried out only for the historical simulation period.

Table 2.1: Plant Functional Types (PFTs) used for the analysis, abbreviations and bioclimatic limits.

| | NE | TBS | GRS |
|------------------------|--|---|----------------|
| PFT | Shade-tolerant needle-leaved evergreen | Shade-tolerant broad-leaved summergreen | Grass |
| Photosynthesis pathway | C ₃ | C ₃ | C ₃ |
| GDDmin ^a | 600 | 1500 | - |
| Tc,min ^b | -30 | -3.5 | - |
| Tc,min ^c | -1.5 | 6 | - |

^aMinimum degree-days sum (5°C base) for establishment (°C).

^bMinimum coldest month temperature for survival (°C).

^cMaximum coldest month temperature for establishment (°C).

2.2.2 Climate data

LPJ-GUESS uses meteorological measurements of daily precipitation, temperature and sunshine hours and annual values of CO₂ concentration as climate forcings. Atmospheric CO₂ concentrations were derived from ice core reconstructions [Sitch *et al.*, 2003; Frank *et al.*, 2010] and the Mauna Loa record [Keeling *et al.*, 2009]. We carried out plot-scale simulations for which no explicit spatial dimension is required. In order to investigate the model sensitivity under different climate conditions, virtual stations, representative of the entire Switzerland, were generated, covering a wet-to-dry gradient and a wide range of elevations. Daily climate forcings were defined following a detailed analysis of 200 Swiss meteorological stations with high quality measurements of precipitation, temperature, and radiation (Figure 2.1). Three stations were identified as representative for dry, normal and wet conditions with about 600 (Sion), 1300 (Chaumont), and 2000 (Ebnat-Kappel) [mm/year] of annual precipitation. Observed precipitation and radiation time series from these stations, from January 1st 1966 to December 31st 2009 (44 years), were used in the analysis (Table 2.2). Temperature time series measured at the meteorological station of Chaumont, 1073m above sea level (a.s.l.), was used to force the model, after applying an environmental temperature lapse rate of 0.65° C/100 m. This operation allows us to generate five virtual elevation bands (i.e., different temperature time series) from 200 m to 2600 m a.s.l. with a 600 m interval (Table 2.2), covering the entire range of vegetated area in Switzerland. The climate types used for the GSA are therefore a combination of the three identified precipitation-cloud cover patterns (dry, normal, and wet) with five different temperature time series

representative of different elevation bands (fifteen virtual stations in total). Although the synthetic climate forcings (virtual stations) were based only on Swiss records, they are likely to be representative of much larger area due to the wide range of precipitation and temperature regimes covered by the analysis (Table 2.2).

Table 2.2: Climatic forcings used for the sensitivity analysis based on observations from 200 Swiss meteorological stations. The temperature-based elevation bands are created according to the meteorological station of Chaumont.

| | Mean Precipitation [mm] | | | Mean Temperature [°C] | | | | |
|--------|-------------------------|--------|------|-----------------------|-------|--------|--------|--------|
| | Dry | Normal | Wet | 200 m | 800 m | 1400 m | 2000 m | 2600 m |
| Annual | 600 | 1245 | 1898 | 11.8 | 7.9 | 4 | 0.1 | -3.8 |
| Winter | 163 | 315 | 414 | 4.4 | 0.5 | -3.4 | -7.3 | -11.2 |
| Spring | 123 | 288 | 457 | 10.6 | 6.7 | 2.8 | -1.1 | -5 |
| Summer | 166 | 336 | 604 | 19.4 | 15.5 | 11.6 | 7.7 | 3.8 |
| Autumn | 148 | 305 | 424 | 12.4 | 8.5 | 4.6 | 0.7 | -3.2 |

2.2.3 Sensitivity analysis

A detailed description of the methodology applied for the GSA is provided in Appendix A, and just the outlines are summarized in the following subsections.

The structure of LPJ-GUESS is complex, including many simulated processes and potentially many interactions, therefore no a priori assumption can be made about the linearity, monotonicity, or additivity of the model response to parameter changes. In these conditions, commonly applied practices of simply changing one-parameter-at-a-time are considered inappropriate [Saltelli and Annoni, 2010]. In the present analysis, LPJ-GUESS is treated as black-box, without assumptions about its structure (i.e., model-free approach). Furthermore, since model outputs are time series, the mean of each output variable over the 44-years of the historical period (i.e., starting from the spun-up conditions) is used for the sensitivity analysis. This allows us to assess the model sensitivity, filtering the influence of variability induced by inter-annual or seasonal climate and vegetation fluctuations. The methodology used for the GSA of LPJ-GUESS is summarized in four steps:

1. Selection of the output of interest. Since LPJ-GUESS has many different output variables (vegetation and soil carbon as well as water fluxes and states), the model sensitivity is expected to be different according to the selected model output. In the present study, we focused on the following variables: net primary productivity, NPP, ($NPP = GPP - R$, where GPP denotes the gross primary production and R is the sum of plant mainte-

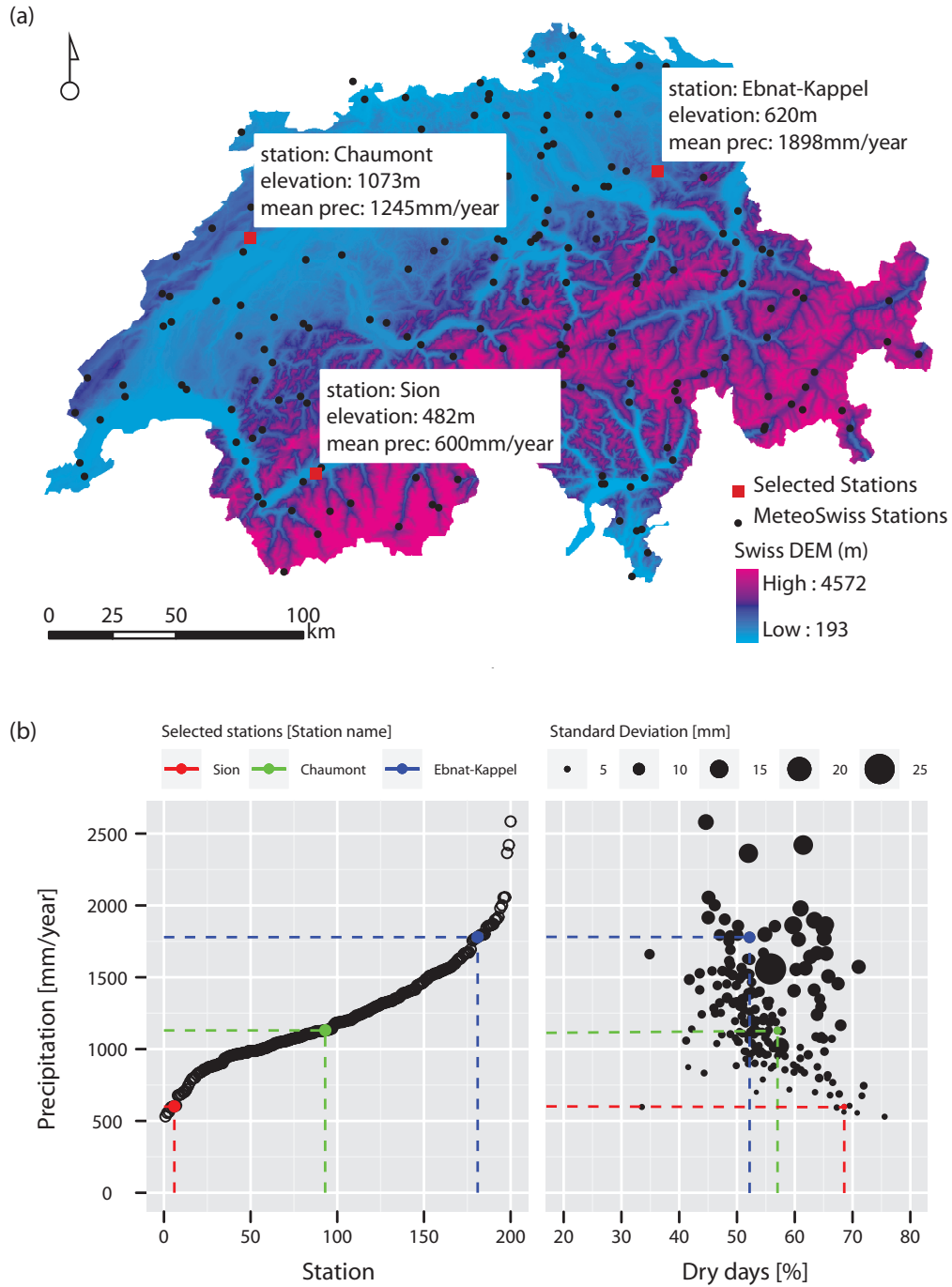


Figure 2.1: (a) The 200 analyzed meteorological stations in Switzerland with the 3 selected stations, representative of dry, normal, and wet conditions. (b) Annual statistics, i.e., mean, standard deviation, and percentage of dry days for the investigated stations. The selected stations are highlighted.

nance and growth respiration) and vegetation carbon pools (i.e., the sum of leaves, sapwood, heartwood, and fine roots, carbon). These are typically the main outputs of DGVMs.

2. Selection of parameter ranges and distributions. The key parameters for the principal processes were identified and included in the analysis (Section 2.2.3.1).
3. Qualitative GSA. A screening test was applied to identify a sub-set of the most important parameters. The purpose of the screening sensitivity analysis is applied to gain insights into the importance of parameters with low computational cost (Section 2.2.3.2).
4. Quantitative GSA. An explicit, quantitative evaluation of parameter importance and interactions was performed for the sub-set of parameters identified in the screening sensitivity analysis. A variance based GSA technique is used for this task (Section 2.2.3.3).

2.2.3.1 *Parameter ranges and assumptions*

On the basis of extensive literature research and model structure investigation, 34 model parameters, which are linked to the main simulated processes, namely, parameters related to plant establishment, growth and mortality, soil organic matter dynamics, plant biochemical and biophysical processes, plant water demand and uptake, and hydrological processes (e.g., runoff and percolation), were selected for the GSA. The model sensitivity to soil texture and soil characteristics was also investigated by including in the GSA the parameter regulating the soil water storage capacity available to plants, SSC (Table 2.3).

Parameter ranges represent a very critical but unavoidable choice for any sensitivity analysis study [Wallach and Genard, 1998], therefore a thorough selection has to be made. According to suggested guidelines [EC, 2009; EPA, 2009], GSA requires a detailed coverage of the entire parameter space over the full range of plausible values. Particular attention is thus paid in defining the uncertainty ranges of the examined parameters (see Table 2.3, and references therein). More specifically, for well documented parameters, the range obtained from measurement variability was used, while for empirical parameters, a plausible range was approximated based on our current knowledge, modeling experience, and literature survey (Table 2.3).

Model parameters are treated as independent random variables and their uncertainty is characterized by a uniform probability density function (PDF). Parameter independence is a crude but necessary assumption since our current knowledge about ecosystem processes does not allow for quantitatively predefined correlations. The orthogonality of the parameter space also facilitates the sensitivity analysis since it enhances applicability and computations of many GSA methodologies.

Table 2.3: Detailed description of the 34 investigated parameters and the processes in which they are involved. Their standard values as well as their uncertainty ranges, based on the literature, are shown.

| Process | Parameter Name | Minimum | Maximum | Standard values | Units | Description | Reference |
|-------------------------|----------------|--|---------|-----------------|---|--|---|
| ESTABLISHMENT | EST_MAX | 0.05 | 0.48 | 0.24 | [indiv m ⁻² year ⁻¹] | Maximum sapling establishment rate, eq.38 in Stich et al., (2003). | Zachle et al., (2005); Wrannebey et al., (2008) |
| | PARFF_MIN | ^{GRS} 300 ^{TBS; NE} 300 | 6500 | 2500 350 | [KJ m ⁻² day ⁻¹] | Minimum growing-season forest-floor PAR required for grass growth and tree establishment. | Wrannebey et al., (2008) |
| | ALPHA_R | 0.1 | 33.3 | 3.0 | [-] | Shape parameter for recruitment-juvenile growth rate relationship, eq.1 in Wrannebey et al., (2008). | Fulton (1991); Wrannebey et al., (2008) |
| | KEST_BG | 0.0 | 1.0 | 0.1 | [-] | Empirical parameter for tree establishment rate, eq.1 in Wrannebey et al., (2008). | Wrannebey et al., (2008) |
| | KEST_REP | 15 | 25 | 20 | [-] | Empirical parameter for tree establishment rate, eq.1 in Wrannebey et al., (2008). | Wrannebey et al., (2008) |
| GROWTH | K_LATOSA | ^{TBS} 2000 ^{NE} 2000 | 8000 | 5000 4000 | [-] | Leaf-to-sapwood area ratio, eq.1 in Stich et al., (2003). | Waring et al., (1982); Novick et al., (2009); Zachle et al., (2005) |
| | TURN_SAP | 0.01 | 0.20 | 0.05 | [frac. year ⁻¹] | Sapwood-heartwood conversion rate, eq.27 in Stich et al., (2003). | Bartelink (1998); Zachle et al., (2005) |
| | LWR_MAX | ^{GRS} 0.1 ^{TBS; NE} 0.1 | 5.0 | 0.5 1.0 | [-] | Maximum leaf-to-root mass ratio under nonwater stressed conditions, eq.2 in Stich et al., (2003). | Read et al., (2010); Sugita and Tateno (2011) |
| MORTALITY | DISTINT | 100 | 500 | 200 | [years] | Disturbance interval, average return time for genetic patch-destroying disturbances. | diagnostic |
| | KMORT_BG | 0 | 3 | 2 | [-] | Shape parameter for background mortality. | Harcombe (1987); Wrannebey et al., (2008) |
| | GREEF_MIN | 0.03 | 0.18 | 0.10 | [kg C m ⁻² leaf year ⁻¹] | Threshold for growth suppression mortality. | Harcombe (1987); Pacala et al., (1993); Wrannebey et al., (2008) |
| | LONGEVITY | 100 | 2100 | 500 | [years] | Expected maximum life span for 99% of population under non-stressed conditions. | Prentice and Helmisaari (1991); Wrannebey et al., (2008) |
| SOIL ORGANIC MATTER | TAU_LITTER | 1.23 | 5.26 | 2.85 | [years] | Litter turnover time at 10 °C. | Meentemeyer (1978); Zachle et al., (2005) |
| | ATM_FRAC | 0.5 | 0.9 | 0.7 | [-] | Fraction of the decomposed litter emitted as CO ₂ to the atmosphere. | Jenkinson (1990); Zachle et al., (2005) |
| | FAST_FRAC | 0.850 | 0.990 | 0.985 | [-] | Fraction of soil-bound decomposed litter entering the intermediate soil pool. | Foley (1995); Zachle et al., (2005) |
| AYTOTROPHIC RESPIRATION | GROWTH_RESP | 0.15 | 0.40 | 0.25 | [-] | Growth respiration per unit NPP, eq.25 in Stich et al., (2003). | Zachle et al., (2005); Wrannebey et al., (2008) |

Table 2.3. (Continued)

| Process | Parameter Name | | | Standard values | Units | Description | Reference |
|----------------|----------------|--|--|--|--|--|--|
| | Minimum | Maximum | | | | | |
| PHOTOSYNTHESIS | ALPHA_C3 | 0.020 | 0.125 | 0.080 | [$\mu\text{mol CO}_2$ μmol^{-1} photons] | Intrinsic quantum efficiency of CO_2 uptake in C_3 plants, eq.17 in Stich et al 2003. | Farquhar et al., (1980); Hallgren and Pitman (2000); Zaehle et al., (2005) |
| | ALPHA_A | 0.3 | 0.7 | 0.4 | [-] | Scaling parameter from leaf to canopy accounting for PAR absorbed by non-photosynthetic structures, thus lost to canopy photosynthesis. | Haxelme and Prentice (1996a,b); Zaehle et al., (2005) |
| | BC3 | 0.010 | 0.021 | 0.015 | [-] | Leaf respiration as a fraction of Rubisco capacity in C_3 plants, eq. 16 in Stich et al., (2003). | Farquhar et al., (1980); Hallgren and Pitman (2000); Zaehle et al., (2005) |
| | THETA | 0.200 | 0.996 | 0.700 | [-] | Shape parameter specifying the degree of colimitation by light and Rubisco activity, eq. 14 in Stich et al., (2003). | Leverenz (1988); Collatz et al., (1990); Zaehle et al., (2005) |
| | LAMBEER_K | 0.4 | 0.7 | 0.5 | [-] | Canopy light extinction coefficient, eq.7 in Stich et al., (2003). | Zaehle et al., (2005) |
| | LAMBDA_MAX | 0.6 | 0.8 | 0.8 | [-] | Optimal (non-water-stressed) ratio of intercellular to ambient CO_2 for C_3 plants. | Haxelme and Prentice (1996a,b); Zaehle et al., (2005) |
| | GM | 2.5 | 18.5 | 5.0 | [mm d^{-1}] | Maximum canopy conductance eq.12 in Stich et al., (2003). | Magnani et al., (1998); Zaehle et al., (2005) |
| AET | ALPHA_M | 1.1 | 1.5 | 1.4 | [-] | Empirical evapotranspiration parameter, eq.12 in Stich et al., (2003). | Monteith (1995); Zaehle et al., (2005) |
| PET | PR_TAYLOR | 1.08 | 1.60 | 1.32 | [-] | Priestley-Taylor coefficient, conversion factor from EET to PET. | Summer and Jacobs (2005) |
| WATER UPTAKE | EMAX | 2.4 | 6.2 | 5.0 | [mm d^{-1}] | Maximum daily transpiration rate. | Steward et al., (1989); Whitehead et al., (1993); Zaehle et al., (2005) |
| | ROOTDIST | $\begin{matrix} GRS \\ NE \\ TBS; NE \end{matrix}$ | $\begin{matrix} 1.0 \\ 0.9 \end{matrix}$ | $\begin{matrix} 0.8 \\ 0.6 \end{matrix}$ | [-] | Fraction of fine roots in the upper soil layer. | Jackson et al., (1996); Zaehle et al., (2005) |
| | GMIN | $\begin{matrix} GRS \\ NE \\ TBS \end{matrix}$ | $\begin{matrix} 0.22 \\ 0.22 \\ 0.42 \end{matrix}$ | $\begin{matrix} 0.58 \\ 0.38 \\ 0.58 \end{matrix}$ | $\begin{matrix} 0.50 \\ 0.30 \\ 0.50 \end{matrix}$ | Minimum canopy conductance which accounts for plant water loss not directly associated with photosynthesis, e.g., cuticular transport, eq.21 Stich et al., (2003). | Zaehle et al., (2005) |
| INTER-CEPTION | INTC | $\begin{matrix} GRS \\ NE \\ TBS \end{matrix}$ | $\begin{matrix} 0.01 \\ 0.01 \\ 0.01 \end{matrix}$ | $\begin{matrix} 0.2 \\ 0.2 \\ 0.2 \end{matrix}$ | [-] | Rainfall interception coefficient, eq.2 in Gerten et al., (2004). | Kergoat (1998); Gerten et al., (2004); Zaehle et al., (2005) |
| HYDROLOGY | DEPTH_EVAP | 0 | 500 | 200 | [mm] | Depth of sublayer at top of upper soil layer from which evaporation is possible. | diagnostic |
| | BASE_FRAC | 0.01 | 0.99 | 0.50 | [-] | Fraction of precipitation amount from lower soil layer that is diverted to baseflow runoff. | diagnostic |
| | PERC_BASE | 0.2 | 5.0 | 4.0 | [mm d^{-1}] | Empirical parameter, Eq.10 in Stich et al., (2003). | Stich et al., (2003); Gerten et al., (2004) |
| | PERC_EXP | 1 | 10 | 2 | [-] | Empirical exponent, eq.10 in Stich et al., (2003). | Neilson (1995) |
| | SSC | 15.00 | 450.00 | 225.00 | [mm] | volumetric water holding capacity (whc) at field capacity minus volumetric whc at wilting point, multiplied by the soil depth. | Stich et al., (2003) |

The choice of a non-informative PDF, such as the uniform, reflects the lack of knowledge which does not allow us to assign a well-defined distribution [see also [Radtko et al., 2001](#); [Medlyn et al., 2005](#)]. It is also coherent with other studies that mostly used uniform PDFs [e.g., [Zaehle et al., 2005](#); [Wramneby et al., 2008](#)]. These conservative assumptions may lead to overestimation of model uncertainty and sensitivity since improbable parameter combinations can be included. In order to partially reduce this effect and preserve the trait differences among plant types, PFT specific parameters were adjusted in their uncertainty range by maintaining a constant ratio between the different PFTs, derived from the standard model parameterization.

2.2.3.2 Screening exercise: Elementary Effects

The basic idea of screening approach is based on the Pareto's principle, i.e., model structures tend to have few very influential parameters and a majority of non-influential ones [[Saltelli et al., 2000a](#)]. A special case of screening sensitivity analysis is the method of elementary effects (EE) which was originally proposed by [Morris \[1991\]](#). The method is based on individually randomized many one-at-a-time designs. Derivatives with wide range of variation are calculated over the parameter space and their average values are used to provide a global sensitivity metric (see Section [A.1](#) for a detailed description).

The basic statistics, mean (μ_{EE}) and standard deviation (σ_{EE}), of a number of incremental ratios (EE), are the sensitivity measures suggested by [Morris \[1991\]](#) for parameter ranking (see Section [A.1](#) for further details). The mean of EE, μ_{EE} , is an estimator of the overall influence of a parameter to the output, and the standard deviation of EE, σ_{EE} , is an indicator of the higher-order parameter effects. The absolute mean value of EE (μ_{EE}^*) is used, instead of μ_{EE} , since it is considered as more robust sensitivity metric especially for the case of non-monotonic functions [[Campolongo et al., 2007](#)]. In this study, to facilitate the interpretation of the results and the ranking of parameters, the Euclidian distance, $\epsilon = \sqrt{\mu_{EE}^{*2} + \sigma_{EE}^2}$, of (μ_{EE}^* , σ_{EE}) from the origin (0,0) was used for parameter ranking. In the case of non-linearities and parameter interactions, this is a fair approximation of the overall parameter sensitivity.

The EE screening test was recursively applied for all the investigated climates to qualitatively assess the relevant importance of each of the 34 parameters. Parameter ranking according to the metric ϵ varies among different output variables and also among different PFTs. An objective selection of the most important parameters was performed using two criteria: (i) the 34 parameters were first ranked according to their mean value of ϵ across the 15 climatic forcings, then (ii) the selection was further restricted by ranking the parameters according to the standard deviation of ϵ . The rationale of this classification is that parameters

presenting high values of mean ϵ in combination with low standard deviation of ϵ , are influential parameters over most climatic scenarios.

While *EE* method is considered as an accurate and efficient screening test [Campolongo and Braddock, 1999; Campolongo et al., 2007], a major drawback is its qualitative character. Since parameters are ranked in terms of relevant importance, no information is provided about how much a given parameter is more important than another or how the different parameters interact [Saltelli et al., 2000a, 2004]. Therefore, after a subset of the most influential parameters is identified through the screening test, a detailed variance-based GSA was applied in order to quantify explicitly the importance of, and interactions among, different parameters.

2.2.3.3 Variance-based sensitivity analysis

The Sobol' methodology [Sobol', 1993], a special type of variance-based sensitivity analysis, is applied on the subset of the few most important parameters selected after the qualitative screening exercise (Section 2.2.3.2). The underlying assumption is that all the information about model uncertainty is captured by its variance.

Sobol' sensitivity analysis is based on the traditional analysis of variance (ANOVA) [Archer et al., 1997]. In summary, assuming that $Y = f(\mathbf{X})$ is a generalized model and $\mathbf{X} = \{X_1, \dots, X_k\}$ is a vector of parameters (random variables), where k is the total number of investigated parameters, then the model response, $f(\mathbf{X})$, is decomposed through a functional ANOVA into summands of increasing dimensionality:

$$\begin{aligned} f(\mathbf{X}) &= f(X_1, \dots, X_k) = \\ &= f_0 + \\ &\quad \sum_{i=1}^k f_i(X_i) + \sum_{i=1}^k \sum_{j>i}^k f_{ij}(X_i, X_j) + \dots + f_{12\dots k}(X_1, \dots, X_k) \end{aligned} \quad (2.1)$$

Note that the following convention is applied in the present work: capital letters are used for random variables, small letters for their realizations and bold for vectors and matrices. Obviously, there are many different ways to decompose $f(\mathbf{X})$ in the form of Equation 2.1, but provided that (i) the vector \mathbf{X} consists of independent parameters, (ii) f_0 is a constant ($f_0 = E[Y]$) and (iii) all the other terms in Equation 2.1 are selected such that they are square integrable with zero mean, then the decomposition is unique [Sobol', 1993]. Once we square and integrate Equation 2.1, we can partition the total output variance, V_Y , into terms of increasing dimensionality:

$$V_Y = V[Y] = V[f(\mathbf{X})] = \sum_i^k V_i + \sum_{i=1}^k \sum_{j>i}^k V_{ij} + \dots + V_{12\dots k} \quad (2.2)$$

where $V_i = V[E[Y|X_i = x_i^*]]$, $V_{ij} = V[E[Y|X_i = x_i^*, X_j = x_j^*]] - V_i - V_j$, and so on. $E[\cdot | \cdot]$ is the conditional expectation, and x_i^* , x_j^* denote the *real* values of the parameters i and j , respectively. In other words, similar to the ANOVA concept, the total output variance is partitioned to different sub-components which contribute to the overall output variability [Archer et al., 1997; Chen et al., 2005].

The sensitivity indices are then derived as the ratios of partial variances contributed by specific parameters of interest over the total output variance:

$$1 = \sum_i^k S_i + \sum_{i=1}^k \sum_{j>i}^k S_{ij} + \dots + S_{12\dots k} \quad (2.3)$$

where S_i is the first order sensitivity index (or main effect) of the i^{th} parameter, S_{ij} is the second order sensitivity index which represents the interactions of the i^{th} and j^{th} parameters and so on. Accordingly, the total sensitivity index, S_{Ti} , which represents the overall parameter importance (first and higher order effects), for the orthogonal case (i.e., independent parameters) is the sum of all the sensitivity indices of Equation 2.3 that include the i^{th} parameter [Saltelli et al., 2004]. The first and total order sensitivity indices are estimated since they include the most essential information and they offer a robust estimation of parameter importance and interactions [Homma and Saltelli, 1996; Saltelli, 2002].

The first order sensitivity index of parameter X_i is defined as:

$$S_i = \frac{V_i}{V_Y} = \frac{V[E[Y|X_i]]}{V[Y]} \quad (2.4)$$

The variance of the conditional expectation $V[E[Y|X_i]]$, represents the expected variance reduction that could be achieved when X_i would become perfectly known (i.e., $X_i = x_i^*$). The expectation of model response Y over the entire variation interval of X_i (i.e., $E[Y|X_i]$) is used since we are not able to know the *real* value x_i^* for each parameter X_i . First order sensitivity indices represent the main effect contribution of individual parameters to the output variance [Saltelli et al., 2008] and are therefore considered an agile measure for sensitivity assessments, but they are not enough for a rigorous GSA because quantification of higher order effects can also be important [Chan et al., 1997].

Total order sensitivity indices attempt to bridge this gap by estimating not only first but also higher order effects. According to variance decomposition pre-

sented in Equation 2.2, the total effect index of the i^{th} parameter can be expressed as: $S_{Ti} = S_i + \sum_{j \neq i}^k S_{ij} + \dots + S_{12\dots k}$ and it is defined as:

$$S_{Ti} = \frac{E[V[Y | \mathbf{X}_{\sim i}]]}{V[Y]} = 1 - \frac{V[E[Y | \mathbf{X}_{\sim i}]]}{V[Y]} \quad (2.5)$$

where $\mathbf{X}_{\sim i}$ is a vector of all the random variables (i.e., parameters) but the i^{th} . The term $E[V[Y | \mathbf{X}_{\sim i}]]$ is the expected amount of variance that would remain unexplained if X_i , and only X_i , were left free to vary over its uncertainty range, all the other parameters (i.e., the vector $\mathbf{X}_{\sim i}$) having been learnt [Homma and Saltelli, 1996; Saltelli et al., 2008]. Similarly to the main effect, the outer expectation is used since the *true* values of the $\mathbf{X}_{\sim i}$ vector are not known. Total effect indices play a pivotal role in distilling information about the overall parameter importance since they highlight nonadditive features of the model structure and allow one to quantify parameter interactions, by subtracting the first order from the total sensitivity indices.

A detailed description of the implemented computational scheme is available in the Section A.2. In summary, for estimating first and total sensitivity indices, the computational strategy originally proposed by Sobol' [1993] and further improved by Saltelli [2002] and Saltelli et al. [2010] was followed. A convergence test was also conducted for defining the number of necessary model evaluations (6656 model runs were selected, see details in Section A.4). The sampling strategy is based on the Sobol' low discrepancy sequences, LP_τ sequences [Sobol', 1967, 1976], because they provide an enhanced convergence rate of the numerical estimators [Chan et al., 2000; Saltelli et al., 2000a, 2004, 2008, 2010]. A better description of LP_τ appealing properties is provided in Section A.3.

2.3 RESULTS

2.3.1 Screening results

The sensitivity metric ϵ gives comparable ranking of the parameters for the case of vegetation biomass and NPP. Parameters that exert high sensitivity for NPP, they also do so for vegetation biomass (Figure 2.2 and 2.3). The variability in the parameter sensitivity induced by different climate forcings is generally lower in comparison to the variability induced by the parameters themselves. A subset of 11 potentially critical parameters was identified according to the ϵ -based ranking (Figures 2.2, 2.3, and Table 2.4). The parameter selection was also corroborated by an analysis of other complementary output variables such as Leaf Area Index, LAI (results not shown).

From the screening emerges that vegetation carbon assimilation and fluxes show low sensitivity to hydrological parameters that define and regulate directly or indirectly the available soil water to plants. Parameters related to the terrestrial water balance, such as runoff generation (BASEFLOW_FRAC) and percolation (PERC_BASE, PERC_EXP) have no important effect on the variability of vegetation carbon fluxes and pools, especially when compared to biochemical or biophysical parameters (Figure 2.2 and 2.3). Only soil texture properties, specifically soil water storage capacity (SCC), defined as the difference between volumetric water content at field capacity and volumetric water content at wilting point multiplied by soil depth is found important. It occurs as the only parameter related to the terrestrial water balance that might significantly influence vegetation carbon sequestration.

Table 2.4: The 11 parameters selected through the screening test, categorized in terms of simulated processes.

| Process | Parameters |
|----------------------------|------------|
| Vegetation establishment | PARFF_MIN |
| | K_LATOSA |
| Plant growth and structure | TURN_SAP |
| | LtoR_MAX |
| | ALPHA_C3 |
| Photosynthesis | ALPHA_A |
| | THETA |
| Mortality | GREFF_MIN |
| Transpiration | GM |
| Water uptake | ROOTDIST |
| Soil hydrology | SSC |

In accordance with Pareto's principle (Section 2.2.3.2), only 11 parameters, out of 34 originally examined, were selected after the *EE* screening analysis (Table 2.4). The importance of these parameters was further investigated by applying a detailed variance-based GSA that allows us to quantitatively assess parameter sensitivity and interactions.

2.3.2 Results of variance-based sensitivity analyses

2.3.2.1 First and total Sobol' sensitivity indices

The distribution of model outputs (mean values over the 44-year historical period) for the 6656 model simulations, where the 11 parameters were varied simultaneously, under different climatic forcings are illustrated in Figure 2.4. The annual NPP of each PFT (Figure 2.4b) facilitates the delineation of stand composition in terms of dominant and sub-dominant PFTs. In our study, evergreen

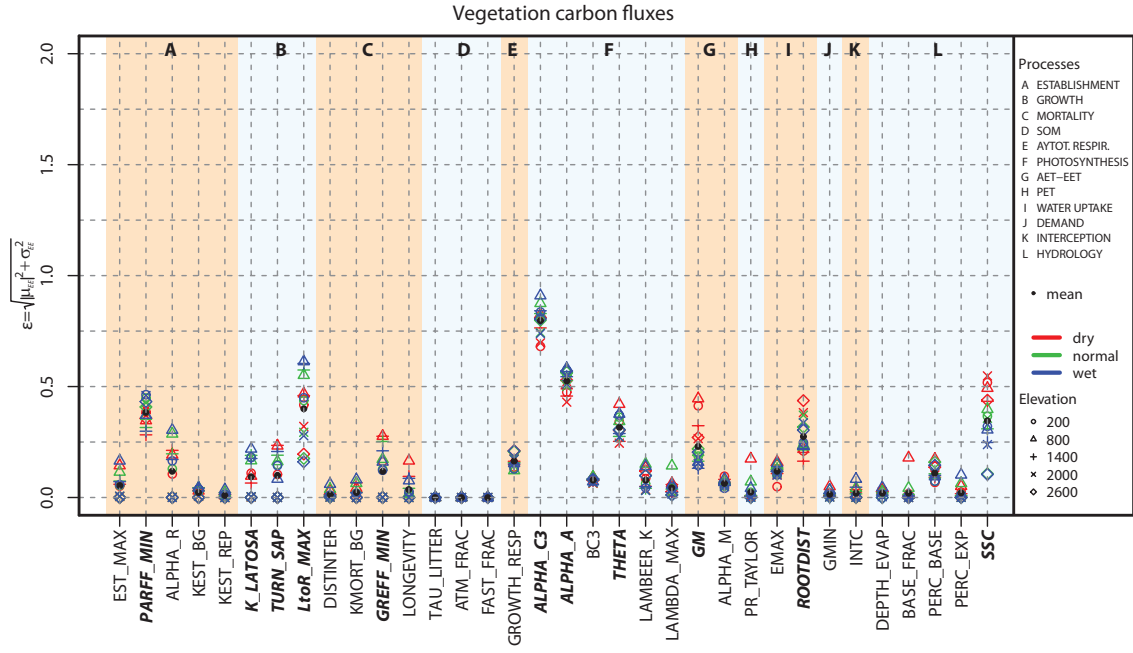


Figure 2.2: Qualitative results of the screening analysis for the total NPP (i.e., vegetation carbon fluxes). The sensitivity metric ϵ under different climate conditions is illustrated. The 11 parameters selected for the detailed analysis are highlighted with bold italic characters.

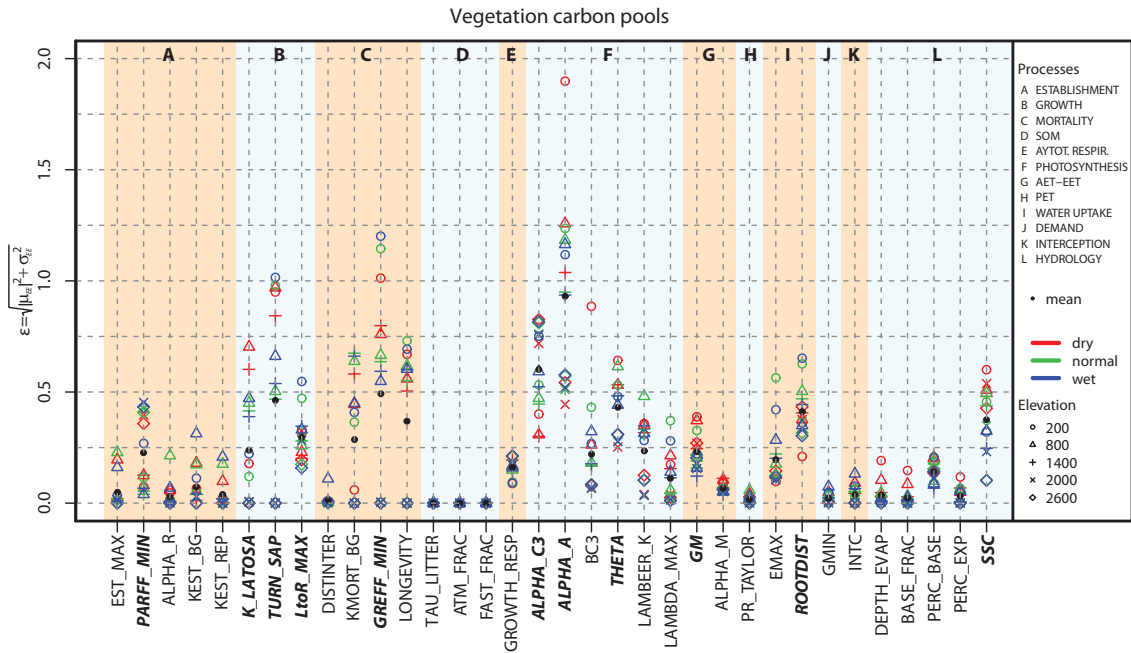


Figure 2.3: Qualitative results of the screening analysis for the total vegetation biomass (i.e., vegetation carbon pools). The sensitivity metric ϵ under different climate conditions is illustrated. The 11 parameters selected for the detailed analysis are highlighted with bold italic characters.

trees can be found between 800 m to 1400 m a.s.l. while deciduous trees occur from 200 m to 800 m a.s.l. of elevation. The simulated herbaceous PFT occurs at all the elevation bands and for high elevations (2000 m and 2600 m a.s.l.) dominates the entire stand, without any woody PFT being present.

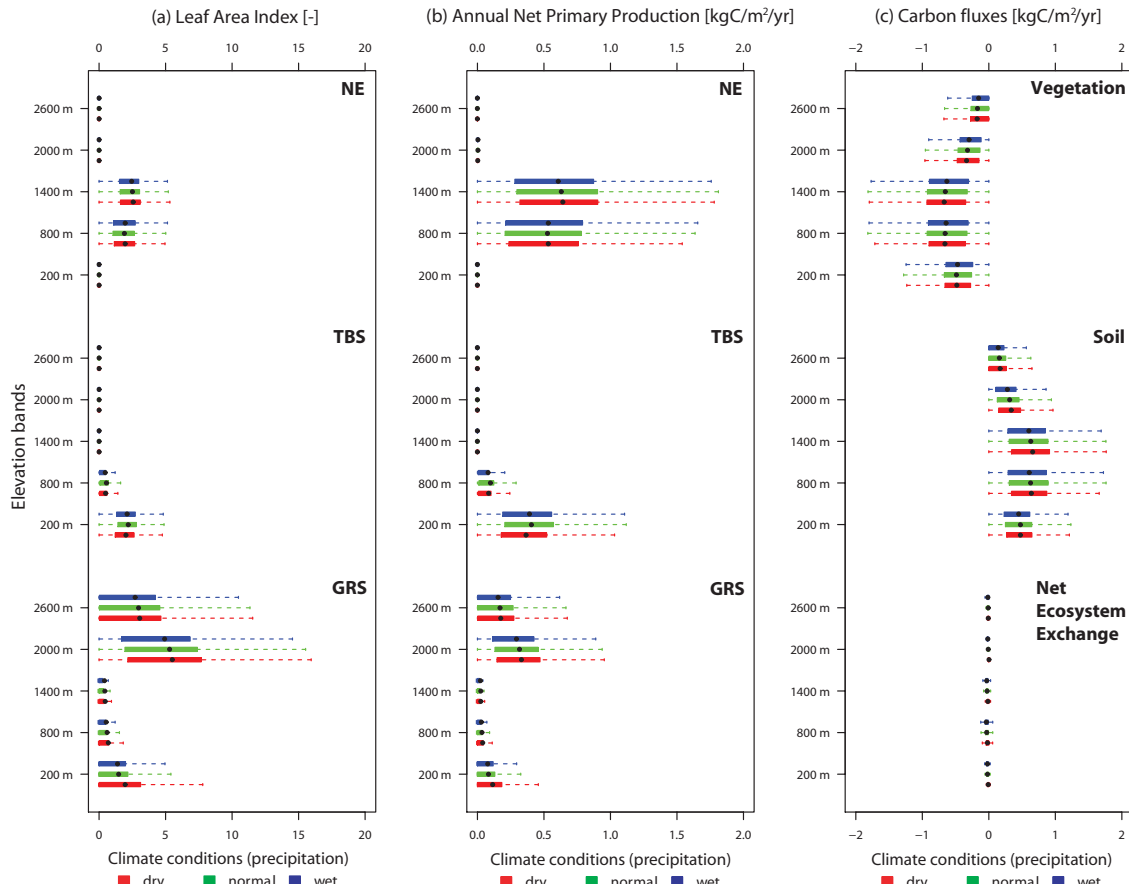


Figure 2.4: Distribution of LAI, NPP, and carbon fluxes for different climatic forcings (from wet to dry conditions and from low to high elevations), when the 11 selected parameters were varied simultaneously (6656 model evaluations). LAI (a), annual NPP (b) as well as carbon fluxes (c) for the different ecosystem components are presented. Boxes are extended from 25% lower quartile ($q_{0.25}$) to 75% upper quartile ($q_{0.75}$) while whiskers represent the range of $[q_{0.5} - 1.5IQR, q_{0.5} + 1.5IQR]$, where $q_{0.5}$ is the median and IQR is the interquartile range ($q_{0.75} - q_{0.25}$).

About 50% to 70% (according to the climate forcing) of the variability in total annual NPP is explained by the uncertainty of ALPHA_C3. Most of this variability is caused by first order effects (40% to 60%) while only 10% is due to interactions with other parameters (Figure 2.5). ALPHA_C3 is the parameter that regulates the initial slope of the light response curve of photosynthesis, representing the maximum efficiency of incident light-energy conversion i.e., light utilization [Haxeltine and Prentice, 1996a, b; Wohlfahrt et al., 1999; von Caemmerer, 2000; Singaas et al., 2001; Gates, 2003; Bonan, 2008a]. The high sensitivity to ALPHA_C3 is consistent through the examined precipitation conditions (from

dry to wet climates), but shows a certain variability across elevation bands due to variability in vegetation composition (Figure 2.4). At high elevations, e.g., 2600 m a.s.l., where grass dominates the simulated stand, the importance of ALPHA_C3 is lower than at 800 m a.s.l., where woody and herbaceous PFTs co-exist and compete. The second most influential parameter for vegetation carbon fluxes is ALPHA_A, i.e., the scaling parameter from leaf to canopy. Roughly 20% of output variability is due to the uncertainty of ALPHA_A. The influence of ALPHA_A in the variability of NPP is relatively constant across the examined environmental conditions. Since ALPHA_C3 and ALPHA_A regulate the efficiency in converting solar radiation to carbon, they essentially control vegetation carbon fluxes, causing high variability in model outputs. The parameter PARFF_MIN, which determines establishment for woody, and growth for herbaceous PFTs, is also a crucial parameter at high elevation (2000 m to 2600 m a.s.l.), where grass tends to dominate the simulated stand. At the elevation band of 2000 m, where grass is abundant, around 40% of the variability in vegetation carbon fluxes is due to the first order effect of ALPHA_C3, while around 30% is induced by the first order effect of PARFF_MIN. At the highest elevation (2600 m a.s.l.), where grass is the only occurring PFT, ALPHA_C3 is again the most influential parameter, accounting for 60% of variability in the simulated NPP, of which about 40% is due to first order effects, while 20% is due to interactions with other parameters. In this non-competitive environment dominated by grass, LtoR_MAX, which affects the partition of below-ground and above-ground biomass, is of similar importance as PARFF_MIN and ALPHA_A, causing around 25% of variability in the vegetation carbon fluxes, out of which 10% is due to interactions.

Since there is ample evidence that patch composition affects the model results (e.g., the performance of the simulated biomes) and therefore the parameter importance [Tilman *et al.*, 1997; Wramneby *et al.*, 2008], we examined the effects of parameter uncertainty in the simulated NPP separately for each PFT (Figures 2.6, 2.7, and 2.8).

Comparing parameter sensitivity of the two woody PFTs, coniferous evergreen (Figure 2.6) and broadleaf deciduous (Figure 2.7), we can highlight different sensitivity patterns. When competition among PFTs occurs, the model shows sensitivity to additional parameters since higher order effects start playing a more important role for the model outcomes. This is particularly evident in Figures 2.6 and 2.7 where parameters related to plant structure are becoming significantly important in terms of total effects while their first order indices are relatively low, underlining the effect of parameter interactions. At 800 m a.s.l. elevation, where evergreen and deciduous trees co-exist and compete for the same resources, parameters related to plant growth and structure (TURN_SAP, LtoR_MAX) are becoming influential for coniferous trees (Figure 2.6). Deciduous trees (Figure 2.7), that are sub-dominant at this elevation, i.e., they have a significantly lower productivity in comparison to coniferous, show

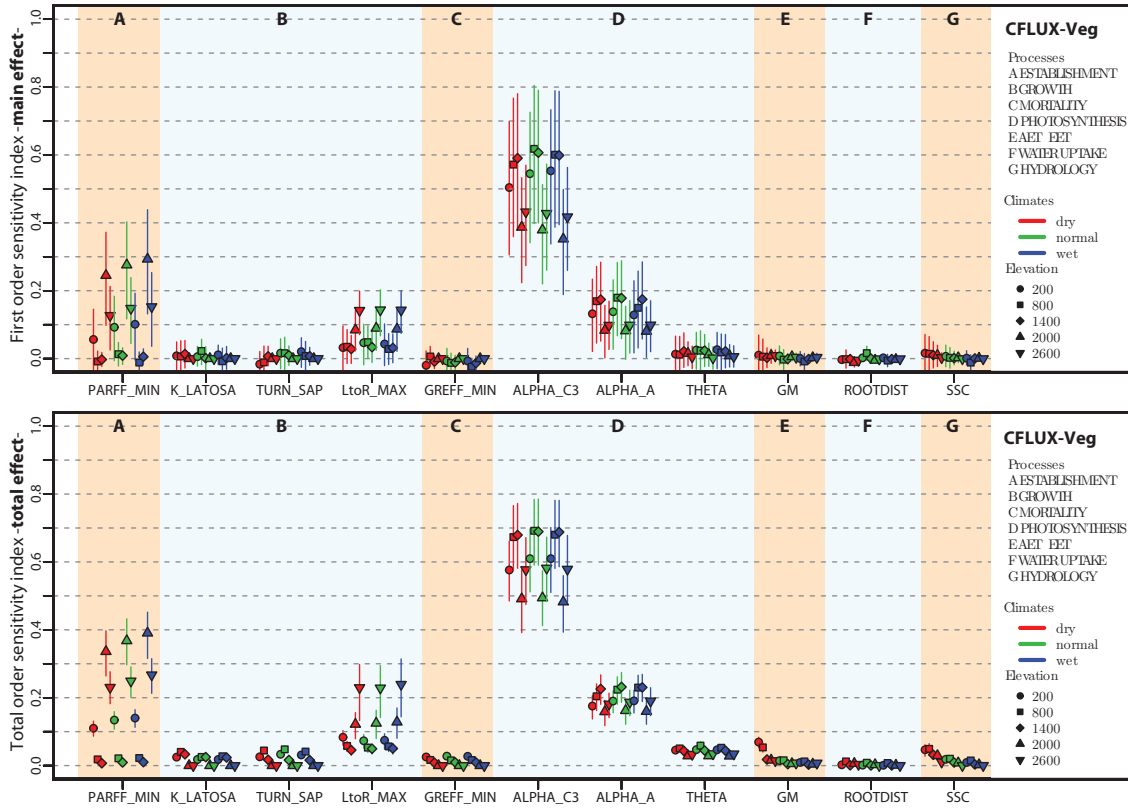


Figure 2.5: First and total Sobol' sensitivity indices of the 11 investigated parameters with their 95% confidence intervals (vertical lines), for total vegetation NPP under different climate forcings (from wet to dry conditions and from low to high elevations).

sensitivity to many parameters controlling their occurrence and growth (e.g., ALPHA_C3, K_LATOSA, TURN_SAP, LtoR_MAX, GREFF_MIN) especially in terms of higher order effects.

The sensitivity of the productivity of grass is also influenced by stand composition. At low and middle elevations (200 m to 1400 m a.s.l.), where woody and herbaceous PFTs co-exist, the productivity of grass is mostly sensitive to PARFF_MIN, which defines a light threshold required for grass to grow (Figure 2.8). Due to tree shadowing effects, the available Photosynthetically Active Radiation (PAR) for grass is reduced and PARFF_MIN becomes very critical for the productivity of grass. The second most influential parameter, responsible for around 30% of the variance in the simulated NPP of grass, is the maximum leaf-to-root mass ratio (LtoR_MAX). At higher elevations where grass does not compete with woody PFTs, the importance of PARFF_MIN and LtoR_MAX significantly decreases. Contemporaneously, intrinsic quantum efficiency becomes the most sensitive parameter, explaining about 50% to 60% of grass NPP variability (Figure 2.8).

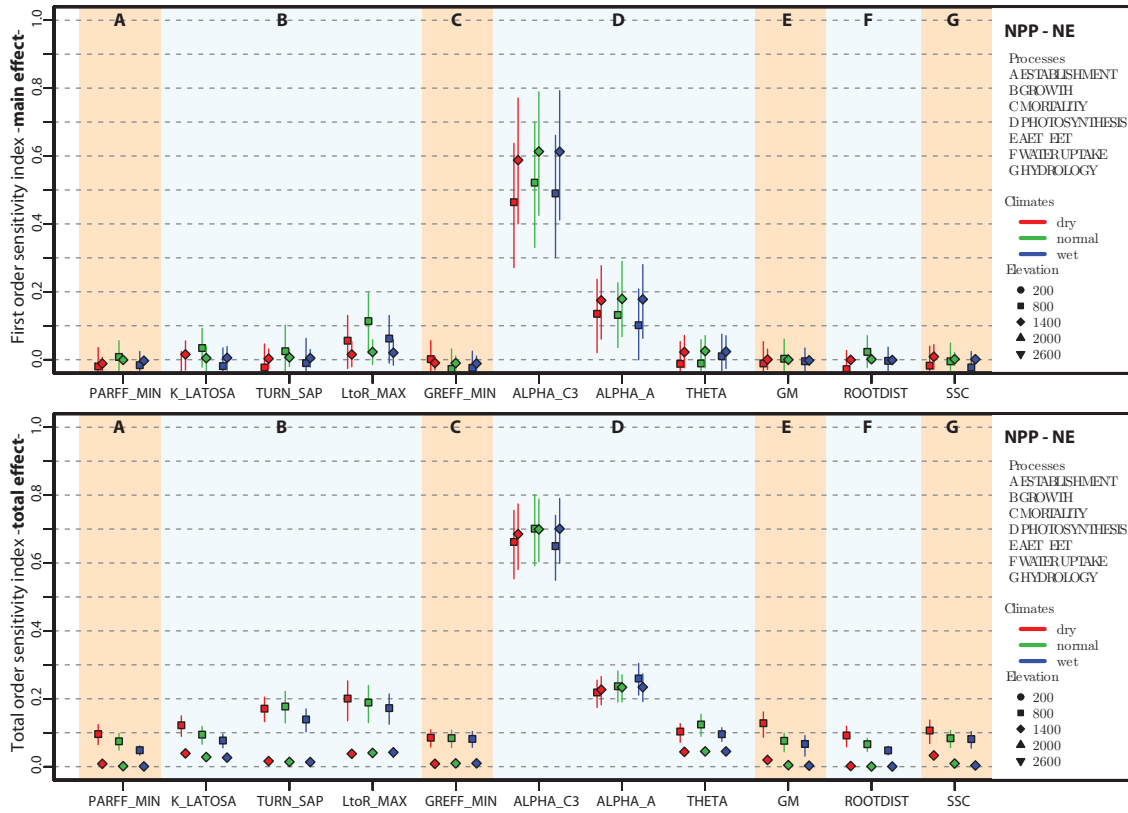


Figure 2.6: First and total Sobol' sensitivity indices of the 11 investigated parameters for the NPP of needle-leaved trees under different climate forcings (from wet to dry conditions and from low to high elevations). The 95% confidence intervals are also plotted (vertical lines). Constrained by the ascribed bioclimatic limits, needle-leaved vegetation occurs only between 800 m and 1400 m a.s.l. elevation.

Finally, intrinsic quantum efficiency is confirmed to be the most important parameter for the total carbon stored by vegetation under all the climate forcings (Figure 2.9), independent of patch composition. ALPHA_C3 alone explains 50% to 60% of the variability in the vegetation carbon pools. ALPHA_A also shows a consistent influence on the output variability across all the elevation bands with a total order effect of ≈ 0.2 . However, the second most important parameter for the carbon stored in vegetation pools, when the simulated stand is occupied by woody PFTs (200 m to 1400 m a.s.l. elevation), is TURN_SAP, which defines the conversion rate between sapwood and heartwood. At high elevations, where grass occupies the entire tile, PARFF_MIN becomes the second most important parameter after ALPHA_C3.

2.3.2.2 Sobol' GSA excluding photosynthesis-related parameters

The strong sensitivity of LPJ-GUESS to the parameterization of photosynthesis scheme may hide the importance of other parameters and processes. Thus, in

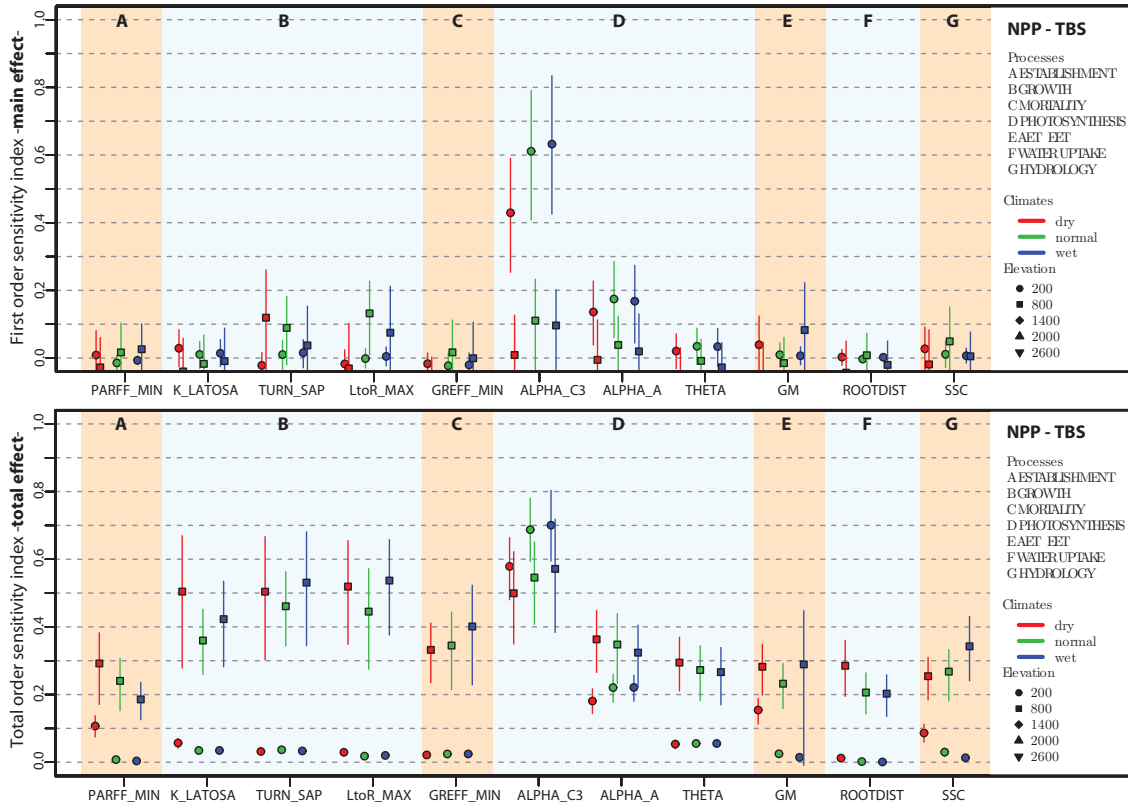


Figure 2.7: First and total Sobol' sensitivity indices of the 11 investigated parameters for the NPP of broad-leaved trees under different climate forcings (from wet to dry conditions and from low to high elevations). The 95% confidence intervals are also plotted (vertical lines). Constrained by the ascribed bioclimatic limits, broad-leaved vegetation occurs only between 200 m and 800 m a.s.l. elevation.

order to consolidate our findings and investigate any potential damping effect in the parameter ranking caused by the overwhelming contribution of intrinsic quantum efficiency, we repeated the GSA by excluding parameters related to photosynthesis. Specifically, ALPHA_C3, ALPHA_A, and THETA were fixed to their standard values (Table 2.3), and the first and total Sobol' sensitivity indices were calculated for the 8 remaining parameters. By excluding the photosynthesis parameters, the importance of light harvesting and plant-structure parameterization were further scrutinized and the low sensitivity of soil water content was also reconfirmed.

Figure 2.10 shows the distribution of the 44-year average values of LAI, NPP, and carbon fluxes. The stand composition is similar as in Figure 2.4, where photosynthesis parameters were included in the analysis. However, the distribution of the output is narrower and with less dispersion. There is no important variation in the examined output and stand composition with the different precipitation patterns (Figure 2.10), i.e., Sobol' sensitivity indices are similar under dry, normal and wet conditions. Therefore, results are illustrated only for the case of

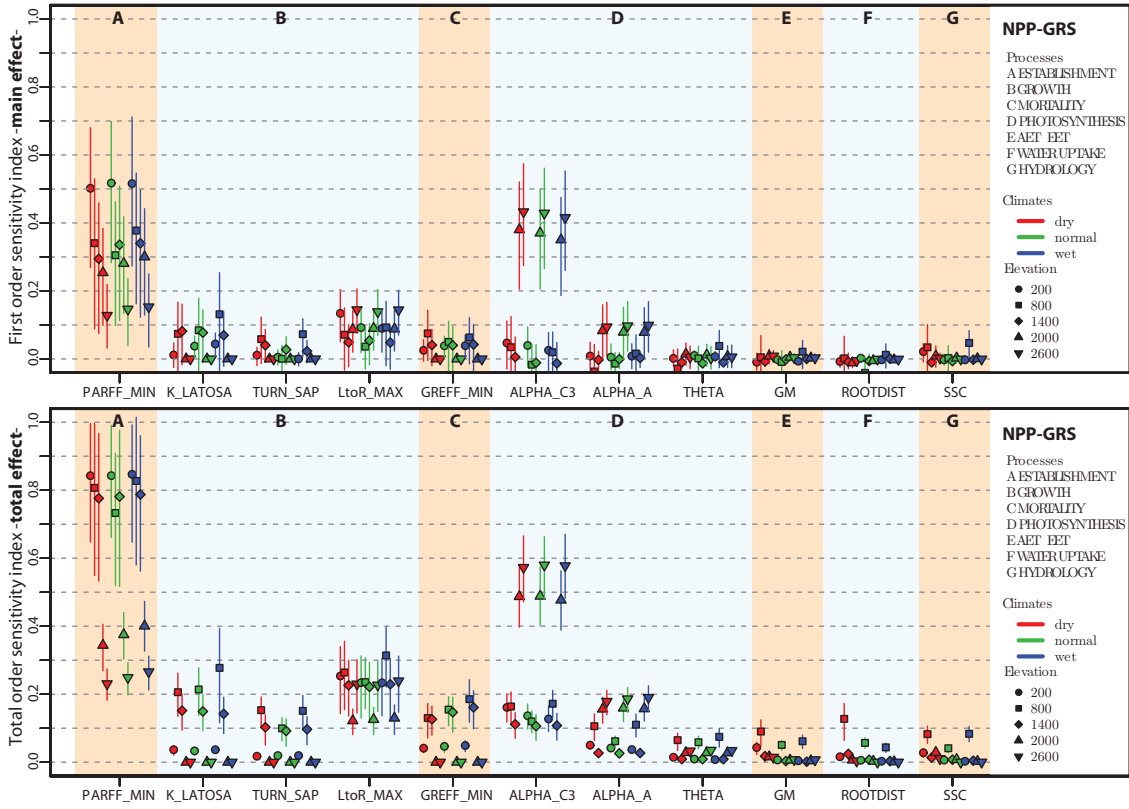


Figure 2.8: First and total Sobol' sensitivity indices of the 11 investigated parameters for the NPP of grass, under different climate forcings (from wet to dry conditions and from low to high elevations). The 95% confidence intervals are also plotted (vertical lines).

normal precipitation forcing (Figures 2.11 and 2.12). Coxcomb plots, which are essentially bar charts in polar coordinates, were used to summarize the parameter ranking of the different stand compositions. Total Sobol' sensitivity indices of the examined parameters are depicted for the elevation bands where each PFT is predominant in the simulated stand (TBS at 200 m a.s.l., NE at 1400 m a.s.l., and GRS at 2000 m a.s.l.), and for the elevation band of 800 m a.s.l., where all the PFTs co-exist and compete (Figures 2.11 and 2.12).

The parameter LtoR_MAX is found to be very important for the vegetation carbon fluxes, independent of stand composition (Figure 2.11a, b). At the elevation of 200 m a.s.l. where TBS is the dominant PFT, PARFF_MIN is the most important parameter explaining 60% of the variability in NPP and LtoR_MAX is the second most important with a total order sensitivity index ≈ 0.4 . At 2000 m a.s.l., where the entire stand is covered by grass, the sensitivity patterns are similar, PARFF_MIN explains most of the variability in vegetation carbon fluxes and LtoR_MAX is the second most important parameter. At the elevation of 800 m a.s.l., where the two woody PFTs and grass co-exist (NE is the dominant PFT and TBS the sub-dominant), LtoR_MAX is the most critical parameter, with a total order sensitivity index ≈ 0.6 .

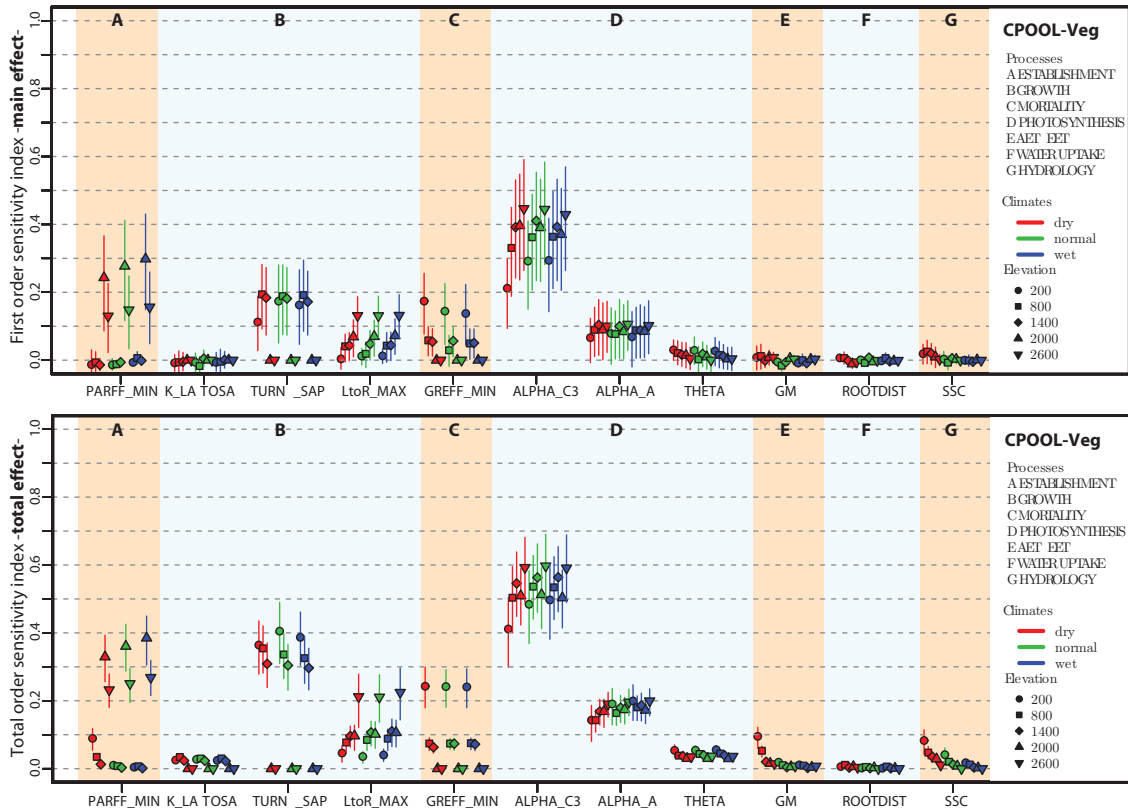


Figure 2.9: First and total Sobol' sensitivity indices of the 11 investigated parameters with their 95% confidence intervals (vertical lines) for the vegetation carbon pools (sum of the carbon allocated in leaves, sapwood, heartwood and fine roots) under different climate forcings.

For the vegetation biomass (vegetation carbon pools, Figure 2.11c, d), parameters regulating plant structure and mortality, TURN_SAP and GREFF_MIN respectively, are the most important parameters for the elevation bands where woody PFTs are dominant (200-1400 m a.s.l.). GREFF_MIN is the most sensitive parameter for vegetation carbon pools when only TBS trees occur and TURN_SAP is the second most important. For stands with only NE trees, TURN_SAP is the most sensitive parameter and GREFF_MIN is the second most sensitive. When grass is the only PFT that occurs in the simulated stand, PARFF_MIN is found to be the most important parameter (Figure 2.11c). At the elevation of 800 m a.s.l., TURN_SAP, GREFF_MIN, and LtoR_MAX emerge as the most influential parameters, as a result of the co-existence of different PFTs.

Summarizing, despite some differences due to stand composition, the parameter ranking is fairly similar for the vegetation carbon fluxes and pools under the entire spectrum of the used climate forcings. PARFF_MIN and LtoR_MAX are the most influential parameters for NPP under all the examined stand compositions. For the vegetation carbon pools TURN_SAP, GREFF_MIN, and LtoR_MAX are the three key parameters when woody PFTs occur. When the simulated stand is

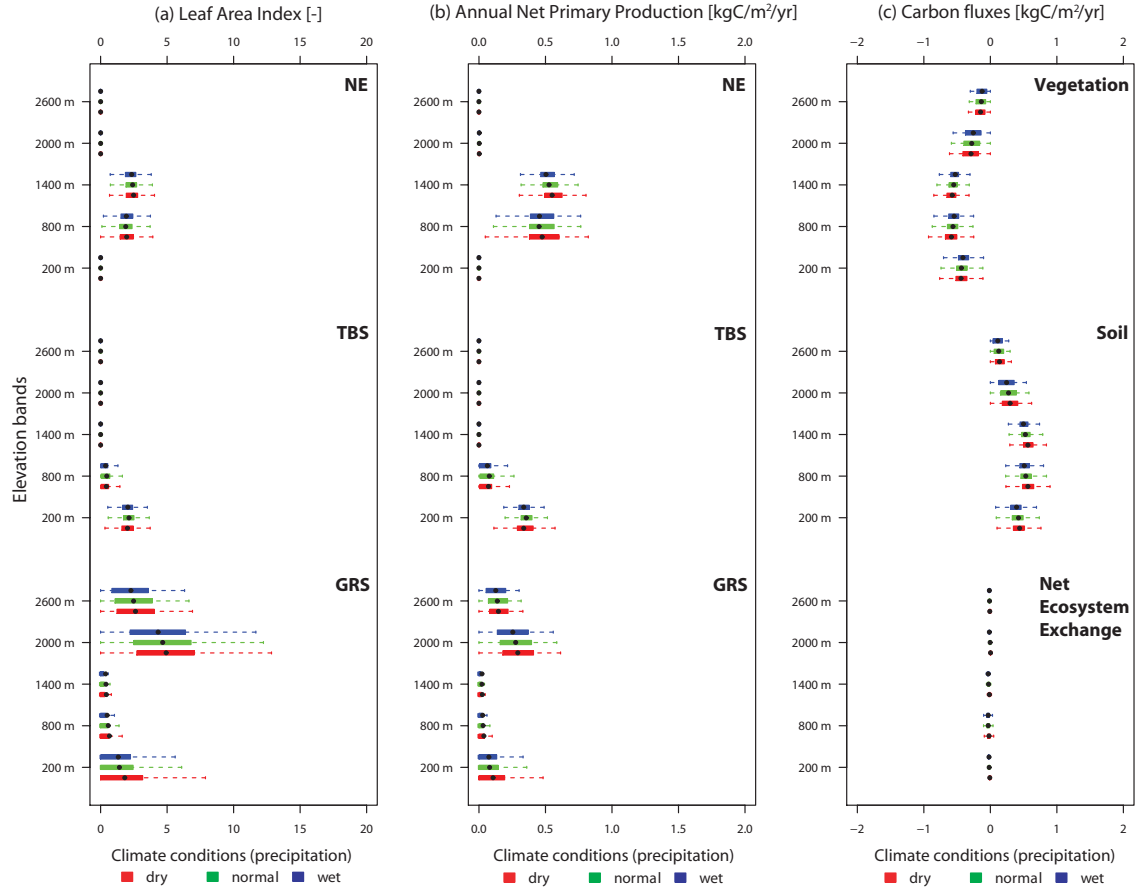


Figure 2.10: Distribution of LAI, NPP, and carbon fluxes for different climatic forcings, when the 8 remaining parameters, after removing photosynthesis parameterization from the GSA, were varied simultaneously (5120 model evaluations). LAI (a), annual NPP (b), as well as carbon fluxes (c) for the different ecosystem components are presented. Boxes are extended from 25% lower quartile ($q_{0.25}$) to 75% upper quartile ($q_{0.75}$) while whiskers represent the range of $[q_{0.5} - 1.5IQR, q_{0.5} + 1.5IQR]$, where $q_{0.5}$ is the median and IQR is the interquartile range ($q_{0.75} - q_{0.25}$).

only covered by herbaceous species, PARFF_MIN is the most important parameter.

Contrary to what we found for vegetation carbon fluxes and pools, the sensitivity metrics at the PFT level, e.g., NPP and LAI of each specific PFT, are strongly conditioned by stand composition. Total sensitivity indices for NPP and LAI of the 8 examined parameters of NE, TBS, and GRS are illustrated in Figure 2.12 for the different stand compositions and normal precipitation conditions. When only one PFT occurs in the simulated stand, there are very few parameters that essentially affect the PFT specific model outputs (Figure 2.12a, c), while at the 800 m a.s.l. elevation band where all the simulated PFTs co-exist, many parameters become influential, affecting NPP and LAI of each PFTs (Figure 2.12b, d). When woody PFTs occupy the entire stand, K_LATOSA and LtoR_MAX, are

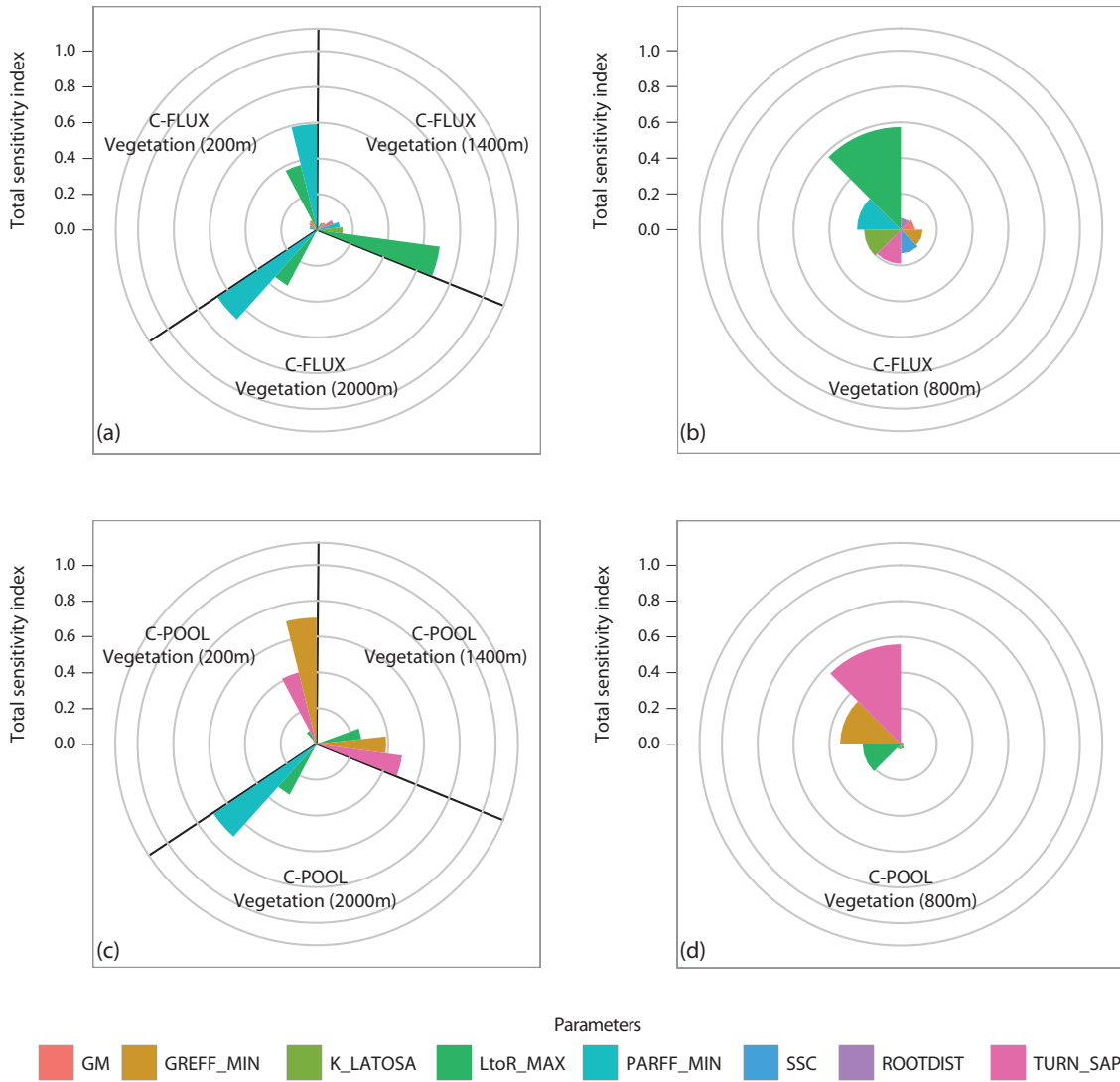


Figure 2.11: Coxcomb plots of the total effect sensitivity indices for vegetation carbon fluxes, subplots (a) and (b), and vegetation carbon pools, subplots (c) and (d). Total effect sensitivity indices are reported for the three different elevation bands where each of the simulated PFT is the dominant (TBS at 200 m a.s.l., NE at 1400 m a.s.l, and GRS at 2000 m a.s.l.) under normal precipitation conditions, subplots (a) and (c), as well as for the elevation band where all the PFTs co-exist (800 m a.s.l.), subplots (b) and (d).

of paramount importance. However, the examination of elevation bands where competition among PFTs takes place, led to the identification of additional crucial parameters. Especially for broad-leaved trees, which are sub-dominant at 800 m a.s.l., the total sensitivity indices of most of the parameters are higher when compared to needle-leaved trees that dominate the forest stand. For grass, PARFF_MIN is the most sensitive parameter independent of forest stand composition, but the sensitivity is higher in the presence of trees. Trees reduce the amount of radiation that penetrates the canopy and reaches the forest-floor and thus light becomes the limiting factor for grass growth. Grass is also strongly

influenced by the maximum leaf-to-root mass ratio (LtoR_MAX), especially at high elevations.

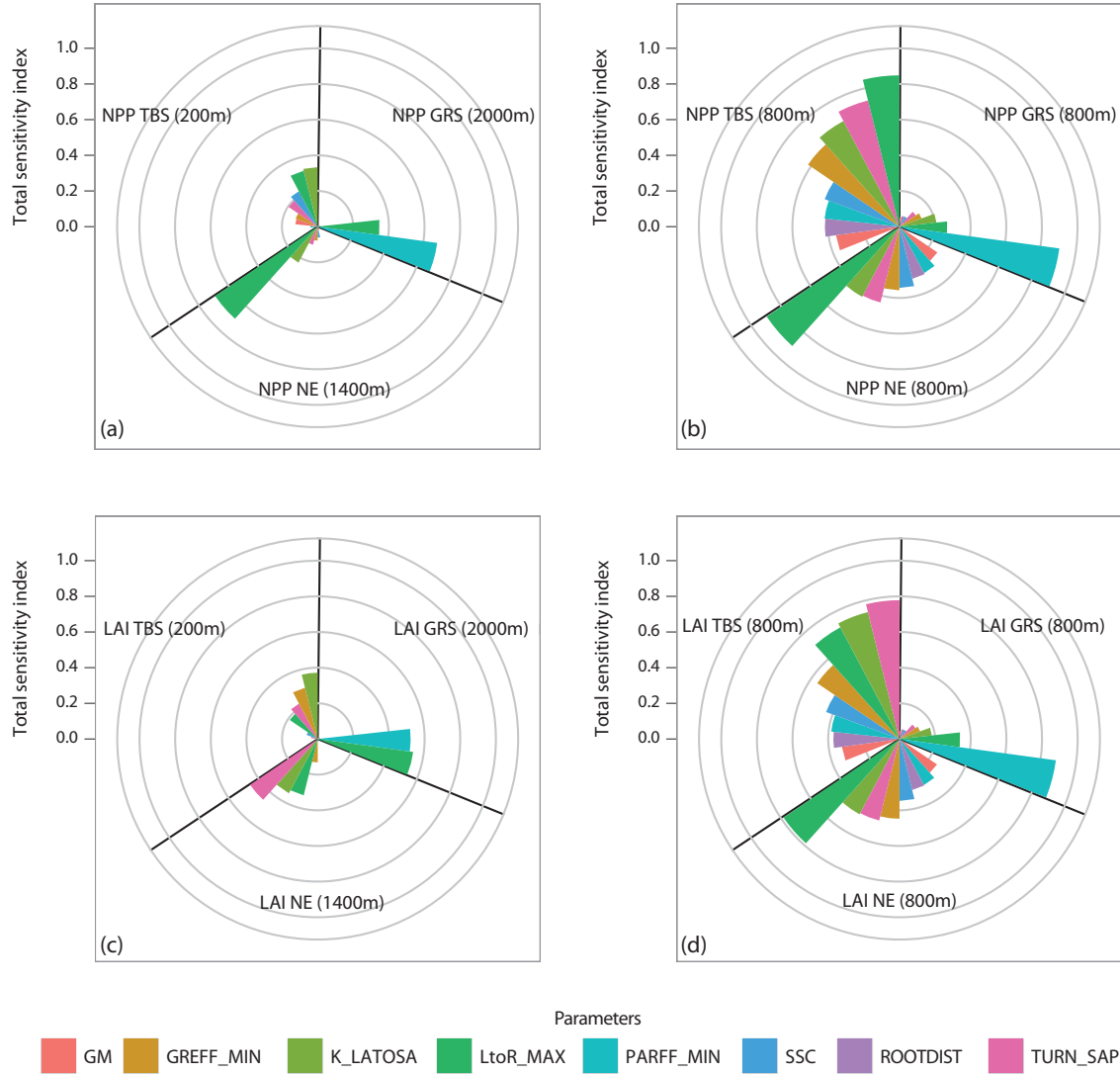


Figure 2.12: Coxcomb plots of the total effect sensitivity indices for NPP, subplots (a) and (b), and LAI, subplots (c) and (d). Total effect sensitivity indices of NPP and LAI are reported for the three different elevation bands where each of the simulated PFT is the dominant (TBS at 200 m a.s.l., NE at 1400 m a.s.l., and GRS at 2000 m a.s.l.) under normal precipitation conditions, subplots (a) and (c), and for the elevation band where all the PFTs co-exist (800 m a.s.l.), subplots (b) and (d).

2.4 DISCUSSION

The results described in the previous sections provide a thorough evaluation of LPJ-GUESS terrestrial ecosystem model. For the first time, advanced sensitivity analysis methodologies are applied to a DGVM for estimating not only

the sensitivity to different parameters, but also for better understanding the importance of the model structure. Since it is widely accepted that mimicking the reality should imply more than a simple agreement with observed variables [Weisberg, 2007], especially when long term or climate non-stationary quantitative predictions are envisioned [Cox *et al.*, 2006; Evans, 2012], such a type of model evaluation is fundamental.

2.4.1 Sensitivity to photosynthesis and plant growth

The Farquhar photosynthesis scheme [Farquhar *et al.*, 1980; Collatz *et al.*, 1991] turned out to include the most sensitive out of the 34 examined model parameters of LPJ-GUESS, in particular the intrinsic quantum efficiency. In agreement with the results of Zaehle *et al.* [2005], intrinsic quantum efficiency is of utmost importance in the LPJ-GUESS parameterization, explaining most of the variability in vegetation carbon fluxes and pools, regardless of stand composition and climate forcings. The essential role of photosynthesis parameterization in controlling the terrestrial ecosystem carbon budget has also been detected in other modeling studies [Hallgren and Pitman, 2000; Medlyn *et al.*, 2005; Zaehle *et al.*, 2005; Alton *et al.*, 2007; Matthews *et al.*, 2007; Chen *et al.*, 2011; Bonan *et al.*, 2011; Dietze *et al.*, 2011]. Specifically, maximum capacity for carboxylation has been found to be a key plant physiological parameter which can strongly influence not only photosynthesis but also the global climate [Bonan *et al.*, 2011].

This critical role of the process of photosynthesis in controlling long-term vegetation carbon fluxes and pools (responsible for about 60% of output variability in the case of LPJ-GUESS) is contradicted by field experiments, which suggest that photosynthesis may be a consequence rather than a driver of plant growth [Körner, 2003a; Zweifel *et al.*, 2006; Muller *et al.*, 2011; Hoch and Körner, 2012]. Thus, the generally simplistic and mostly static carbon allocation schemes of DGVMs [e.g., Shinozaki *et al.*, 1964; Huang *et al.*, 1992; Zeide, 1993] create high sensitivity of plant growth to photosynthesis, neglecting processes such as direct growth limitation by temperature [Oberhuber *et al.*, 2011; Hoch and Körner, 2012; Körner, 2012] or water [Würrth *et al.*, 1998; Muller *et al.*, 2011]. We acknowledge the fundamental role of photosynthesis in controlling short-term carbon fluxes and in this regard more accurate representations of canopy layers, leaf temperature, and light harvesting can be very important [e.g., De Pury and Faruhar, 1997; Dai *et al.*, 2004; Kobayashi *et al.*, 2012]. However, we underline that forest growth and development (and therefore long-term carbon fluxes) result from complex interactions and should not be dominated by the process of photosynthesis. For instance, the importance of plant structure and architecture in determining carbon assimilation has been recognized recently [Luyssaert *et al.*, 2008; Ishii and Asano, 2010; Hardiman *et al.*, 2011] and is confirmed by our GSA with fixed photosynthesis parameters. Overall, we suggest that these contradictions call for

a more mechanistic representation of carbon allocation and translocation [e.g., carbon sink rather than carbon source driven, *Leuzinger et al., 2013*] and it represents one of the key challenges for future model improvements [*Hurt et al., 1998; Daudet et al., 2002; Litton et al., 2007; Fisher et al., 2010; De Schepper and Steppe, 2011; Franklin et al., 2012; Mäkelä, 2012; Sala et al., 2012*].

2.4.2 Photosynthesis in the LPJ model family

LPJ-GUESS (as well as LPJ-DGVM), originates from the BIOME model family [*Prentice et al., 1992; Haxeltine and Prentice, 1996a; Haxeltine et al., 1996*]. In these models, the implemented photosynthesis scheme, for both C₃ and C₄ species, is based on a simplified mechanistic approach [*Farquhar et al., 1980; Collatz et al., 1991, 1992*], that allows for an analytical solution as demonstrated by *Haxeltine and Prentice [1996a, b]* and *Haxeltine et al. [1996]*. Net photosynthesis and stomatal conductance are calculated at a daily time scale using a non rectangular hyperbola formulation describing the transition between light-limited and Rubisco limited photosynthesis rates [*Haxeltine and Prentice, 1996b; Cannell and Thornley, 1998*]. However, the analytical expressions of daily photosynthesis emerge from the assumption that for any PAR level there is an optimal photosynthetic enzyme activity that maximizes net photosynthesis [*Haxeltine and Prentice, 1996a, b*]. Specifically, the canopy-average maximum Rubisco capacity (V_{\max}) of each simulated average individual, is not predefined, as it is required by the original Farquhar photosynthesis scheme and implemented in other models [e.g., *Knorr, 2000; Krinner et al., 2005; Bonan et al., 2011; Ivanov et al., 2008a; Fatichi et al., 2012a*], but it is adjusted daily in an optimal way, under the assumption that leaf nitrogen distribution through the canopy maximizes daily canopy net assimilation. This optimality constraint is likely responsible for the strong sensitivity of LPJ-GUESS to ALPHA_C3. In LPJ-GUESS, ALPHA_C3 represents more than intrinsic quantum efficiency and does not only affect the light-induced carbon fixation [Equation 2 and 4 in *Haxeltine and Prentice, 1996a*]. Therefore, variations in ALPHA_C3, indirectly affect the optimized value of V_{\max} [Equation 11 in *Haxeltine and Prentice, 1996a*], and this sequentially affects the Rubisco-limited assimilation [Equation 5 in *Haxeltine and Prentice, 1996a*]. In other words, the optimization procedure, applied for obtaining analytical solutions of daily photosynthesis, implies that the uncertainty originally attributed to the intrinsic quantum efficiency, also reflects the uncertainty propagated by the internal adjustment of V_{\max} . Therefore, the biochemical processes of photosynthesis and specifically the light use efficiency of plants (mediated by the intrinsic quantum efficiency parameter and entailing V_{\max} variation as well) is found to be the cornerstone of LPJ-GUESS framework.

Given the computational cost of concurrently solving processes involved in plant photosynthesis, namely water and energy exchanges, analytical solutions

of this highly non-linear system have been provided through optimization assumptions. Despite the appeal of finding analytical solutions of plant photosynthesis processes [Baldocchi, 1994; Lloyd *et al.*, 1995; De Pury and Faruham, 1997; Baldocchi and Amthor, 2001], this study suggests that optimality assumptions might be too simplistic leading to undesirable sensitivity confined to few parameters.

2.4.3 Sensitivity to soil moisture

According to our extensive analysis, both with (Section 2.3.2.1) and without (Section 2.3.2.2) photosynthesis-related parameters, the model has a very low sensitivity, in relation to the vegetation outcomes (e.g., biomass, NPP, LAI), to parameters controlling the terrestrial water balance (Figure 2.13). This contradicts empirical evidence that emphasizes the effect of water availability on primary production [e.g., Beer *et al.*, 2010; Reichstein *et al.*, 2007]. While it is true that Swiss climate is rather wet, the lack of sensitivity to values of SCC, which directly defines the available water to plants, is also evident in the dry alpine climate regime of Sion, where water controls have shown to be important [Zweifel *et al.*, 2007].

The lack of sensitivity to water is likely ascribed to both an inaccurate representation of water stress effects on vegetation functioning (photosynthesis, autotrophic respiration, carbon allocation) that are still not fully understood [Tezara *et al.*, 1999; Tuzet *et al.*, 2003; Zweifel *et al.*, 2006; Vico and Porporato, 2008; Lawlor and Tezara, 2009; Keenan *et al.*, 2010; McDowell, 2011; Tardieu *et al.*, 2011], and to the simplistic approach used by LPJ-GUESS and several other DGVMs in representing soil hydrology [Pitman, 2003; Jung *et al.*, 2007b]. Specifically, the “bucket model” assumption which is implemented in LPJ-GUESS (and in many other DGVMs) [Haxeltine and Prentice, 1996a; Neilson, 1995; Gerten *et al.*, 2004], might lead to unreliable model results, especially for the case of dry climates, reducing the importance of water limitations [Churkina *et al.*, 1999; Gordon *et al.*, 2004; Matthews *et al.*, 2007; Morales *et al.*, 2007; Jung *et al.*, 2007a; Dietze *et al.*, 2011; Wood *et al.*, 2011]. More detailed approaches for computing surface and soil water dynamics in an ecohydrological framework [e.g., Ivanov *et al.*, 2008a; Hwang *et al.*, 2009; Fatichi *et al.*, 2012a] or at the tree scale [e.g., Bohrer *et al.*, 2005; Janott *et al.*, 2010; Bittner *et al.*, 2012] might improve the simulation of carbon and water fluxes especially in arid and semiarid regimes [Hanan *et al.*, 1998; Law *et al.*, 2000; Baldocchi and Wilson, 2001; Ivanov *et al.*, 2008b; Quillet *et al.*, 2010; Fatichi *et al.*, 2012b]. In these ecosystems, DGVMs are prone to a poorer performance when compared to temperature-limited northern ecosystems [Smith *et al.*, 2001; Hickler *et al.*, 2004; Morales *et al.*, 2005, 2007; Jung *et al.*, 2007a; Keenan *et al.*, 2011b], illustrating that moisture availability is not a primary driver of their performance [Churkina *et al.*, 1999; Matthews *et al.*, 2007].

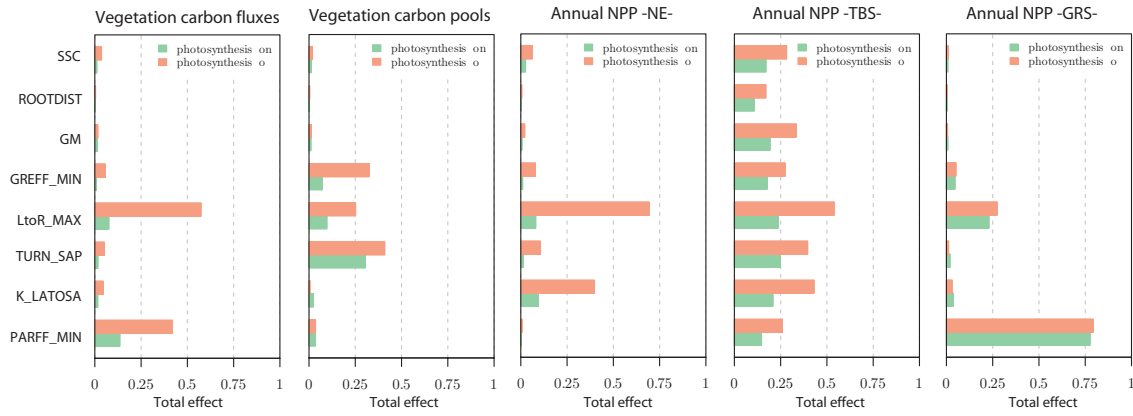


Figure 2.13: Total order sensitivity index of the subset of 8 examined parameters with the different GSA experiments, including (photosynthesis on) and excluding (photosynthesis off) parameters related to the Farquhar photosynthesis parameterization (ALPHA_C3, ALPHA_A and THETA). The median of Sobol' total order sensitivity indices over the 15 examined climatic forcings is plotted.

A more mechanistic representation of plant-water relationships should be thus embedded in the current model frameworks of DGVMs. This implies not only a better coupling of the intertwined dynamics of photosynthesis, stomatal regulation, and transpiration but also an explicit modeling of water controls on biochemical process, carbon transport, and plant growth as well as a better representation of the driving force, i.e., soil moisture temporal and spatial variability.

2.4.4 Sensitivity to stand composition

The role of stand composition in assessing model sensitivity was demonstrated to be of noticeable importance. The importance of certain parameters with regard to PFT-specific outputs is different when compared to the overall parameter sensitivity for the entire stand, highlighting that parameter importance can be strongly affected by the composition of the simulated stand [Wramneby et al., 2008]. Especially parameters controlling the capability of vegetation biomes to establish and grow become very critical when multiple PFTs compete for the same resources and might undergo stress. As the number of co-existing PFTs in a patch increases, the interactions among parameters also increases leading to a highly susceptible non-linear system where small variations in the model parameterization may cause considerable differences in the final vegetation composition.

The broad-leaved trees are found more sensitive to different parameterizations, in comparison to needle-leaved trees. This is probably attributed to a different phenology of deciduous PFTs and partially explain the fact that DGVMs are

able to simulate evergreen phenology (LAI cycle) and interannual productivity better than the phenology of deciduous trees which is characterized by a strong seasonal variability [Morales *et al.*, 2005; Kucharik *et al.*, 2006; Jung *et al.*, 2007a; Richardson *et al.*, 2011].

The increasing sensitivity to parameterization as a result of a more heterogeneous forest highlights another important challenge for DGVMs. Since the simulated species competition is strongly dependent on the choice of the parameters, the robustness of future projections of carbon fluxes might be questionable, especially for conditions different from the ones where parameter values are estimated.

2.5 CONCLUSIONS

Global Sensitivity Analysis is a very powerful tool for pinpointing principal mechanisms of model functioning and for highlighting critical aspects of model parameterization and structure. Using this framework, we could show that vegetation carbon fluxes and pools simulated by LPJ-GUESS are highly sensitive to parameters related to photosynthesis, especially to intrinsic quantum efficiency. At the same time, the sensitivity to parameters controlling water availability was found to be very low. Both of these results tend to be in contradiction with recent evidence showing that photosynthesis is not the primary driver of growth while plant-water relations are fundamental. We therefore argue that future amendments of DGVMs should concentrate on a more mechanistic representation of plant water relations and carbon trans- and allocation. This, together with an adequate parameterization of plant functional traits will allow for a better understanding of terrestrial carbon cycle.

ACKNOWLEDGMENTS

We would like to thank Veiko Lehsten, and the LPJ course team from the Department of Earth and Ecosystem Sciences at Lund University, for organizing the ClimBEco graduate research school: “Applications of LPJ-GUESS to research problems within Earth System Sciences”, where C.P. participated, for the fruitful discussions during the course, and for providing the source code of LPJ-GUESS. The authors would also like to thank the developers of the R programming environment [RCoreTeam, 2012], where all the statistical calculations were conducted, and of packages fOptions [Wuertz *et al.*, 2011], ggplot2 [Wickham, 2009], and sensitivity [Pujol *et al.*, 2012], for making them freely available. The meteorological data were kindly provided by the Swiss Federal Office of Meteorology and Climatology (MeteoSwiss, Switzerland). We are grateful to the Editor, Dennis D. Baldocchi and two anonymous reviewers for their constructive comments

that helped us to improve the presentation of the study. This study was funded by the Swiss National Science Foundation, in the frame of NRP 61 project HydroServ (C.P.: project no. 4061-125926) and partially by the European project ACQWA, Framework Programme 7, contract 212250.

THE ROLE OF LOCAL SCALE HETEROGENEITIES IN TERRESTRIAL ECOSYSTEM MODELING

ABSTRACT

The coarse-grained spatial representation of many terrestrial ecosystem models hampers the importance of local scale heterogeneities. To address this issue, we combine a range of observations (forest inventories, eddy flux tower data, remote sensing products) and modeling approaches with contrasting degrees of abstraction. The following models are selected: (i) LPJ, a well-established, area-based, Dynamic Global Vegetation Model (DGVM); (ii) LPJ-GUESS, a hybrid, individual-based approach that additionally considers plant population dynamics in greater detail; and (iii) D-LPJ, a spatially explicit version of LPJ, operating at a fine spatial resolution ($100 \text{ m} \times 100 \text{ m}$), which uses an enhanced hydrological representation accounting for lateral connectivity of surface and subsurface water fluxes. By comparing model simulations with a multivariate dataset available at the catchment scale, we argue that: (i) local environmental and topographic attributes that are often ignored or crudely represented in DGVM applications exert a strong control on terrestrial ecosystem response; (ii) the assumption of steady-state vegetation and soil carbon pools at the beginning of simulation studies (e.g., under “current conditions”), as embedded in many DGVM applications, is in contradiction with the current state of many forests that are often out of equilibrium; (iii) model evaluation against vegetation carbon fluxes does not imply an accurate simulation of vegetation carbon stocks. Having gained insights about the magnitude of aggregation-induced biases due to smoothing of spatial variability at the catchment scale, we discuss the implications of our findings with respect to the global scale modeling studies of carbon cycle and we illustrate alternative ways forward.

3.1 INTRODUCTION

The Earth’s carbon balance and its variability under changing climatic conditions and anthropogenic disturbances are topics of great societal and scientific importance [e.g., *Le Quéré et al., 2009, 2013; Regnier et al., 2013*]. Terrestrial

Pappas, C., S. Fatichi, S. Rimkus, P. Burlando, and M. Huber, The role of local scale heterogeneities in terrestrial ecosystem modeling, *Journal of Geophysical Research: Biogeosciences*, under review-a

ecosystems often undergo state transitions imposed by climate variability, anthropogenic interventions and/or natural disturbances [e.g., *Bonan, 2008b; Luo and Weng, 2011*]. However, understanding and modeling these trajectories still remain very challenging [*Levin et al., 1997; Hurtt et al., 1998; Schellnhuber, 1999; Landsberg, 2003; Moorcroft, 2006; Purves and Pacala, 2008b; Evans et al., 2012; Papas et al., 2013*]. A bulk of numerical representations, with different degrees of abstraction, has been developed to mimic complex terrestrial ecosystem processes across different scales [see *Martin, 1993; Perry and Enright, 2006; Jeltsch et al., 2008; Levis, 2010*, for extensive reviews]. Dynamic Global Vegetation Models [DGVMs; *Prentice et al., 2000; Quillet et al., 2010*] are among the most widely used tools, not only in global carbon cycle research, but also as integrated part in Earth System Models [e.g., *Cox et al., 2000; Prinn, 2012*].

The embedded physical mechanisms and causalities allow DGVMs to operate across a wide range of spatial scales, e.g., from the footprint of eddy flux towers, where their performance is often assessed, to global scale applications, where local parameterizations are extrapolated to larger domains. While the process-based framework of DGVMs makes them very appealing for analyzing future scenarios, any model-based inference is strongly conditioned on their underlying assumptions. Therefore, it is important to investigate whether the causal relations incorporated in these models mimic realistically the observed vegetation dynamics and whether the effects of a spatially heterogeneous vegetation are correctly reproduced. The importance of spatial heterogeneities has been recognized recently for ecosystem carbon budgets at the regional scale (*Zhao and Liu [2014]*, but see *Hall et al. [2015]*), and when terrestrial carbon, energy, and water fluxes are simulated with land surface models [e.g., *Li et al., 2013; Melton and Arora, 2014*], but has not yet been properly quantified for DGVMs.

In the present study, we combine a range of observations and modeling approaches for assessing the importance of spatial representation in forest-growth dynamics at the catchment scale. By analyzing the problem of terrestrial ecosystem modeling in a well-restricted domain, such as the catchment area, where multivariate datasets are available, rather than at the continental or global scale, where DGVMs often operate, a better assessment of the strengths and weaknesses of the models is expected. In addition, the regional and catchment scales represent scales at which management decisions are taken [e.g., *Korzukhin et al., 1996; Mäkelä et al., 2000*]. We focus on comparing different approaches for treating spatial vegetation heterogeneities. More specifically, three terrestrial ecosystem models with different degrees of abstraction and spatial representation of vegetation are applied: (i) LPJ [*Sitch et al., 2003*], a well established DGVM (section 3.2.1.1); (ii) LPJ-GUESS [*Smith et al., 2001*], a hybrid approach that incorporates a mechanistic description of population dynamics into DGVMs (section 3.2.1.1); and (iii) D-LPJ, that is presented for the first time in this study (section 3.2.1.2) and consists of a spatially explicit version of LPJ operating on a fine resolution grid, which is distributed in space and accounts for lateral water

fluxes among the simulated grid cells through an enhanced hydrological representation. The experimental setup is designed to preserve commonly applied practices in each modeling approach (section 3.2.5).

By comparing model simulations with multiple observed variables, the following questions are addressed: (i) which is the role of landscape heterogeneity (e.g., local climate, topography) in terrestrial ecosystem modeling? (ii) Does the simulated ecosystem response obtained averaging out subgrid heterogeneities, as is typically done in LPJ or LPJ-GUESS simulations (i.e., $f(\overline{\mathbf{X}})$, where f is a model, \mathbf{X} the ecosystem properties, and the overline denotes averaging operator), correspond to the mean simulated response of the system when spatial heterogeneities are explicitly taken into account, as done in D-LPJ simulations (i.e., $\overline{f(\mathbf{X})}$)? By answering these questions, we provide an explicit quantification of the potential biases in DGVMs applications, due to smoothing of local heterogeneities, induced by aggregation ($f(\overline{\mathbf{X}})$ versus $\overline{f(\mathbf{X})}$), as well as detailed explanations for their mismatch. In addition, building upon our findings at the catchment scale, we investigate implications for the modeling of global carbon cycle, where similar tools are often applied without scrutiny of underlying assumptions.

3.2 METHODOLOGY

3.2.1 Models

3.2.1.1 Ecosystem models: LPJ and LPJ-GUESS

LPJ (Lund-Potsdam-Jena) Dynamic Global Vegetation Model [Sitch *et al.*, 2003] and LPJ-GUESS (Lund-Potsdam-Jena General Ecosystem Simulator; Smith *et al.* [2001]) are established terrestrial ecosystem models. Many studies have been published showing their skills in predicting potential natural vegetation and primary production at global and regional scales [e.g., Badeck *et al.*; Hickler *et al.*, 2004; Koca *et al.*, 2006; Smith *et al.*, 2008; Ahlström *et al.*, 2012; Tang *et al.*, 2012; Piao *et al.*, 2013]. Both models are not spatially explicit but provide lumped, area-averaged representations (i.e., $f(\overline{\mathbf{X}})$, following the symbolism introduced in the previous section).

LPJ and LPJ-GUESS share the same process-oriented representation of plant physiology and ecosystem biogeochemistry, but have different approaches for simulating the distribution of vegetation. In LPJ vegetation within a grid cell is described in terms of fractional coverage of different Plant Functional Types (PFTs) and each simulated PFT reflects average properties of the entire population (e.g., tree height, vegetation carbon pools; population-based approach). In LPJ-GUESS forest dynamics and local scale vegetation heterogeneities are

approximated following a gap-model approach [Bugmann, 2001] accounting for ecosystem demography: forest structure is represented by averaging several spatially independent patches (100 patches in the current model configuration) of PFTs with different age classes (cohorts; individual-based approach) [Smith et al., 2001]. The use of several replicated patches accommodates for the variability induced by stochastic processes, such as plant establishment and mortality.

Photosynthesis, respiration, stomatal regulation, plant phenology and soil biogeochemistry are simulated at the daily scale while processes related to forest successional dynamics such as plant growth, establishment, and mortality are computed at the annual scale. Fire disturbances are disabled in the current study. Only a generic background mortality represented by stochastic disturbances (e.g., storms, diseases) is instead considered. Soil hydrological processes are modeled at the daily scale with a simple “bucket” hydrological model and do not consider lateral flows, as detailed in Gerten et al. [2004]. The meteorological forcings are daily values of precipitation, temperature, and radiation, and annual values of CO₂ concentration. Instead of the commonly used generic PFTs, a species-based parameterization of European biomes, proposed by Hickler et al. [2012], is adopted. To better capture Swiss vegetation functioning, some plant physiological parameters are also adjusted, such that data from Swiss eddy covariance flux measurements are better simulated (see Section 3.2.4.1 as well as the detailed discussion in Section B.3). Detailed model descriptions of LPJ and LPJ-GUESS are provided in Sitch et al. [2003] and Smith et al. [2001], respectively.

Since vegetation grows dynamically in both LPJ and LPJ-GUESS, each model simulation started with no vegetation (bare ground). An initialization period (equal to 500 years in our study) is used to spin-up the model and reach a state where carbon pools and vegetation cover are in equilibrium with the historical climatic conditions. The climate forcings used for spinning-up the model are constructed by repeating randomly years of the observed climate and using the preindustrial CO₂ levels. The use of a spin-up period to initialize vegetation and soil carbon pools represents a common and unavoidable step in DGVM applications [Pietsch and Hasenauer, 2006; Carvalhais et al., 2008; Williams et al., 2009].

3.2.1.2 Ecohydrological scheme: D-LPJ

D-LPJ (“D” stands for distributed in space) is a novel ecohydrological scheme built upon state-of-the-art ecological and hydrological tools. It combines the LPJ process-based vegetation model, which mimics short- and long-term vegetation dynamics, with the TOPKAPI-ETH hydrological model, which mechanistically simulates soil and surface water dynamics. The coupling strategy incorporated in the D-LPJ scheme is illustrated in Figure 3.1.

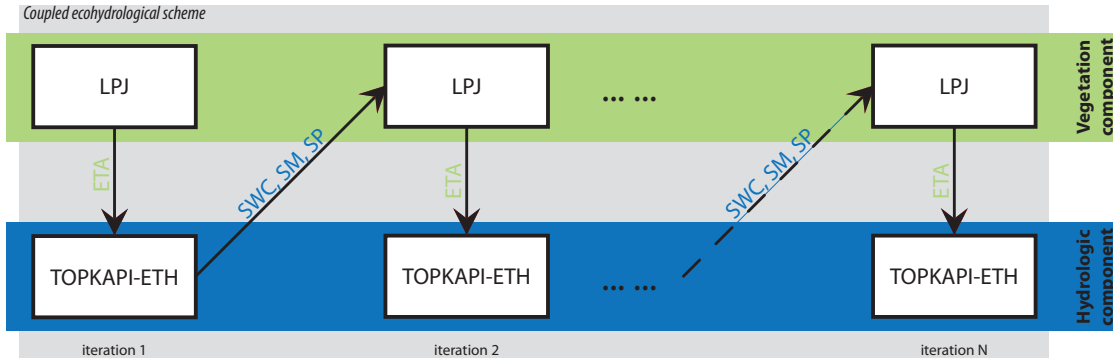


Figure 3.1: Representation of the D-LPJ ecohydrological scheme. D-LPJ is based on an iterative coupling of the LPJ ecosystem model with the TOPKAPI-ETH hydrological model. LPJ provides an estimate of evapotranspiration fluxes (ETA; soil evaporation, evaporation from interception, and plant transpiration) to TOPKAPI-ETH which then feeds back to LPJ an estimate of the soil water content (SWC), snow pack (SP), and snow melt (SM). Several iterations of the exchange variables (ETA and SWC, SP, SM) are performed until convergence of estimated fluxes over the simulated area is achieved.

TOPKAPI-ETH is a spatially explicit hydrological model that originates from the TOPKAPI (TOpographic Kinematic APproximation and Integration) rainfall-runoff model [Ciarapica and Todini, 2002; Liu and Todini, 2002]. The process-based framework of the model allows for a detailed spatial and temporal representation of the major hydrological processes at the catchment scale, accounting not only for runoff generation and routing but also for evapotranspiration, snow, and glacier dynamics [e.g., see Paschalis *et al.*, 2014, for a recent application of TOPKAPI-ETH on catchment flood response]. Spatial heterogeneity is represented by discretizing the domain as a fine-resolution regular grid, while the temporal dynamics of the hydrological processes are solved at an hourly time-step. The meteorological input variables are hourly values of precipitation and temperature and daily cloud cover transmissivity. The shortwave radiation fluxes are computed internally, accounting for topographic effects, based on clear-sky radiation [Bird and Hulstrom, 1981; Iqbal, 1983], skyview factor and terrain shading [Corripio, 2003], cloud cover transmissivity, and surface albedo. The spatially distributed nature of TOPKAPI-ETH facilitates a high-resolution representation of topography. Different computational elements are connected in the surface and in the subsurface according to topographic gradients. A kinematic wave approximation is applied to route water in the surface, sub-surface, and channels [Liu and Todini, 2005]. Three soil layers are used for mimicking the vertical soil-water dynamics; the first two (schematized as non-linear reservoirs) represent shallow and deep soil horizons, while the third layer (schematized as a linear reservoir) represents slow flow components, such as groundwater.

D-LPJ operates in a spatially explicit mode. Precipitation, temperature, and radiation fields are used to drive LPJ at a daily time step. The original hydrological

module of LPJ is used for estimating soil- and snow-water dynamics only during the spin-up period. Once the spin-up period is completed, distributed fields of soil water content, snow melt, and snowpack, computed with TOPKAPI-ETH, are provided as input to LPJ. When a simulation of LPJ is completed, distributed evapotranspiration fluxes (soil evaporation, plant transpiration, and evaporation from interception) are fed-back to TOPKAPI-ETH. Several iterations are conducted until a convergence of the exchange state variables is achieved (evapotranspiration fluxes and soil water content; Figure B.1). This information is exchanged at the end of the simulation period, i.e., 10 years in the present study. Contrary to the approach of using potential natural vegetation of LPJ and LPJ-GUESS, as well as of most DGVM applications, for obtaining the vegetation cover of the examined area, a land use map is imposed on D-LPJ in order to prescribe a realistic vegetation distribution over the simulated domain.

In summary, when compared to the original, area-averaged, lumped watershed representations of LPJ and LPJ-GUESS, D-LPJ includes (i) distributed vegetation cover based on the current land use map, (ii) spatially explicit topographic and meteorological attributes, defined on a fine resolution grid, (iii) refined soil-moisture dynamics computed with a spatially explicit hydrological module that solves the lateral connectivity of surface and subsurface water fluxes (see Table 3.1).

Table 3.1: Summary of the model configurations used for the numerical experiments. Model settings are assigned based on typical practices, i.e., coarse resolution for LPJ and LPJ-GUESS and a spatially explicit representation for D-LPJ.

| | Climate forcing | Topography | Initial conditions | | Soil hydrology | | Vegetation dynamics |
|-----------|--------------------|--------------------|------------------------------|--------------------|-----------------------|-------------------------|---------------------|
| | | | Land cover | Soil depth | Vertical fluxes | Horizontal fluxes | |
| LPJ | domain average | domain average | potential natural vegetation | uniform | "bucket" hydrology | no | population-based |
| LPJ-GUESS | domain average | domain average | potential natural vegetation | uniform | "bucket" hydrology | no | individual-based |
| D-LPJ | spatially explicit | spatially explicit | current land cover | spatially explicit | non-linear reservoirs | kinematic approximation | population-based |

3.2.2 Case study

The Kleine Emme basin is located in the central part of Switzerland, on the northern edge of the Alps (Figure 3.2). It covers about 477 km² with an average elevation of 1050 m a.s.l., ranging from 2329 m a.s.l. on the southern edge to

431 m a.s.l. at the catchment outlet (Littau; 47°4'0.1" N, 8°17'2.6" E). Most of the catchment area is covered by forest and grassland (Figure 3.4). The long-term (from January 2000 to December 2009) precipitation and air temperature averaged over the entire catchment are 1650 mm yr⁻¹ and 7.7 °C respectively (Figure 3.3). The river flow is unregulated with a mean discharge at the outlet of about 1023 mm yr⁻¹.

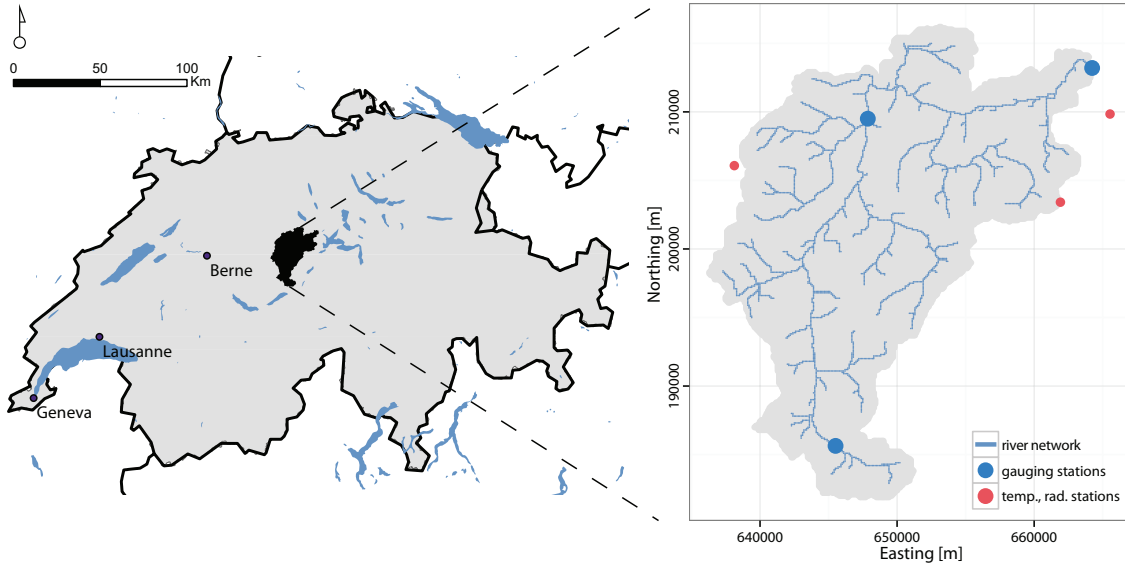


Figure 3.2: The Kleine Emme catchment is located in the central part of Switzerland. Three stream gauges operate in the main river network (blue circles) and three meteorological stations (red circles) with high quality temperature and radiation measurements are located close to the catchment boundaries.

3.2.3 Input data

3.2.3.1 LPJ and LPJ-GUESS input variables

Assigning mean meteorological and topographic properties over a large area is a common practice for simulations with LPJ and LPJ-GUESS since they are typically used for regional or global scale applications with relatively coarse spatial resolution. Accordingly, daily values of spatially averaged meteorological variables (precipitation, temperature, radiation) available in the Kleine Emme region, are used for the simulations with LPJ and LPJ-GUESS (see section 3.2.3.2 and Figure 3.3). Annual values of atmospheric CO₂ concentrations are derived from ice core reconstructions [Sitch *et al.*, 2003; Frank *et al.*, 2010] and the Mauna Loa record [Keeling *et al.*, 2009]. Mean soil properties are also prescribed following the FAO global soil map [FAO, 1991].

3.2.3.2 D-LPJ input variables

For the hydrological component of D-LPJ, meteorological forcings as well as topographic, land cover, and soil data should be provided for each computational element, since TOPKAPI-ETH is spatially explicit. In the present model setup a regular grid of $100 \text{ m} \times 100 \text{ m}$ resolution is used to account for spatial heterogeneity, resulting in a total of 47707 computational elements over the Kleine Emme catchment.

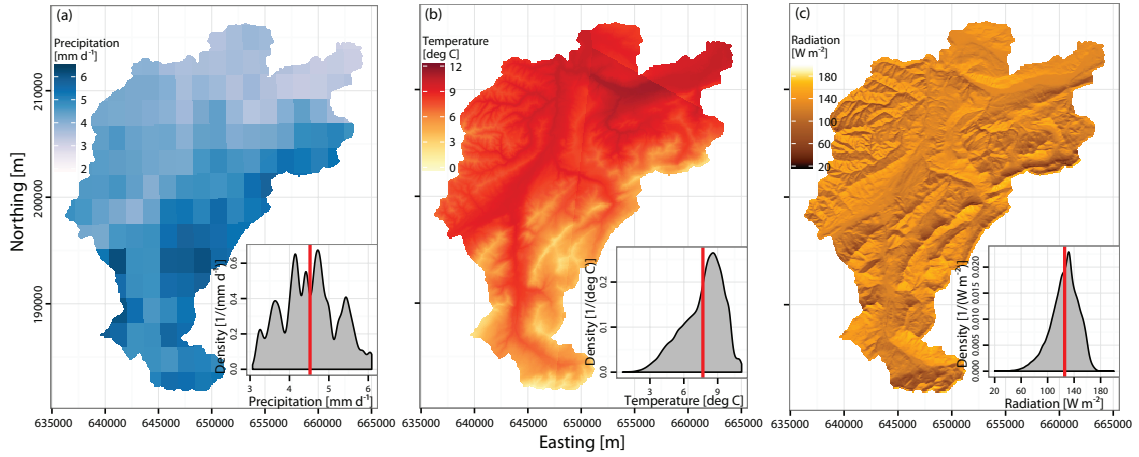


Figure 3.3: Spatial distribution ($100 \text{ m} \times 100 \text{ m}$ resolution) of mean daily (a) precipitation, (b) temperature, and (c) radiation, averaged over the examined period (January 2000 to December 2009) for the Kleine Emme catchment. Inner plots illustrate the areal probability density function with the areal mean denoted by a continuous red line. D-LPJ simulations are driven with spatially explicit meteorological forcings while area-averaged values are used for the simulations with LPJ and LPJ-GUESS.

Historical data are available from the Swiss meteorological service. Hourly precipitation and temperature gridded fields [Wüest *et al.*, 2010], with $100 \text{ m} \times 100 \text{ m}$ resolution, for the period January 2000 through December 2009, are used (Figure 3.3). Daily values of cloud transmissivity, uniformly distributed over the catchment, are estimated with a weather generator [Fatichi *et al.*, 2011], comparing simulated clear sky shortwave radiation with ground measurements from three radiometers in the catchment area (Figure 3.2). A detailed description of the meteorological products is provided in Section B.2.

Topographic data are obtained by resampling a fine resolution ($25 \text{ m} \times 25 \text{ m}$) digital terrain model of Switzerland to $100 \text{ m} \times 100 \text{ m}$ resolution (Figure 3.4a). The Global Land Cover Product [GlobCover; Bontemps *et al.*, 2009] and the Swiss soil map [GEOSTAT, 2000] are used to assign spatially distributed land cover and soil properties (Figure 3.4).

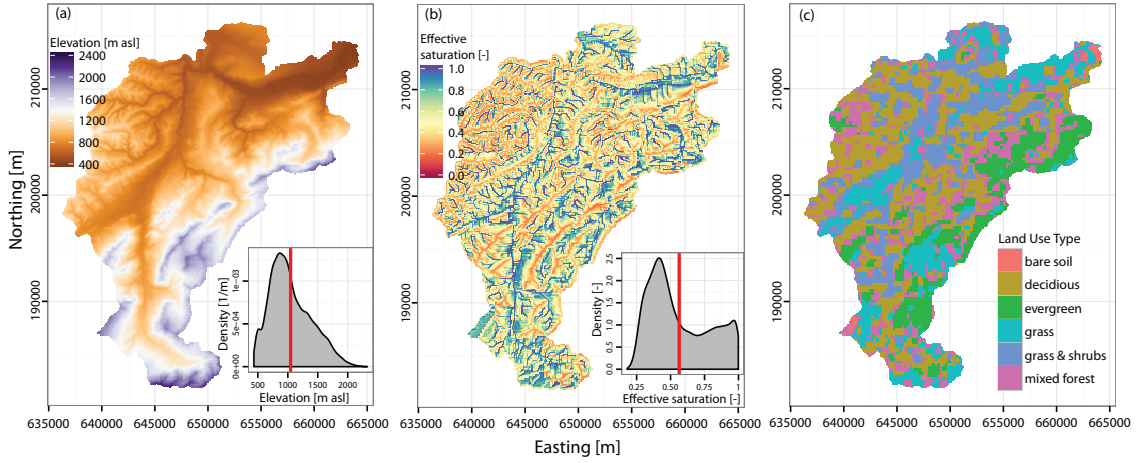


Figure 3.4: Landscape-level information, in a $100 \text{ m} \times 100 \text{ m}$ regular grid, used for the D-LPJ simulations over the Kleine Emme area: (a) digital elevation model, (b) effective saturation, averaged over the period January 2000 to December 2009, for the first soil layer, and (c) land cover map imposed on the D-LPJ simulations. Inner plots illustrate the areal probability density function with the areal mean denoted by a continuous red line.

The vegetation component of D-LPJ also operates in a spatially explicit mode with a $100 \text{ m} \times 100 \text{ m}$ resolution regular grid but with a daily temporal resolution. Hourly precipitation and temperature fields are thus aggregated to daily scale and used for the D-LPJ simulations together with the radiation fields calculated by TOPKAPI-ETH (Figure 3.3). Annual values of atmospheric CO_2 concentrations, the same as for LPJ and LPJ-GUESS, are assumed to be uniformly distributed over the catchment area. In addition, spatially distributed fields of soil water content, snow melt, and snowpack, computed using TOPKAPI-ETH, are used as inputs to D-LPJ after the spin-up period (Figure 3.4b).

A land use map, based on GlobCover, is imposed to constrain the occurrence of different vegetation types (Figure 3.4c). More specifically, generic land use classes (e.g., deciduous, evergreen, mixed forest) are used to restrict the species distribution over the catchment. Evergreen species, for example, can only occur in computational elements where land use map indicates evergreen or mixed forest. This allows us to preserve the observed land use and to obtain a better spatial representation of the current vegetation cover.

3.2.4 Confirmation datasets

3.2.4.1 Eddy covariance flux measurements

Eddy covariance (EC) flux measurements available from the Swiss FLUXNET (<http://www.swissfluxnet.ch>), which is part of the international research net-

work FLUXNET [Baldocchi *et al.*, 2001; Baldocchi, 2003], are incorporated in the analysis to refine the parameterization of carbon assimilation for vegetation in Switzerland. More specifically, we compare model simulations of LPJ with observations of carbon fluxes at five EC towers. Plant physiological parameters are adjusted to improve the representation of vegetation functioning in the Swiss environment (see Section B.3). We use measurements from two forested areas: a deciduous forest (mostly dominated by European beech, *Fagus sylvatica*) in the Laegeren mountain (tower coordinates: 47°28'42.0" N and 8°21'51.8" E at 682 m a.s.l.; examined period: 2004-2009) and a subalpine coniferous forest in Davos (mostly covered by Norway spruce, *Picea abies*) in the Eastern Swiss Alps (tower coordinates: 46°48'55.2" N and 9°51'21.3" E at 1639 m a.s.l.; examined period: 2000-2005). In addition, EC data from three grassland sites are included in the analysis: Chamau (tower coordinates: 47°12'36.8" N and 8°24'37.6" E at 393 m a.s.l.; examined period: 2006-2008), Fruebuel (tower coordinates: 47°6'57.0" N and 8°32'16.0" E at 982 m a.s.l.; examined period: 2006-2008), and Oensingen (tower coordinates: 47°16'59.9" N, 7°43'59.9" E at 451 m a.s.l.; examined period: 2002-2003). A more detailed description of the use of EC flux measurements is provided in Section B.3.

3.2.4.2 MODIS products

Spatial and temporal dynamics of two variables (Gross Primary Production, GPP, and Leaf Area Index, LAI) from the MODerate resolution Imaging Spectroradiometer, [MODIS; Huete *et al.*, 2002] are also used for a qualitative assessment of the models. The spatial resolution of these vegetation indices is $1 \times 1 \text{ km}^2$ while the temporal resolution is eight days. The mismatch in the spatial resolution between MODIS and D-LPJ ($100 \text{ m} \times 100 \text{ m}$), as well as the uncertainties related to these products [e.g., Tian *et al.*, 2002; Kang *et al.*, 2005; Heinsch *et al.*, 2006; Pan *et al.*, 2006; Zhao *et al.*, 2006; Fang *et al.*, 2012, 2013] hamper a quantitative evaluation of simulated vegetation metrics over the Kleine Emme area. Only a qualitative comparison of the spatial distributions and seasonality of GPP and LAI is therefore attempted, aiming at the visual comparison of long-term spatial patterns in the catchment and of the area-averaged seasonal dynamics. The implemented pre-processing procedure (e.g., quality control, temporal smoothing and interpolation) of the raw MODIS data for the examined simulation period is detailed in Section B.4.

3.2.4.3 Forest inventory data

The Swiss National Forest Inventory (NFI; <http://www.lfi.ch>) is a joint project of the Federal Office for the Environment and the Swiss Federal Institute for Forest, Snow and Landscape Research. It records different vegetation variables related to the area, structure and status of forests in Switzerland. The NFI

database consists so far of three surveys: the first was conducted over the period from 1983 to 1985, the second one from 1993 to 1995, and the third one from 2004 to 2006. Inventory plots influenced by anthropogenic disturbances (e.g., plant cuttings, replanting) are excluded from our analysis. More details on the NFI are reported in Section B.5. Here, we focus on the rate of long-term changes in vegetation carbon stocks, $\Delta C_{\text{veg}}/\Delta t$, where C_{veg} is the total vegetation carbon (i.e., carbon in the foliage, wood, and roots) and Δt refers to the examined time period. Simulated values of $\Delta C_{\text{veg}}/\Delta t$ can be compared with the inventory-based estimates since forest plots with anthropogenic disturbances are excluded from our analysis. Changes in vegetation carbon stocks can be mainly attributed to the balance between vegetation growth and natural disturbances, assuming other components affecting the vegetation carbon balance (e.g., natural herbivory, emission of volatile organic compounds) to be of minor importance for the purpose of our study [Luyssaert et al., 2010].

3.2.4.4 River discharge

We complement the validation datasets with measurements of river discharge distributed in the main river corridor (Figure 3.2). Hourly data from January 2000 through December 2009 at the catchment outlet at Littau (station coordinates: 47°4'0.1" N, 8°17'2.6" E; elevation: 431 m a.s.l.) and at Werthenstein (station coordinates: 47°2'5.6" N, 8°4'6.4" E; elevation: 595 m a.s.l.; draining area: 311 km²) are provided by the Swiss Federal Office for the Environment. A cantonal station at Soerenberg (LU14; station coordinates: 46°49'13.3" N, 8°2'6.0" E; elevation: 1150 m a.s.l.; draining area: 23 km²) covering a period of January 2005 to December 2009 is also included in the analysis even though the station-data is likely characterized by a lower quality (Figure 3.2). River discharge can be considered as an aggregated ecosystem property, encompassing both biotic (e.g., plant transpiration) and abiotic (e.g., evaporation, river routing) processes. Therefore, realistic simulation of streamflow reinforces our confidence about model consistency in reproducing the principal physical mechanisms determining the hydrological response of the catchment.

3.2.5 Experimental design

The experimental approach is designed to respect the configurations that are commonly applied in each of the models we used. More specifically, the three examined models, namely LPJ, LPJ-GUESS, and D-LPJ, are configured using either domain average or spatially-explicit local-scale information ($f(\bar{X})$ and $f(X)$; Table 3.1). While, theoretically, both LPJ and LPJ-GUESS could have been used with a fine resolution configuration, e.g., by prescribing the current vegetation cover and using fine resolution climatic forcings, this would have been at odds with common applications carried out with these types of models. Furthermore,

simplifications in process representation that can be acceptable at coarse spatial or temporal scales, are not valid at finer resolutions. For instance, the “bucket-type” hydrological representation, which ignores lateral water fluxes can be a fair approximation at coarse spatial scales but typically fails at finer scales where lateral exchanges may be important (*Li et al.* [2013]; *Tang et al.* [2014a]; see also detailed discussion in Section 3.4.4). Therefore, in order to preserve the assumptions applicable at the different scales, we use LPJ and LPJ-GUESS with coarse scale boundary conditions and forcings, and D-LPJ with heterogeneous forcings at $100 \text{ m} \times 100 \text{ m}$ resolution (Table 3.1). With this configuration, we investigate aggregation-induced biases ($f(\overline{\mathbf{X}})$ versus $\overline{f(\mathbf{X})}$) comparing the three contrasting approaches for modeling vegetation dynamics. However, for the sake of completeness, the results of a full factorial experimental design (e.g., simulations of LPJ with fine resolution inputs and current land use information, as done for D-LPJ simulations) are included in Sections B.8 and B.9. In essence, as illustrated in Figure B.1, the preliminary D-LPJ simulation (i.e., “iteration-0”; Figure B.1) corresponds to a LPJ simulation which is forced with fine resolution inputs but lacks the mechanistic hydrological representation of TOPKAPI-ETH (Figure 3.1).

3.3 RESULTS

3.3.1 Regionalizing the parameterization of vegetation

The parameterization proposed by *Hickler et al.* [2012] is used for a first comparison of vegetation carbon fluxes. However, a considerable mismatch is found between EC-based GPP and the simulated values (Figure B.2). In this regard, the case of the evergreen forest in Davos is striking; the site is dominated by Norway spruce (*Picea abies*) with an observed mean annual GPP of about $1100 \text{ gC m}^{-2} \text{ yr}^{-1}$ [*Etzold et al.*, 2011], while the simulated GPP with LPJ, using the original parameterization of *Picea abies*, is about $2000 \text{ gC m}^{-2} \text{ yr}^{-1}$ for the period 2000 to 2005 (Figure B.2). This mismatch is not entirely surprising since the parameterization of LPJ, as well as that of LPJ-GUESS, is made envisioning global or continental scale applications [see *Hickler et al.*, 2012, for the European continent]. It is therefore expected that average parameter values, developed for example to describe vegetation properties in a $1^\circ \times 1^\circ$ grid, will not be representative of the fine scale heterogeneities encapsulated in the footprint of eddy-flux towers [e.g., *Pappas et al.*, 2013; *Rogers*, 2014]. Manual adjustments of some plant physiological properties are therefore applied to LPJ, LPJ-GUESS, and D-LPJ simulations, providing a more accurate representation of vegetation carbon fluxes for the Swiss environment (Figure B.3). Section B.3 provides a detailed description of the adjusted parameters and the rationale behind the modifications. After these modifications, the skill of the model in reproducing carbon fluxes for the Swiss

FLUXNET sites is significantly improved, enabling the model to achieve a coefficient of determination between daily simulated and observed GPP equal to 0.62, 0.71, 0.69, 0.69, 0.53, respectively in Chamau, Davos, Fruebuel, Laengern, and Oensingen (see also Figure B.3).

3.3.2 *Confirming the hydrological consistency*

Satisfactory results of river discharge are obtained with D-LPJ without significant calibration efforts. This model captures fairly well both the short-term and the seasonal dynamics of river flow in all the examined locations (Figure B.4). The long-term water budget of the catchment is also realistically simulated, although evapotranspiration is slightly underestimated. For the period 2000-2009, out of the 1650 mm yr⁻¹ of precipitated water, 1170 mm yr⁻¹ are simulated as discharge at the outlet and around 480 mm yr⁻¹ as evapotranspiration, while the observed discharge at the outlet is 1023 mm yr⁻¹.

3.3.3 *Bird's-eye view on vegetation indices*

3.3.3.1 *Vegetation cover*

The two implemented approaches for initialization of vegetation cover i.e., potential natural vegetation for LPJ and LPJ-GUESS, as opposed to a constrained vegetation distribution based on current land cover for D-LPJ, lead to distinct results (Figure 3.5). The potential natural vegetation, obtained after the end of the spin-up period, varies significantly from the actual vegetation distribution in the area. In D-LPJ simulations, both evergreen and deciduous species have an important role in the overall vegetation carbon dynamics, reflecting the information of the current land use map in the area (Figure 3.5b). Since land cover information is not imposed in LPJ and LPJ-GUESS simulations, a considerable discrepancy occurs between the actual vegetation cover and the simulated potential natural vegetation over the Kleine Emme catchment (Figure 3.4c and 3.5d,e, respectively). Both LPJ and LPJ-GUESS overestimate the proportional abundance of deciduous forest (Figure 3.5d,e). In addition, significant differences also occur when vegetation carbon stocks and their long-term dynamics are compared (Figure 3.5c,d,e).

3.3.3.2 *Spatial dynamics of GPP and LAI*

For both GPP and LAI, the spatially explicit nature of D-LPJ, accounting for current land cover as well as local topography and climatic conditions, allows for a reasonable representation of spatial heterogeneities (Figure 3.6a,b for GPP; and

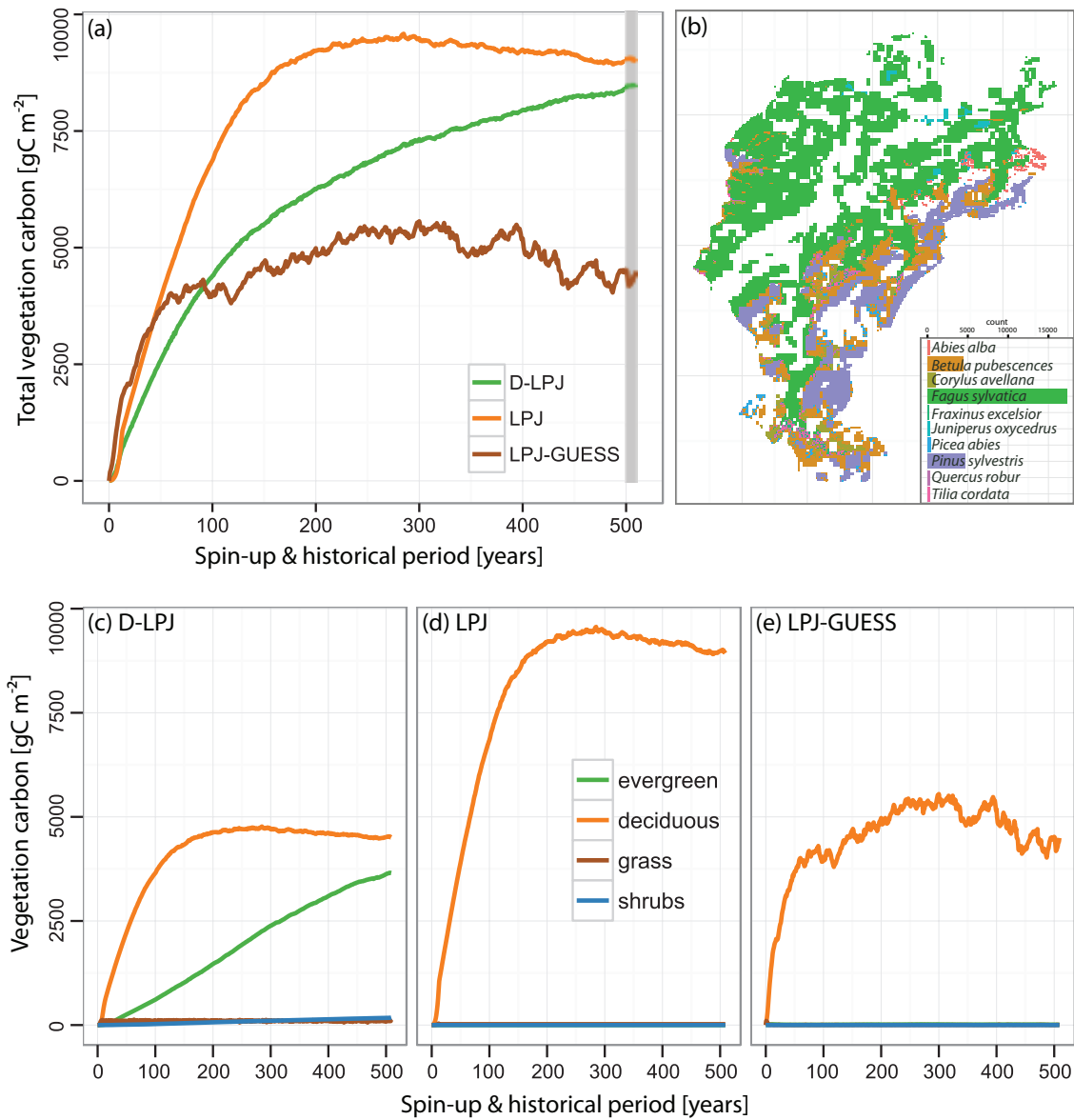


Figure 3.5: (a) Total vegetation carbon as simulated with D-LPJ, LPJ, and LPJ-GUESS for the spin-up (500 years) and the historical period (10 years; shaded area). (b) Distribution of vegetation types over the catchment area, at the end of the simulation period, as estimated by D-LPJ (based on the current land cover map; Figure 3.4c). Long-term vegetation-carbon dynamics over the Kleine Emme catchment, as obtained through the spin up period, for simulations with (c) D-LPJ, (d) LPJ, and (e) LPJ-GUESS. Different plant types are grouped in major plant life forms, i.e., evergreen, deciduous, grass, and shrubs.

Figure 3.7a,b for LAI). Since LPJ and LPJ-GUESS are not spatially explicit, estimates of mean GPP and LAI over the examined area, computed using mean climate conditions, $f(\bar{X})$, are compared with the area-averaged D-LPJ and MODIS estimates, $\bar{f(X)}$ (Figure 3.6c,d for GPP; and Figure 3.7c,d for LAI).

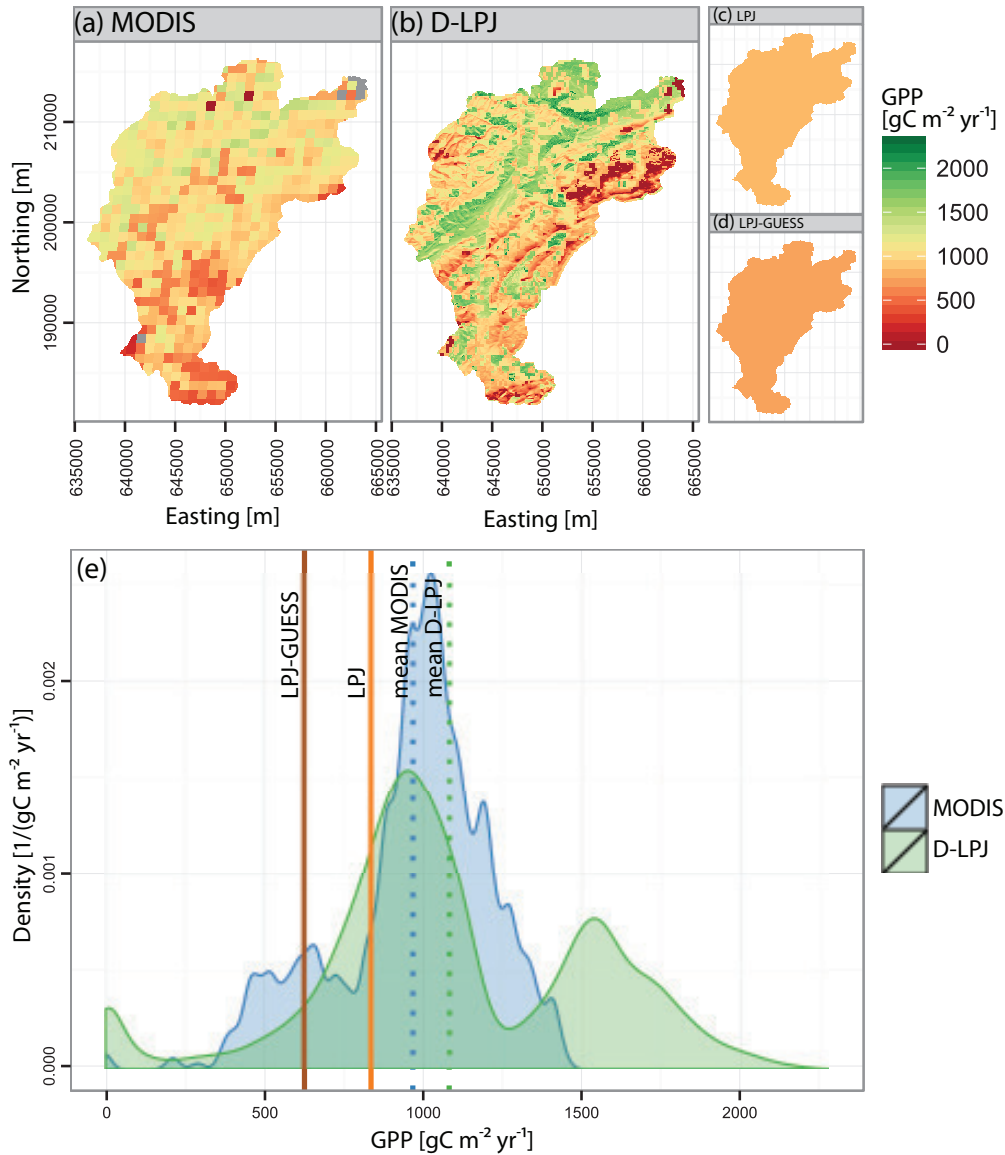


Figure 3.6: Spatial patterns of mean Gross Primary Production (GPP) for the period 2000 through 2009, over the Kleine Emme catchment, as estimated by: (a) MODIS, (b) D-LPJ, (c) LPJ, and (d) LPJ-GUESS as well as (e) a comparison of the spatial distribution among the four different estimates. The mean of the distributions are denoted by dashed lines. Note that since LPJ and LPJ-GUESS are not spatially explicit, a single value, representative for the entire catchment, is provided.

Visual similarities exist between GPP estimated by MODIS and D-LPJ values (Figure 3.6a,b). The mean aggregated response over the catchment is comparable: about $970 \text{ gC m}^{-2} \text{ yr}^{-1}$ for MODIS, and about $1080 \text{ gC m}^{-2} \text{ yr}^{-1}$ for D-LPJ. However, MODIS fails, due to algorithmic limitations, to capture the high productivity of the grasslands located in the lowland valleys, while D-LPJ simulation provides a second peak in the GPP distribution, at around $1500 \text{ gC m}^{-2} \text{ yr}^{-1}$, highlighting such contribution to the overall GPP of the area (Figure 3.6e).

The D-LPJ results cannot be considered an artefact of the model simulations since the high productivity of grasslands in Switzerland is confirmed by the Swiss FLUXNET sites (see Section 3.3.1). Conversely, uncertainties in MODIS product, related to the transfer of the absorbed radiation into carbon assimilation for grassland as well as frequent periods with cloud- or snow-cover in the catchment, may cause these discrepancies [e.g., *Kang et al., 2005*; *Heinsch et al., 2006*; *Zhao et al., 2006*].

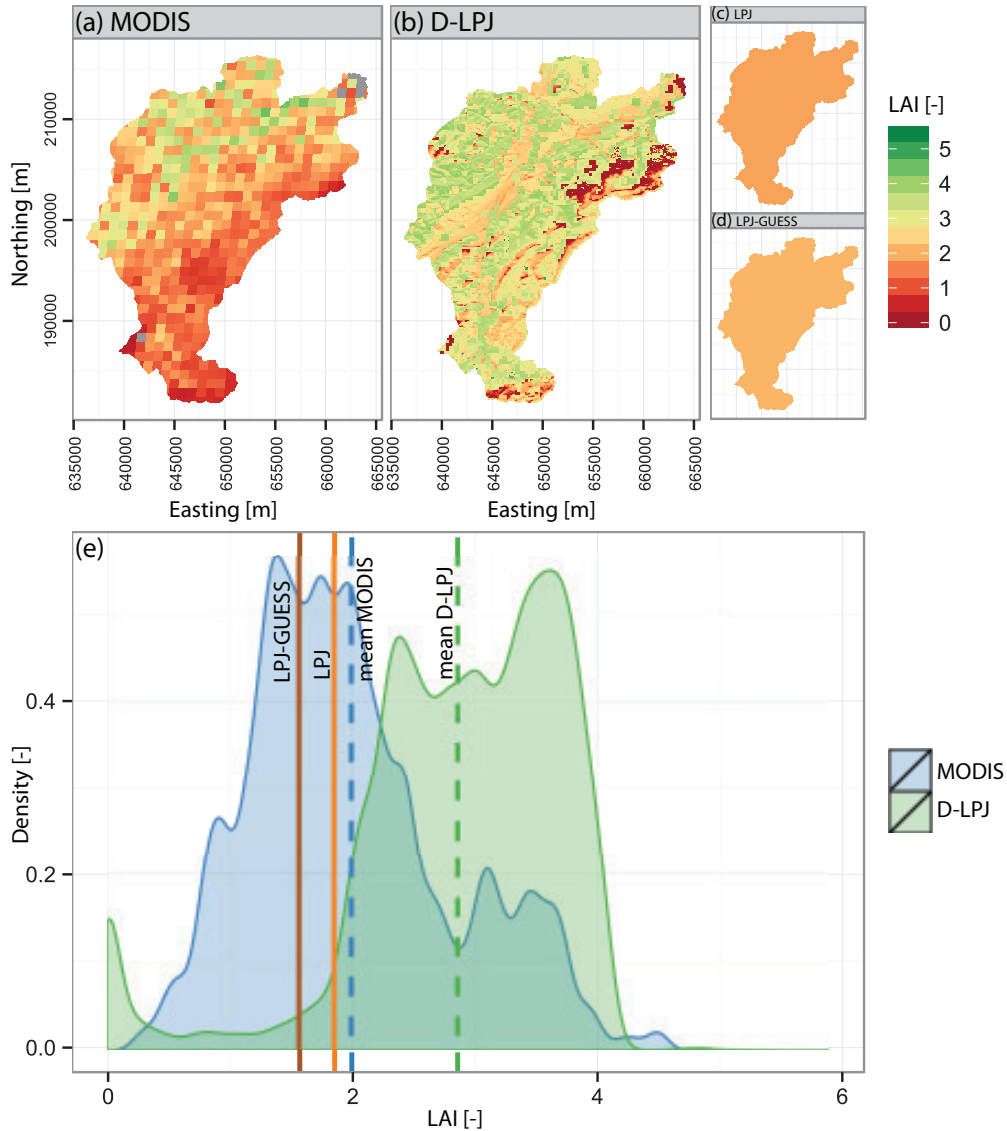


Figure 3.7: Spatial patterns of mean Leaf Area Index (LAI) for the period 2000 through 2009, over the Kleine Emme catchment, as estimated by: (a) MODIS, (b) D-LPJ, (c) LPJ, and (d) LPJ-GUESS as well as (e) a comparison of the spatial distribution among the four different estimates. The mean of the distributions are denoted by dashed lines. Note that since LPJ and LPJ-GUESS are not spatially explicit, a single value, representative for the entire catchment, is provided.

The LPJ and LPJ-GUESS estimates of GPP are significantly different from those retrieved by MODIS and simulated by D-LPJ, i.e., $f(\bar{X}) \neq \overline{f(X)}$. LPJ-GUESS gives a value of GPP of about $650 \text{ gC m}^{-2} \text{ yr}^{-1}$ (averaged over the simulated period) while the LPJ value is slightly higher (about $835 \text{ gC m}^{-2} \text{ yr}^{-1}$) but still considerably below the D-LPJ or MODIS values. This can be attributed to differences in vegetation composition as well as in local meteorological/hydrological conditions underlying D-LPJ, LPJ, and LPJ-GUESS simulations. In both LPJ and LPJ-GUESS simulations, deciduous forest is the dominant vegetation type over the area, while in D-LPJ simulations the current vegetation cover is preserved (Figure 3.5).

The coarse resolution of the MODIS product cannot capture some of the heterogeneities in the LAI patterns as simulated by D-LPJ (Figure 3.7a,b). The importance of local climate (particularly the spatial patterns of radiation and temperature, Figures 3.3b,c) in shaping the LAI dynamics is reflected in the D-LPJ simulations (Figure 3.7b). The annual mean LAI estimated by MODIS (Figure 3.7a; $\text{LAI} \approx 2.0$), is lower than the mean of D-LPJ estimate (Figure 3.7b; $\text{LAI} \approx 2.9$). This is more likely to reflect a poor reliability of MODIS estimates rather than the real LAI magnitude in the catchment [Tian *et al.*, 2002; Yang *et al.*, 2006; Fang *et al.*, 2012, 2013]. The simulated values of LPJ (Figure 3.7c; $\text{LAI} \approx 1.8$) and LPJ-GUESS (Figure 3.7d; $\text{LAI} \approx 1.6$) are low due to the predominance of deciduous forest (Figure 3.5).

3.3.3.3 Temporal dynamics of GPP and LAI

The seasonal dynamics of GPP simulated with D-LPJ are in good agreement with vegetation activity estimated with MODIS (Figure 3.8a). MODIS products capture greening phase dynamics with less uncertainty than its magnitude [e.g., Heinsch *et al.*, 2006]. However, some source of error can still be present, for instance, related to data processing algorithms and missing values. For instance, while the length of the growing season is fairly comparable between MODIS and D-LPJ estimates, a mismatch in the intra-season variability of LAI occurs (Figure 3.8b). The seasonal patterns of GPP and LAI as simulated by LPJ and LPJ-GUESS are also similar to the D-LPJ results, since the underlying phenology modules are identical in all three models and the effect of local climatic differences is smoothed out by averaging them over the entire domain (Figure B.5).

3.3.4 Ant's-eye view on carbon stocks

Vegetation carbon dynamics, expressed as the rate of long-term changes in vegetation carbon stocks, denoted as $\Delta C_{\text{veg}}/\Delta t$, for the last 10 years of simulations with D-LPJ, LPJ, and LPJ-GUESS (i.e., 2000 to 2009), are significantly different

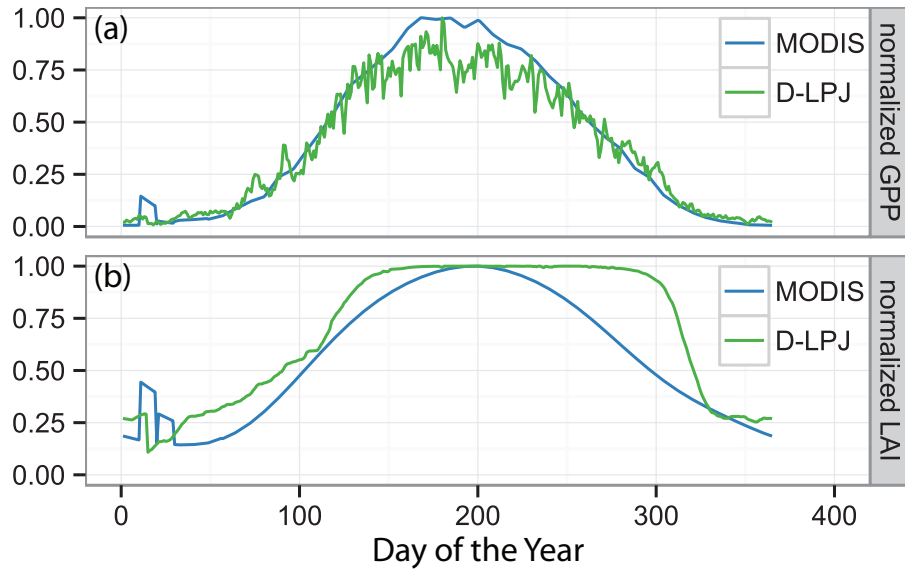


Figure 3.8: Seasonal dynamics of normalized Gross Primary Production (GPP) and normalized Leaf Area Index (LAI), averaged over the Kleine Emme catchment, for the period 2000 to 2009, based on MODIS and D-LPJ.

when compared to estimates from the in situ forest inventory observations (Figure 3.9). In the spatial domain of the catchment, $\Delta C_{veg}/\Delta t$ values estimated by D-LPJ are close to zero for most of the grid cells except for few sites on the South-West part of the region where evergreen and mixed forest occur. Even for these cells, the values of $\Delta C_{veg}/\Delta t$ simulated by D-LPJ are much lower than the range of variability of the forest inventories sites, which exhibit values of the first and third quantile around 100 and 400 $\text{gC m}^{-2} \text{yr}^{-1}$, respectively (Figure 3.9b). This does not come as a surprise, since it is the result of imposing in the simulations carried out with D-LPJ, LPJ, and LPJ-GUESS a spin-up period, as it is generally done in all DGVMs. The spin-up is designed to provide a state of vegetation in equilibrium with the prevailing environmental conditions. Therefore, in absence of significant climatic changes, the simulated changes in vegetation carbon stocks with D-LPJ, LPJ, and LPJ-GUESS, are intrinsically low (practically close to zero, as shown by Figure 3.9b). Conversely, the observations obtained from the forest inventories give a mean rate of increase in vegetation carbon stocks of about 210 $\text{gC m}^{-2} \text{yr}^{-1}$ in the examined forests (Figure 3.9b), because they represent measurements of actual and likely non-stationary conditions, which are influenced for example by environmental controls and natural disturbances. Discrepancies occur also when $\Delta C_{veg}/\Delta t$ values at the beginning of the spin-up period are compared with the inventory-based estimates. The slope of the vegetation carbon pools for the first 100 years of the spin-up, computed as the derivatives of the vegetation carbon stock accumulation over 10-year time-windows (Figure 3.5a), varies in the range of 35-120, 15-135, 25-65 $\text{gC m}^{-2} \text{yr}^{-1}$ for LPJ, LPJ-GUESS, and D-LPJ, respectively, contrasting with the

mean estimated changes in vegetation carbon stocks from the forest inventories which is considerably higher ($210 \text{ gC m}^{-2} \text{ yr}^{-1}$; Figure 3.9b).

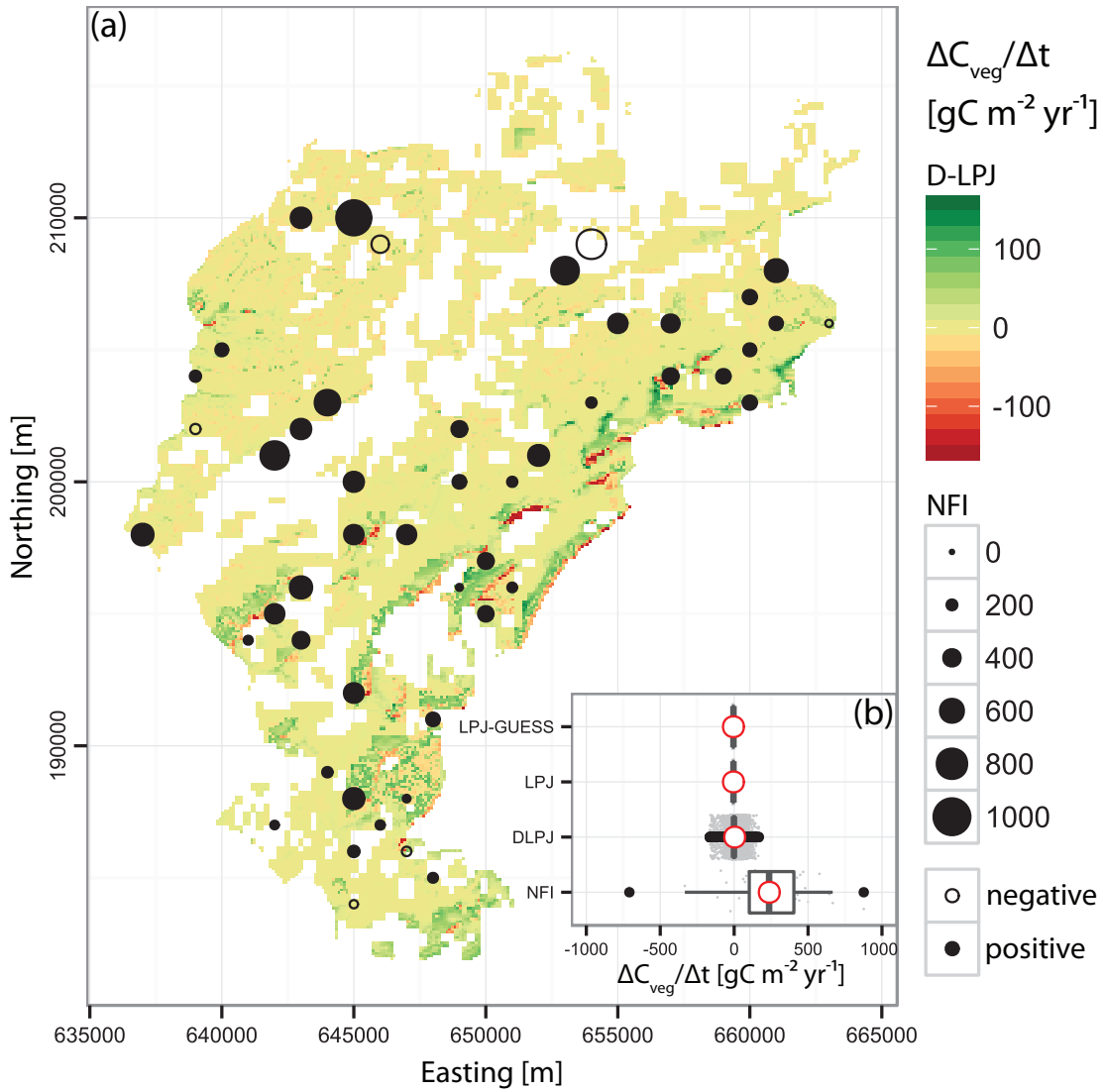


Figure 3.9: (a) Spatial patterns of the rate of long-term changes in vegetation carbon stocks (denoted as $\Delta C_{veg}/\Delta t$) of forested areas in Kleine Emme as estimated by D-LPJ, and by the National Forest Inventories (NFI; black dots; filled symbols are used for increase while open circles are used for decrease in total vegetation carbon). (b) Box-plot of $\Delta C_{veg}/\Delta t$ values over the Kleine Emme region, based on LPJ-GUESS, LPJ, D-LPJ, and NFI. Grey dots correspond to $\Delta C_{veg}/\Delta t$ values either in each simulated grid-cell (case of D-LPJ), or in each of the forest inventory plots (case of NFI). The areal mean is indicated with red circles.

3.4 DISCUSSION

The results presented in the previous sections provide a comprehensive evaluation of several approaches for modeling terrestrial ecosystems, scrutinizing modeling assumptions and spatial aggregation rules. We explicitly quantified how the coarse spatial representations of DGVMs lead to aggregation-induced biases for the orographically complex landscape of the Kleine Emme catchment. Hereafter, we discuss the insights gained at the catchment scale which have possible implications for applying such modeling approaches at the regional and global scales.

3.4.1 *Aggregating landscape heterogeneity: DGVMs, gap-models, and ecohydrological schemes*

Since LPJ, LPJ-GUESS and D-LPJ apply an identical formulation to mimic biophysical and biochemical processes, discrepancies among the simulated vegetation dynamics can be attributed to the following three main reasons, further discussed in the following sections: (i) initialization with different vegetation cover, i.e., potential natural vegetation (LPJ and LPJ-GUESS) versus constrained vegetation distribution derived from current land cover information (D-LPJ); (ii) effects of local topography, climate, and hydrological representation, i.e., mean field approach of LPJ and LPJ-GUESS versus ecohydrological approach of D-LPJ; (iii) different approaches for simulating vegetation structure and dynamics, i.e., population-based (LPJ, D-LPJ) versus individual-based approach (LPJ-GUESS). Moreover, in order to quantify the relative importance of land cover initialization versus that of local climate, topography, and hydrology, the following additional simulation are included in the Appendix: (i) LPJ simulations with mean climatic conditions over the area, but with prescribed land cover instead of the potential natural vegetation hypothesis (Section B.8), and (ii) LPJ simulations with high resolution inputs (meteorological forcings and land cover information; same as D-LPJ approach) but without the enhanced hydrological representation of TOPKAPI-ETH (Section B.9).

3.4.1.1 *The importance of actual rather than potential vegetation cover*

In agreement with other model- and data-based studies, the role of land use history cannot be easily neglected when fragmented landscapes, such as the Kleine Emme catchment, are simulated [Harmon, 2001; Barnes and Roderick, 2004; Hurtt *et al.*, 2004; Gimmi *et al.*, 2008, 2012; Williams *et al.*, 2009]. Even though vegetation cover is initialized in the three approaches (LPJ, LPJ-GUESS, and D-LPJ), since the successional dynamics of vegetation are simulated starting from an unvegetated state, the imposition of a land use map allows for a better representation

of the current state of the system. This was reflected in the D-LPJ results in terms of species distribution (Figure 3.5b), GPP (Figure 3.6a) and LAI (Figure 3.7a) dynamics. In addition, by comparing simulation results of LPJ using the current land cover map with the D-LPJ results (Section B.8), the following additional conclusions can be drawn: (i) the role of land cover initialization is most relevant for the carbon fluxes (GPP; Figure B.6), and (ii) the role of local climate, topography, and hydrological regime is predominant in controlling the leaf area pattern (Figure B.7). These results highlight the importance of accounting for anthropogenic impacts on the land cover history within the model setup, rather than using the hypothesis of potential natural vegetation, where predefined bioclimatic limits regulate the vegetation distribution over the landscape.

3.4.1.2 The importance of being spatially explicit

A strong disagreement is observed between the areal estimates of GPP and LAI obtained from the spatially distributed model (D-LPJ) and those obtained from the lumped representations of LPJ, and LPJ-GUESS. When D-LPJ is run, using high resolution gridded information of climatic and topographic variables, the spatial patterns of vegetation activity appear to be realistic, reflecting observed local heterogeneities (Figure 3.6a,b,e, and 3.7a,b,e). A comparison of MODIS and D-LPJ spatial patterns of GPP (Figure 3.6a,b) underlines qualitatively the plausibility of the simulated heterogeneity at the landscape level and supports the hypothesis of the influence of local variability of both climate and topography in shaping vegetation response. As illustrated in Figure 3.6e and 3.7e, for both GPP and LAI, LPJ and LPJ-GUESS results (i.e., $f(\bar{\mathbf{X}})$) do not correspond to the mean response of the spatially explicit D-LPJ model (i.e., $\overline{f(\mathbf{X})}$).

The importance of a detailed spatial representation for simulating complex, spatially distributed systems has been often emphasized [e.g., *Pacala and Deutschman, 1995; Bugmann and Fischlin, 1996; Baldocchi et al., 2005; Strigul et al., 2008; Sears et al., 2011; Wood et al., 2011; Potter et al., 2013; Zhao and Liu, 2014*] and demonstrated theoretically [*Levin, 1974, 1976; Rastetter et al., 1992; Norman, 1993; Durrett and Levin, 1994*]. However, models that are widely used in the global carbon cycle research do not account yet for local heterogeneities, as it is done for example in this study with the D-LPJ simulations. The rationale behind the coarse, lumped representation of LPJ, LPJ-GUESS and other DGVMs is, conversely, that the mean response of the system, $\overline{f(\mathbf{X})}$, can be captured reasonably well by characterizing and forcing to the model with the mean properties of the system, $f(\bar{\mathbf{X}})$. However, this assumption fails when nonlinear processes are simulated, as pointed by Jensen's inequality, $\overline{f(\mathbf{X})} \neq f(\bar{\mathbf{X}})$; *Jensen, 1906*], so that the approach commonly used by DGVM simulations leads to the *fallacy of the averages* [*Wagner, 1969*], i.e., “the false assumption that the mean of a nonlinear function of several variables equals the function of the means of those variables” [*Welsh et al., 1988*].

Most of terrestrial ecosystem models rely only upon coarse spatial representations of the Earth surface, dictated by computational limitations and lack of local information. Such an approach averages out local scale heterogeneities of climate and topography that, as demonstrated by our analysis, as well as by experimental evidence [e.g., *Scherrer and Körner, 2009; Adams et al., 2014*], have a significant impact in ecosystem functioning, particularly in areas with complex terrains. In addition, the coarse spatial resolution, implemented in LPJ and LPJ-GUESS, provides a crude representation of the system which goes beyond the simple averaging of heterogeneities; it implies that the simulated computational elements are treated independently without spatial interactions such as lateral water flows (see Figure B.8, where the implications of this assumptions on the hydrological regime of the catchment are illustrated). In summary, we argue on the basis of numerical experiments, which are confirmed by observational evidence, that the coarse spatial resolution and the area-averaged representation of terrestrial ecosystems in heterogeneous topography are likely to be questionable in general, and, in particular, for impact studies. Ecohydrological approaches as implemented here as well as in other ecohydrological models [e.g., *Tague and Band, 2004; Ivanov et al., 2008b; Fatichi et al., 2012b; Tang and Bartlein, 2012; Tague et al., 2013; Tang et al., 2014b*] might conversely represent a valuable alternative.

3.4.1.3 *The role of forest structure and dynamics*

Different representations of the canopy (i.e., population- versus individual-based approach; Section 3.2.1.1) cause differences in simulated vegetation carbon dynamics (Figure 3.5). As already highlighted by *Smith et al. [2001]*, the population-based model provides higher values of GPP and LAI in comparison to the individual-based approach (Figure 3.6e and 3.7e). This is due to differences in the light distribution throughout the canopy. In LPJ-GUESS the simulated forest stand is more heterogeneous and light harvesting is less efficient because of leakages in the vegetation canopy, while the vertical homogeneity of LPJ allows to capture more radiation [*Smith et al., 2001*]. However, it is worth underlining that, the variability of vegetation dynamics, induced by local scale forest disturbances as well as climatic heterogeneities and hydrological regime, appears to be more influential, overcoming the variability induced by the individual-based approach. Mechanistic representations of forest demography using the gap-model approach [*Bugmann, 2001*] are often introduced with the aim to account for the spatial heterogeneity of the forest stand thus improving the area-averaged representation of most DGVMs [e.g., *Liu et al., 2011*]. Nonetheless, they still fail in including local scale heterogeneities (disturbances, meteorological and topographic attributes, soil-water content spatiotemporal variability) that, in meso-scale and fairly heterogeneous catchments, like Kleine Emme, appear to exert a strong signature in vegetation response (Figure 3.6 and 3.7).

3.4.2 Equilibrium vegetation and the rate of carbon sequestration

The concept of potential vegetation in equilibrium with historical climate conditions is often incorporated in DGVMs for the initialization of several of their state variables (e.g., vegetation, soil, and litter carbon pools). Given the daunting task of initializing every single variable for which often no information is available, a spin-up period, starting from an unvegetated state, is a convenient and unavoidable way for model initialization [Pietsch and Hasenauer, 2006; Carvallhais et al., 2008, 2010; Williams et al., 2009]. Our results provide a direct quantification of the implications of such a simplified assumption and are consistent with observations from an increasing number of studies indicating that many forest ecosystems are not in equilibrium but rather in a growing stage [e.g., Buchmann and Schulze, 1999; Liski et al., 2002; Ciais et al., 2008; Keith et al., 2009; Luyssaert et al., 2010]. This is particularly true for the highly productive Swiss forest [Gehrig-Fasel et al., 2007], where carbon sequestration is estimated to be 60% higher than an average forest of Central Europe [SAEFL/WSL, 2005; Etzold et al., 2011]. The legacy of the place shapes the landscape in a much different way than what can be obtained using the potential vegetation hypothesis, i.e., assuming vegetation in equilibrium with historical climate. The history of local scale disturbances controls ecosystem equilibrium or a lack thereof, thus influencing its response in terms of productivity and capacity to store carbon [e.g., Sprugel, 1991; Durrett and Levin, 1994; Körner, 2003b; Gehrig-Fasel et al., 2007; Smith, 2014].

While the inventory based estimate of $\Delta C_{veg}/\Delta t$ for our case study is about $210 \text{ gC m}^{-2} \text{ yr}^{-1}$, all the three models, LPJ, LPJ-GUESS, and D-LPJ simulate a value at the end of the spin-up period which is close to zero (Figure 3.9). D-LPJ allows, however, for some variability, which make the results more comparable to NFI estimates (Figure 3.9). Because LPJ-GUESS, in comparison to LPJ and D-LPJ, allows for generic disturbances, simulated as random events with pre-defined expected return periods, it can maintain a dynamic equilibrium by balancing between disturbance events and forest recovery leading to a more variable carbon balance dynamics (Figure 3.5a). However, while these patch scale disturbances may lead to realistic simulations at the global or continental scales [e.g., Badeck et al.; Smith et al., 2001; Hickler et al., 2004], our analysis demonstrates that they become questionable at basin meso-scales like that of our test case (Figure 3.9). At these scales, approaches based on the specific local disturbance history should be applied.

Model simulations of terrestrial ecosystem functioning can therefore be significantly improved using a better description of the boundary conditions [Liu et al., 2011]. The increasing data availability through Earth-observation programs [e.g., Pan et al., 2013; Butler, 2014] and advanced remote sensing techniques [Kerr and Ostrovsky, 2003; Hurtt et al., 2004; Antonarakis et al., 2014] provide already a rich amount of information, such as vegetation type, biomass, stand age class, phenology, leaf area index, tree height [Lucas and Curran, 1999; Turner et al., 2004;

Nightingale et al., 2004; *Shugart et al.*, 2010], which can be conveniently used for model initialization. While enhancing model initialization with global scale distributed observations comes without additional computational cost, it can improve significantly model simulations.

3.4.3 *Vegetation carbon fluxes and stocks: towards a better model-data integration*

Eddy covariance flux measurements and forest inventories are the two main strategies for tracing vegetation carbon fluxes and stocks, respectively. As eddy-flux towers are becoming widespread worldwide (e.g., CarboeuropelP, Ameri-Flux, Ozflux) and biosphere and atmosphere fluxes are getting widely accessible, many model-data comparisons are conducted for flux tower sites, mainly focusing on ecosystem level carbon fluxes (GPP, e.g., *Schaefer et al.* [2012], or Net Ecosystem Exchange, NEE, e.g., *Dietze et al.* [2011]). At the same time, several tree census datasets are available worldwide [*Anderson-Teixeira et al.*, 2014], offering a great potential for model-data integration [*Lichstein et al.*, 2010]. However, few studies so far have compared model simulations with carbon stock measurements or demographic stand characteristics [e.g., *Hurt et al.*, 2004; *Weng and Luo*, 2011; *Medvigy and Moorcroft*, 2012; *Antonarakis et al.*, 2014].

Model confirmation against vegetation carbon fluxes at flux tower sites does not imply a realistic simulation of vegetation carbon stock dynamics in areas with similar vegetation cover and environmental conditions. While D-LPJ performs fairly well in capturing the spatial (Figure 3.6) and temporal dynamics (Figure 3.8a) of vegetation carbon fluxes, and shows a reasonable agreement with the Swiss FLUXNET sites (Figure B.3), remarkable differences occur when modeled and observed values of forest carbon stock changes are compared (Figure 3.9). Disturbances, aging, and turnover processes may have more significant contribution to the landscape's carbon budget than the assimilated carbon through plant activity [*Dolman et al.*, 2003; *Körner*, 2003b; *Friend et al.*, 2014]. In this respect, the legacy of the place, i.e., local scale disturbances, individual-level plant establishment, growth and mortality rates, control the vegetation carbon storage. The localized nature of these phenomena is thus the likely cause of the strong mismatch between simulated and observed carbon stocks changes [e.g., *Harmon*, 2001; *Fisher et al.*, 2008].

Furthermore, our analysis reveals that the inventory-based estimates also differ from the simulated carbon sequestration rate when the system is not yet balanced (i.e., derivative of the vegetation carbon pools at the beginning of the spin-up; Figure 3.5a). This underlines not only that the state of the forest obtained after the spin-up is not realistic, but allows us also to speculate that there could be structural issues in how forest growth is simulated in the models. Accordingly, in long-term analyses focusing mainly on the carbon stored in forest stands, special caution should be paid to model-based inferences regarding veg-

etation carbon storage when evidence shows that the simulated fluxes are only confirmed by observations in eddy flux tower sites.

3.4.4 *Broader implications and ways forward*

Organisms do not experience climate at coarse scales [Sears *et al.*, 2011; Potter *et al.*, 2013]. Thus, aggregation biases can be significant not only when past and current ecosystem dynamics are simulated, but also when model projections under climate change scenarios are carried out [Trivedi *et al.*, 2008]. When process-based models are used, and confidence on their results is based on their “physical-correctness and consistency”, then the “physics” should be solved at appropriate scales with appropriate forcings. In this study we quantified the biases occurring in terrestrial ecosystem modeling when this is not done. Model complexity and process representation should therefore match with the adopted spatiotemporal representation, as well as with the quality and resolution of the available data [Costanza and Maxwell, 1994]. Advanced statistical tools, such as emulators, together with enhanced computing capabilities can provide viable options to cope with the additional computational burden [Neelin *et al.*, 2010; Castelletti *et al.*, 2012].

If solving processes at the appropriate scales is computationally too demanding, given the available resources, then statistical and/or top-down approaches may represent a conceptually better approximation of terrestrial ecosystem functioning. For instance, a statistical-dynamical approach [e.g., Giorgi and Avissar, 1997] can be incorporated in terrestrial ecosystem modeling using the empirical probability density function of local scale attributes, thus describing the heterogeneity of the meteorological forcings in the examined domain or that of plant traits [Reich, 2014]. The potential of using well established approaches from other disciplines dealing with spatial aggregation of complex non-linear systems [e.g., population and community ecology, Auger *et al.*, 2012; Chesson, 2012], as well as organizing principles [e.g., Mäkelä *et al.*, 2002; Whitfield, 2007; Dewar, 2010], is also worth of exploring.

3.5 CONCLUSIONS

Our study revealed that local scale spatial heterogeneities, which are often ignored or at best crudely represented in terrestrial ecosystem models, exert a strong control on ecosystem response. Therefore, preservation of local environmental and topographic attributes, as proposed with the fine spatial resolution grid of the D-LPJ model, represents an important feature to achieve a more realistic representation of terrestrial ecosystem dynamics. In addition, we showed that model initialization, and therefore forest historical legacy, has a remarkable

importance on carbon balance assessments and specifically on the capacity of the forest to store carbon. The assumption of steady-state vegetation and soil carbon pools, incorporated in DGVMs for pragmatic reasons, is in contradiction with the current state of many forests, which are often far from an equilibrium and with different states of succession due to natural or anthropogenic disturbances. A realistic assessment of future carbon stocks cannot be separated from an accurate representation of these heterogeneities and local scale trajectories. The light shed by this study on model limitations, emphasizes the importance of solving biophysical and biogeochemical processes at the appropriate scales and with the appropriate boundary conditions.

ACKNOWLEDGEMENTS

We would like to thank Veiko Lehsten and the LPJ team from the Department of Earth and Ecosystem Sciences at Lund University for providing the source code of LPJ, LPJ-GUESS. The authors would also like to thank the developers of the R programming environment [*RCoreTeam*, 2012], where all the statistical calculations and figures are made. Fruitful discussions with Harald Bugmann and Valeriy Ivanov are gratefully acknowledged. The meteorological data are kindly provided by the Swiss Federal Office of Meteorology and Climatology (MeteoSwiss, Switzerland). Flux towers observations are obtained from the network Swiss FLUXNET (<http://www.swissfluxnet.ch>). This study was funded by the Swiss National Science Foundation, in the frame of NRP 61 project HydroServ (C.P.: project no. 4061-125926). Simulation results are available upon request from the corresponding author.

MODELING TERRESTRIAL CARBON AND WATER DYNAMICS ACROSS CLIMATIC GRADIENTS: DOES PLANT DIVERSITY MATTER?

ABSTRACT

Vegetation diversity in many terrestrial ecosystem models is crudely represented using a discrete classification of a handful of “plant types” (named Plant Functional Types; PFTs). The parameterization of PFTs reflects mean properties of observed plant traits over broad categories ignoring most of the inter- and intra-specific trait variability. Taking advantage of well-established plant-trait cross-correlations described by the Leaf Economics Spectrum as well as documented plant drought strategies, we generated an ensemble of hypothetical species with coordinated attributes, rather than using few PFTs. The behavior of these proxy species is tested using a mechanistic ecohydrological model that translates plant traits into plant performance. Simulations are carried out for a range of climates representative of different elevations and wetness conditions in the European Alps. Using this framework we investigated the sensitivity of ecosystem responses to species-induced variability and compared it with climate-induced variability. Trait diversity leads to highly divergent vegetation carbon dynamics (fluxes and pools) and to a lesser extent water fluxes (transpiration). Abiotic processes, such as soil water dynamics and evaporation, are only marginally affected. These results highlight the need for improving species representation in vegetation models. Probabilistic approaches, based on empirical multivariate distributions of coordinated plant trait spectra, provide a viable alternative.

4.1 INTRODUCTION

Understanding the terrestrial ecosystem functioning and its responses under changing climatic conditions requires the development of mechanistic numerical models to simulate carbon, water, and nutrient dynamics. Modeling is the art of the appropriate approximation [Jennings, 2007]. In an attempt to conceptualize the terrestrial ecosystem from a modeler’s perspective, the following components can be identified: (i) the initial and boundary conditions; (ii) the

Pappas, C., S. Fatichi, and P. Burlando, Modeling terrestrial carbon and water dynamics across climatic gradients: does plant diversity matter?, *New Phytologist*, under review-b

abiotic factors, consisting essentially of the environmental drivers (e.g., precipitation, temperature); and (iii) the biotic attributes, representing the living organisms (plant parameters for the case of vegetation models) that thrive within the system's boundaries. The immense diversity occurring in terrestrial ecosystems has to be reflected in the aforementioned conceptual components. Several techniques have been therefore developed for approximating natural heterogeneity within models, particularly in deterministic, process-based schemes.

While variability in boundary conditions and abiotic component of the system can be captured sufficiently well by numerical models imposing local scale information from modern remote-sensing data [e.g., imaging spectrometry and waveform lidar; *Antonarakis et al.*, 2014] and using fine resolution spatiotemporal representations [e.g., *Tague and Band*, 2004; *Ivanov et al.*, 2008a; *Hwang et al.*, 2009; *Wood et al.*, 2011; *Fatichi et al.*, 2012a; *Pappas et al.*, under review-a], the biotic attributes and the related species heterogeneities are often simplistically represented.

Nature is rich in plant properties and functional forms. Hot-spots of biodiversity exist with more than 5000 species per plot [see *Mutke and Barthlott*, 2005, for a global perspective of vascular plant diversity]. Accounting for this immense diversity is very challenging and bottom-up approaches (e.g., based on individual, species-specific parameterizations) are hampered by species abundance. For pragmatic reasons (e.g., computational constraints and data scarcity), a handful of broad vegetation categories, named Plant Functional Types (PFTs, e.g., temperate broadleaf deciduous forest) preserving major phenological, environmental and leaf shape characteristics is typically used for mimicking plant diversity and functioning [*Woodward*, 1992; *Box*, 1996; *Lavorel et al.*, 1997; *Bonan et al.*, 2002; *Harrison et al.*, 2010]. The PFT-conceptualization is based on static physiological parameters and bioclimatic variables [e.g., minimum coldest-month temperature for survival; *Sitch et al.*, 2003] that define their occurrence. The PFT concept is widely incorporated in terrestrial ecosystem models [such as Dynamic Global Vegetation Models DGVMs; *Sitch et al.*, 2003; *Prentice et al.*, 2007; *Sitch et al.*, 2008] and Earth System Models [ESMs; *Cox et al.*, 2000; *Friedlingstein et al.*, 2006; *Friedlingstein and Prentice*, 2010; *Prinn*, 2012], since it offers a simple way for dealing with biotic variability and floristic complexity, but has several weaknesses and limitations as outlined hereafter.

Grouping plant traits in broad categories (PFTs) captures an important fraction of trait variation [*Kattge et al.*, 2011], but the discrete and static species parameterization poses serious constraints, especially when long-term, prognostic simulations are envisioned. The drawbacks underlying this conceptualization have been recently recognized [*Kleidon and Mooney*, 2000; *Lavorel and Garnier*, 2002; *Kleidon et al.*, 2007; *Lavorel et al.*, 2007; *Prentice et al.*, 2007; *Reich et al.*, 2007; *Thuiller et al.*, 2008; *Ordoñez et al.*, 2009; *Williams et al.*, 2009; *Harrison et al.*, 2010; *Quillet et al.*, 2010; *McMahon et al.*, 2011; *Van Bodegom et al.*, 2012; *Stoy et al.*, 2013; *Wullschlegel et al.*, 2014]. The importance of representing plant diversity within

models has been also highlighted using statistical tools [e.g., *Pappas et al.*, 2013, for a detailed sensitivity analysis of a DGVM], or by embedding trait variations in vegetation [e.g., *Wang et al.*, 2012], or Earth System Models [e.g., *Verheijen et al.*, 2013, but see also *Higgins et al.* [2014]].

Plants are not static, they respond dynamically to local conditions (resources availability) by adjusting their metabolism. Different levels of plant adjustments exist, for example phylogenetic selection, genotypic differentiation, morphological modifications, physiological acclimation [*Ackerly*, 2003; *Korner*, 2012]. These adjustments are reflected in plant functional traits, defined as plant morphological, phenological or physiological characteristics that control plant functioning and thus its fitness [*Violle et al.*, 2007; *Laughlin and Laughlin*, 2013], leading to significant divergence among plant properties [limiting similarity; *MacArthur and Levins*, 1967], and strong spatiotemporal variation. Functional traits vary significantly not only among [e.g., *Reich et al.*, 1997; *Wright et al.*, 2004], but also within species [*Albert et al.*, 2010a, b; *Bolnick et al.*, 2011; *Albert et al.*, 2011; *Cadotte et al.*, 2011; *Violle et al.*, 2012; *Kichenin et al.*, 2013], as well as among plant communities [*Messier et al.*, 2010]. They may vary also throughout plant's lifespan due to plant adaptation to prevailing environmental conditions.

An illustrative example is that of leaf photosynthetic properties (e.g., maximum Rubisco carboxylation capacity, V_{cmax}). Variation of V_{cmax} is not limited across species, where it has been observed to vary by almost two orders of magnitude [*Wullschlegel*, 1993; *Medlyn et al.*, 1999, 2002b; *Kattge and Knorr*, 2007; *Kattge et al.*, 2009], but also across different locations [*Wilson et al.*, 2000; *Fyllas et al.*, 2009; *Castanho et al.*, 2013], and plant age-class [*Thomas*, 2010]. It has also been shown to undergo seasonal variation [*Wilson et al.*, 2000; *Baldocchi and Xu*, 2005; *Bonan et al.*, 2011; *Medvigy et al.*, 2013], and to be controlled by photoperiod [*Bauerle et al.*, 2012]. V_{cmax} is included in almost all vegetation models that mechanistically simulate carbon assimilation [*Rogers*, 2014] and has been found to be the cornerstone of their performance [*Pappas et al.*, 2013]. While V_{cmax} is crucial for vegetation modeling, its variation is hidden by the PFTs parameterization where discrete values, that often do not even correspond to the mean of the empirical distribution of the measured values are used [see a detailed discussion in *Kattge et al.*, 2011].

Taking advantage of the recently assembled global databases of plant-traits, e.g., GLOPNET, *Wright et al.* [2004] and TRY initiative, *Kattge et al.* [2011], alternative traits-based vegetation modeling approaches have been proposed, moving beyond the paradigm of PFTs [*Westoby et al.*, 2002; *Lavorel and Garnier*, 2002; *McGill et al.*, 2006; *Webb et al.*, 2010; *Cadotte et al.*, 2011; *Van Bodegom et al.*, 2012; *Laughlin and Laughlin*, 2013]. Trait-based approaches build upon well documented cross-correlations across multivariate plant trait spectra, such as leaf traits [Leaf Economics Spectrum, LES; *Reich et al.*, 1997; *Wright et al.*, 2004], plant hydraulic properties [e.g., *Manzoni et al.*, 2013], wood properties [wood economics spectrum; *Chave et al.*, 2009] or seed mass properties [*Westoby et al.*, 2002; *Moles et al.*,

2005a, b], as well as their covariations with environmental conditions [Díaz *et al.*, 1998; Wright *et al.*, 2004, 2005; Ordoñez *et al.*, 2009; Maire *et al.*, 2012] and nutrient availability [Reich *et al.*, 1997; Reich and Oleksyn, 2004; Wright *et al.*, 2004; Ordoñez *et al.*, 2009; Maire *et al.*, 2012]. Coordinated proxy plant species can be therefore generated and embedded in vegetation models, maintaining the empirical distributions and cross-correlations of plant traits, their dominant stoichiometric constraints (e.g., nitrogen dependencies), and environmental controls (e.g., water availability).

Accordingly, we adopt in the present study a trait-based approach to analyze the importance of species representation in terrestrial ecosystem modeling and their relation to the simulated water and carbon dynamics. Following the conceptual framework introduced by Webb *et al.* [2010], our analysis consists of three main elements: (i) distribution of plant traits (Section 4.2.3), (ii) performance filter (Section 4.2.1), and (iii) environmental gradients (Section 4.2.2). Coordinated proxy plant species are generated, across a continuous spectrum of plant traits, using the well-established empirical plant-trait cross-correlations (LES, using the freely available GLOPNET dataset; Wright *et al.* [2004]) as well as different drought tolerances. The behavior of these proxy species is then tested using an ecohydrological model [T&C; Fatichi *et al.*, 2012a] that simulates mechanistically plant performance. Simulations are carried out for a range of climatic conditions representative of naturally occurring meteorological gradients in Switzerland, which are exemplary for a large variety of climatic boundary conditions.

Using this framework we quantify explicitly the implications of a pluralistic trait-specific representation of vegetation functioning in simulating water and carbon fluxes and stocks. The main questions addressed are thus: (i) which is the importance of trait diversity in simulating terrestrial ecosystem responses in terms of carbon- and water-related variables? (ii) Which are the aggregation biases induced by smoothing of species variability through PFTs? (iii) Is the trait-induced variability comparable to the variability induced by climate heterogeneity?

4.2 MATERIALS AND METHODS

4.2.1 Modeling ecosystem functioning

4.2.1.1 Model description

Numerical simulations were carried out using the Tethys-Chloris (T&C) model [Fatichi *et al.*, 2012a, b; Fatichi and Leuzinger, 2013; Fatichi *et al.*, 2014; Fatichi and Ivanov, 2014]. T&C is a mechanistic distributed ecohydrological model designed to simulate essential components of terrestrial hydrological and carbon cycle

resolving exchanges of energy, water, and CO₂ at an hourly resolution. Mass and energy fluxes control the temporal evolution of vegetation (carbon pools) that in turn can feed back land-atmosphere exchanges through its biophysical structure and physiological properties. Soil moisture dynamics in saturated and unsaturated soils are solved using the one-dimensional (1D) Richards equation for vertical flow and the kinematic approximation for lateral subsurface flow. Photosynthesis is simulated with a biochemical model [Farquhar *et al.*, 1980; Bonan *et al.*, 2011] where sunlit and shaded leaves are treated separately for the computation of net assimilation and stomatal resistance. An exponential decay of photosynthetic capacity is used to upscale photosynthesis from the leaf to the plant scale [Ivanov *et al.*, 2008a; Bonan *et al.*, 2011].

The dynamics of seven carbon pools are explicitly simulated in the model and include (i) green aboveground biomass (leaves), (ii) living sapwood (woody plants only), (iii) fine roots, (iv) carbohydrate reserve (non-structural carbohydrates), (v) standing dead leaf biomass, (vi) fruit and flowers, and (vii) heartwood and dead sapwood. The carbon assimilated through photosynthetic activity is used for growth, and reproduction and is lost in the process of respiration and tissue turnover. Carbon allocation and translocation are dynamic processes that account for resource availability (light and water), allometric constraints and phenology. Organic matter turnover of the different carbon pools is controlled by tissue longevity and environmental stresses, i.e., drought and low temperatures. Phenology is simulated considering four states [Arora and Boer, 2006]: dormant, maximum growth, normal growth, and senescence.

Forest demography and nutrient dynamics are neglected in the model, which always considers a mature vegetation in equilibrium with its nutritional and hydrometeorological environments. The domain of the simulation is typically represented by a regular grid as described by digital elevation models and includes topographic effects of incoming radiation and lateral water transfers. However, in this study, each computational element was treated in isolation, without an explicit areal dimension, i.e., point-scale simulations were carried out. A detail description of the model structure and process parameterizations is presented in Fatichi *et al.* [2012a].

4.2.1.2 Simulation protocol

Plot scale simulations were performed using a 3 m deep soil column, discretised into 19 layers of various thickness (10-500 mm). Soil properties correspond to a typical loam with 40% sand, 20% clay, and 2.5% organic matter [percentages are expressed by weight basis; Saxton and Rawls, 2006]. The meteorological forcing of T&C consists of hourly values of solar radiation subdivided into two wavebands (including Photosynthetically Active Radiation, PAR), precipitation, air temperature, water vapour pressure, cloud cover, atmospheric pressure, wind speed, and atmospheric CO₂ concentration. The latter was fixed to 380 ppm.

Thirty years long T&C simulations were carried out, using synthetic time series of the meteorological variables (see Section 4.2.2). The first five years of the simulations were used for model spin-up (i.e., initialization of state variables). We consider five years to be sufficient since the model starts from a mature forest condition and only soil moisture and living carbon pools have to be initialized. The results presented in the following sections are based on long-term averages of the remaining 25 yr. T&C specific parameters are detailed in Table C.2.

4.2.2 *Meteorological forcing across climatic gradients*

Cross-correlated long-term meteorological time series are generated using an advanced weather generator [Advanced WEather GENerator, AWE-GEN; *Fatichi et al., 2011*], which makes use of meteorological records, provided by the Swiss meteorological service (MeteoSwiss), across elevational and precipitation gradients. A weather generator is required to obtain a smooth interpolation of observed climate across elevation, which otherwise is not feasible, due to irregular spacing of meteorological stations. The implemented methodology as well as the validation of the generated climatic gradients with ground measurements are detailed in Appendix C (Section C.1). In brief, thirty years of synthetic hourly time series of solar radiation, precipitation, air temperature, vapour pressure, cloud cover, atmospheric pressure, and wind speed are generated for two precipitation regimes, i.e., a dry, sheltered internal alpine valley and a wet, exposed mountain side, and for elevations ranging from 500 to 2500 m a.s.l (Figure 4.1). While the selected environmental transects are nested within the alpine region (i.e., prescribed latitude, day length, seasonality), they cover a wide range of variations of meteorological conditions across elevation and precipitation regimes (e.g., mean annual values of precipitation from 600 to 2350 mm yr⁻¹; temperature from -1 to 10 °C; and PAR from 65 to 82 W m⁻²), so that they are representative of a broader set of meteorological forcings. In the following sections, simulation results are presented across the elevation gradient, for the two examined wetness conditions. It is worth underlining that meteorological input variables vary and co-vary in a coordinated manner respecting the observed high-frequency (hourly) and climatological changes with elevation (Figure 4.1).

4.2.3 *Mimicking plant diversity*

Plant diversity is included in our analysis through a Monte-Carlo framework, sampling vegetation-related properties from the T&C parameter space. Proxy plant species are generated combining: (i) three categories of plant-life forms, deciduous, evergreen trees, and grass, reflecting structural and phenological differences among plant species (Section C.2.1); (ii) three discrete plant drought

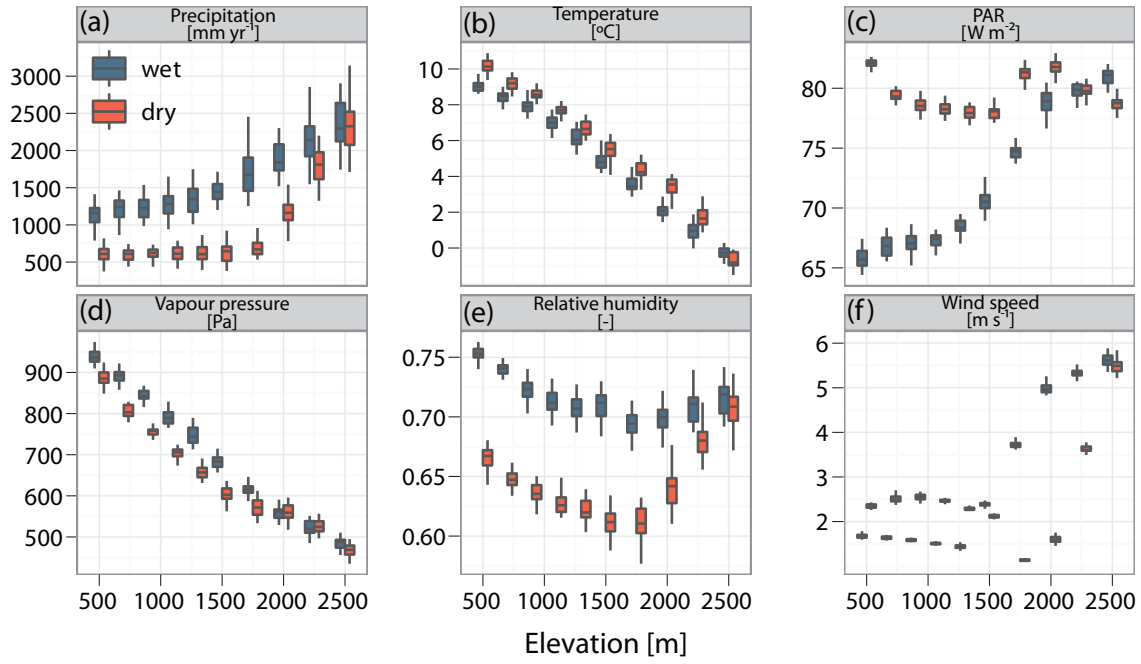


Figure 4.1: Variation of the mean annual values of major environmental variables across the examined precipitation (wet, dry), and elevation gradients over the 30 yr of simulated climate. Boxes extend from the 25th to the 75th percentile, while whiskers extend to 1.5 times the interquartile range of the lower and upper quartiles respectively. PAR [W m^{-2}] stands for Photosynthetically Active Radiation.

tolerances (Table 4.1 and Section C.2.2); and (iii) four major leaf traits (Table 4.1 and Figure 4.2), constructed using a continuous spectrum of values across the observed LES (Section C.2.3).

Differences in drought tolerance between species can be characterized using hydraulic limits [Sperry, 2000]. Three drought strategies (low, medium, and high drought tolerance) are simulated varying not only the rooting depth and the stomatal regulation but also the plant water-stress limits through variation of soil water potential values at incipient stomatal closure and wilting point (Table 4.1). For each plant-life form (deciduous, evergreen, or grass) and plant-drought strategy (low, medium, or high), 100 proxy species, each corresponding to a unique set of parameters, were generated sampling coordinated leaf traits (Figure 4.2). More specifically, the following leaf traits are investigated: (i) critical age for leaf shed, A_{cr} ; (ii) maximum Rubisco capacity, V_{cmax} , obtained through the conversion from measured photosynthetic capacity rates, A_{mass} (see Section C.2.4); (iii) carbon-nitrogen mass ratio for the foliage, N_f ; and (iv) plant specific leaf area, SLA, using the empirical distributions and cross-correlations from the GLOPNET database [Global Plant Trait Network; Wright *et al.*, 2004]. The sampled (proxy) plant species are not necessarily identical to real plant species, but they preserve realism and leaf-level coordination reflected in the GLOPNET

Table 4.1: Description of the parameters used for generating proxy plant species as well as the main processes where they play a role (P: photosynthesis, R: respiration, T: transpiration, TT: tissue turnover, VS: vegetation structure).

| Process | Parameter ID | Units | Description |
|--------------------------|-------------------|--|---|
| <i>Drought tolerance</i> | | | |
| P, T | α | [-] | Empirical parameter in Leuning's equation for stomatal conductance. |
| P, T | PSI _{ss} | [MPa] | Soil water potential at which stomatal closure begins. |
| P, T | PSI _{wp} | [MPa] | Soil water potential at full stomatal closure (wilting point). |
| VS, T | ZR95 | [m] | Rooting depth that contains 95% of the root biomass. |
| <i>Leaf traits</i> | | | |
| TT | A _{cr} | [d] | Critical age for leaf shed. |
| P | V _{cmax} | [$\mu\text{mol CO}_2 \text{ s}^{-1} \text{ m}^{-2}$] | Leaf-level values of maximum Rubisco capacity at 25 °C. |
| R | N _f | [gC gN ⁻¹] | Carbon-nitrogen mass ratio for foliage. |
| VS | SLA | [m ² LAI gC ⁻¹] | Specific leaf area. |

database (Figure 4.2 and Figure C.7, C.8, C.9). A description of the sampling procedure is detailed in Section C.2. In total 900 proxy plant species (3 plant-life forms, 3 drought strategies, and 100 proxies with coordinated leaf traits) are used in the simulations.

4.2.4 Variance partitioning

In order to partition the total variance of model outputs across the examined sources of variation, namely trait variability and environmental heterogeneity, the variance of the conditional expectations (conditioning across the two sources of variation) is estimated and normalized using the total (unconditional) variance. More specifically, the following importance measure is calculated: $S_x = \frac{\text{Var}[E[Y|x=x_i]]}{\text{Var}[Y]}$, where x is the (random) variable under consideration (either trait diversity encapsulating variation in plant leaf-traits and drought tolerances, denoted by *species*, or environmental heterogeneity, represented by the examined elevation and precipitation gradients, denoted by *environ*), x_i refers to a particular value in the domain of variation of the random variable x (e.g., elevation band of 500 m a.s.l., or one out of the 100 simulated proxy species per drought tolerance and plant-life form), and Y is the examined model output (e.g., photosynthetic activity, transpiration). S_x is therefore the percentage of total variance that can be explained due to variability of x , and varies between 0 and 100% [see Pappas *et al.*, 2013, for a detailed explanation of the use of conditional variances of model outputs as importance measures]. Since species

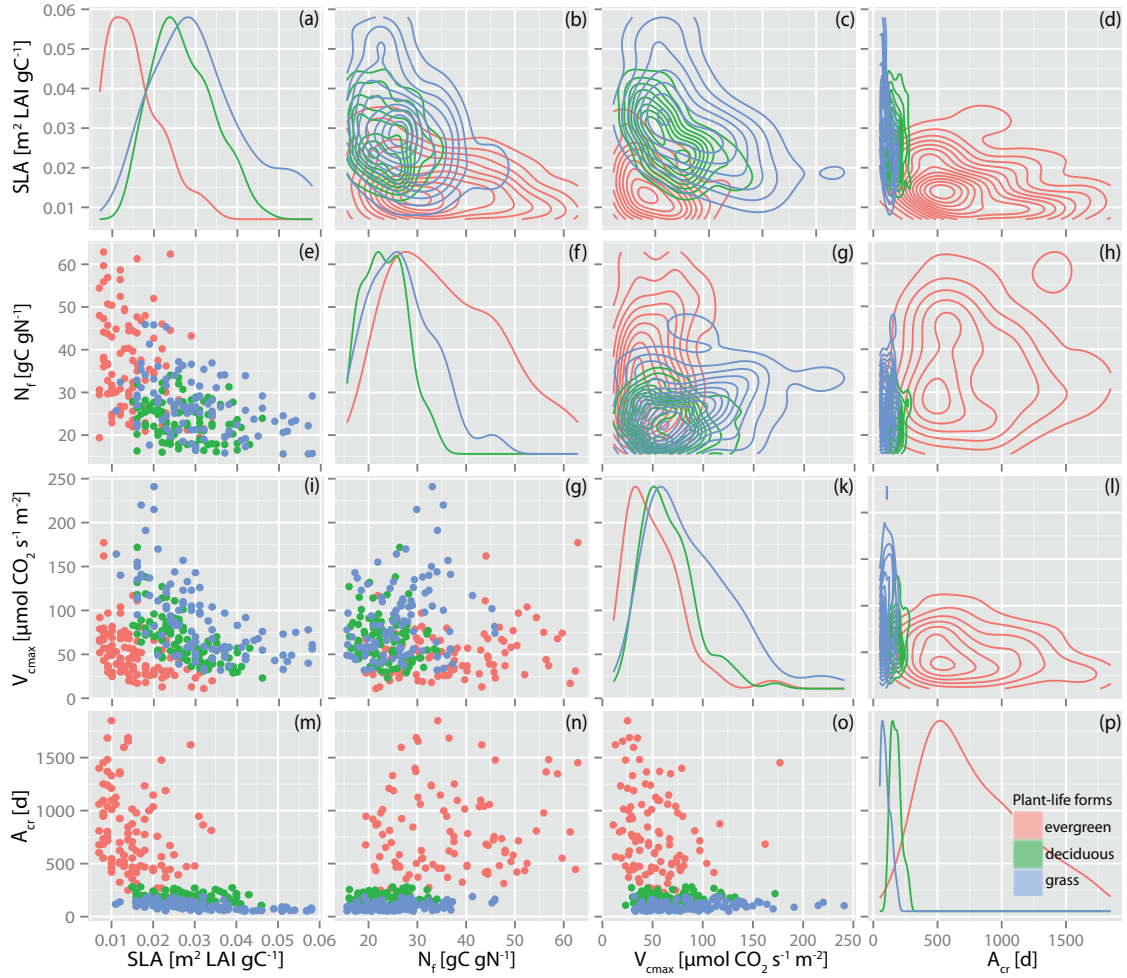


Figure 4.2: Covariation among the examined leaf-traits for the 100 generated proxy species per plant-life form (evergreen: red, deciduous: green, grass: blue). Scatter- (e, i, j, m, n, o), probability density- (a, f, k, p) as well as contour-plots (b, c, d, g, h, l) of the generated leaf-traits are shown.

variability and environmental heterogeneity are treated as independent sources of variation in this analysis (i.e., no interaction effects), the sum of the partial variances is equal to the total output variance i.e., $S_{\text{species}} + S_{\text{environ}} = 1$.

4.2.5 Data

Three datasets were compiled in our analysis for a qualitative data-based assessment of simulated model responses: (i) photosynthetic activity (Gross Primary Production, GPP) estimated from eddy covariance technique across different elevations and plant types, in the central European Alps (Switzerland and Italy), (ii) MODerate Resolution Imaging Spectroradiometer (MODIS) estimates of GPP and Leaf Area Index (LAI) in the European Alps, and (iii) estimates of forest growth (i.e., net increase in forest biomass) of surviving trees in Switzerland,

provided by Swiss National Forest Inventories [NFI; [WSL, 2012](#)]. A detailed description of the datasets and their preprocessing are detailed in [Pappas et al. \[under review-a\]](#) as well as in Section [C.3](#).

4.3 RESULTS

4.3.1 *Species variability and long-term vegetation dynamics*

The long-term mean response of simulated vegetation dynamics across the examined species variation and the elevation gradients is in a good qualitative agreement with the data-based estimations of GPP and LAI from MODIS, and in a good quantitative agreement with the few eddy covariance data points and biomass estimates from forest inventories (Figure [4.3](#)).

Species-induced variability, due to plant leaf-trait and drought tolerance variations, in the long-term simulated Gross Primary Productivity (GPP; Figure [4.3a, b, c](#)), Leaf Area Index (LAI; Figure [4.3d, e, f](#)), and changes in the Above Ground (woody) Biomass (ΔAGB ; Figure [4.3g, h](#)), tends to prevail when compared to differences imposed by elevation and precipitation gradients. At low elevations, where environmental conditions are favorable for plant activity (Figure [4.1](#)), species variability enhances the variance of the simulated GPP, LAI, and ΔAGB . As elevation increases, environmental conditions become “harsher” (Figure [4.1](#)), causing a tapering response of GPP, LAI, and ΔAGB (Figure [4.3](#)). Species variability leads to coefficients of variation (defined as the ratio of the standard deviation to the mean, averaged across the elevation gradient; expressed in %) of simulated GPP, LAI, and ΔAGB , for the dry (wet) precipitation conditions of about 48 (48), 42 (39), 46 (35) for deciduous trees, while for evergreen species they are about 46 (53), 36 (43), 53 (60), respectively (Figure [4.3](#)).

Species-induced variability in the dry precipitation gradient leads to lower plant performance, when compared to wet environmental conditions because of the stronger environmental constraints. For example, at the elevation band of 900 m a.s.l., the simulated GPP averaged over proxy species, for deciduous, evergreen, and grass plant-life forms and for dry (wet) wetness conditions is $960 \text{ gC m}^{-2} \text{ yr}^{-1}$ ($1667 \text{ gC m}^{-2} \text{ yr}^{-1}$), $1063 \text{ gC m}^{-2} \text{ yr}^{-1}$ ($1705 \text{ gC m}^{-2} \text{ yr}^{-1}$), and $828 \text{ gC m}^{-2} \text{ yr}^{-1}$ ($1928 \text{ gC m}^{-2} \text{ yr}^{-1}$) respectively (Figure [4.3a, b, c](#)). This is because resources availability (water) affects plant performance, highlighting the competitive advantage of different drought strategies. Species with higher drought tolerance outperform those with medium or low tolerance, leading to higher values of GPP, LAI, and ΔAGB . These results are more pronounced for evergreen plant-life forms (Figure [4.3](#)), mainly due to their phenology that allows them to interact with climate over the entire year, as compared to deciduous or grass plant-life forms that have a limited growing season (A_{cr} ; Figure [4.2p](#)).

4.3.2 *Species variability and water fluxes*

Evidence of species-induced variability on vegetation dynamics suggests that such variability is expected to affect also biotic water fluxes (transpiration; Figure 4.4a, b, c) and related hydrological variables, such as total evaporation (Figure 4.4d, e, f) and soil water content (Figure 4.4g, h, i). This is shown by the numerical experiments, though the effect is less pronounced. Across the dry precipitation gradient, species-induced variability to simulated transpiration dynamics is smaller (e.g., the coefficient of variation averaged across the elevation gradient is about 24% and 30% for evergreen and deciduous plant-life forms respectively), when compared to wet conditions (e.g., the coefficient of variation averaged across elevation of about 36% and 37% for evergreen and deciduous species respectively), since the decreasing availability of water poses a strong constraint to root water uptake. Under water-limiting conditions (low elevations in the dry precipitation gradient; Figure 4.1a) the strategic advantage of species with high drought tolerance becomes very clear (blue bars in Figure 4.4a, b, c). Variability in simulated long-term transpiration losses due to species parameterization is higher in evergreen plant-life forms than that in deciduous or grass, due to their phenological dynamics (A_{cr} ; Figure 4.2p).

However, abiotic water fluxes (total evaporation; Figure 4.4d, e, f) as well as soil-water dynamics (Soil Water Content available to plants, SWC; Figure 4.4g, h, i) are mostly controlled by water availability -i.e., climatic conditions- rather than trait parameterization. Total evaporation including all sources of water evaporation (i.e., ground evaporation, evaporation and sublimation from the snowpack at the ground, evaporation from intercepted water and snow) is mostly independent from variation in plant traits (Figure 4.4d, e, f). Long-term variation in simulated SWC shows low variability with plant parameterization in ample water availability (wet precipitation gradient). The interactions between SWC dynamics and species variability become more variable for the dry precipitation gradient at low elevations. In precipitation-limited environments (Figure 4.1a), different plant transpiration rates exert a stronger control on SWC dynamics (Figure 4.4g, h, i).

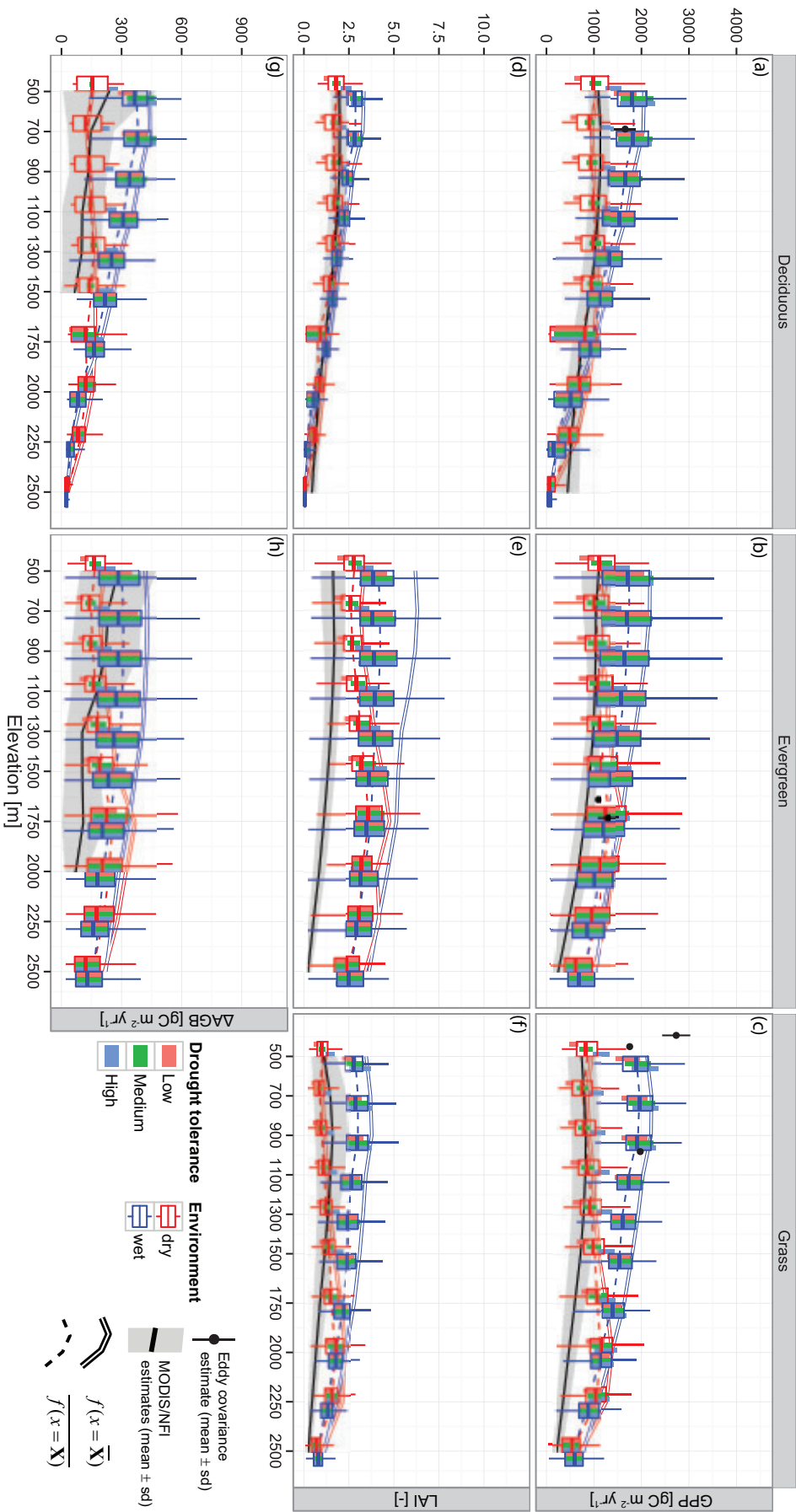


Figure 4.3 (*previous page*): Vegetation activity of proxy plant species across different elevation and precipitation gradients. Box-plots illustrate the long-term variability (25 yr) of 100 generated proxy plant species per plant-life form (deciduous, evergreen, and grass) and per drought tolerance (low, medium, and high) for the case of photosynthetic activity (GPP; a, b, c), leaf area dynamics (LAI; d, e, f) and changes in woody aboveground biomass (ΔAGB ; g, h, note that grass consists only of fine roots and leaves, no wood components, thus it is not included in the comparison). Red and blue box-plots illustrate the dry and wet precipitation gradients respectively. Boxes extend from the 25th to the 75th percentile, while whiskers extend to 1.5 times the interquartile range of the lower and upper quartiles respectively. Bar-plots, included within each box-plot, depict the response of proxy plant species, grouped according to their drought tolerance. Light red, green, and blue fill colors correspond to low, medium, and high drought tolerance respectively. Bar-plots cover the 25th to 75th percentile of the distribution. Dashed red and blue lines highlight the mean model response across the elevation gradient ($\overline{f(x = \mathbf{X})}$, i.e., mean of the box-plots) as obtained using all the simulated proxy species ($x = \mathbf{X}$), while continuous lines illustrate the obtained model response ($f(x = \overline{\mathbf{X}})$) when only mean values of the empirical distribution of plant trait are used ($x = \overline{\mathbf{X}}$), for dry and wet precipitation gradients respectively. Vertical lines with points in the middle, denoted in black, represented estimates of GPP (mean \pm standard deviation), as obtained from eddy covariance measurements for several locations in the European Alps with similar plant types and elevation (a, b, c). Continuous black lines and shaded areas represent the mean and the range of variation (mean \pm standard deviation) of vegetation variables across the elevation gradient based on MODIS estimates from European Alps (a, b, c, for the case of GPP; and d, e, f, for the case of LAI) and Swiss National Forest Inventory estimates (NFI; g, h, for the case of ΔAGB).

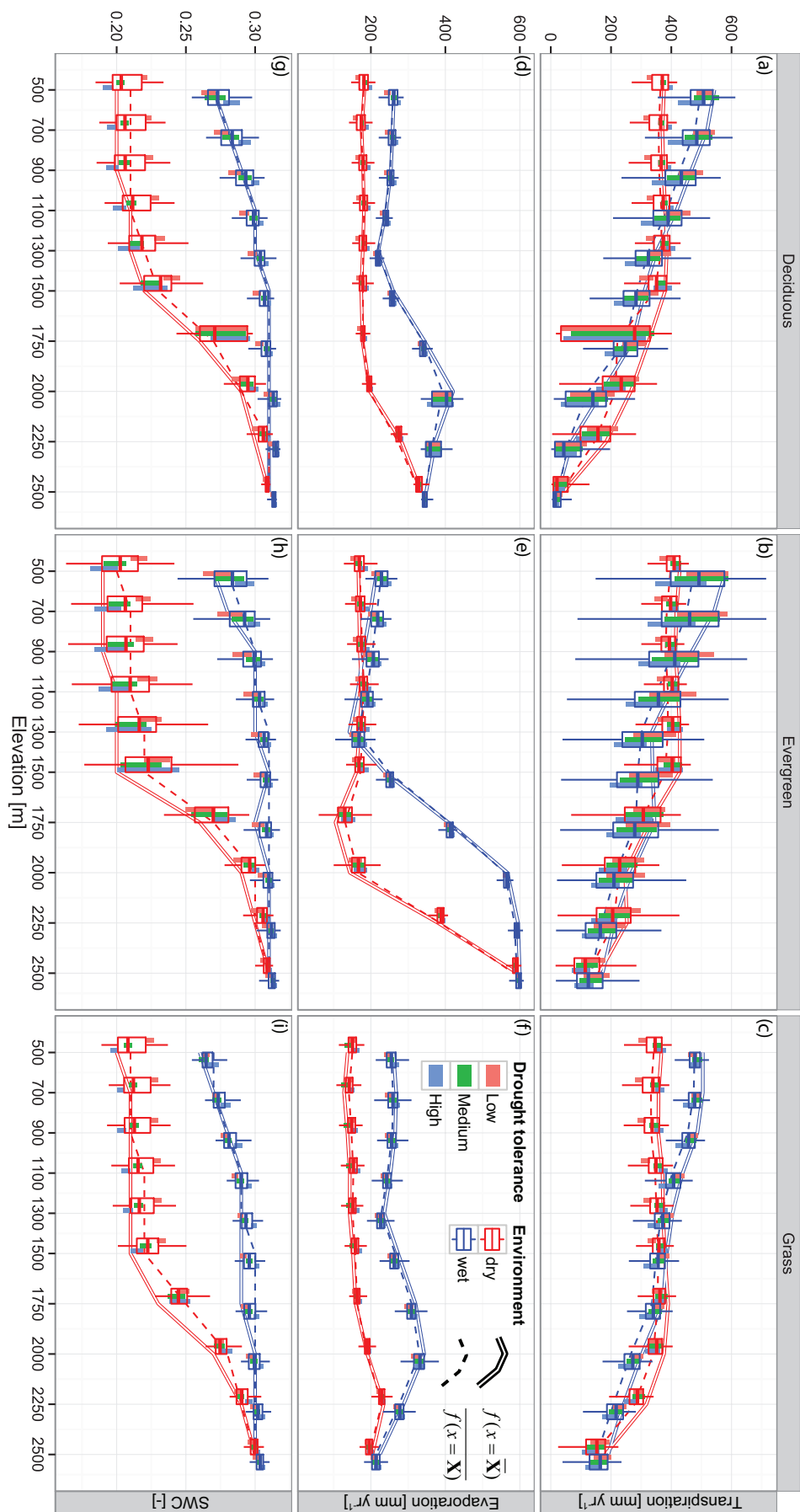


Figure 4.4 (*previous page*): Biotic (transpiration) and abiotic (total evaporation i.e., sum of ground evaporation, evaporation and sublimation from the snowpack at the ground, evaporation from intercepted water and snow) water fluxes and soil water dynamics (soil water content available to plants, SWC) across different elevation and precipitation gradients, simulated using different proxy plant species. Box-plots illustrate the long-term variability (25 yr) of 100 generated proxy plant species per plant-life form (deciduous, evergreen, and grass) and per drought tolerance (low, medium, and high) for the case of plant transpiration (a, b, c), total evaporation (d, e, f) and soil water content (SWC, g, h, i). Red and blue box-plots illustrate the dry and wet precipitation gradients respectively. Boxes extend from the 25th to the 75th percentile, while whiskers extend to 1.5 times the interquartile range of the lower and upper quartiles respectively. Bar-plots, included within each box-plot, depict the response of proxy plant species, grouped according to their drought tolerance. Light red, green, and blue fill colors correspond to low, medium, and high drought tolerance respectively. Bar-plots cover the 25th to 75th percentile of the distribution. Dashed red and blue lines highlight the mean model response across the elevation gradient ($f(x = \bar{X})$, i.e., mean of the box-plots) as obtained using all the simulated proxy species ($x = \bar{X}$), while continuous colored lines illustrate the obtained model response ($f(x = \bar{X})$) when only mean values of the empirical distribution of plant trait are used ($x = \bar{X}$), for dry and wet precipitation gradients respectively.

4.3.3 Species variability and aggregation-induced biases

Simulated carbon and water dynamics using an average proxy species, i.e., based on the mean values of the empirical distribution of plant traits, do not correspond to the mean of model responses obtained using proxy species from the entire plant trait distribution (solid and dashed lines in Figure 4.3 and 4.4). When the mean parameterization is used, the simulated carbon dynamics are consistently overestimated (solid lines in Figure 4.3). Simulated GPP, LAI, and ΔAGB with mean plant traits correspond often to the upper quartile, or even to the tail of the distribution of the results obtained using the entire empirical distribution of plant traits, underlining therefore positive aggregation-induced biases due to smoothing of trait variability (solid and dashed lines in Figure 4.3). Positive aggregation biases occur also for the case of biotic water fluxes (solid and dashed lines in Figure 4.4a, b, c), but less pronounced in comparison to that of the carbon dynamics. Since abiotic water fluxes are not significantly affected by species-induced variability (Section 4.3.2), the occurring aggregation biases

are smaller (solid and dashed lines in Figure 4.4d, e, f). Aggregation biases are also less pronounced when soil water dynamics are analyzed, with the exception of dry precipitation gradient where negative biases are identified. More specifically, in dry conditions the simulated SWC dynamics with an average species are lower than the species mean across the elevation gradient and correspond to the lower quartile of the full range of proxy species (solid and dashed lines in Figure 4.4g, h, i).

4.3.4 *Partitioning the output variance between climate- and species-induced variability*

In order to obtain a more traceable assessment of the importance of species variability, a variance decomposition was employed. This allows us to disentangle the influence of the two sources of variation in our modeling framework, namely heterogeneity in trait parameterization and climate.

As shown in Figure 4.3, simulated vegetation dynamics (GPP, LAI, and ΔAGB) are mostly controlled by species-induced variability in evergreen and grass plant-life forms. The variance decomposition shows that, particularly for the case of evergreens more than 80% of the variance in GPP, LAI, and ΔAGB is attributed to species parameterization (Figure 4.5a). In deciduous species, this effect is less pronounced since environmental conditions prevail at high elevations and constrain their performance and occurrence (Figure 4.3a, d, g), overwhelming the importance of trait variability (responsible for about 20-30% of variability in GPP, LAI, and ΔAGB ; Figure 4.5b). About 60% of the overall output variance in long-term simulated GPP and LAI for species with grass plant-life form is explained by trait variability. Environmental heterogeneity dominates biotic water fluxes, particularly for deciduous and grass plant-life forms (Figure 4.5a, c), while for evergreens, trait-induced differences still explain about 40% of the variability in annual transpiration (Figure 4.5b). Variability in abiotic water fluxes (total evaporation and soil water dynamics), for all the examined plant-life forms, is dominated by environmental conditions, which explain more than 90% of the total variance in evaporation and SWC (Figure 4.5).

4.3.5 *Leaf traits and their contribution to simulated plant responses*

The influence of leaf-trait variability and environmental heterogeneity on simulated carbon and water fluxes is illustrated in Figure 4.6 and 4.7. Among the four examined leaf-traits (specific leaf area, SLA, carbon-nitrogen mass ratio for the foliage N_f , maximum Rubisco capacity, V_{cmax} , and critical age for leaf shed, A_{cr} ; Figure 4.2), V_{cmax} has a consistent influence on the long-term simulated GPP (Figure 4.6) and transpiration (Figure 4.7) across all the examined environ-

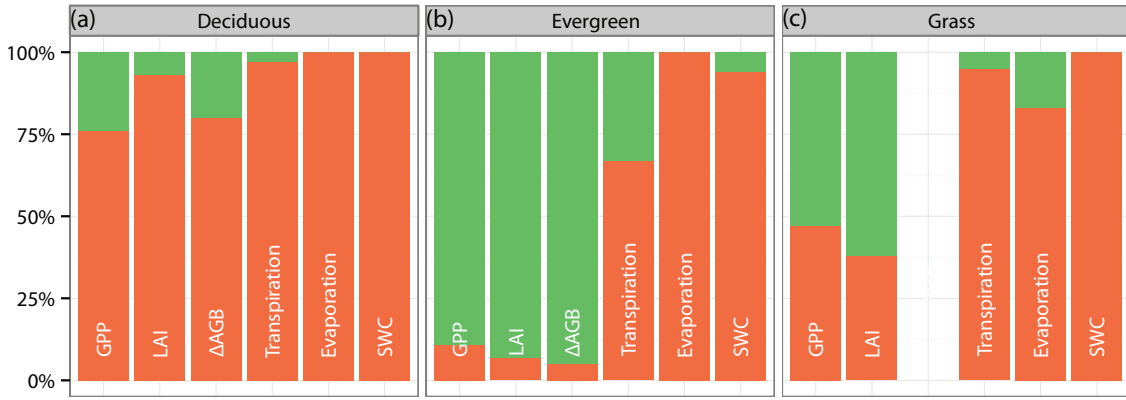


Figure 4.5: Partitioning of total variance in annual Gross Primary Productivity (GPP), Leaf Area Index (LAI), changes in woody aboveground biomass (ΔAGB), transpiration, total evaporation, and Soil Water Content available to plants (SWC) due to environmentally induced variability (i.e., elevation and precipitation gradients; depicted in orange) and trait variability (i.e., variability in leaf-traits and drought strategies; depicted in green) for deciduous (a), evergreen (b), and grass (c) plant-life forms.

mental conditions. For all plant-life forms, as V_{cmax} increases, annual GPP and transpiration increase (Figure 4.6c, g, k, and 4.7c, g, k, respectively). The variability in GPP induced by changes in V_{cmax} (i.e., horizontal axis in Figure 4.6c, g, k) is comparable (and for the case of evergreen species higher) to the variability due to environmental changes, expressed on the vertical axis in Figure 4.6c, g, k by elevation. SLA, N_f , and A_{cr} influence the model response but their relatively high cross-covariance with V_{cmax} (Figure 4.2) that exerts a predominant role in the model performance, does not allow for a clear signal in the surface plots (Figure 4.6 and 4.7).

4.4 DISCUSSION

The results presented in the previous sections highlight the importance of including floristic complexity (inter- and intra-specific trait variability) in terrestrial ecosystem models for a realistic representation of interactions between climate, hydrology and vegetation dynamics. An important role of trait-specific behavior, consistent across the examined climatic gradients, emerged from our simulation results. While the limitations of the PFTs conceptualization are well documented and widely recognized, our study, quantifies, for the first time in a controlled numerical experiment, the importance of considering multivariate trait distributions (accounting not only for the mean, but also for higher moments) in ecosystem modeling. An alternative, trait-based approach, is applied and results are illustrated using a state-of-the-art mechanistic model that combines land surface energy and water exchanges with plant functioning.

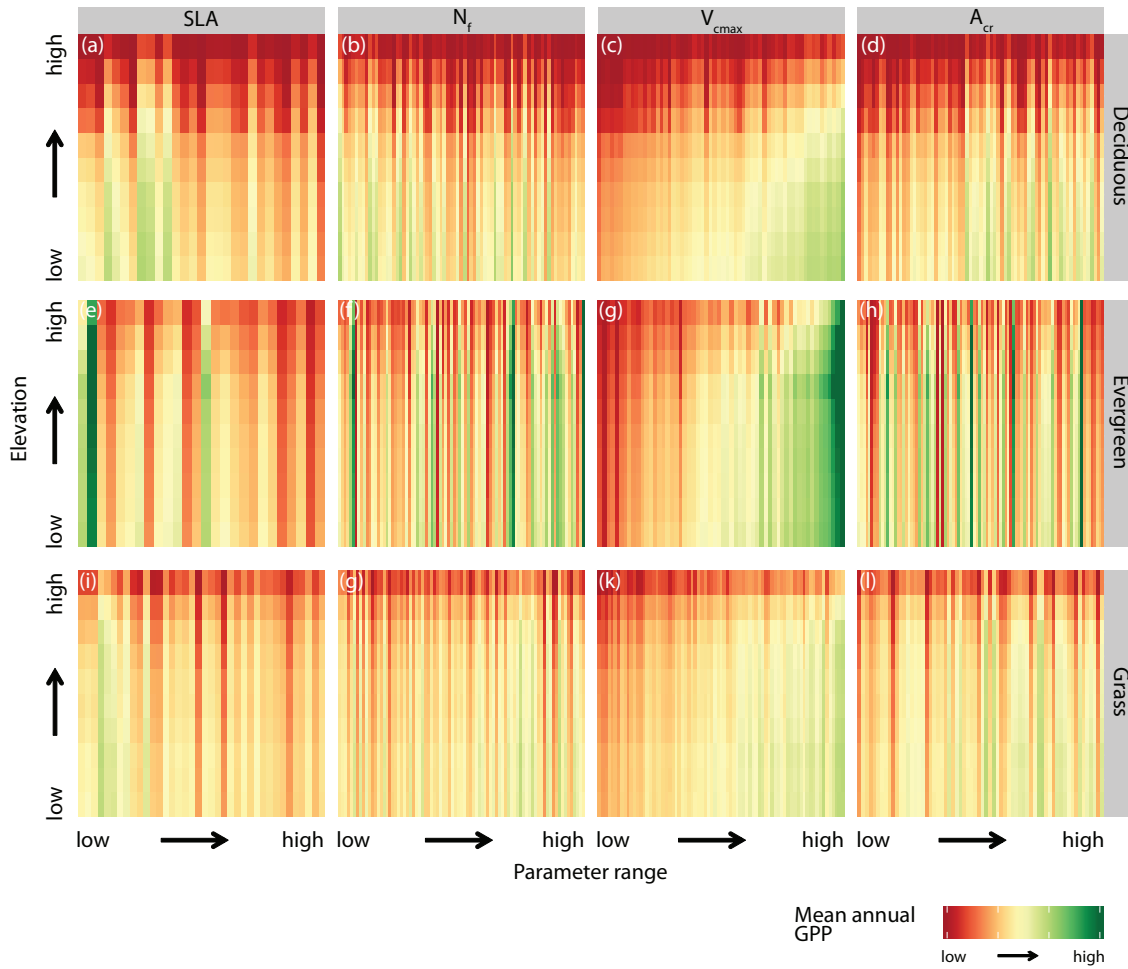


Figure 4.6: Surface-plots of the long-term response (25 yr) of photosynthetic activity (GPP) to environmental variability (summarized by elevation; vertical axis) and to major leaf-traits (specific leaf area, SLA, carbon-nitrogen mass ratio for the foliage N_f , maximum Rubisco capacity, V_{cmax} , and critical age for leaf shed, A_{cr} ; horizontal axis). The reported annual GPP corresponds to mean values over the precipitation gradients (wet, dry) and drought tolerances (low, medium, high).

4.4.1 Converging and diverging ecosystem responses to species-induced variability

Trait diversity leads to a broad range of plant functioning and thus to a highly divergent vegetation response when carbon and water dynamics are analyzed. Contrary to biotic, abiotic water dynamics show convergence with a relatively modest influence of trait-specificity. Ecosystem carbon fluxes are more affected, causing high variability in photosynthetic activity, leaf dynamics, and growth rates. Since carbon and water cycles are tightly coupled at the plant level, trait-induced variability also creates a divergent response of transpiration. In addition, different plant strategies for dealing with drought-tolerance (i.e., rooting depth, water-stress thresholds, and stomatal regulation) enhance the variability

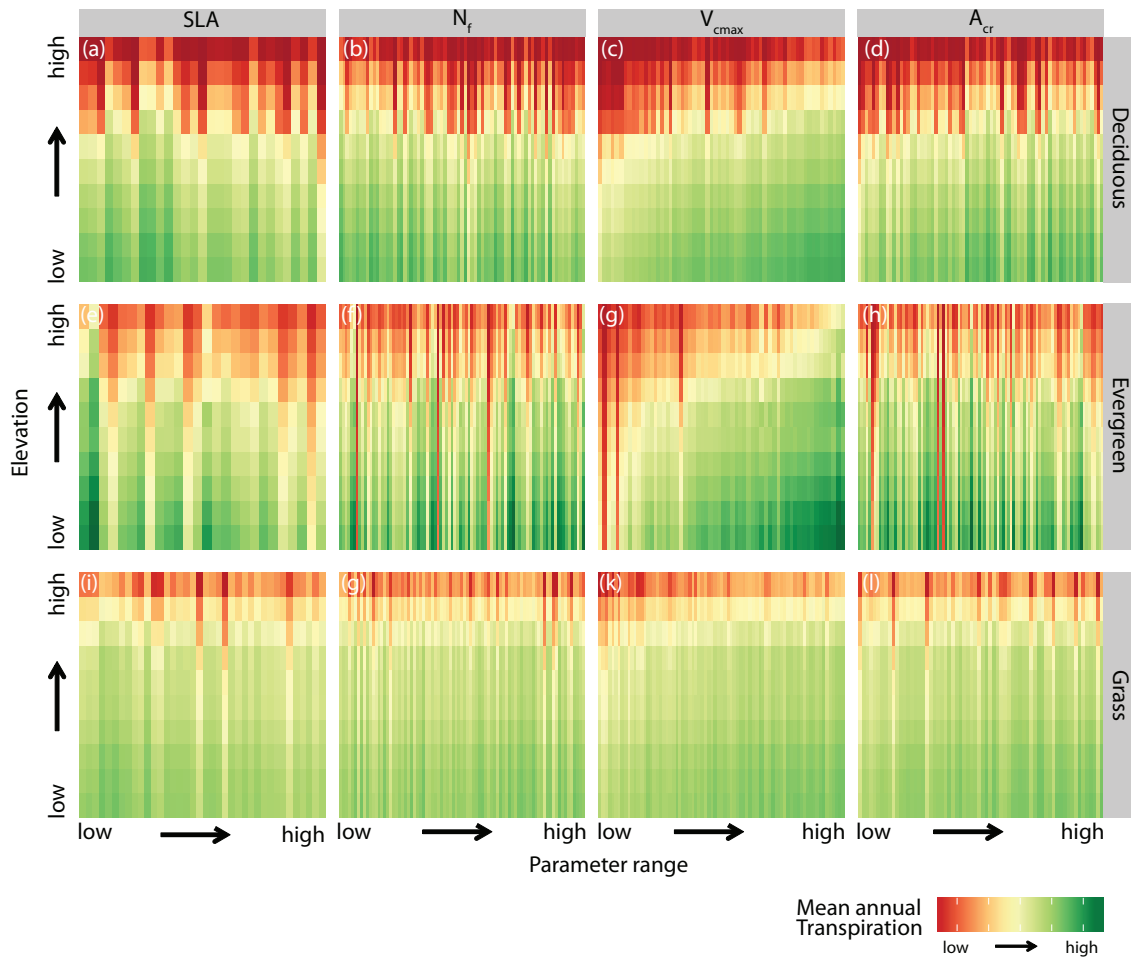


Figure 4.7: Surface-plots of the long-term response (25 yr) of plant-water fluxes (transpiration) to environmental variability (summarized by elevation; vertical axis) and to major leaf-traits (plant specific leaf area, SLA, carbon-nitrogen mass ratio for the foliage N_f , maximum Rubisco capacity, V_{cmax} , and critical age for leaf shed, A_{cr} ; horizontal axis). The reported annual transpiration corresponds to mean values over the precipitation gradients (wet, dry) and drought tolerances (low, medium, high).

of plant carbon and water dynamics, particularly in water-limited ecosystems (i.e., dry precipitation gradient, low elevations; Figure 4.1a). Water deficit poses constraints on plant functioning, forcing them to downregulate water-losses (transpiration) and, as a consequence, carbon assimilation. For instance, for the dry precipitation gradient, in the same elevation, species with high drought tolerance outperform the ones with medium or low tolerances, as shown in Figure 4.3 and Figure 4.4a, b, c. These high divergent responses among species, revealed by our controlled simulations, have been widely supported by field observations. Some recent experimental evidence showed indeed how species-specific sensitivities to environmental conditions (not only climate, but also nutrient availability as well as community effects) lead to different plant physiolog-

ical responses in terms of carbon assimilation [Niu *et al.*, 2012] and transpiration [Link *et al.*, 2014].

4.4.2 *Variety versus evenness: the fallacy of averages and the emerging aggregation biases*

Using a Monte-Carlo framework for mimicking plant diversity, our analysis quantifies explicitly the aggregation-induced biases due to smoothing for species variability and supports the idea that higher moments of the empirical trait distribution deserve further consideration. Parameterizing plant functioning using mean values of observed trait distribution hides the inter- and intra-specific trait variability that is often not negligible, as shown by our experiments and supported by recent literature [Albert *et al.*, 2010a, b; Messier *et al.*, 2010; Albert *et al.*, 2011; Bolnick *et al.*, 2011; Cadotte *et al.*, 2011; Violle *et al.*, 2012; Kichenin *et al.*, 2013]. As some recent experimental evidence demonstrates: “the amount of variation around the mean trait value of a species can be as important as the mean itself” [Messier *et al.*, 2010]. Biodiversity and floristic complexity that are reflected in higher moments (e.g., variance) of the trait distribution [Ackerly, 2003; Webb *et al.*, 2010; Violle *et al.*, 2012] can be incorporated in terrestrial ecosystem models, as our study demonstrates, to obtain a more realistic representation of the vegetation component.

Parameterizing species diversity using discrete categories with prescribed (and static) properties is hampered by the nonlinearities of vegetation functioning. Even when the mean values of the empirical (observed) trait distributions are used [mean-field approach; Violle *et al.*, 2012], the high nonlinearities of biophysical and plant physiological processes (e.g., stomatal conductance and photosynthesis coupling) downgrade the information content of the first moment of the distribution [Jensen’s inequality; Jensen, 1906] leading to the so called *fallacy of averages* [Wagner, 1969; Welsh *et al.*, 1988; Pappas *et al.*, under review-a]. Aggregation biases therefore emerge when average plant parameterizations are employed such as the case of using a handful of discrete PFTs. The mean response of highly diverging plant characteristics does not necessary coincide with the response obtained using mean plant attributes, as clearly highlighted in Section 4.3.3 and Figure 4.3 and 4.4. Even though mean values of detailed plant physiological properties are often used for model-data comparisons, e.g., to match observations from eddy covariance fluxes, they have a limited predictive power due to nonlinearities of the processes in which they are involved [Medlyn *et al.*, 2002b; Laughlin *et al.*, 2011].

4.4.3 *Species variability outweighs environmental heterogeneity*

While the dominant role of climate in biological processes is indisputable, since climatic and energetic factors can limit plant functioning, occurrence, and performance [Paruelo *et al.*, 1999; Kleidon and Mooney, 2000; Körner, 2000; Kleidon *et al.*, 2007, 2009; Reu *et al.*, 2011; Araújo and Costa-Pereira, 2013; Gao *et al.*, 2013; Hurlbert and Stegen, 2014], our analysis brings quantitative evidence that species representation plays a significant role in ecosystem responses. When plant carbon- and water-dynamics are jointly analyzed, species variability is often comparable to climate-induced heterogeneity (Figure 4.5). This contrasts with the much larger attention that has been paid to the environmental forcing in the realm of Earth system modeling, especially with regard to analyses of interactions between climate, hydrology and ecosystems.

It is true that living organisms do not experience climate in coarse resolution [Potter *et al.*, 2013]. There has been a great effort therefore during the last decade towards finer resolution meteorological forcings which was reflected in the increasing spatial resolution of climate model outputs [from 500 km at the beginning of '90s to 50 km at the end of 2010; Jones, 2013] or through the development of high-resolution modeling tools [Tague and Band, 2004; Ivanov *et al.*, 2008a; Hwang *et al.*, 2009; Wood *et al.*, 2011; Fatichi *et al.*, 2012a; Pappas *et al.*, under review-a]. The spatial resolution of environmental forcing, in global scale application (e.g., with ESMs and DGVMs), has been therefore increased by roughly one order of magnitude. On the contrary, an equivalent change did not happen with respect to modeling plant diversity. Even the carbon cycle analyses in the Fifth Assessment Report (AR5) of the United Nations Intergovernmental Panel on Climate Change are still based on a handful of PFTs [IPCC, 2013, Ch. 6]. This uneven progress in model developments between boundary conditions and environmental drivers on the one hand, and floristic complexity, on the other, does not provide the appropriate framework to highlight the mechanisms that control terrestrial ecosystem dynamics. Simulated carbon- and water-dynamics are strongly controlled by species-specific attributes. There is therefore a compelling need -especially in studies focusing on the response of vegetation to climate change- for enhancing the ecological realism within models by accounting for inter- and intra-specific trait variability, as well as for how traits evolve, e.g., plant adaptation, dispersal, and community dynamics [see for example Norberg *et al.*, 2012, where these aspects are highlighted].

4.4.4 *Broader implications and ways forward*

Trait variation can change the outcome of ecological responses and therefore deserves further consideration in local and global scale assessments, for instance when the response of terrestrial ecosystem under extremes [Reichstein *et al.*, 2013;

Bahn et al., 2013], or global carbon cycle dynamics [*Cox et al.*, 2013; *Graven et al.*, 2013] are analyzed. Redundancy in plant traits and functioning has, however, also broader implications. Biodiversity is intrinsically coupled with plant physiological responses [see *Hooper et al.*, 2005, for a detailed review]. There is growing experimental evidence that species diversity enhances productivity [*Tilman et al.*, 1997; *Tilman*, 1999; *Hector et al.*, 1999; *Grace et al.*, 2007; *Morin et al.*, 2011] and affects ecosystem resilience [*Naeem and Li*, 1997; *Peterson et al.*, 1998; *McCann*, 2000; *Pfisterer and Schmid*, 2002; *Díaz et al.*, 2006; *Tilman et al.*, 2006]. These effects should therefore be accounted for in climate change studies that investigate plant extinction risks, species range shifts or carbon source-sink dynamics.

Building upon the community ecology, trait-based approaches have been recently articulated for dealing with plant functional dissimilarity within terrestrial ecosystem models (aDGVM2, *Scheiter et al.* [2013]; JeDi, *Pavlick et al.* [2013]). Along these lines, we would like to advocate the need for: (i) incorporating species inter- and intra-specific variability using multi-trait spectra (Table 4.1), (ii) parameterizing plant functioning preserving the entire empirical multivariate distribution of plant-trait variation (Figure 4.2) rather than preserving, at best, only the first moment of the distribution, (iii) communicating model simulation results in a probabilistic manner (e.g., Figure 4.3 and 4.4) rather than providing single-value outputs (obtained using discrete and static plant attributes). In this regard, insightful simulations would profit from knowing not only the probability distributions of plant traits and their cross-correlations, but also their frequency of occurrence in different geographical areas. Remote sensing is in this respect a promising observational technique.

Plant trait spectra are not panacea, but offer a remedy for increasing the level of plant functional diversity within models. Following the recently popularized traits manifesto [*Reich*, 2014], an integrated whole-plant economics spectrum will allow for an elegant approximation of plant attributes within terrestrial ecosystem models. The origin of LES is still an open question and several hypothesis have been proposed [see *Sack et al.*, 2013, for a recent review]. Some trait cross-correlation may be spurious [*Jasienski and Bazzaz*, 1999; *Osnas et al.*, 2013; *Lloyd et al.*, 2013], and the identified correlations do not necessary imply causalities [*Osnas et al.*, 2013; *Lloyd et al.*, 2013]. Nonetheless, accounting for the observed trait variances and covariances within models improves model consistency, since it allows for a realistic representation of plant responses to resources availability thus unfolding whole plant economic strategies with respect to water, light, and nutrients [*Westoby et al.*, 2013; *Poorter et al.*, 2014]. While traits correlations have been partly already implemented in DGVMs -for example SLA is calculated through leaf longevity using an empirical relation presented in *Reich et al.* [1997] in the LPJ [*Sitch et al.*, 2003]- or by constraining the parameter space using observed leaf-trait covariances [*Wang et al.*, 2012], these implementations are of deterministic nature. We would like to emphasize the need for a probabilistic approach for simulating plant diversity, which propagates the ob-

served whole-plant multivariate trait distribution within models and not only cross-correlations among traits. Our analysis illustrates this approach by generating proxy plant species from an observed leaf-trait pool. This concept is well established within the frame of uncertainty analysis [e.g., [Ziehn et al., 2012](#); [LeBauer et al., 2013](#)] and Bayesian inference [[Clark, 2004](#); [Clark and Gelfand, 2006](#); [Hartig et al., 2012](#); [Efron, 2013](#)], but with different objectives. Here, we are not searching for the best parameter set (i.e., proxy species) that reproduces the observed responses (single-value outputs), but we propagate into the model the observed empirical multivariate trait probability distribution by Monte-Carlo simulations, since all the observed (measured) trait values have a probability of occurrence, related to the trait distribution in a given area. In this way, we obtain realistic, probabilistic representation of ecosystem responses. The increasing data availability [e.g., [Reich, 2014](#), for a recent review] and monitoring techniques (e.g., remote sensing, [Homolová et al. \[2013\]](#); plant phenotyping platforms [Granier and Vile \[2014\]](#)) facilitate the identification of probability distributions underlying multi-trait spectra and thus the applicability of such probabilistic approaches.

4.4.5 *Uncertainties and limitation*

Species richness is approximated in our simulations using three plant-life forms (deciduous, evergreen, and grass), three discrete plant drought strategies (low, medium, and high drought tolerance), and 100 proxy-species with coordinated leaf traits based on empirical statistical properties from the LES. This is a moderate, first approximation of species diversity. Several (continuous and not discrete) plant drought strategies exists and the LES covers only 1% of the documented vascular plant species [[Wright et al., 2004](#)]. Therefore, evidence from our results can potentially be more pronounced especially when whole-plant trait spectra are used, accounting for trait variation in other organs apart from leaf (e.g., root, sapwood). At the same time, we also assume that traits are following the LES distribution without weighting the values according to the frequency of species occurrence. This may increase the overall trait variability, particularly for the evergreen plant-life form, affecting also the variance partitioning (Figure 4.5).

Our analysis is moreover characterized by few additional limitations due to the numerical tools used for simulating ecosystem responses. More specifically, T&C simulates vegetation in a mature state without accounting for plant competition, establishment and mortality different from carbon starvation. The response of each proxy-species is also tested in isolation, ignoring the demographic effects related to species establishment and competition, community dynamics, as well as disturbances. Nutrient limitations, although very important [[Fernández-Martínez et al., 2014](#)], are not directly simulated in T&C. Finally, while

biotic and abiotic factors are intrinsically coupled in nature [land-atmosphere interactions and feedbacks; *Pielke et al.*, 1998; *Pielke*, 2001; *Currie*, 2007; *Field et al.*, 2007; *Bonan*, 2008b; *Chapin et al.*, 2008; *Seneviratne et al.*, 2010; *Pielke et al.*, 2011; *Kichenin et al.*, 2013], in these simulations environmental conditions (model input) and species representation (model parameters) are independent, i.e., plant traits do not affect the climatic forcing, and vice versa. This is a simplified assumption since prevailing environmental conditions and nutrient availability at a given site can shape plant functional traits [e.g., *Díaz et al.*, 1998; *Savage et al.*, 2007; *Ordoñez et al.*, 2009; *Messier et al.*, 2010; *Cadotte et al.*, 2011; *Wright and Sutton-Grier*, 2012; *Kichenin et al.*, 2013]. However, this assumption allows for a complete variance decomposition of model outputs (Figure 4.5). Carbon- and water-fluxes and their variation across elevation, are also reasonably simulated as illustrated by the good agreement with the compiled eddy flux measurements, MODIS, and NFI data. Thus, we are persuaded that the conclusions of our study are not significantly affected by the aforementioned assumptions.

4.5 CONCLUSIONS

To the question if plant diversity matters with regard to the simulated ecosystem responses, our conclusions are three-fold: (i) simulated carbon dynamics are strongly conditioned by trait-specific attributes; (ii) transpiration is also affected but to a lesser extent; and (iii) abiotic water fluxes are generally unaffected by trait-induced variability. These findings highlight the need for revising the representation of biotic attributes (species representation) within terrestrial ecosystem models, moving beyond the discrete and static conceptualization of PFTs and the associated limitations. Alternative, probabilistic approaches should be thus adopted, which mimic the floristic complexity using multivariate distributions of coordinated whole-plant trait spectra, enhanced with trait abundance information from remote sensing. This will allow for a better representation of terrestrial ecosystem dynamics and their responses under climate variability.

CONCLUSIONS AND OUTLOOKS

5.1 MAJOR CONCLUSIONS

5.1.1 *On a comprehensive model evaluation*

Process-based numerical models of terrestrial ecosystem functioning are necessary tools for an holistic understanding of water and carbon dynamics and the underlying mechanisms and feedbacks. However, they are often characterized by high complexity and dimensionality due to the multiple encapsulated processes, ranging for example from the leaf level (e.g., photosynthesis, transpiration), to the stand scale (e.g., plant resource competition), to the landscape (e.g., disturbances such as fire events) and beyond. Therefore, model intercomparison studies and model evaluation against observations are not enough for scrutinizing model strengths and weaknesses. Mimicking terrestrial ecosystem dynamics imply more than a simple agreement with observed variables, especially when long term or climate non-stationary quantitative predictions are envisioned.

Advanced statistical tools, such as the global sensitivity analysis presented in Chapter 2, offer an elegant way for a comprehensive evaluation of high dimensional, non-linear models, assessing not only the importance of model parameters, but also model structural limitations. Since process-based tools embed physical causalities, the sensitivity of the simulated processes should reflect the observed, real-world sensitivities. Using state-of-the-art statistical methodologies I could show that photosynthesis is the cornerstone of LPJ-GUESS, and possibly of other, structurally similar, dynamic vegetation models. Simulated vegetation carbon fluxes and pools are highly sensitive to plant physiological parameters related to photosynthesis. At the same time, the sensitivity to parameters controlling water availability was found to be very low. Both of these results highlighted the urgent need for (i) revising vegetation models with regards to the representation of spatial heterogeneities and soil water dynamics and feedbacks (issue addressed in Chapter 3), (ii) enhancing the representation of plant trait variability that significantly control vegetation responses such as carbon assimilation (issue addressed in Chapter 4).

5.1.2 *On the spatial heterogeneities and boundary conditions*

By spatially disaggregating a dynamic vegetation model and applying it at the catchment scale, where multivariate observations are available, I quantified how the coarse spatial representation leads to aggregation-induced biases (Chapter 3). A novel ecohydrological scheme (D-LPJ) was developed, operating at a fine spatial resolution, using not only detailed meteorological inputs, but also enhanced, spatially explicit representations of vertical and lateral water fluxes as well as local scale information of the current land cover.

Combining tools with contrasting degrees of abstraction and spatiotemporal representations, I could show that local scale spatial heterogeneities, which are often ignored or at best crudely represented in model applications at the regional and global scales, exert a strong control on plant response. Preservation of local environmental and topographic attributes, as proposed with the fine resolution grid of the D-LPJ model, represents therefore an important feature to achieve a more realistic approximation of ecosystem dynamics, particularly at the regional or catchment scales with complex topography.

Model initialization using local scale information is also crucial, since the boundary conditions (soil and vegetation carbon stocks in particular), affect the long term terrestrial carbon balance, as well as the capacity of the forest to store carbon. A realistic assessment of future carbon stocks cannot be separated from an accurate representation of these heterogeneities and local scale trajectories. The assumption of steady-state vegetation and soil carbon pools, incorporated in vegetation models for pragmatic reasons, needs therefore to be revised, and eventually replaced using local scale information, incorporating tree demography inputs from forest inventories, as for example the results of D-LPJ simulations highlight, or using advanced remote sensing products.

Ecosystems are often out of equilibrium and do not experience climate at coarse scales, but react to local controls, particularly with respect to soil-vegetation interactions. When process-based models are therefore used, and confidence on their results is based on their “physical-correctness and consistency” as well as the embedded causalities, then the “physics” should be solved at appropriate scales with appropriate forcings.

5.1.3 *On the ecological realism and species variability*

Vegetation diversity in many terrestrial ecosystem models is crudely represented using a discrete classification of a handful of “plant types” (named Plant Functional Types; PFTs). The parameterization of PFTs typically reflects mean properties of observed plant functional traits over broad categories ignoring most of the inter- and intra-specific trait variability. A novel Monte Carlo frame-

work was developed to address this issue, simulating proxy plant species from observed multivariate trait distribution, and assessing their performance across continuous environmental gradients with a mechanistic ecohydrological model (Chapter 4).

Having investigated the sensitivity of ecosystem responses to species-induced variability and compared it with climate-induced variability, the importance of species diversity in simulated carbon and water dynamics was quantified. Species diversity leads to highly divergent vegetation carbon dynamics (fluxes and pools) and to a lesser extent water fluxes (transpiration). Abiotic processes, such as soil water dynamics and evaporation, are only marginally affected. These findings highlight the need for revising the representation of biotic attributes (species representation) within terrestrial ecosystem models, moving beyond the discrete and static conceptualization of PFTs and the associated limitations.

Floristic complexity (inter- and intra-specific trait variability) should be enhanced in terrestrial ecosystem models in order to achieve a realistic representation of interactions between climate, hydrology and vegetation dynamics. Probabilistic approaches, based on empirical multivariate distributions of coordinated plant trait spectra, as presented in Chapter 4, provide a viable alternative. This will allow for a better representation of terrestrial ecosystem dynamics, as well as their responses and resilience under climate variability.

5.2 OUTLOOK FOR FURTHER RESEARCH

5.2.1 *Towards better resource allocation schemes*

Carbon allocation remains the Achilles' heel of vegetation models [Le Roux *et al.*, 2001]. As demonstrated by the detailed sensitivity analysis, presented in Chapter 2, the generally simplistic and static carbon allocation schemes underlying current terrestrial ecosystem models (from plot scale forest growth models, to catchment scale ecohydrological representations, and to regional and global scale dynamic vegetation models) create high sensitivity of plant functioning and growth to photosynthesis, neglecting processes such as carbon reserve dynamics and direct growth limitation by temperature, water, or nutrient. Such processes may have a significant implications for many studies assessing for example the source or sink dynamics of forested areas or the ecosystem resilience under changing environmental conditions.

Several approaches for modeling resources allocation (carbon and nutrients) have been proposed, and reviewed by Cannell and Dewar [1994] as well as recently by Franklin *et al.* [2012]. Five main categories can be distinguished, following the classification presented by Franklin *et al.* [2012], namely: (i) empirical

approaches, using data-derived fix ratios of resource partitioning among plant organs; (ii) allometric scaling approaches, using for example species specific allometric relations documented by forest inventories; (iii) functional balance approaches where resources are allocated on the basis of the limiting environmental factor (e.g., under water-limited conditions, more resources are allocated to water-abstraction organs); (iv) eco-evolution based approaches including optimality principles, game-theory, and adaptive population dynamics; (v) thermodynamic approach, using the well established principle of Maximum Entropy Production (MEP).

Unfortunately, within the frame of vegetation modeling, not all the aforementioned approaches have been implemented and extensively tested. A common practice in vegetation models is to model resource allocation as a static component, using mostly the empirical and static allometric rules, enhanced, in some cases, with predefined environmental controls such as water or light. The results presented in Chapter 2 highlight the urgent need for revising such approaches since they do not allow for comprehensive modeling of plant functioning and thus for robust long-term carbon dynamics (fluxes and stocks).

Allocation cannot be considered as an individual process, such as for example photosynthesis, but emerges as a consequence of several coordinated processes [Franklin *et al.*, 2012; Mäkelä, 2012]. In addition, defining the way in which plants allocate their resources to different organs implies defining not only their ecological strategy, but also their structural advantages over other species [Le Roux *et al.*, 2001; Franklin *et al.*, 2012]. In this regard, the formalism of MEP offers a great potential for a more tractable simulation of plant resource dynamics, imposing a well-established top-down guiding principle to plant functioning. It is worth therefore to be implemented and tested in vegetation modeling studies. The increasing data availability of forest architecture and demography, e.g., through forest inventories and modern remote-sensing data, offers a great potential of evaluating such approaches at larger simulation domains. A better representation of plant resource allocation within terrestrial ecosystem models will enhance our understanding of forest growth and the intrinsically coupled carbon and water dynamics.

5.2.2 *Towards better up-scaling approaches*

Having gained insights into the magnitude of aggregation-induced biases due to smoothing of spatial heterogeneities, hereafter I advocate the need of solving the processes at the appropriate scales, when bottom-up modeling tools are used. This is particularly true when topographically complex landscapes are analyzed (Chapter 3). Organisms do not experience climate in coarse scales [Potter *et al.*, 2013]. Therefore a more realistic representation of spatial heterogeneities within process-based terrestrial ecosystem models should be implemented. This can be

done, as presented in Chapter 3, using a fine resolution spatial representation, accounting for topographic attributes, lateral water fluxes, and local scale land cover, following the process-based ecohydrological paradigm. However, when larger domains are examined, the computational burden often poses limitations on the applicability of such numerical tools.

If solving processes at the appropriate scales is computationally too demanding, given the available resources, then alternative, statistical and/or top-down approaches may represent a conceptually better approximation of the functioning of global scale terrestrial ecosystem. For instance, a statistical-dynamical approach [e.g., *Giorgi and Avissar, 1997*] can be incorporated in terrestrial ecosystem modeling using the observed (empirical) probability density function of local scale attributes, thus describing the heterogeneity of the meteorological forcing in the examined domain, or that of vegetation traits [*Reich, 2014; Pappas et al., under review-b*]. The potential of using well established approaches from other disciplines dealing with complex non-linear systems, such as the scale transition theory developed within the frame of population and community ecology [*Chesson, 2012*], the multiscale modeling and simulation framework developed explicitly for dealing with non-linear, multidimensional hierarchical systems [*Chopard et al., 2014*], as well as organizing principles [e.g., *Prentice et al., 2014; Dyke and Kleidon, 2010; Dewar, 2010; Dewar et al., 2009; Whitfield, 2007; Mäkelä et al., 2002*], is also worth to be explored. Similarly to the thermodynamic approach of modeling resources allocation (Section 5.2.1), organizing principles can provide a top-down constrain to simulated ecosystem responses at large scales, correcting therefore potential aggregation-induced biases due to scale mismatches. The applicability and efficiency of organizing principles, such as the MEP [e.g., *Dewar and Porté, 2008; Dewar, 2009, 2010; Kleidon, 2010*] has already been extensively demonstrated at local scales [e.g., *Schymanski et al., 2010*] and remains to be further explored at global scale and for terrestrial ecosystem simulations.

5.2.3 Towards a predictive framework of terrestrial ecosystem responses

Numerical models of terrestrial ecosystem functioning are developed not only for purely scientific curiosity, i.e., better process understanding, but ultimately for societal purposes, through a predictive framework of ecosystem responses under climate variability and anthropogenic interventions. To this end, synthesizing the results and outlooks articulated in the previous Sections, I would conclude that a predictive framework of terrestrial ecosystem functioning is possible only by confining our process understanding with probabilistic theory.

Three definitive arguments towards this direction are summarized below:

- *Fixed values vs random variables*

Natural processes are approximated in models using parameters. The word parameter is not chosen by chance; it comes from the Greek word *παρά* meaning *beside, beyond*, and *μέτρον*, meaning *measure*¹. In essence, parameters are used to describe and infer properties that go beyond measurements. Even in process-based models, where parameters are often claimed to have a physical meaning, the spatiotemporal scale mismatch between measurements and model applications hampers direct inference of parameter values from observations. Furthermore, the spatiotemporal heterogeneities, together with inter- and intra-specific variability of plant traits, make the extrapolation of plot-scale observations to the simulation domain even more difficult. Therefore, parameters should be treated as random variables, using well-established concepts of probabilistic theory rather than discrete and static values inferred from observations.

- *Mean values vs entire probability distribution*

Assigning parameter values based on the empirical mean of the observed values may be misleading due to the non-linearities of the simulated processes, leading to the, so called, *fallacy of averages*. This is demonstrated in Chapter 3, where the aggregation-biases caused by the smoothing of spatial heterogeneities are quantified, as well as in Chapter 4, where the importance of the higher moments in the plant trait distribution is discussed. By prescribing not only the mean but also higher moments of empirical distribution of the random variables (model parameters), would therefore allow for a better system representation. In addition, this will allow for a better representation of the underlying uncertainties, single-value model outputs would be replaced with probabilistic statements, following the distribution of the simulated outputs.

- *Static vs dynamic parameterizations*

Motivated by the aphorism of Theodosius Dobzhansky that “*nothing in biology makes sense except in the light of evolution*” [Dobzhansky, 1973], I would argue that the static parameterization of plant activity, ignoring short- and long-term plant physiological adjustments is a major drawback for current vegetation models analyzing the long-term terrestrial ecosystem responses. Parameterizing plant activity by means of random variables together with top-down thermodynamic constraints such as the MEP, will allow for a more mechanistic representation of short- and long-term plant adaptive dynamics and their implications for the carbon and water cycle.

¹<http://en.wikipedia.org/wiki/Parameter>

APPENDIX A: SENSITIVITY ANALYSIS OF A PROCESS-BASED ECOSYSTEM MODEL: PINPOINTING PARAMETERIZATION AND STRUCTURAL ISSUES

A.1 SCREENING EXERCISE: ELEMENTARY EFFECTS

Screening methodologies provide adequate qualitative information of model sensitivity with low computational cost [Saltelli et al., 2000a]. The basic idea of screening approach is based on the Pareto's principle. Many studies have shown that model structures tend to have few very influential parameters and a majority of non-influential ones [Saltelli et al., 2000a].

A special case of screening sensitivity analysis is the method of elementary effects (EE) which was originally proposed by Morris [1991]. The method is based on individually randomized many one-at-a-time designs. One-at-a-time design is refereing to a design where one parameter is changing each time while keeping all other fixed. After the permutation, the parameter is fixed back to its standard value (baseline). The same applies sequentially to all the examined parameters. Derivatives with wide range of variation are calculated over the parameter space and their average values are used to provide a global sensitivity metric. Assuming that $Y = f(\mathbf{X})$ is a generalized model and $\mathbf{X} = \{X_1, \dots, X_k\}$ is a vector of parameters (random variables), where k is the total number of investigated parameters, then each of the random variables is assumed to vary across p selected levels of its uncertainty range. Thus, the parameter space consists of a k -dimensional p -level grid. The EE of the i^{th} parameter is defined as

$$EE_i = \frac{Y(x_1, \dots, x_i + \Delta, \dots, x_k) - Y(x_1, \dots, x_k)}{\Delta} \quad (\text{A.1})$$

where $\{x_1, \dots, x_k\}$ is a realization of the random variables $\{X_1, \dots, X_k\}$, representing a point in the k -dimensional p -level grid and Δ is the variation size taking values in $\{1/(p-1), \dots, 1 - 1/(p-1)\}$. Note that capital letters are used for random variables, small letters for their realizations and bold for vectors and matrices.

The basic statistics, mean (μ_{EE}) and standard deviation (σ_{EE}), of a number of incremental ratios (EE), are the sensitivity measures suggested by Morris for parameter ranking. The mean of EE, μ_{EE} , is proposed by Morris [1991] as an estimator of the overall influence of a parameter to the output, and the standard

deviation of EE, σ_{EE} , as an indicator for the higher-order parameter effects. The total cost of the analysis (model evaluations) depends on the number of parameters (k) and the number of randomly generated trajectories (r), i.e., EE calculated for each parameter, and it is calculated as $r \times (k + 1)$. As previous experiments have demonstrated [Campolongo and Saltelli, 1997; Campolongo et al., 1999; Saltelli et al., 2000a, 2008], a reasonable choice of r , p , and Δ , which we also adopted for this study, is $r = 10$, $p = 4$, and $\Delta = p/[2(p - 1)] = 2/3$.

The importance of model parameters is categorized according to μ_{EE} and σ_{EE} in three types: (i) negligible (low values of μ_{EE} , σ_{EE}), (ii) linear and additive (high values of μ_{EE} and low values of σ_{EE}) or (iii) non-linear or involved in interactions with other parameters (high values of σ_{EE}). For an easier interpretation of the results, Morris suggested a graphical representation: μ_{EE} and σ_{EE} estimators for each parameter are displayed in a plane (scatterplot) whose Cartesian coordinates are the (μ_{EE}, σ_{EE}) pairs.

The recent improvements suggested by Campolongo et al. [2007] are also applied to the original Morris experiment. The absolute mean value of EE (μ_{EE}^*) is used instead of μ_{EE} . As Campolongo et al. [2007] demonstrated, μ_{EE}^* is considered as more robust sensitivity metric especially for the case of non-monotonic functions. Furthermore, in order to maximize the coverage and the spread of the sampled points in the k -dimensional p -level grid, we first generated $R = 1000$ trajectories and the $r = 10$ trajectories with the highest spread (i.e., highest relative distance among them) were finally selected [Campolongo et al., 2007]. Maximizing the spread of the trajectories, improves the coverage of the sampling, without increasing the computational cost of the method (i.e., number of model evaluations). In this study, to facilitate the interpretation of the results and the ranking of parameters, instead of using (μ_{EE}, σ_{EE}) plots suggested by Morris, the Euclidian distance, $\epsilon = \sqrt{\mu_{EE}^{*2} + \sigma_{EE}^2}$, of $(\mu_{EE}^*, \sigma_{EE})$ from the origin $(0, 0)$ was used for parameter ranking. In the case of non-linearities and parameter interactions, this is a fair approximation of overall parameter sensitivity.

A.2 VARIANCE-BASED SENSITIVITY ANALYSIS

Variance-based sensitivity methods are elegant tools for performing model-free, coherent and quantitative Global Sensitivity Analysis (GSA). The underlying assumption is that all the information about model uncertainty is captured by its variance. The aim is to apportion a fraction of the overall output variability to each of the model parameters (conditional variances), accounting also for their interactions.

Sobol' sensitivity indices are based on Sobol's variance decomposition [Sobol', 1993] and offer a thorough evaluation of parameter importance and interactions. First and higher order effects are explicitly assessed after a detailed, compu-

tationally expensive, travel across the multidimensional parameter space. The method of Sobol' is based on the traditional analysis of variance (ANOVA) [Archer et al., 1997]. In summary, a function (i.e., the model response), $Y = f(\mathbf{X})$ is decomposed through a functional ANOVA into summands of increasing dimensionality:

$$\begin{aligned} f(\mathbf{X}) &= f(X_1, \dots, X_k) = \\ &= f_0 + \\ &\quad \sum_{i=1}^k f_i(X_i) + \sum_{i=1}^k \sum_{j>i}^k f_{ij}(X_i, X_j) + \dots + f_{12\dots k}(X_1, \dots, X_k) \end{aligned} \quad (\text{A.2})$$

Obviously, there are many different ways to decompose $f(\mathbf{X})$ in the form of Equation A.2, but provided that (i) the vector \mathbf{X} consists of independent parameters, (ii) f_0 is a constant ($f_0 = E[Y]$) and (iii) all the other terms in Equation A.2 are selected such that they are square integrable with zero mean, then the decomposition is unique [Sobol', 1993]. Once we square and integrate the Equation A.2, we can partition the total output variance, V_Y , into terms of increasing dimensionality:

$$V_Y = V[Y] = V[f(\mathbf{X})] = \sum_i^k V_i + \sum_{i=1}^k \sum_{j>i}^k V_{ij} + \dots + V_{12\dots k} \quad (\text{A.3})$$

where $V_i = V[E[Y|X_i = x_i^*]]$, $V_{ij} = V[E[Y|X_i = x_i^*, X_j = x_j^*]] - V_i - V_j$, and so on. $E[\cdot | \cdot]$ is the conditional expectation, and x_i^* , x_j^* denote the *real* values of the parameters i and j , respectively. In other words, similar to the ANOVA concept, the total output variance is partitioned to different sub-components which contribute to the overall output variability [Archer et al., 1997; Chen et al., 2005]. The sensitivity indices are then derived as the ratios of partial variances contributed by specific parameters of interest over the total output variance:

$$1 = \sum_i^k S_i + \sum_{i=1}^k \sum_{j>i}^k S_{ij} + \dots + S_{12\dots k} \quad (\text{A.4})$$

where S_i is the first order sensitivity index (or main effect) of the i^{th} parameter, S_{ij} is the second order sensitivity index which represents the interactions of the i^{th} and j^{th} parameters and so on. Accordingly, the total sensitivity index, S_{Ti} which represents the overall parameter importance (first and higher order effects), for the orthogonal case (i.e., independent parameters) is the sum of all the sensitivity indices of Equation A.4 that include the i^{th} parameter [Saltelli et al., 2004]. The first and total order sensitivity indices are estimated

since they include the most essential information and they offer a robust estimation of parameter importance and interactions [Homma and Saltelli, 1996; Saltelli, 2002].

The first order sensitivity index of parameter X_i is defined as:

$$S_i = \frac{V_i}{V_Y} = \frac{V[E[Y|X_i]]}{V[Y]} \quad (\text{A.5})$$

The variance of the conditional expectation $V[E[Y|X_i]]$, known also as main effect, represents the expected variance reduction that could be achieved when X_i would become perfectly known (i.e., $X_i = x_i^*$). The expectation of model response Y over the entire variation interval of X_i (i.e., $E[Y|X_i]$) is used since we are not able to know the *real* value x_i^* for each parameter X_i . First order sensitivity indices represent the main effect contribution of individual parameters to the output variance [Saltelli et al., 2008] and are therefore considered an agile measure for sensitivity assessments, but they are not enough for a rigorous GSA since quantification of higher order effects may be also important [Chan et al., 1997].

Total order sensitivity indices attempt to bridge this gap by estimating not only first but also higher order effects. According to variance decomposition presented in Equation A.3, the total effect index of the i^{th} parameter can be expressed as: $S_{Ti} = S_i + \sum_{j \neq i}^k S_{ij} + \dots + S_{12\dots k}$. This theoretical definition of total effect is not very useful for practical applications since it implies the estimation of the $2^k - 1$ terms in Equation A.4. Nonetheless, S_{Ti} can be calculated based on the following statistical identity [Papoulis, 1965]:

$$V[Y] = V[E[Y | X_i]] + E[V[Y | X_i]] \quad (\text{A.6})$$

If we substitute in Equation A.6 the parameter X_i with the vector $\mathbf{X}_{\sim i}$ which refers to a vector of all the random variables (i.e., parameters) but the i^{th} , then we obtain the following identity:

$$\begin{aligned} V[Y] &= V[E[Y | \mathbf{X}_{\sim i}]] + E[V[Y | \mathbf{X}_{\sim i}]] \\ &\Leftrightarrow \\ E[V[Y | \mathbf{X}_{\sim i}]] &= V[Y] - V[E[Y | \mathbf{X}_{\sim i}]] \end{aligned} \quad (\text{A.7})$$

The term $E[V[Y | \mathbf{X}_{\sim i}]]$ is the expected amount of variance that would remain unexplained if X_i , and only X_i , were left free to vary over its uncertainty range, all the other parameters (i.e., the vector $\mathbf{X}_{\sim i}$) having been learnt [Homma and Saltelli, 1996; Saltelli et al., 2008]. Similarly to the main effect, the outer expectation is

used since the *true* values of the $\mathbf{X}_{\sim i}$ vector are not known. The total effect index of the i^{th} parameter is obtained by normalizing $E[V[Y | \mathbf{X}_{\sim i}]]$ by the total, unconditional output variance:

$$S_{Ti} = \frac{E[V[Y | \mathbf{X}_{\sim i}]]}{V[Y]} = 1 - \frac{V[E[Y | \mathbf{X}_{\sim i}]]}{V[Y]} \quad (\text{A.8})$$

Total effect indices play a pivotal role in distilling information about the overall parameter importance since they highlight nonadditive features of the model structure and allow one to quantify parameter interactions, by subtracting the first order from the total sensitivity indices. Since a robust identification of influential and non-influential parameters implies quantification not only of first order effects but also of interaction, the calculation of total effect indices is a very crucial sensitivity measure for GSA [Saltelli *et al.*, 2008].

The most important properties of first and total Sobol' sensitivity indices are summarized as [Saltelli *et al.*, 2000a, 2004, 2008]:

1. $0 \leq S_i \leq S_{Ti} \leq 1$,
2. $\sum_{i=1}^k S_i \leq 1$,
3. if $\sum_{i=1}^k S_i = 1$ then the model is additive otherwise $1 - \sum_{i=1}^k S_i$ is a measure of the non-additive model structure,
4. $S_i = 1$ indicates that the model depends only on the parameter X_i ,
5. $S_{Ti} = 0$ indicates that the model is independent of parameter X_i ,
6. $S_{Ti} = S_i$ means absence of interaction between parameter X_i and the other parameters.

Although the presented equations for estimating the first and total sensitivity indices are analytical, their practical implementation is feasible under a Monte-Carlo integration approach. In the present study we followed the computational strategy originally proposed by Sobol' [1993] and further improved by Saltelli [2002]. This computational scheme is parsimonious and is based on the manipulation of two independent sampling matrices \mathbf{A} and \mathbf{B} of dimensions $N_{\text{mat}} \times k$ each, where N_{mat} is the number of rows, the sampled parameter sets and k is the number of columns, i.e., the number of parameters under examination. The computational cost of the enhanced Sobol' methodology is $N_{\text{mat}} \times (k + 2)$ model evaluations [Saltelli, 2002] for calculating both first and total sensitivity indices ($2 \times k$ indices in total).

The formulae used for calculating Sobol' indices are based on recent findings of Saltelli *et al.* [2010], according to which the best estimators for first and total Sobol' sensitivity indices are given by:

$$V[E[Y|X_i]] = \frac{1}{N_{\text{mat}}} \sum_{j=1}^{N_{\text{mat}}} f(\mathbf{B})_j [f(\mathbf{A}_{\mathbf{B}}^{(i)})_j - f(\mathbf{A})_j] \quad (\text{A.9})$$

$$E[V[Y | \mathbf{X}_{\sim i}]] = \frac{1}{2N_{\text{mat}}} \sum_{j=1}^{N_{\text{mat}}} [f(\mathbf{A})_j - f(\mathbf{A}_{\mathbf{B}}^{(i)})_j]^2 \quad (\text{A.10})$$

where $f(\mathbf{A})_j$ and $f(\mathbf{B})_j$ is the model output when it is forced with the parameter combination from the j^{th} row of matrix \mathbf{A} and \mathbf{B} respectively. $\mathbf{A}_{\mathbf{B}}^{(i)}$ symbolizes a manipulated matrix where the i^{th} column comes from the matrix \mathbf{B} and all the other $k - 1$ columns come from the matrix \mathbf{A} (i.e., \mathbf{A} may be considered as sampling matrix and \mathbf{B} as re-sampling matrix). Further details about this computational scheme and a review of alternative numerical estimators are provided by [Saltelli \[2002\]](#), [Saltelli et al. \[2010\]](#) and references therein.

The use of sophisticated sampling strategies is also widely suggested since they improve the computational efficiency of numerical integrations [[Chan et al., 2000](#); [Saltelli et al., 2000a, 2004, 2008, 2010](#)]. Many practical studies have shown that the Sobol' low discrepancy sequences, known as LP_{τ} sequences [[Sobol', 1967, 1976](#)] provide an enhanced convergence rate of the numerical estimators. LP_{τ} sequences are deterministic numbers that fulfil predefined properties, offering a very efficient coverage of the entire input parameter space. The next section provides a better description of LP_{τ} appealing properties and a justification of this selection as the most appropriate sampling approach for a uniform coverage of the parameter space.

A.3 PARAMETER SAMPLING: SOBOLEW LOW DISCREPANCY SEQUENCES VERSUS PSEUDO-RANDOM NUMBERS

"It is suggested that, instead of clinging to vague concepts of randomness, it might be better to aim at working with sequences making no pretence of random origin, but so devised as to give the best possible guarantee of accuracy in computations." [Zarembka \[1968\]](#)

Covering a k -dimensional parameter space in a uniform way is not a panacea, especially for problems with high dimensionality. Parameter sampling is indeed a very critical step not only for global sensitivity analyses, but generally for numerical integration, optimization, and calibration problems. Despite a vast amount of sampling techniques is available in the scientific literature (e.g., random sampling, stratified sampling, low discrepancy sequences, etc.), very often pseudo random numbers are preferred without solid justification. The advantages of Sobol' Low Discrepancy Sequences (LDS), in comparison to the widely

used (pseudo) random numbers are summarized below, illustrating their appealing properties and justifying their use for sampling the parameter values from a multidimensional (in our case 11–dimensional) parameter space.

Discrepancy is a measure of deviation from uniformity of a sequence of points in the k -dimensional space. A detailed review of the mathematical concept of discrepancy is provided in [Niederreiter \[1978, 1992\]](#); [Morokoff and Caflisch \[1994\]](#); [Sobol' \[1994\]](#). LDS are uniformly distributed deterministic numbers with very high dispersion. Unlike (pseudo) random numbers, LDS have memory. Thus, instead of filling the space in a random way, LDS produce successive points that follow a deterministic sequence, attempting to minimize the empty *spaces* and reducing point clustering and overlapping. Sobol' LDS are used in this study as many practical applications have shown their superior performance [[Bratley et al., 1992](#); [Paskov and Traub, 1995](#); [Sobol', 1998](#); [Kucherenko and Sytsko, 2005](#); [Sobol' and Kucherenko, 2005](#); [Kucherenko et al., 2011](#)]. A detailed description of the Sobol' LDS can be found in [Bratley and Fox \[1988\]](#) as well as in the original works of [Sobol' \[1967, 1976\]](#). Figure [A.1](#) provides a comparison of Sobol' LDS sequences against pseudo random numbers generated with the classical Mersenne-Twister random number generator [[Matsumoto and Nishimura, 1998](#)] for two different sample sizes. Note that the sample sizes are of power of two as the Sobol' LDS use a base of two to form successively finer uniform partitions of the unit interval.

Sobol' LDS, also known as LP_τ sequences [[Sobol', 1967, 1976](#)], are per definition constructed such that they fulfill the following criteria [[Sobol', 1976, 1994](#); [Chan et al., 2000](#); [Kucherenko and Sytsko, 2005](#)]:

1. Best uniformity of distribution as the sample size goes to infinity.
2. Good distribution for fairly small initial sets.
3. A very fast computational algorithm.

Since the objective of a sensitivity analysis sampling (but also of optimization or integration problems) is to obtain as much information as possible with a minimum computational cost (i.e., number of sampled points), these very appealing properties of LP_τ sequences make them ideal candidate for sampling strategies. Figure [A.1](#) illustrates these properties: as the sample size increases, Sobol' LDS produce new points in a way that the previous gaps are filled, leading to a very uniform distribution even for small sample sizes, while (pseudo) random numbers, independently from the sample size, are less equidistributed as they do not have information about the position of the previously sampled points.

The Monte Carlo (MC) integration of multidimensional integrals is the most common way for comparing the efficiency of different sampling strategies [[Niederreiter, 1992](#); [Sobol', 1994](#)]. In the MC framework, for a k -dimensional space (H^k), the integrand $f(\mathbf{x})$ is evaluated at a multiple number, N , of points, $\mathbf{x} = \{\mathbf{x}_1, \dots, \mathbf{x}_N\}$, and the integration error ϵ is defined as:

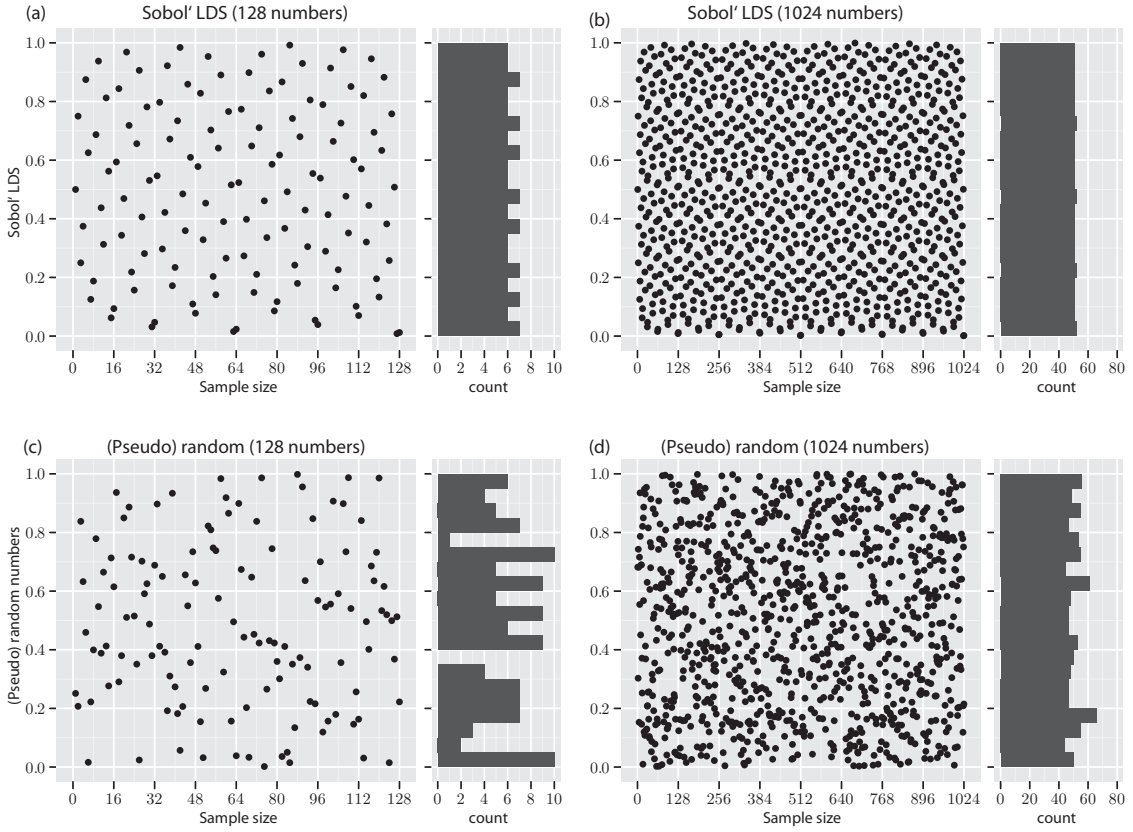


Figure A.1: Scatter plots and histograms for the case of LP_τ sequences and (pseudo) random numbers scaled in $[0,1]$ interval, for different sample sizes. LP_τ sequences fill out the space in an evenly dispersed manner such that the new points fill in the previous gaps.

$$\epsilon = |I[f] - I_N[f]| \quad (\text{A.11})$$

where

$$I[f] = \int_{H^k} f(\mathbf{x}) \, d\mathbf{x}$$

and

$$I_N[f] \simeq \frac{1}{N} \sum_{i=1}^N f(x_i)$$

The expected error of the classical MC integration method, i.e., with (pseudo) random numbers, is $\epsilon_{MC} = \mathcal{O}(N^{-1/2})$. This rather slow convergence rate requires sufficiently large sample sizes N in order to achieve the desirable accuracy. LDS offer a deterministic version of MC integration, the quasi-MC integration (QMC) where LDS also known as quasi-random numbers are used for sampling the required points. The theoretical upper bound of their convergence rate according to the Koksma-Hlawka inequality is proved to be $\epsilon_{QMC} = \mathcal{O}(\frac{\log^k(N)}{N})$

[Niederreiter, 1978, 2010; Morokoff and Caflisch, 1994]. The dependence of the error on the dimensionality of the problem, k , creates the impression that ϵ_{QMC} would be higher than the ϵ_{MC} especially for problems with high dimensionality. However, due to the non-isotropic character of most practical problems [Papageorgiou, 2000] (i.e., many problems tend to follow the Pareto principle), the convergence rate of the LDS becomes asymptotically independent of the dimensions k . Therefore, as many practical applications have shown, the QMC integration can provide a rate of convergence $\sim \mathcal{O}(N^{-1})$ [Press, 2007], which is much faster than classical MC integration. The faster convergence rate of LDS in comparison to (pseudo) random numbers and their enhanced capability in exploring the space (i.e., more uniform coverage) are the two main assets of LP_τ sequences which justify our preference in this type of sampling strategy.

A.4 CONVERGENCE TEST OF SENSITIVITY INDICES

Monte-Carlo studies aim to draw conclusions about the probability distribution of model outputs by recursively performing many model evaluations with different parameter sets. The selection of the number of model evaluations (sample size) is not a trivial decision and very often arbitrary sample sizes are selected without further justification. A *sufficiently large* sample size should be objectively chosen such that the entire parameter space is covered. This is especially true in problems with high dimensionality, as it is the case in this study, with an 11-dimensional parameter space. A convergence test was employed to estimate which sample size leads to robust estimations of the first and total Sobol' sensitivity indices.

The estimation of first and total Sobol' sensitivity indices is based on two matrices of equal dimensions, the sample matrix **A** and the re-sample matrix **B** (Section A.2). The convergence test allows us to define the optimal size, i.e., the number of rows, N_{mat} , of these two matrices. Figure A.2, depicts first and total Sobol' sensitivity indices of vegetation carbon pools for the case of normal precipitation conditions at middle elevation (1400 m a.s.l.). The sensitivity indices were estimated by using different values of N_{mat} from 64 to 2048, covering two order of magnitude sample sizes. Note that N_{mat} equal to 64 leads to $(11 + 2) \times 64 = 832$ model evaluations, while N_{mat} equal to 2048 leads to $(11 + 2) \times 2048 = 26624$ model runs. The 95% confidence bounds of the sensitivity indices estimators, calculated according to the classical bootstrapping technique [Efron, 1979; Efron and Tibshirani, 1993; Archer et al., 1997], with 1000 bootstrap replicates, are also shown in Figure A.2. $N_{\text{mat}} = 512$, i.e., $(11 + 2) \times 512 = 6656$ model evaluations, provides a robust estimation of first and total order Sobol' sensitivity indices with relatively narrow uncertainty bounds. The same sample size (6656 model evaluations) led also to robust estimates of Sobol' sensitivity indices for

other model outputs e.g., NPP, LAI, and vegetation carbon fluxes (results not shown).

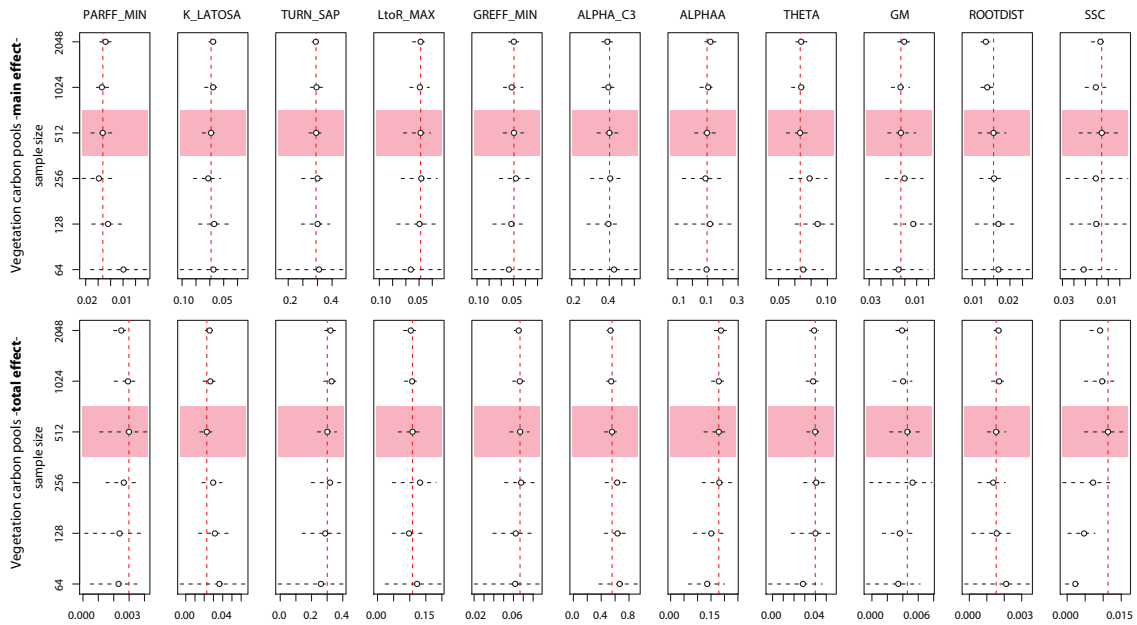


Figure A.2: Convergence test for the estimators of the first and the total order effects with their uncertainty bounds, for vegetation carbon fluxes under normal precipitation conditions at 1400 m a.s.l. The sample size corresponds to the number of rows of the sample and re-sample matrices **A** and **B**, respectively. A sample size of 512, highlighted in the plots, is found to be sufficient for the convergence of the estimators, with relatively narrow uncertainty bounds.

APPENDIX B: THE ROLE OF LOCAL SCALE HETEROGENEITIES IN TERRESTRIAL ECOSYSTEM MODELING

B.1 D-LPJ ECOHYDROLOGICAL SCHEME: CONVERGENCE TEST

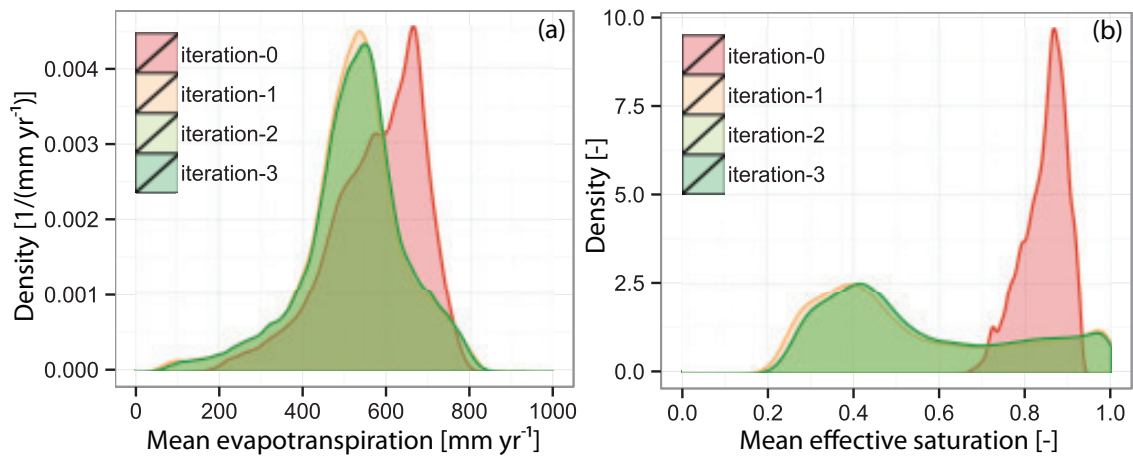


Figure B.1: Convergence test of the density functions of the exchange variables of D-LPJ ecohydrological scheme. Four iterations are enough for achieving a convergence over the simulated area of (a) evapotranspiration (soil evaporation, evaporation from interception, and plant transpiration) as well as of (b) the effective saturation.

B.2 DISTRIBUTED METEOROLOGICAL VARIABLES

The meteorological data used for the present model application are provided by the Swiss Federal Office of Meteorology and Climatology (MeteoSwiss) and refer to the period January 2000 through December 2009.

B.2.1 Precipitation

Precipitation fields (Figure 3.3a) used to drive the models (TOPAKPI-ETH and D-LPJ) are based on a gridded daily precipitation product of 2×2 km² resolution (RhiresD; *Schwarb [2000]*; *Wüest et al. [2010]*) combined with hourly point-scale measurements from three meteorological stations located in the catchment area

(see Figure 3.2). The point-scale measurements are used for disaggregating the daily values of RhiresD product to hourly temporal resolution. Thiessen polygon interpolation of the hourly gauge precipitation data is used for defining weights (i.e., hourly partition of the daily precipitation) used for the RhiresD disaggregation. When precipitation values greater than zero occur only in the gridded product, a uniform precipitation was assumed for a duration of 7 h. This occurs only for very low intensity. According to the available data, this corresponds to a typical duration of precipitation events in Switzerland. The spatial distribution of precipitation, outlined in the RhiresD gridded product, reflects a more realistic representation of precipitation patterns in comparison to classical interpolation methods from station data (e.g. Thiessen polygons or Inverse Distance Weighting). This is particularly true in complex terrains, as is the case for the Kleine Emme area (Figure 3.3a).

B.2.2 *Temperature*

Temperature maps over the catchment were obtained by interpolating spatially (with Thiessen polygons and a constant air temperature lapse rate of $5.5\text{ }^{\circ}\text{C km}^{-1}$), observations from the three meteorological stations in the area (Figure 3.3b).

B.2.3 *Cloud transmissivity and shortwave radiation*

A time series of daily cloud transmissivity, representative for the catchment area, is calculated based on the observed values of shortwave radiation in the three meteorological stations (Figure 3.2) and clear sky shortwave radiation simulated using the AWE-GEN weather generator [Fatichi et al., 2011]. Daily shortwave radiation inputs for each computational element of D-LPJ were then calculated based on TOPKAPI-ETH algorithms (see Section 3.2.1.2), accounting explicitly for local topographic effects (Figure 3.3c).

B.3 VEGETATION CARBON FLUXES: LPJ SIMULATIONS VS EDDY COVARIANCE ESTIMATES

Five different Swiss FLUXNET sites, covering a wide altitudinal range as well as the major land use types in Switzerland: evergreen forest (Davos; 1639 m a.s.l.), deciduous forest (Laengern; 682 m a.s.l.), and grassland (Chamau, 393 m a.s.l.; Fruebuel, 982 m a.s.l.; Oensingen, 451 m a.s.l.), are incorporated in the analysis. More details on the grassland sites can be found in Ammann et al. [2007]; Gilgen and Buchmann [2009]; Lazzarotto et al. [2009]; Zeeman et al. [2010]. Figure B.2 de-

picts the temporal dynamics of Gross Primary Production (GPP) as estimated by the Eddy-Covariance measurements, as well as by the LPJ simulations with original and adjusted parameter values. It is clear from Figure B.2 that the original species-based parameterization of LPJ (based on *Hickler et al.* [2012]) is not reproducing very well the observed vegetation fluxes in Switzerland. This parameterization was developed for regional or continental scale applications, and thus discrepancies occur when point-scale comparisons are attempted. To overcome this issue, key plant physiological properties related to photosynthesis, carbon allocation, and phenological cycle were adjusted manually within their uncertainty ranges in order to achieve a better agreement with the measured carbon fluxes.

More specifically, for Davos (evergreen forest), the disagreement among the observed values of GPP and the simulated GPP with the original parameterization of LPJ is striking (Figure B.2). The intrinsic quantum efficiency of the photosynthetic machinery and leaf-to-root ratio were therefore adjusted (reduced) in order to mimic this lower productive forest stand [*Etzold et al.*, 2011]. The same approach was followed also for re-parameterizing the deciduous forest in Laegeren and obtaining GPP values closer to the observed magnitude. Intrinsic quantum efficiency in LPJ encapsulates information about the canopy-average maximum Rubisco capacity, V_{\max} (see detailed discussion in *Pappas et al.* [2013]). V_{\max} is known to be highly variable among species and sites, therefore the preformed adjustments are well justified. The empirical parameter defining the partition between above- and below-ground biomass is also very uncertain, and the performed adjustments are within the range of typical values [*Pappas et al.*, 2013]. Grassland sites in Switzerland are very productive and often highly managed [e.g., *Lazzarotto et al.*, 2009; *Zeeman et al.*, 2010]. Therefore, intrinsic quantum efficiency was increased, and some adjustments of the parameters regulating the carbon allocation (above- and below-ground) and the phenological cycle were performed. More specifically the leaf-to-root ratio, the leaf longevity, and the growing degree sum on a 5 degree base required for full leaf cover, were decreased in order to achieve not only a good agreement of carbon fluxes but also lower values of Leaf Area Index (LAI). With the new, adjusted parameterization, tailored to the Swiss area, the carbon fluxes of the examined sites are better captured (Figure B.2, B.3).

B.4 MODIS PRE-PROCESSING

Gross Primary Production (GPP) is based on the MODIS land product MOD17A2 (Version 005) and Leaf Area Index (LAI) on the MOD15A2 (Version 005). The resolution of both products is $1 \times 1 \text{ km}^2$ with a eight-days regular time-step. Apart from the usual quality assurance layer of MODIS products, an additional analysis was conducted following the methodology presented by *Hwang et al.*

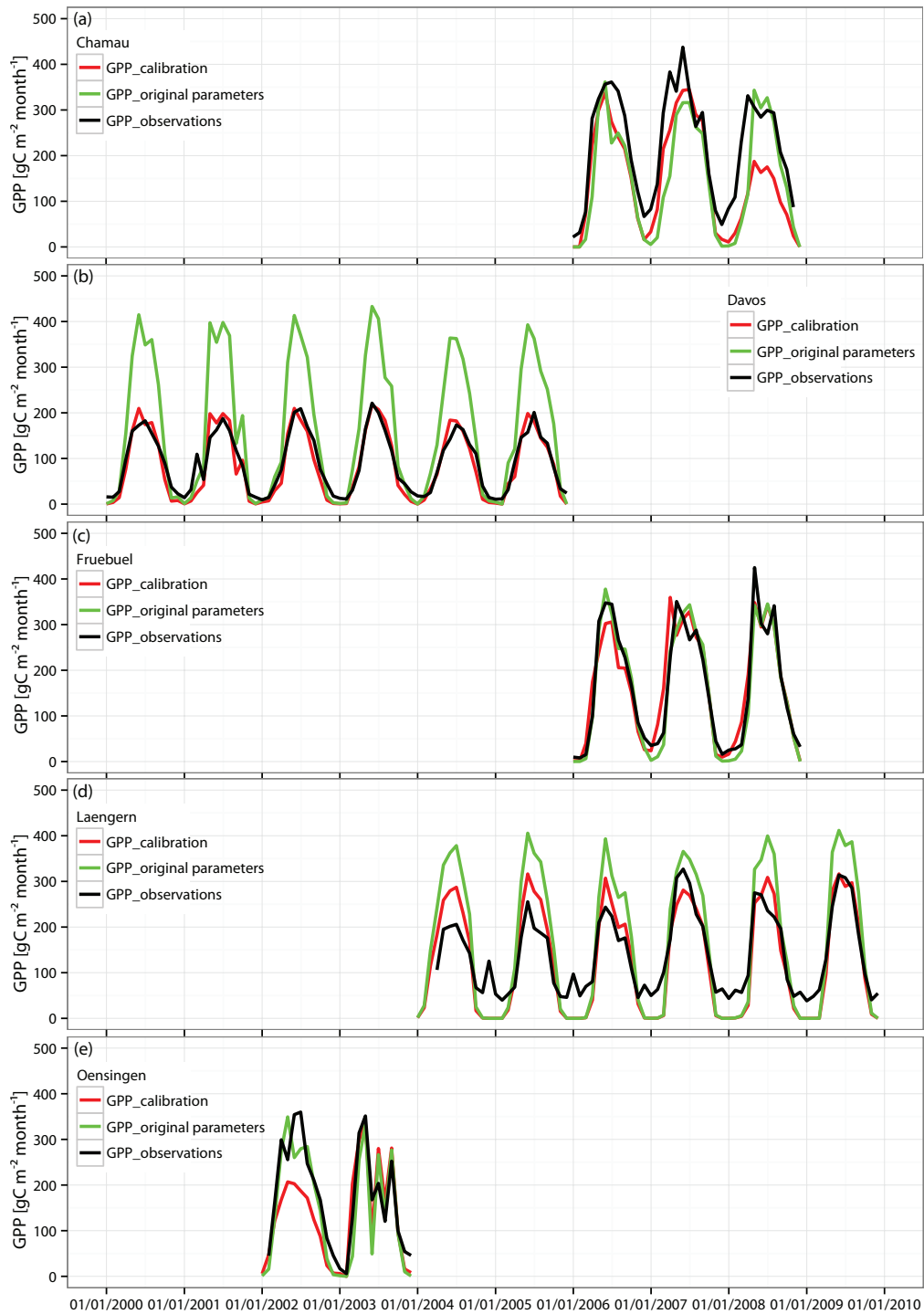


Figure B.2: Monthly gross Primary Productivity (GPP) in five Swiss FLUXNET sites estimated by Eddy-Covariance measurements (black lines) as well as with LPJ with the original parameterization (green lines), and LPJ with the adjusted plant physiological parameters (red lines).

[2011]. A detailed description of MODIS pre-processing for the Alpine region is provided in *Bogler* [2013].

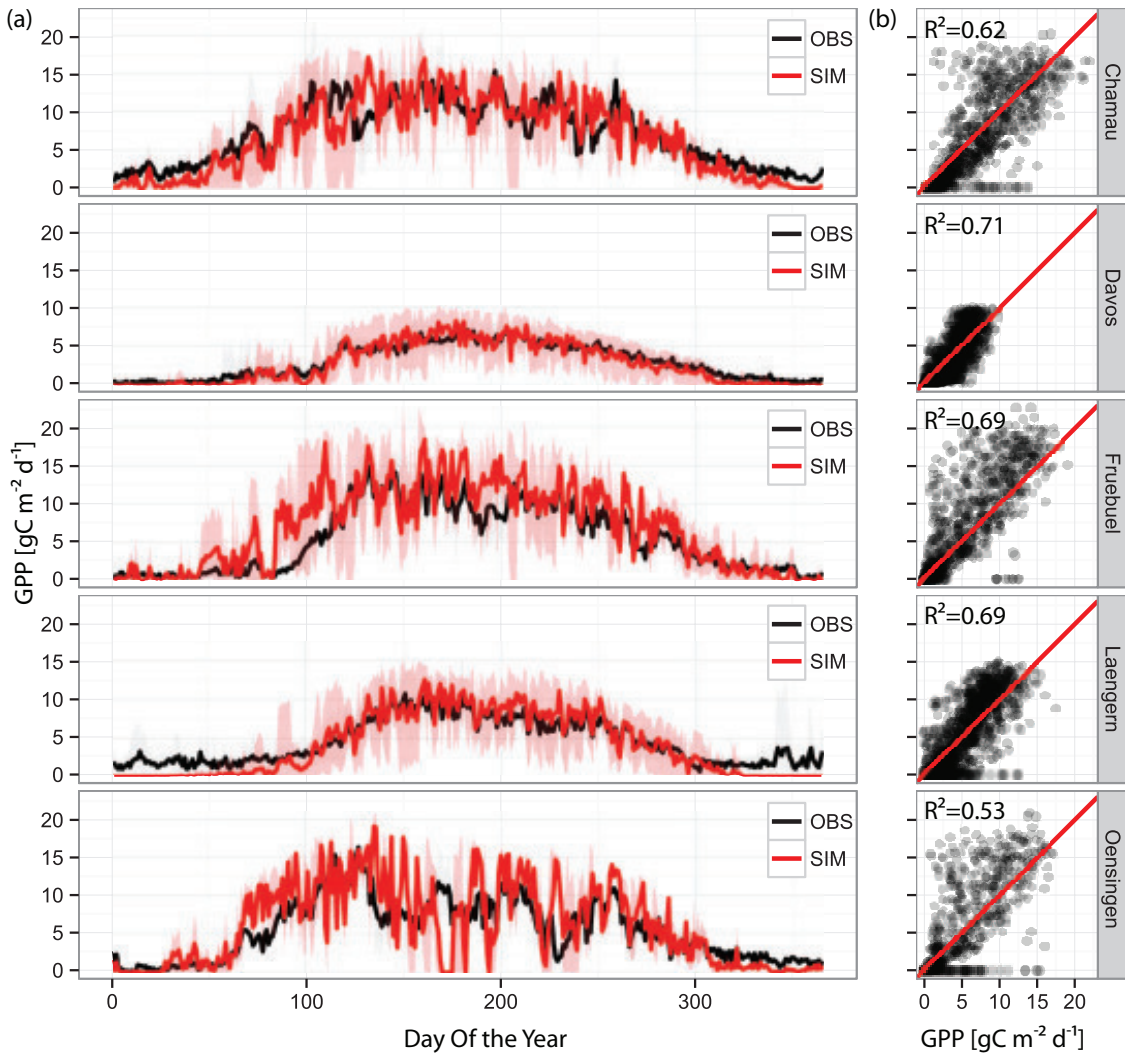


Figure B.3: (a) Seasonality and (b) scatter plots of Gross Primary Productivity (GPP) in five Swiss FLUXNET sites estimated by Eddy-Covariance measurements (black lines) as well as with LPJ with the adjusted plant physiological parameters (the mean response over the simulated period is depicted with the red lines, while the light red areas illustrate the variation among the different years of the simulated period).

In summary, for GPP data pre-processing, values from all the years were combined to compute quantiles, assuming that change of GPP between years is smaller than within a year [Hwang *et al.*, 2011]. In order to reduce the noise of the product, only values included in 1.5-times the interquartile range from lower and upper quartiles are selected. A linear interpolation is then performed for the selected values. As for the LAI, instead of discarding all values below two thirds of the 25% quantile, as it is done for GPP, all values below the 25% quantile are discarded. In order to investigate the temporal dynamics of LAI without misleading effects from the intrinsic noise of the product, a smoothing approach was applied. Based on the methodology described by Jönsson and Ek-

lundh [2004, 2002], the Savitzky-Golay filter was used for smoothing the time series. This filter replaces each value by one derived from the surrounding points inside a specified moving window. The new value is computed by fitting a polynomial function (third degree in the present application) using least squares estimation, to the points within the window (here eleven points) *Bogler* [2013]; *Jönsson and Eklundh* [2004, 2002]. While Savitzky-Golay filter is appropriate for highlighting fast changes in a time series, it is sensitive to noisy data [*Hwang et al.*, 2011]. This is the reason why a stricter selection of LAI raw data, comparing to GPP, was applied. A second smoothing is additionally conducted, with the loess (local regression) method. A polynomial function is fitted to the remaining data points by local regression, based on the least square method, but here the points are weighted. A linear interpolation between the data points and the smoothing results was finally applied.

B.5 SWISS NATIONAL FOREST INVENTORY: DATA DETAILS

Various sources of data, such as terrestrial forest surveys, aerial photos, GIS information, are compiled in the NFI product. In situ records of tree height and diameter at breast height, are incorporated into allometric relationships to provide estimates of vegetation biomass (e.g., above-ground biomass, as well as carbon stocks in specific tissues) and vegetation growth increments. The first NFI used a 1 km square grid over Switzerland, in total about 41000 clusters. In the following periods NFI2 and NFI3 only half of the clusters were re-sampled on a 2^{0.5} km square grid diagonal to the grid used in period NFI1. In a first step raster-based aerial image interpretation was used to distinguish between forest and non-forest clusters. In a second step the forest clusters were sampled in the field. Two concentric circles were used for sample tree selection: a horizontal circle of 200 m² for trees with 12 cm ≤ diameter at breast height (1.3 m, dbh) < 36 cm, and a horizontal circle of 500 m² for trees with dbh ≥ 36 cm. For each tree, species, survival status, stem damages etc. were recorded. Dbh was measured for each sample tree, but tree height, height to the crown base and stem diameter at a height of 7 m was measured only for a sub-sample. This sub-sample was then used to develop species- and site-specific allometric individual-tree stem volume functions [*Kaufmann*, 2001]. Other species specific allometric functions were used to estimate the volume of twigs and branches [*Kaufmann*, 2001], and bark volume [*Altherr et al.*, 1978]. Tree above ground woody biomass was derived by multiplying the tree volume with species specific wood densities given by *Assmann* [1961]. Foliage biomass and woody coarse root biomass was estimated using the function presented by *Perruchoud et al.* [1999]. For more details on the Swiss NFI and its methods see *Brassel and Lischke* [2001] and www.lfi.ch. In the present study, in order to convert tree biomass to carbon amounts, a fixed proportion of 50% C per kg of dry biomass was assumed. Long-term changes in vegetation carbon stocks over the Kleine Emme area are

examined. Mean changes in vegetation carbon stocks simulated by LPJ, LPJ-GUESS, and D-LPJ, for the period 2000 to 2009, are compared with the two estimates of average changes in carbon-stock derived from the consecutive forest inventories: NFI1; from 1983 to 1985, NFI2; from 1993 to 1995, NFI3; from 2004 to 2006.

B.6 CONFIRMING THE HYDROLOGICAL CONSISTENCY

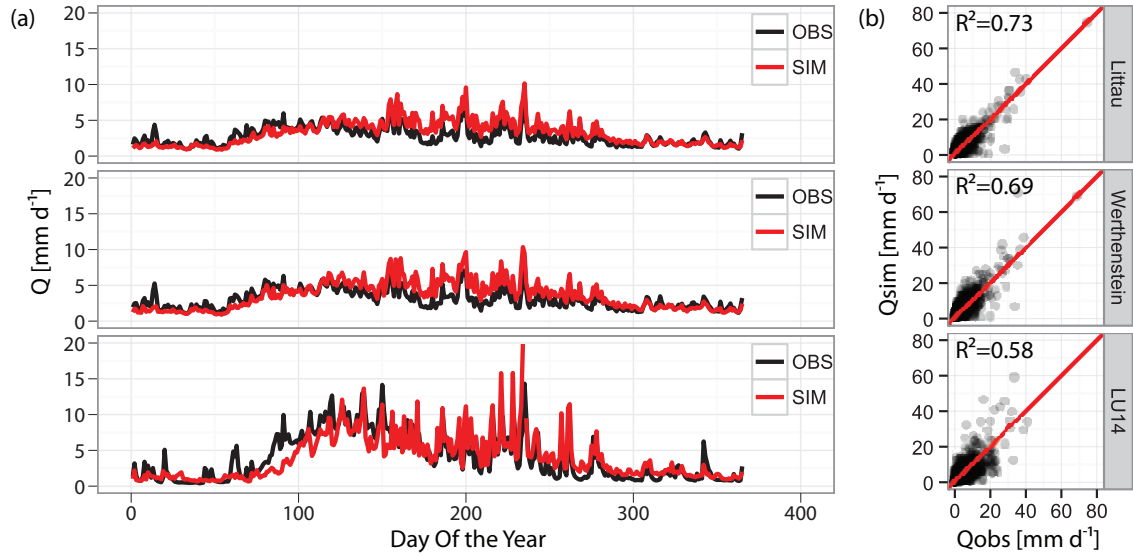


Figure B.4: (a) Seasonality and (b) scatter plots of river discharge, for the period 2000 through 2009, in three locations over the Kleine Emme catchment.

B.7 TEMPORAL DYNAMICS OF GPP AND LAI OVER THE KLEINE EMME CATCHMENT

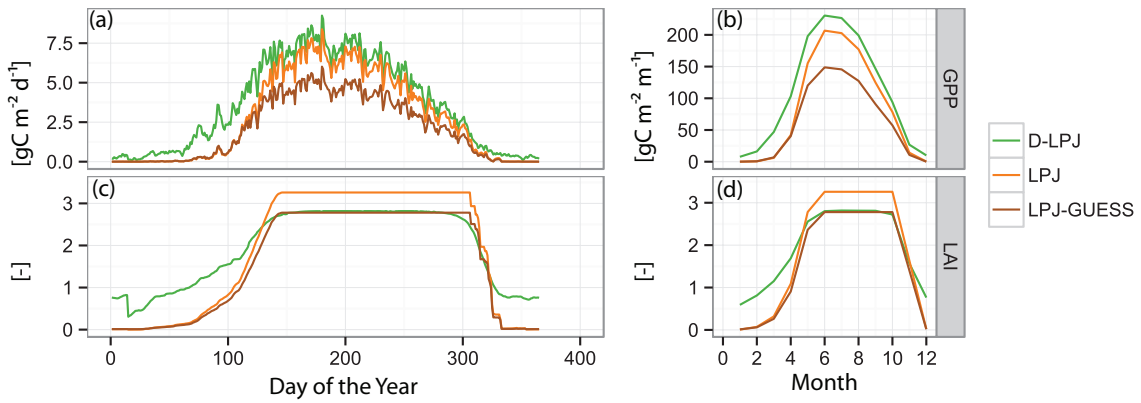


Figure B.5: Seasonality plots of (a, b) Gross Primary Productivity (GPP) and (c, d) Leaf Area Index (LAI) over the Kleine Emme catchment as estimated by D-LPJ, LPJ, and LPJ-GUESS over the 2000-2009 period.

B.8 DISENTANGLING THE ROLE OF LAND COVER INITIALIZATION

In order to quantify the importance of correct land cover initialization, LPJ simulations are carried out with mean climatic conditions over the area, but with prescribed land cover instead of the potential natural vegetation hypothesis. The results of these simulations are compared with the D-LPJ outputs in Figure B.6 and B.7. For the case of GPP, when land cover information is provided to LPJ simulations the bias (defined as the difference with the D-LPJ area-averaged values) is about 4%, much lower than the bias of the original simulations with LPJ ($\approx 23\%$) and LPJ-GUESS ($\approx 42\%$) based on the potential natural vegetation hypothesis. However, biases in area-averaged LAI values are not significantly affected with the modified version of LPJ, i.e., accounting for the current land cover in the simulated domain. In comparison to the D-LPJ simulations of LAI, the modified version of LPJ, accounting for the current land cover, underestimates the area-averaged LAI over the catchment by $\approx 42\%$, when compared to the 35% and 45% bias of the original LPJ and LPJ-GUESS simulations.

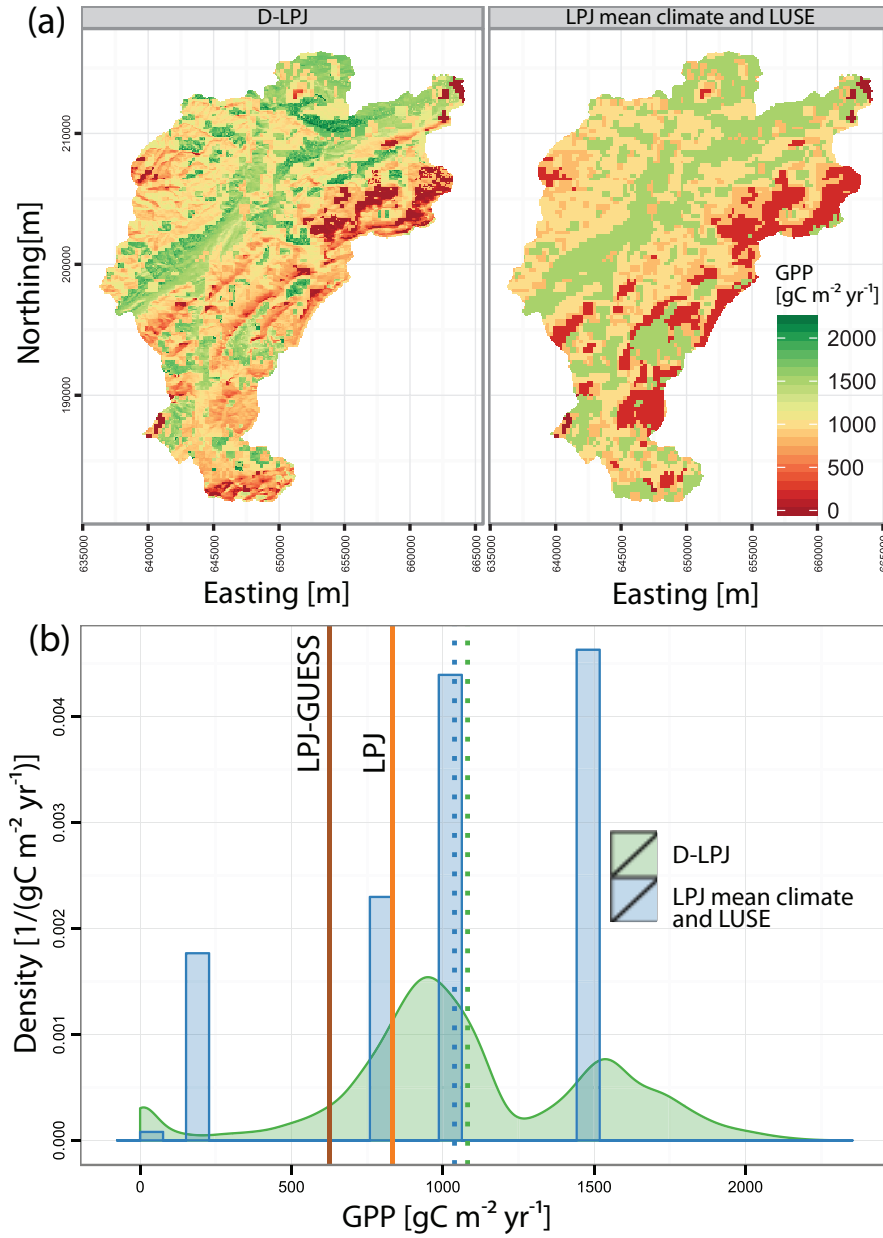


Figure B.6: (a) Spatial patterns of mean Gross Primary Production (GPP) for the period 2000 to 2009, over the Kleine Emme catchment, as estimated by D-LPJ and LPJ with mean climatic conditions but with prescribed land cover (based on the current land use map, as in D-LPJ simulations). (b) Distribution of GPP over the catchment as estimated by the spatially explicit D-LPJ and the LPJ simulations with mean climate forcing but prescribed land cover. Solid lines depict the estimates based on LPJ and LPJ-GUESS, while dashed lines highlight the mean of the distributions.

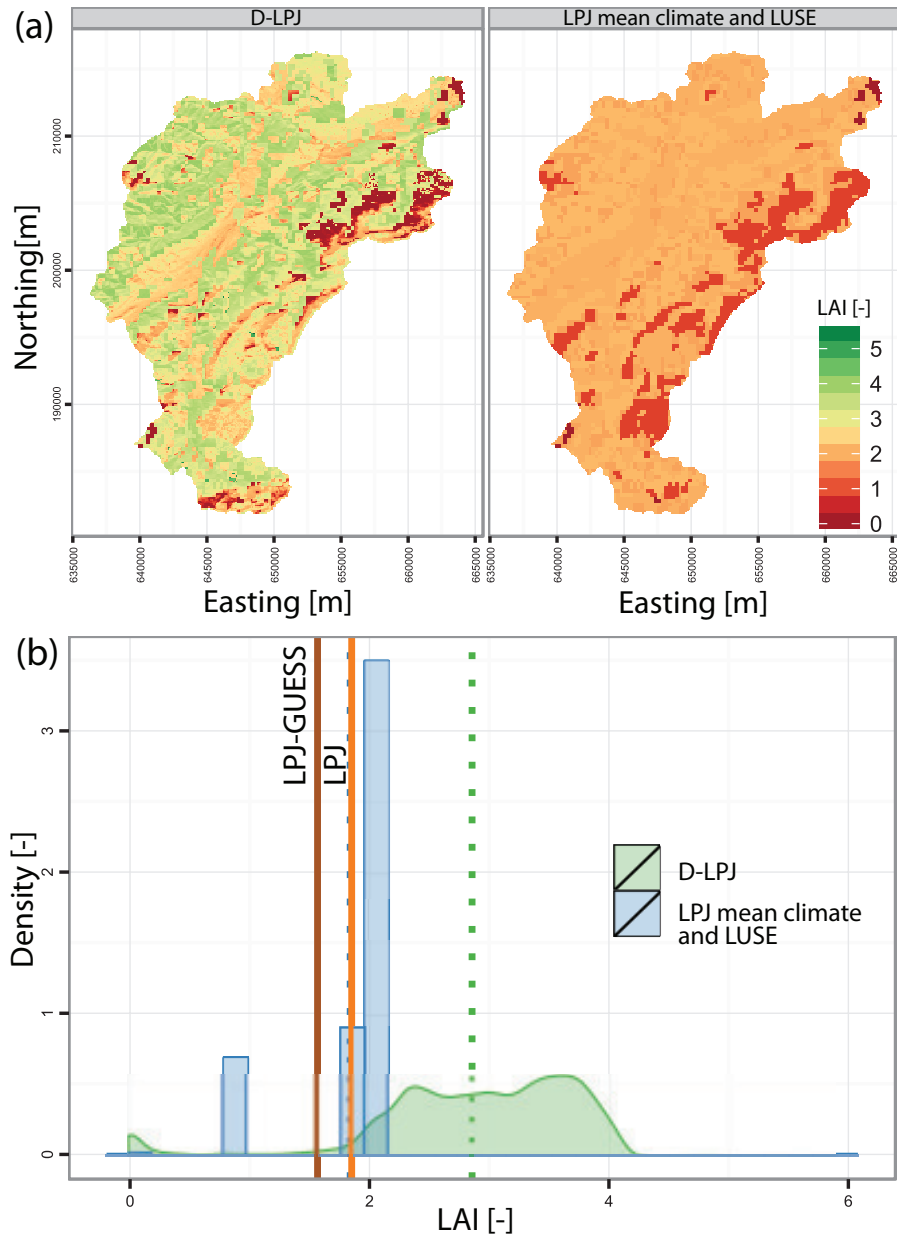


Figure B.7: (a) Spatial patterns of mean Leaf Area Index (LAI) for the period 2000 to 2009, over the Kleine Emme catchment, as estimated by D-LPJ and LPJ with mean climatic conditions but with prescribed land cover (based on the current land use map, as in D-LPJ simulations). (b) Distribution of LAI over the catchment as estimated by the spatially explicit D-LPJ and the LPJ simulations with mean climate forcing but prescribed land cover. Solid lines depict the estimates based on LPJ and LPJ-GUESS, while dashed lines highlight the mean of the distributions.

B.9 DOWNSCALING DYNAMIC VEGETATION MODELS USING FINE RESOLUTION GRID: FINE RESOLUTION LPJ AND D-LPJ RESULTS

In order to further demonstrate the role of local scale information (meteorological forcing, local land use, topography, as well as mechanistic representation of lateral and vertical water fluxes), in this section we illustrate simulation results with LPJ, but now driven with fine scale information (similarly to D-LPJ; i.e., spatially explicit meteorological forcing and current land use instead of natural potential vegetation) and with D-LPJ. In D-LPJ apart from the local scale detailed meteorological forcing and current land use attributes, lateral and vertical water fluxes are additionally explicitly simulated, using the TOPKAPI-ETH hydrological model. The results presented in this section are in essence an explicit illustration of Figure B.1, since iteration-0 in the coupling scheme of LPJ with TOPKAPI-ETH corresponds to the results of the original LPJ forced with detailed meteorological inputs and using the current land use, while iteration-3 corresponds to the D-LPJ simulations (i.e., coupled LPJ and TOPKAPI-ETH simulation).

The simple hydrological representation of LPJ, leads to unrealistic representation of soil moisture patterns over the Kleine Emme catchment, with almost the entire catchment domain close to saturation. D-LPJ on the other hand, using a more mechanistic hydrological representation captures reasonably well the spatial soil moisture dynamics caused by the complex topography and the lateral and vertical water fluxes (Figure B.8). LPJ, once forced with fine resolution meteorological information, is capturing fairly well the spatial patterns of evapotranspiration, mainly due to the strong control of radiation on plant activity. The detailed hydrological representation embedded in D-LPJ enhances the spatial patterns of simulated ETA, reflecting additional local scale attributes mainly due to lateral water fluxes (Figure B.9). Both LPJ with detailed meteorological forcing and local land use information and D-LPJ yield similar spatial patterns of annual NPP and LAI (Figure B.10 and B.11). Vegetation in Kleine Emme region is mostly energy, rather than water limited, therefore the advantages of the enhanced hydrological representation through D-LPJ simulations are not reflected in the long-term simulated NPP. In addition, the lack of sensitivity to water availability and dynamics can be attributed to parameterization issues embedded in LPJ and possibly other structurally similar models, as well as lack of direct environmental controls on the simulated plant growth, as recently highlighted by *Pappas et al.* [2013].

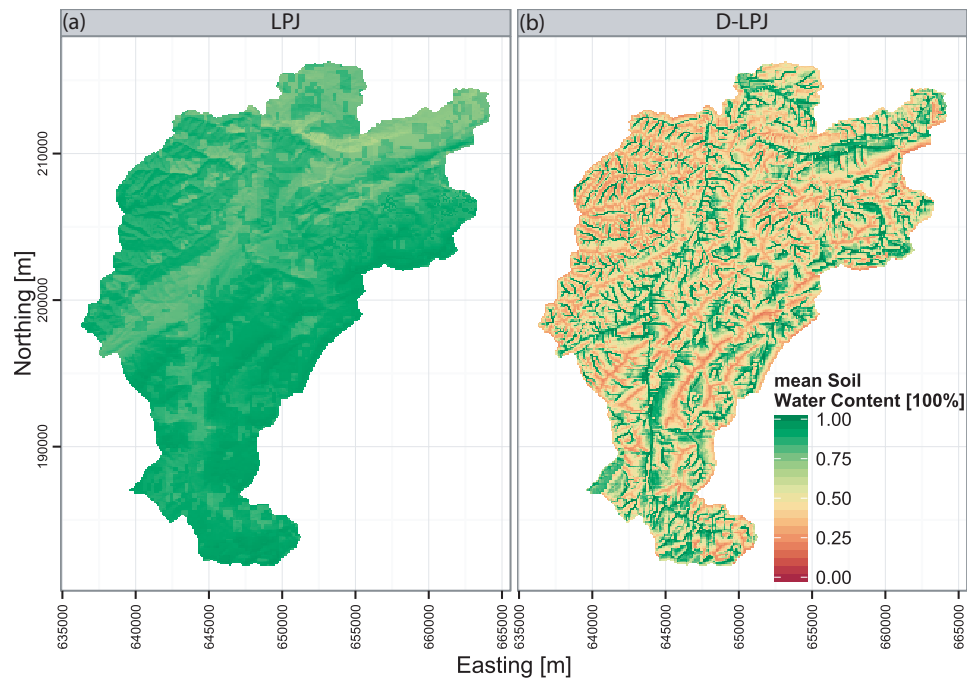


Figure B.8: Spatial patterns of mean soil water content for the period 2000 to 2009, over the Kleine Emme catchment, as estimated by (a) LPJ using exactly the same inputs as D-LPJ (i.e., fine resolution meteorological forcing and local land use information) and (b) D-LPJ (i.e., fine resolution meteorological forcing, local land use map, and in addition, detailed hydrological representation of vertical and lateral fluxes using TOPKAPI-ETH distributed hydrological model).

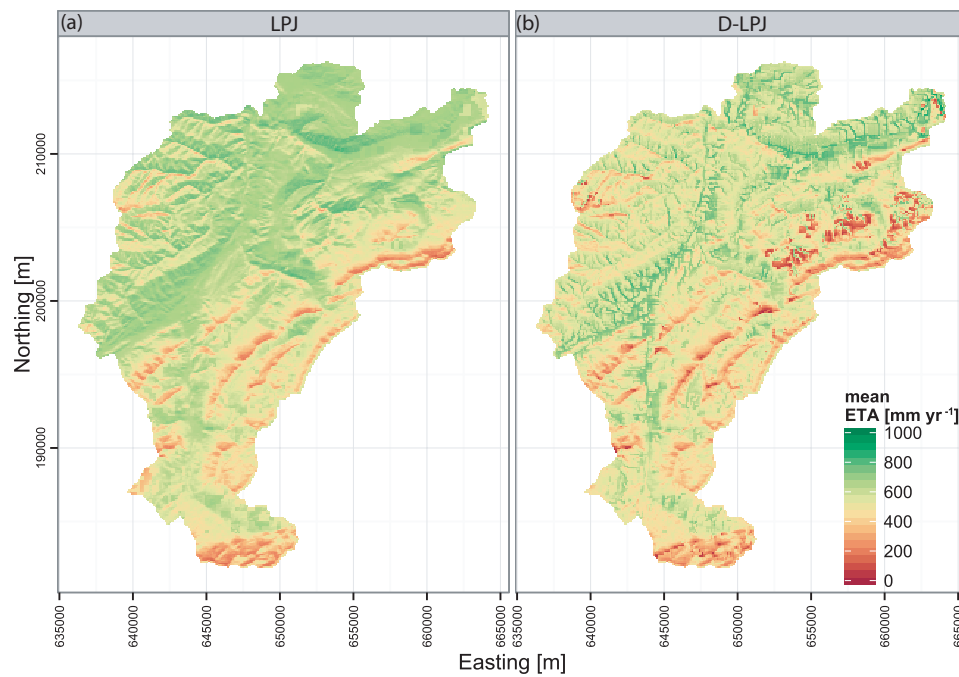


Figure B.9: Same as Figure B.8, but for evapotranspiration (ETA).

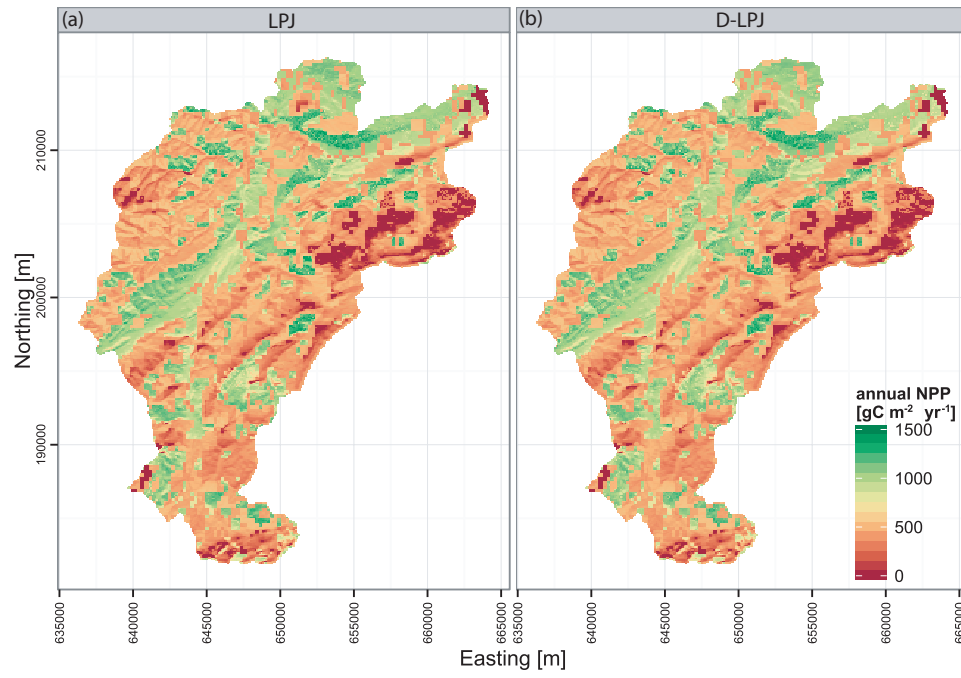


Figure B.10: Same as Figure B.8, but for annual net primary production (NPP).

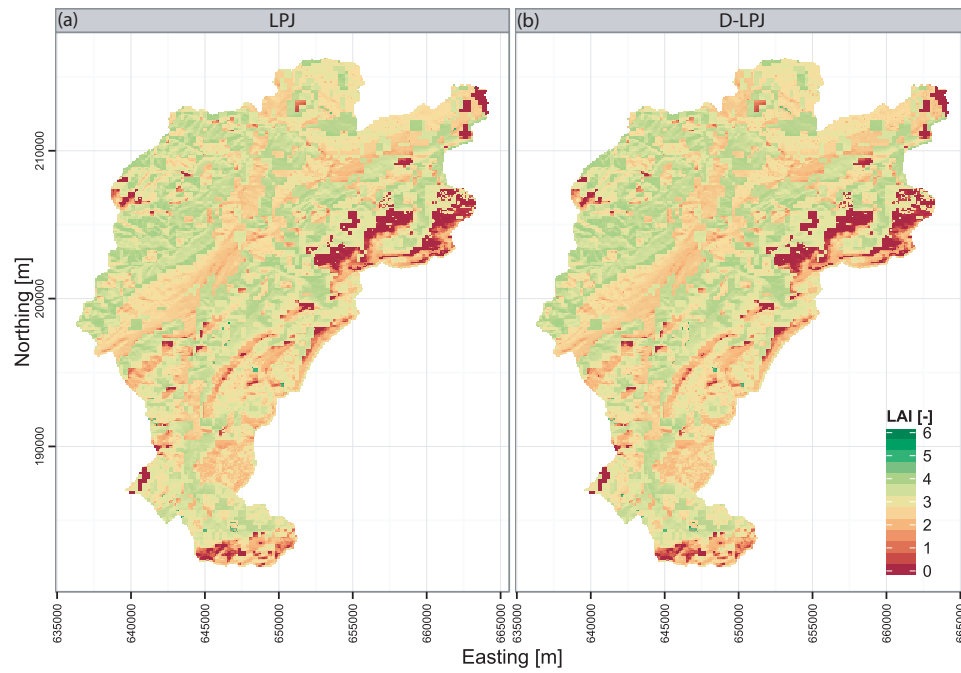


Figure B.11: Same as Figure B.8, but for Leaf Area Index (LAI).

APPENDIX C: MODELING TERRESTRIAL CARBON AND WATER DYNAMICS ACROSS CLIMATIC GRADIENTS: DOES PLANT DIVERSITY MATTER?

C.1 CLIMATIC FORCINGS

Environmental conditions are important in shaping vegetation performance and functioning. While deriving spatially averaged long-term climatic field is rather common in literature, continuous time series of meteorological variables across elevation bands are rarely available at the fine, sub-daily time scales. Few meteorological networks have the density capable of capturing climate conditions to characterize altitudinal differences of few hundred meters. Simple interpolation of meteorological variables is problematic and generates “smoothed” fields, especially for highly dynamic variables such as precipitation, solar radiation, and wind speed. In the present study, in order to analyze the effects of climate variability in terrestrial ecosystem functioning, long-term cross-correlated meteorological variables, at the hourly time scale, are generated using an advanced weather generator, calibrated with a large amount of meteorological data across altitudinal and precipitation gradients.

C.1.1 *Generating the climatic gradients: methodology*

A stochastic methodology for simulating long-term hourly time series of meteorological variables across a continuous range of elevations is implemented (Figure C.1). More specifically, ground observations from the MeteoSwiss network and an hourly weather generator (Advanced WEather GENerator, AWE-GEN, [Fatichi et al. \[2011\]](#)), are combined to construct synthetic climatic gradients of the meteorological variables used for driving T&C simulations (e.g., precipitation, air temperature, cloud cover, relative humidity, wind speed, solar radiation, and atmospheric pressure).

AWE-GEN is an hourly weather generator capable of reproducing characteristics of hydrometeorological variables across a wide range of temporal scales, from interannual to hourly [[Fatichi et al., 2011](#)]. It generates realistic climatic gradients (not only consistent with the observed meteorological variables but also maintaining the cross-correlations among them). The weather generator uses both physically-based and stochastic approaches and is a significant evolution

of the model presented by *Ivanov et al.* [2007]. It includes a formulation of the precipitation module based on the Poisson-Cluster process, and additional modules for generating cloud cover and air temperature time series. It further simulates vapour pressure, wind speed, atmospheric pressure, and shortwave radiation partitioned into various wavebands (e.g., Photosynthetically Active Radiation, PAR) and in the diffuse and direct components. AWE-GEN theoretical framework and parameter estimation can be found in *Fatichi et al.* [2011]. A technical reference of AWE-GEN is available online (<http://www-personal.umich.edu/ivanov/HYDROWIT/Models.html>).

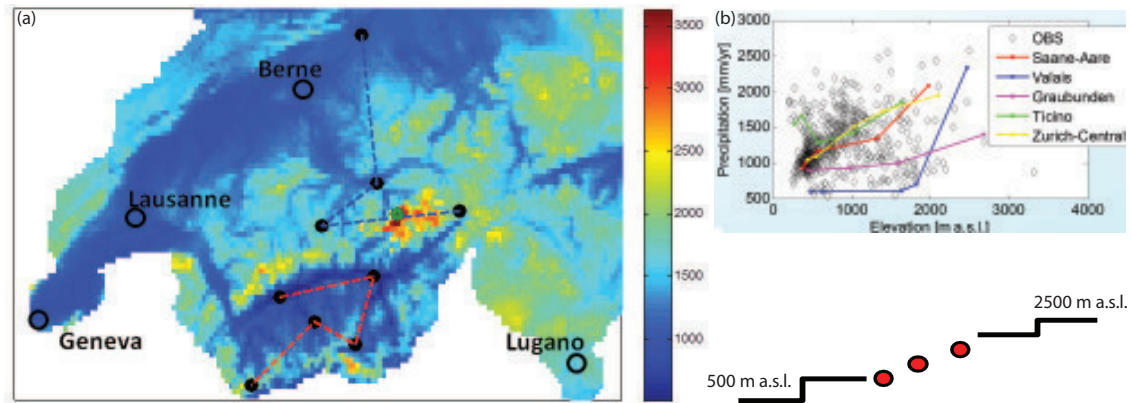


Figure C.1: (a) Map of mean annual precipitation [mm yr⁻¹] in the South-West of Switzerland. Red and blue lines depicted the selected meteorological stations for generating the dry and wet gradients respectively. (b) Mean annual precipitation vs elevation in Switzerland based on data from the MeteoSwiss network.

The developed methodology uses observed data from stations located along an altitudinal gradient (see Figure C.1 and Table C.1) for parameterizing the weather generator for each single station. The estimated parameters are successively interpolated at different elevations using both linear and non-linear functions. The re-parameterized weather generator is able to produce a consistent gradient of climate across the elevation range, preserving the co-variation among meteorological variables. The methodological steps for generating the climatic gradients can be summarized as follows:

1. Sort the available stations with observations of hourly meteorological variables (precipitation, air temperature, cloud cover, relative humidity, wind speed, solar radiation, atmospheric pressure) across an elevation gradient.
2. Estimate the parameters needed for the hourly weather generator, AWE-GEN.
3. Interpolate the estimated parameters across elevation bands (ranging from 500 to 2500 m a.s.l. in the present study).

4. Generate long-term (30 yr in our study) time series of climatic variables for each elevation band and precipitation gradient (wet, dry).

Two synthetic climate gradients, which correspond to two significantly different precipitation regimes, are generated (Table C.1). The first corresponds to a dry gradient (sheltered internal valley in Valais, Figure C.1a) and the second to a wet gradient (exposed mountain side, Bernese Oberland, Figure C.1a). Thirty year long time series of cross-correlated precipitation, air temperature, relative humidity, wind speed, solar radiation, and atmospheric pressure for elevation bands from 500 up to 3500 m a.s.l. are generated to represent the climatic differences. For the T&C simulations of this study, only elevations ranging from 500 to 2500 m a.s.l. are used, since vegetation cover is usually rare above 2500 m a.s.l.

Table C.1: Selected stations (with mean values of different meteorological variables) used for generating the dry and wet climatic gradients across the different elevation bands.

| Station | Number of years available | Elevation [m a.s.l.] | Precipitation [mm yr ⁻¹] | Air temperature [°C] | Wind speed [m s ⁻¹] | Relative humidity [-] | Solar radiation [W m ⁻²] | Atmospheric pressure [hPa] |
|---------------------------|---------------------------------|-------------------------|---|----------------------------|------------------------------------|-----------------------------|--|-------------------------------|
| <i>Dry gradient</i> | | | | | | | | |
| Sion | 30 | 482 | 597 | 10.1 | 2.16 | 0.70 | 189 | 960 |
| Visp | 30 | 639 | 589 | 9.43 | 2.99 | 0.68 | 182 | 941 |
| Zermatt | 29 | 1638 | 626 | 4.33 | 1.84 | 0.64 | 183 | 834 |
| Evolene | 24 | 1825 | 719 | 4.36 | 0.71 | 0.64 | 191 | 815 |
| Col du Gr. St. Bernard | 29 | 2472 | 2359 | -0.48 | 5.53 | 0.74 | 184 | 751 |
| <i>Wet gradient</i> | | | | | | | | |
| Wynau | 30 | 422 | 1195 | 9.08 | 1.78 | 0.79 | 154 | 967 |
| Interlaken | 30 | 577 | 1158 | 8.83 | 1.63 | 0.77 | 156 | 949 |
| Adelboden | 30 | 1320 | 1319 | 6.05 | 1.42 | 0.73 | 159 | 867 |
| Grimsel | 22 | 1980 | 1833 | 1.2 | 4.83 | 0.72 | 183 | 802 |
| Jungfrauoch | 30 | 3580 | - | -7.9 | 7.34 | 0.7 | 205 | - |

C.1.2 Climatic gradients: validation

The simulated hourly time series reproduce well the statistics of observed meteorological variables. First and high-order statistics as well as seasonality, show a consistent transition across all of the elevations and are in a close agreement with the station-based records (Figure C.2, C.3, and C.4 respectively).

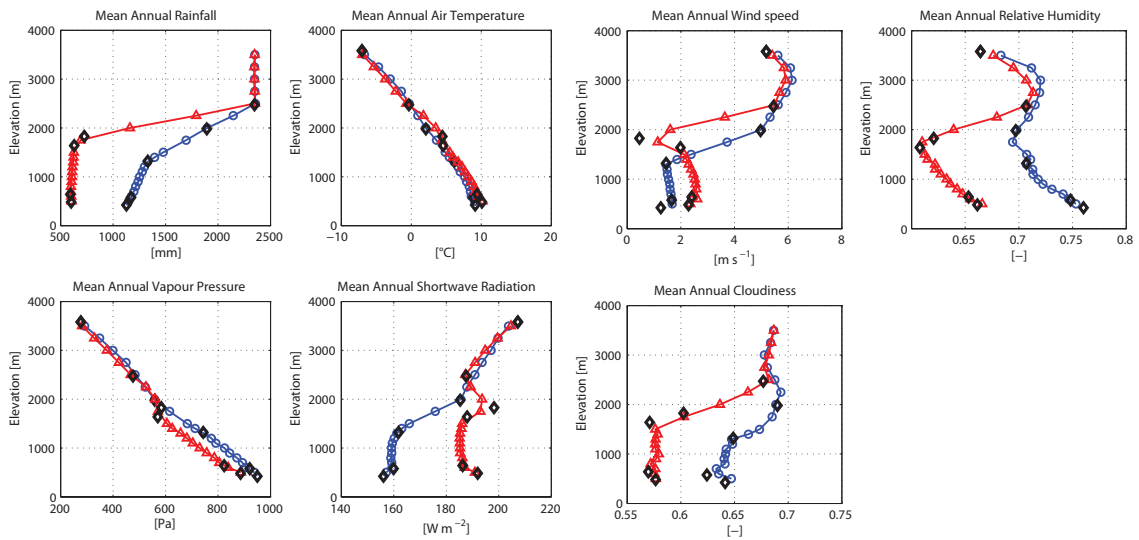


Figure C.2: Mean climate gradients for the examined meteorological variables, as simulated with the weather generator (blue and red points correspond to wet and dry precipitation regimes respectively) as well as the observed mean climatic variables based on the station data (black diamonds).

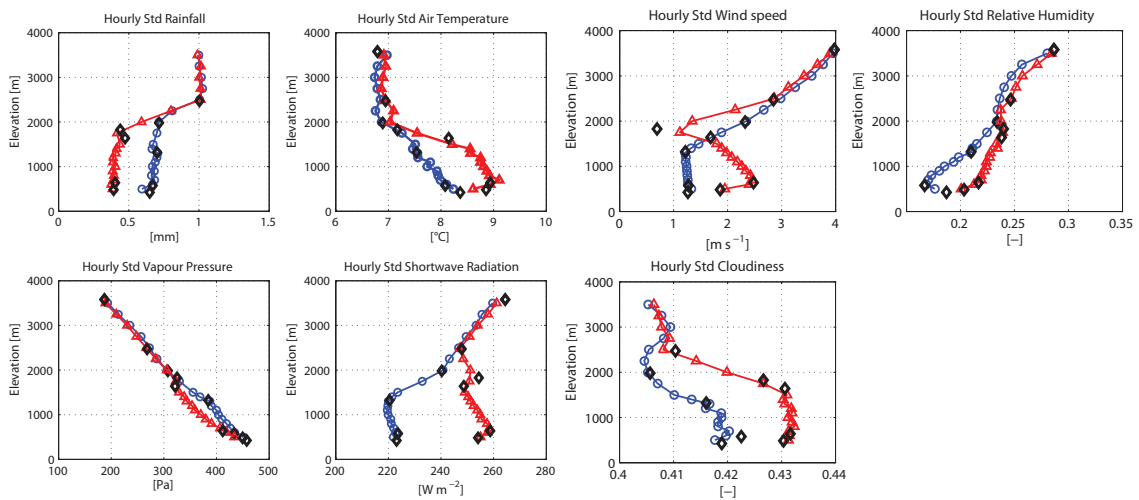


Figure C.3: Hourly standard deviations of the climate gradients for the examined meteorological variables, as simulated with the weather generator (blue and red points correspond to wet and dry precipitation regimes respectively) as well as of the observed climatic variables based on the station data (black diamonds).

C.1.3 Climatic gradients: long-term dynamics

The long term dynamics (i.e., average values over the 30 yr of the simulated time series) of the major environmental drivers of T&C simulations across the altitudinal and precipitation gradients are illustrated in Figure C.5.

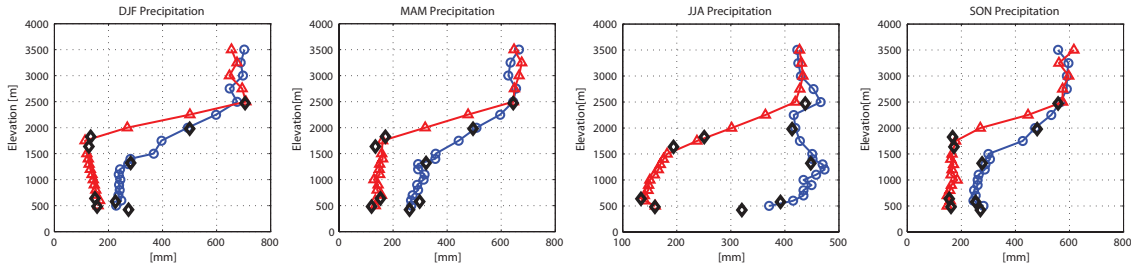


Figure C.4: Seasonal precipitation as simulated with the weather generator (blue and red points correspond to wet and dry precipitation regimes respectively) as well as the observed seasonality based on the station data (black diamonds).

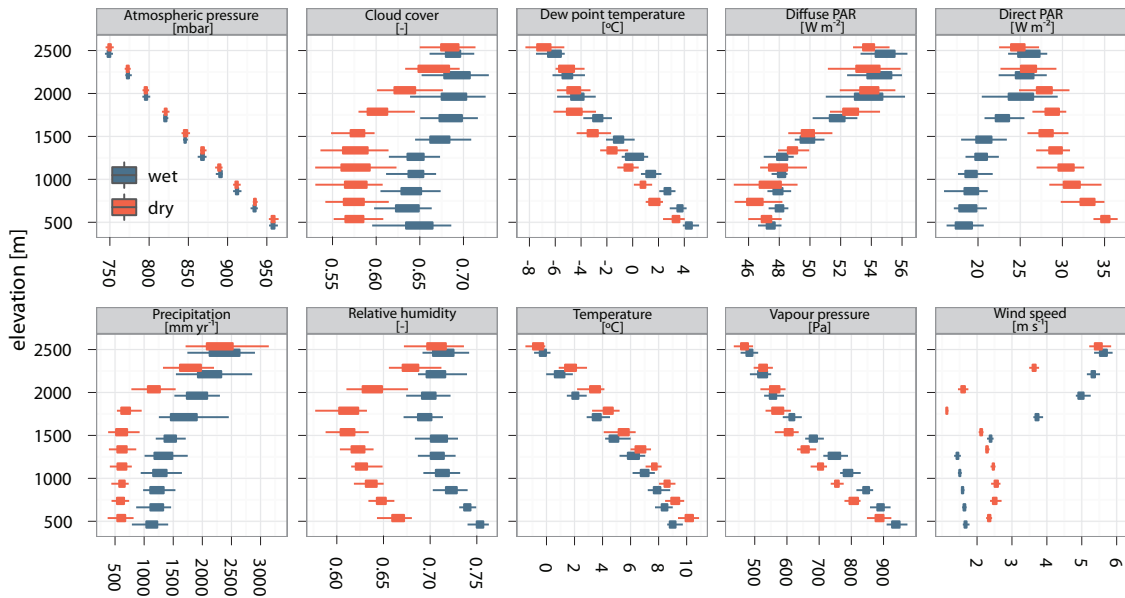


Figure C.5: Variation of the mean annual values (averaged over 30 yr) of major environmental variables across the examined precipitation (wet, dry), and elevation gradients. Boxes extend from the 25th to the 75th percentile, while whiskers extend to 1.5 times the interquartile range of the lower and upper quartiles respectively.

C.2 METHODOLOGICAL DETAILS ON THE GENERATION OF PROXY PLANT SPECIES

Proxy plant species are generated combining: (i) three categories of plant-life forms (reflecting structural and phenological differences among plant species; Section C.2.1); (ii) three discrete plant drought tolerances (Section C.2.2); and (iii) four major leaf traits, constructed using a continuous spectrum of values across the observed leaf economics spectrum (Section C.2.3).

C.2.1 *Separating plant-life forms*

The immense diversity of plant-life strategies and their structural (e.g., plant tissues) and phenological differences are tackled in the T&C framework using three discrete plant-life forms (denoted as “evergreen”, E, “deciduous”, D, and “grass”, G). Vegetation species that share the same life form (tree or grass) and structural attributes (phenology and carbon pools) are considered to belong to the same T&C plant-life form [also called “broad vegetation categories” in [Fatichi et al., 2012a](#)]. This differentiation is necessary because the three vegetation categories have substantially different phenology and carbon pool dynamics. In T&C, the following attributes vary among the simulated plant-life forms:

- the number of carbon pools (in the grass life form, there is no carbon pool corresponding to sapwood and heartwood),
- the phenology of allocation to and translocation from the carbohydrate reserves,
- the phenology of allocation strategies, i.e., in evergreen plant-life form, carbon is allocated to all of their compartments, including reserves throughout the entire year,
- the leaf turnover rates,
- the phenological states, i.e., deciduous and grass plant-life forms experience all phenological states (dormant, maximum growth, normal growth, and senescence), while for evergreen plant-life forms senescence and dormant states are merged,
- the transition across phenological states varies also for the three plant-life forms (i.e., changes from normal growth to senescence and from senescence to dormant statuses).
- the allometric constraints, i.e., leaf-to-root ratio varies among different plant-life forms (higher values for woody in comparison to herbaceous species),
- the translocation rate (higher values for plants that attain faster grow rates after leaf onset e.g., grasses, temperate deciduous species),

More details regarding the differentiation and parameterization of the three plant-life forms within the frame of T&C can be found in [[Fatichi et al., 2012a](#)]. Table [C.2](#) summarizes the T&C parameters that vary across the simulated plant-life forms in this study.

Table C.2: T&C parameters used for generating proxy plant species for the three examined plant life forms (E: evergreen, D: deciduous, G: grass). More information, and justification of the selected values can be found in *Fatichi et al. [2012a, 2014]*.

| Parameter ID | Value | Description | Units |
|------------------------|-----------|---|--|
| d_{root}^{-1} | E: 1460 | Turnover rate of fine roots. | [d] |
| | D: 900 | | |
| | G: 550 | | |
| d_{sapw}^{-1} | E: 730 | Living sapwood to heartwood conversion rate. | [d] |
| | D: 550 | | |
| | G: - | | |
| K_n | E: 0.35 | Control parameter for the exponential decay of the canopy nitrogen profile. | [-] |
| | D: 0.35 | | |
| | G: 0.20 | | |
| R_{ltr} | E: 0.80 | Maximum leaf-to-root or shoot-to-root ratio (allometric constraint). | [-] |
| | D: 0.80 | | |
| | G: 0.35 | | |
| r_r | E: 0.050 | Respiration rate coefficient on a 10°C base. | [gC gN ⁻¹ d ⁻¹] |
| | D: 0.030 | | |
| | G: 0.045 | | |
| T_{day} | E: 13.0 | Mean duration of day for leaf onset. | [h] |
| | D: 12.8 | | |
| | G: 10.7 | | |
| TrC | E: 1.0 | Carbohydrate translocation rate. | [gC m ⁻² PFT d ⁻¹] |
| | D: 3.5 | | |
| | G: 2.0 | | |
| $T_{\text{s,LO}}$ | E: 4.5 | Prescribed temperature threshold for the beginning vegetation growth. | [°C] |
| | D: 4.0 | | |
| | G: 1.0 | | |
| gcI | 3.7 | Interception exponential decay parameter. | [mm ⁻¹] |
| KcI | 0.06 | Interception drainage rate coefficient. | [mm h ⁻¹] |
| Sp_SN_In | 5.9 | Maximum specific snow intercepted by vegetation. | [mm SWE LAI ⁻¹] |
| Sp_LAI_In | E: 0.1 | Maximum specific water intercepted by vegetation. | [mm LAI ⁻¹] |
| | D, G: 0.2 | | |
| d_{leaf} | E: 0.25 | Characteristic leaf dimension. | [cm] |
| | D: 4.00 | | |
| | G: 0.80 | | |
| FI | 0.081 | Intrinsic quantum efficiency. | [μmol CO ₂ μmol photons ⁻¹] |
| go | 0.01 | Cuticular conductance. | [mol CO ₂ s ⁻¹ m ⁻²] |
| gR | 0.25 | Growth respiration coefficient. | [-] |
| Mf | 1/50 | Fruit maturation turnover rate. | [d ⁻¹] |

Table C.2. (continued)

| Parameter ID | Value | Description | Units |
|--------------|------------------------------------|--|--|
| DSE | E, D: 0.649 G: 0.656 | Entropy factor. | [kJ mol ⁻¹] |
| Ha | E, D: 72 G: 55 | Activation energy. | [kJ mol ⁻¹ K ⁻¹] |
| rjv | E: 2.0 D: 2.5 G: 2.6 | Scaling factor between J _{max} (canopy maximum electron transport) and V _{max} (maximum Rubisco capacity). | [μmol Eq μmolCO ₂ ⁻¹] |
| Ns | N _f /0.145 | Sapwood carbon-nitrogen content as a fraction of foliage carbon-nitrogen mass ratio (N _f). | [gC gN ⁻¹] |
| Nr | N _f /0.860 | Fine root carbon nitrogen content as a fraction of foliage carbon-nitrogen mass ratio (N _f). | [gC gN ⁻¹] |
| dd_max | E: 1/360 D, G: 1/365 | Maximum leaf turnover rate induced by drought. | [d ⁻¹] |
| dc_C | E: 78/365 D: 32/365 G: 6/365 | Linear coefficient for foliage loss due to cold temperature. | [d ⁻¹ °C ⁻¹] |
| Tcold | E: -20 D: 4 G: 0 | Temperature threshold for foliage loss. | [°C] |
| Bfac_lo | E, D: 0.95 G: 0.99 | Moisture stress threshold for the beginning of vegetation growth. | [-] |
| dmg | E: 30 D: 35 G: 20 | Number of days of maximum growth. | [d] |
| LAI_min | E: 0.001 D: 0.010 G: 0.100 | Minimum leaf area index at which canopy is considered completely defoliated. | [m ² leaf m ⁻² ground] |
| mjDay | E: 180 D, G: 250 | Maximum Julian day for leaf onset. | [-] |
| eps_ac | E: 0.1 D: 1.0 G: 0.2 | Parameter controlling the allocation to carbohydrate reserve. | [-] |
| LDay_cr | E: 9.65 D: 11.50 G: 10.70 | Day light threshold for senescence. | [h] |
| Klf | E: 1/40 D: 1/28 G: 1/50 | Dead leaves fall turnover rate. | [d ⁻¹] |
| fab | E, D: 0.74 G: 0 | Fraction above-ground sapwood and heartwood reserve. | [-] |
| fbe | E, D: 0.26 G: 1.00 | Fraction below-ground sapwood and heartwood carbohydrate reserve. | [-] |

C.2.2 Parameterizing plant drought tolerance

In order to mimic different plant strategies for responding to drought-induced stress, four T&C parameters, related to plant water abstraction, were adjusted, corresponding to “low” (L), “medium” (M), and “high” (H) drought tolerances

(see Table C.3). More specifically, plants with low drought tolerance can uptake water only at high values of soil water potential (at the beginning as well as at full stomatal closure), in comparison to plants with medium and high drought tolerances that are capable of uptaking water at lower water potentials, allowing them to perform better under water-limited conditions. In addition, deeper plant rooting depth moving from low to higher drought tolerances, therefore allowing species with high drought tolerance to uptake water from a deeper soil profile. Finally, we assigned different sensitivities of stomatal conductances to species with high drought tolerance (in T&C stomatal dynamics are simulated through the coupled photosynthesis-stomatal resistance scheme proposed by *Leuning* [1990]; *Collatz et al.* [1991, 1992]; *Leuning* [1995]). Based on Eq. (5) in *Fatichi et al.* [2012a], species with high (low) drought tolerance, are characterized by low (high) values of the empirical parameter in the Leuning's stomatal conductance equation (parameter α in Table C.3) leading therefore to larger (lower) water use efficiency. Note that it is rare in nature to have all the considered traits (soil water potentials impairing functional activities, rooting depth, and stomatal dynamics) playing in the same direction of "drought tolerance" vs "drought intolerance". The selected strategies are therefore rather extreme, but still plausible drought strategies.

Table C.3: Description of the parameters used for mimicking different plant strategies for drought tolerance (L: low, M: medium, H: high).

| Parameter ID | Value | Description | Units | References |
|-------------------|--------|---|-------|--|
| α | L:10 | Empirical parameter in Leuning's equation for stomatal conductance. | [-] | Fatichi et al. 2012a; Leuning, 1995, 1990 |
| | M:8 | | | |
| | H:6 | | | |
| PSI _{ss} | L:-0.5 | Soil water potential at which stomatal closure begins. | [MPa] | Manzoni et al. 2013 |
| | M:-1.2 | | | Scoffoni et al. 2012 |
| | H:-2.0 | | | Blackman et al. 2010 Meinzer et al. 2009 Maherali et al. 2004 |
| PSI _{wp} | L:-1.0 | Soil water potential at full stomatal closure (wilting point). | [MPa] | Manzoni et al. 2013 |
| | M:-3.0 | | | Scoffoni et al. 2012 |
| | H:-5.0 | | | Blackman et al. 2010 Meinzer et al. 2009 Maherali et al. 2004 |
| ZR95 | grass | L:0.10 | [m] | Canadell et al., 1996; Jackson et al 1996, 1997; Schenk & Jackson 2002a,b Manzoni et al. 2013 |
| | | M:0.25 | | |
| | | H:0.50 | | |
| | trees | L:0.5 | | |
| | | M:1.0 | | |
| | | H:1.5 | | |

C.2.3 *Sampling proxy species with coordinated leaf traits*

There is empirical evidence that several plant traits are cross-correlated [e.g., [Reich et al., 1997](#); [Wright et al., 2004](#); [Kattge et al., 2011](#)]. In the present study, the freely available GLOPNET dataset [<http://bio.mq.edu.au/~iwright/glopnet.htm>; [Wright et al., 2004](#)], is used for generating proxy plant species with coordinated leaf-level plant traits. More specifically, using data from the leaf economics spectrum [[Wright et al., 2004](#)], the following leaf properties are investigated: (i) critical age for leaf shed, A_{cr} , (ii) maximum Rubisco capacity (obtained through the conversion from the photosynthetic capacity rates, A_{mass} , see detailed discussion in Section C.2.4), (iii) carbon-nitrogen mass ratio for the foliage N_f , and (iv) specific leaf area, SLA (equal to $1/LMA$, where LMA is the Leaf Mass per Area). A_{cr} , A_{mass} , N_f , and SLA are selected since they are well-documented, quantitative plant traits, with high species coverage worldwide [[Kattge et al., 2011](#)].

Using the GLOPNET records, three major plant categories are identified, corresponding to two growth forms (i.e., tree and grass) and two phenological states (i.e., evergreen and deciduous). Regarding the photosynthesis pathway, only C₃ type of plants were selected. Having distinguished the three subsets, empirical cross-correlations among the leaf-traits were conserved by sampling values from a multivariate normal distribution with the same statistical properties as the inferred from GLOPNET. In order to avoid outliers that correspond to species that cannot occur in the European Alpine environment, values below the 5 % and above the 95 % quantile of the traits distribution are discarded. Table C.4 provides a detail description of the aforementioned variables as well as their ranges of variability.

C.2.3.1 *Sampling leaf traits from a truncated multivariate normal distribution*

We generate 100 proxy species (hypothetical species with realistic properties) for each plant-life form. We use a truncated multivariate normal distribution, fitted using the empirical statistical properties (mean, variance, and cross-correlations) from the GLOPNET dataset. Since the goal of the study is to investigate the role of inter- and intra-specific trait variability in the simulated carbon and water fluxes and states, 100 proxy species are considered a number large enough for covering the multi-dimensional space of major plant traits within T&C. The package *tmvtnorm* in R environment [[RCoreTeam, 2012](#)] was used.

C.2.3.2 *Evaluating the assumption of normally distributed plant traits*

The assumption of normality in the log-transformed leaf-traits facilitates the sampling procedure. The well-established multivariate normal distribution can

Table C.4: A description of leaf-traits used for generating proxy plant species with coordinated properties. The empirical covariances from the GLOPNET dataset are conserved among the leaf traits. The ranges from the multivariate normal sampling are reported as minimum (Min.) and maximum (Max.) values, while in parentheses are the ranges from the original GLOPNET dataset. E, D, G, correspond to the three investigated plant life forms, i.e., evergreen, deciduous, and grass, respectively.

| Parameter ID | Min. | Max. | Description | Units |
|--------------|--|--|---|---|
| A_{cr} | E: 228 (144) D: 107 (87) G: 51 (30) | E: 1848 (8652) D: 280 (329) G: 189 (1371) | Critical age for leaf shed. | [d] |
| A_{mass} | E: 1.63 (1.41) D: 3.48 (3.80) G: 4.69 (4.27) | E: 25.99 (28.18) D: 25.26 (23.44) G: 35.14 (35.48) | Photosynthetic assimilation rates measured under high light, ample soil moisture and ambient CO_2 . | $[\mu\text{mol } CO_2 \text{ s}^{-1} \text{ m}^{-2}]$ |
| V_{cmax} | E: 11 D: 23 G: 32 | E: 177 D: 172 G: 241 | Leaf-level values of maximum Rubisco capacity at 25 °C. | $[\mu\text{mol } CO_2 \text{ s}^{-1} \text{ m}^{-2}]$ |
| N_f | E: 19.40 (11.70) D: 16.00 (10.60) G: 15.60 (11.60) | E: 62.90 (122.20) D: 34 (58.20) G: 45.90 (72.40) | Carbon-nitrogen mass ratio for foliage. | $[\text{gC gN}^{-1}]$ |
| SLA | E: 0.007 (0.001) D: 0.015 (0.009) G: 0.011 (0.003) | E: 0.034 (0.078) D: 0.046 (0.078) G: 0.058 (0.066) | Specific leaf area. | $[\text{m}^2 \text{ LAI gC}^{-1}]$ |

be therefore used for sampling values (proxy species) with prescribed statistical properties (i.e., corresponding to the observed values and their empirical covariances). In order to assess the robustness of the normality assumption the quantile-quantile (Q-Q) plots of the analyzed plant traits were considered (Figure C.6) and we conducted three statistical tests (Shapiro-Wilks, Kolmogorov-Smirnov, Anderson-Darling) (Table C.5).

From the Q-Q plots (Figure C.6) we can conclude that the assumption of normality in the examined traits can be considered a fair approximation. For evergreen and deciduous plant-life forms most of the points fall on a line with only few deviations (i.e., there are a few outliers in the datasets). There are important deviations from normality for the grass plant-life form regarding the four examined leaf traits. Several points are lying out of the theoretical vs sample quantile line. This left-end of pattern below the line and the right-end of pattern above the line underlies the existence of long tails at both ends of data distribution. Leaf mass per area (LMA) has also a deviation from normality: the data distri-

bution is skewed to the right since the Q-Q plot shows a curved pattern with the slope increasing from left to right. A possible explanation for these deviations of normality is the small sample size (the available data from GLOPNET that correspond to C_3 grass are 19, 47, 45, 21 for A_{cr} , LMA, N_f , and A_{mass} respectively) rather than a strong evidence for a distribution of the population different from the normal.

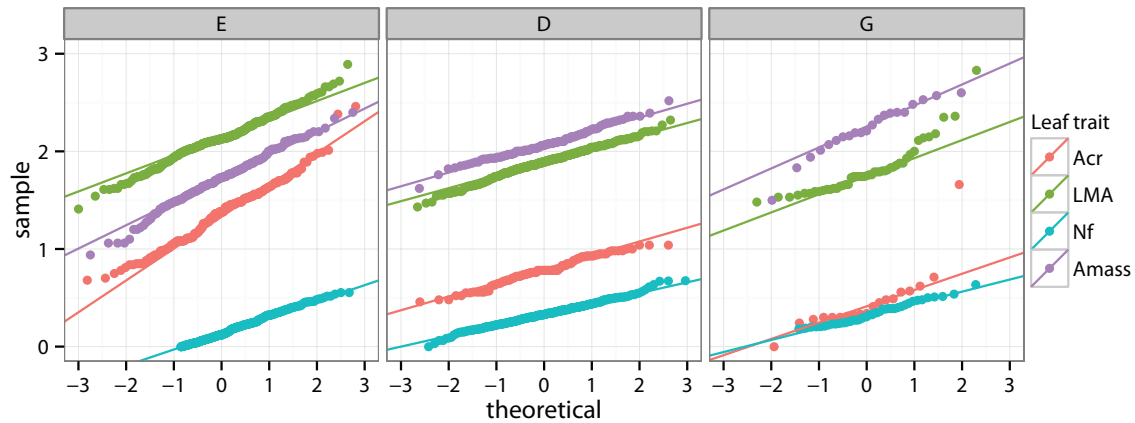


Figure C.6: Quantile-quantile plots for the three analyzed plant-life forms (evergreen, E, deciduous, D, and grass, G), for the examined leaf traits (plotted in the logarithmic scale; A_{cr} [mo]: leaf lifespan; LMA [$gDM\ m^{-2}$]: Leaf Mass per Area; N_f [%]: leaf N per leaf dry mass; A_{mass} [$nmol\ C\ gDM^{-1}\ s^{-1}$]: photosynthetic capacity), as obtained from the GLOPNET dataset. Units are indicated prior to \log_{10} transformation.

In order to evaluate the assumption of normality with a more formal approach, we carried out three well established statistical tests. The results are summarized in Table C.5. A significance value of 0.05 is used as a cutoff for the statistical tests. In the Shapiro-Wilks and Kolmogorov-Smirnov tests, the null hypothesis is that the sample comes from a normal distribution. The p-values of these tests therefore reflect the chances that the sample comes from a normal distribution, i.e., the lower the p-value the smaller the chance. In other words, p-values higher than 0.05 support the null hypothesis, while small p-values imply deviation from normality. The Anderson-Darling test is evaluating whether data-sample came from a population with a specific distribution. This is a modification of the Kolmogorov-Smirnov test with additional weight to distribution's tails. The null hypothesis is again that the data come from a normal distribution and low p-values therefore imply a rejection of the normality hypothesis.

We conclude that despite small deviations from normality, in the scope of our application, the use of a multivariate normal distribution for sampling plant species with coordinated leaf traits (in the logarithmic scale, using the GLOPNET dataset) is a good approximation, and it is in accordance with other studies [e.g., *Kattge et al., 2011*], where the distribution of many plant traits is identified as log-normal.

Table C.5: Sample size of the examined sub-sets from the GLOPNET dataset as well as the obtained p-values of the implemented statistical test for assessing the normality of the sampled data for the three examined plant life forms (E: evergreen, D: deciduous, G: grass).

| | | A_{cr} | LMA | N_f | A_{mass} |
|--------------------|---|--------------|--------------|--------------|--------------|
| Number of values | E | 203 | 370 | 404 | 168 |
| | D | 109 | 375 | 324 | 113 |
| | G | 19 | 47 | 45 | 21 |
| Shapiro-Wilks | E | 0.014 | 0.001 | 0.319 | 0.442 |
| | D | 0.028 | 0.130 | 0.080 | 0.340 |
| | G | 0.000 | 0.000 | 0.006 | 0.253 |
| Kolmogorov-Smirnov | E | 0.431 | 0.083 | 0.327 | 0.939 |
| | D | 0.153 | 0.357 | 0.964 | 0.346 |
| | G | 0.381 | 0.115 | 0.329 | 0.976 |
| Anderson-Darling | E | 0.038 | 0.000 | 0.080 | 0.503 |
| | D | 0.017 | 0.047 | 0.393 | 0.152 |
| | G | 0.000 | 0.000 | 0.022 | 0.495 |

C.2.3.3 Sampled vs observed covariation of plant traits

The selected leaf traits (LL: leaf lifespan, LMA: Leaf Mass per Area, Nmass: leaf N per leaf dry mass, Amass: photosynthetic capacity) of the generated proxy plant species for each plant-life form are compared with the observed values from the GLOPNET dataset (Figures C.7, C.8, C.9, for evergreen, deciduous, and grass life forms). The fitted multivariate normal distribution is capturing well the cross-correlations of the examined leaf traits, providing therefore an efficient sampling across the continuous spectrum of observed leaf-plant properties.

C.2.4 Converting values of photosynthetic capacity (A_{mass}) to maximum Rubisco capacity at 25 °C (V_{cmax})

Similarly to other vegetation models, photosynthetic activity in T&C is modeled using an enhanced version of the biochemical model introduced by *Farquhar et al.* [1980]. A detailed description of the embedded photosynthesis scheme can be found in *Fatichi et al.* [2012a]. Contrary to other approaches for modeling photosynthesis [e.g., no-rectangular hyperbola; *Johnson and Thornley, 1984*], the photosynthetic capacity (A_{mass}) is not used directly in the model parameterization and three limiting factors are assumed to regulate the leaf level carbon assimilation: (i) Rubisco-limitation, (ii) light-limitation, and (iii) export-limited assimilation rates. The Rubisco activity is included in the biochemical model of photosynthesis through the maximum Rubisco capacity (V_{cmax}). Photosynthetic

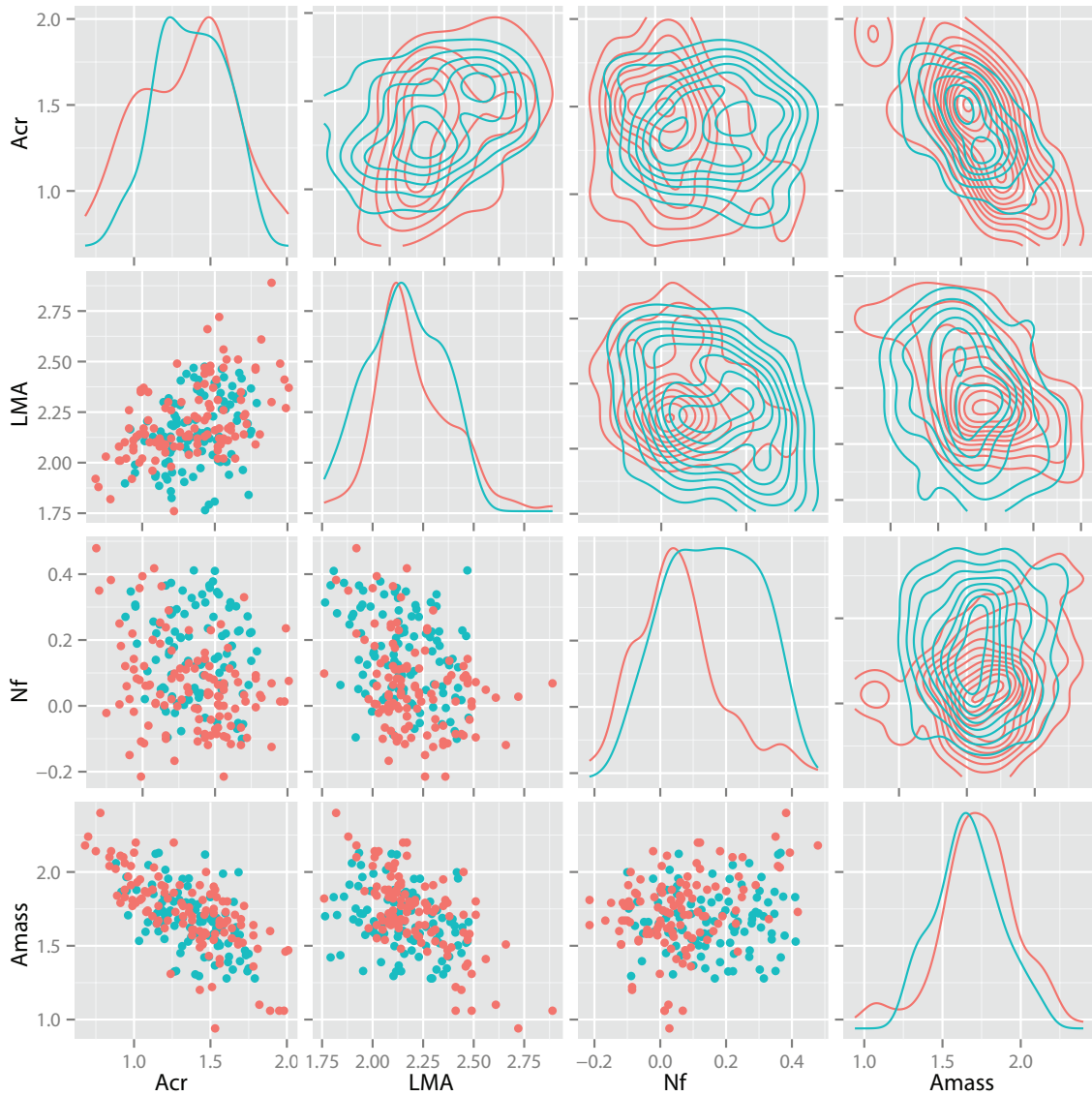


Figure C.7: Major plant functional traits (Acr [mo]: leaf lifespan; LMA [gDM m^{-2}]: Leaf Mass per Area; Nf [%]: leaf N per leaf dry mass; Amass [$\text{nmol C gDM}^{-1} \text{s}^{-1}$]: photosynthetic capacity) for evergreen trees as obtained by the GLOPNET database (<http://bio.mq.edu.au/~iwright/glopian.htm>), denoted in red, as well as the 100 generated plant strategies (denoted in blue) based on the GLOPNET statistics (mean, variance, and covariances of the examined traits). Units are indicated prior to \log_{10} transformation. In order to avoid rare/extreme values of plant traits, only values in the 5 to 95% quantile of the probability density function are included in the analysis.

capacity (A_{mass}) can be therefore used as a surrogate for the maximum Rubisco capacity [e.g., *Collatz et al., 1992*] providing that light, temperature, and humidity are not downregulating carbon assimilation. In the present study, leaf-level values of V_{cmax} are inferred from the sampled values of A_{mass} (maintaining the empirical cross-correlations from the GLOPNET database). A detailed biochemical model of photosynthesis was used for converting the maximum pho-

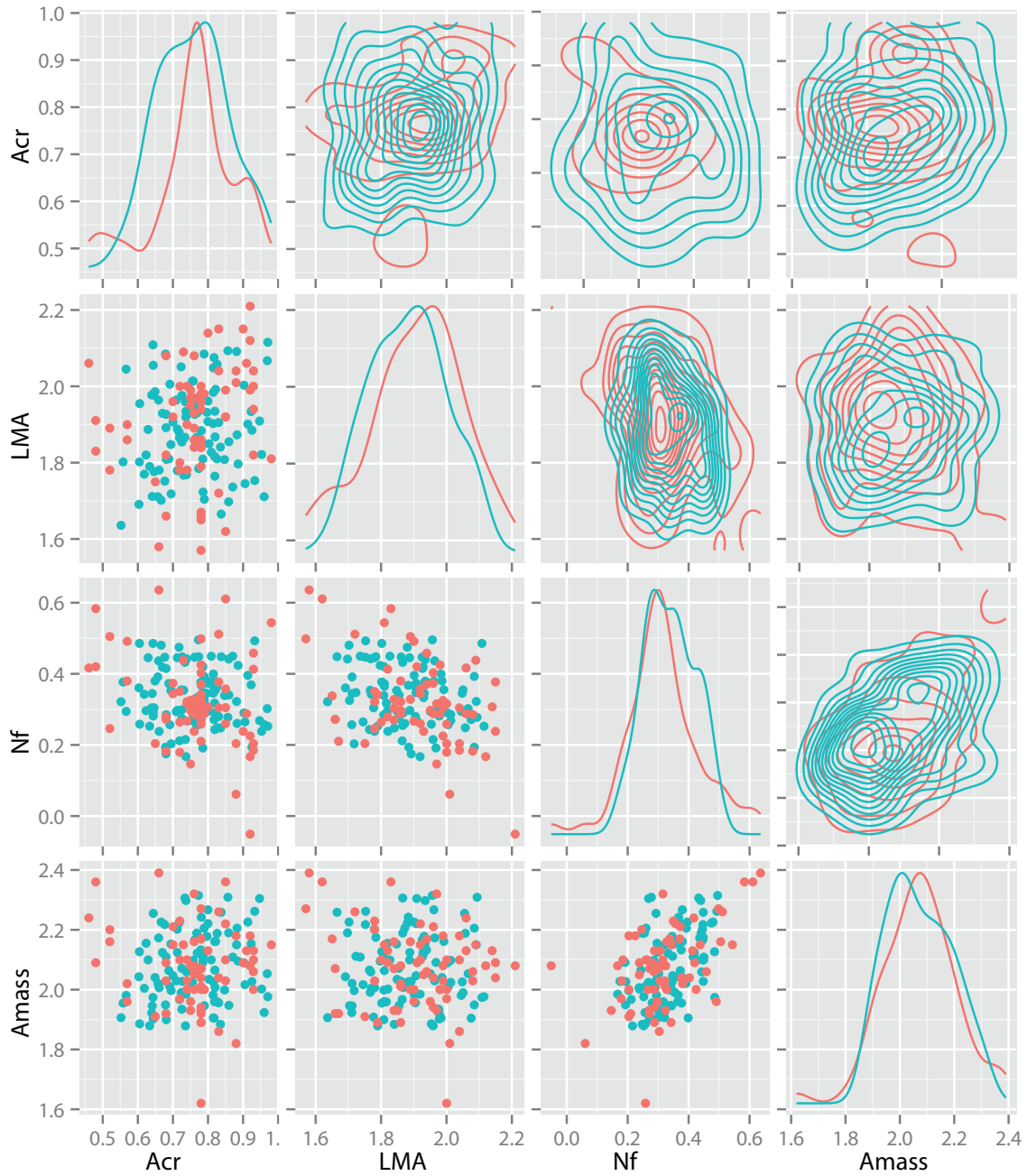


Figure C.8: Same as Figure C.7, but for deciduous trees.

tosynthetic capacity to the corresponding maximum Rubisco capacity at 25 °C (V_{cmax}).

The computer code of the implemented photosynthesis model is provided in a separate file [R format *RCoreTeam*, 2012]. In summary, it is based on a model described by *Bonan et al.* [2011], with the temperature dependence parameterization provided by *Kattge and Knorr* [2007]. The enclosed computer code provides all the necessary documentation for the implemented equations and param-

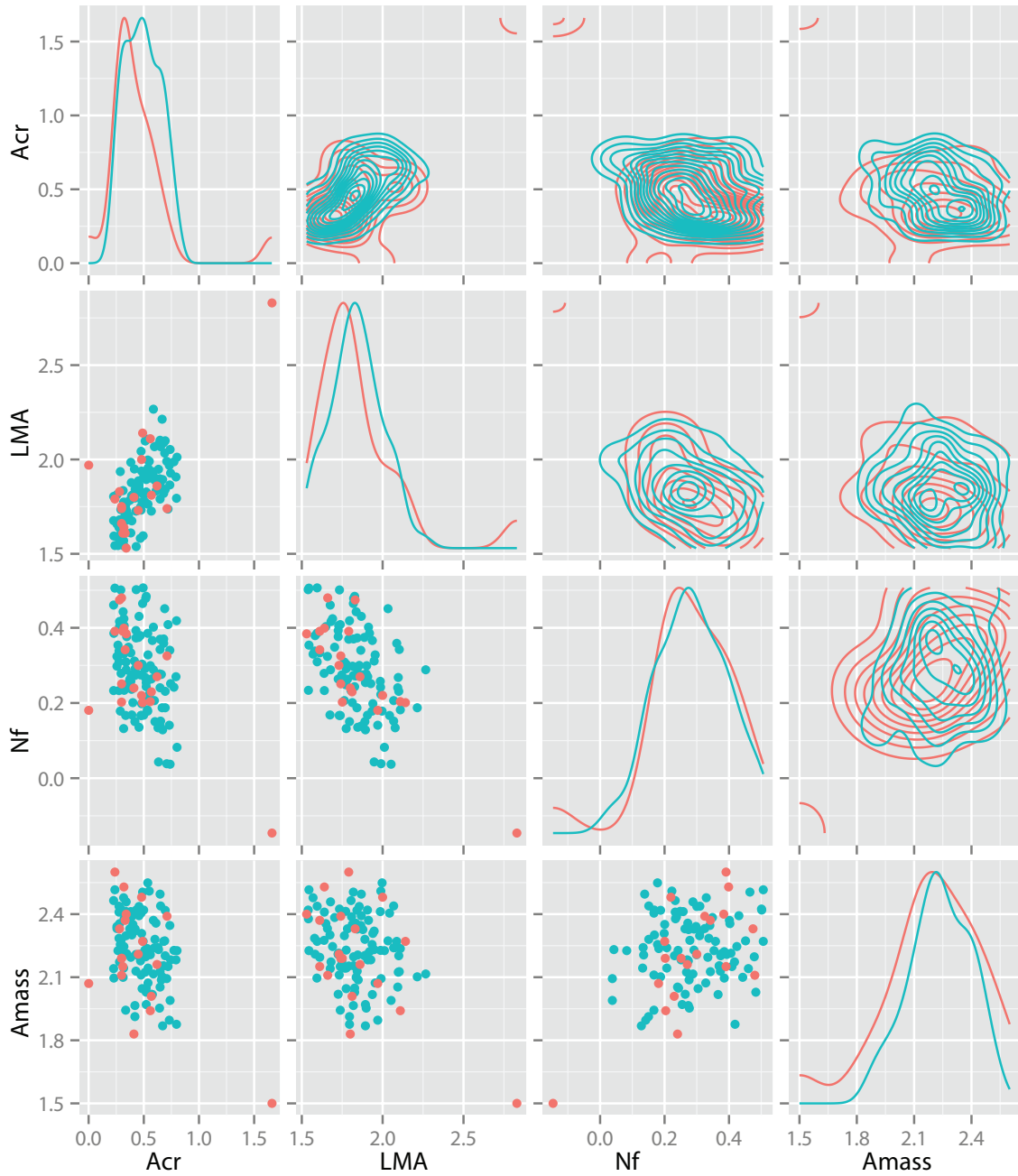


Figure C.9: Same as Figure C.7, but for grass.

terization of the photosynthesis scheme, therefore assuring reproducibility and providing a useful toolbox for mechanistic conversion of A_{mass} to V_{cmax} .

According to *Wright et al. [2004]*, reported values of photosynthetic capacity (A_{mass}) correspond to photosynthetic assimilation rates measured under favorable environmental conditions, i.e, light saturation, favorable temperature, high soil moisture, no restriction due to vapour pressure deficit, and ambient CO_2 concentration. In quantitative terms, we mimic these favorable environmental conditions using the aforementioned photosynthesis model driven with a wide

range of incoming photosynthetically active radiation (0-500 W m⁻²), so as to obtain light saturation. Average CO₂ concentration over the last 20 years with no imposed soil moisture or vapour pressure deficit limitations were also used. The optimal temperature for photosynthesis was calculated following *Kattge and Knorr* [2007]. More specifically, we used a modified Arrhenius function [*Johnson et al.*, 1942; *Medlyn et al.*, 2002b] to describe the temperature dependence of V_{cmax} . The optimum temperature for photosynthesis for A_{mass} and thus the optimum temperature for estimating V_{cmax} is [*Medlyn et al.*, 2002b]:

$$T_{\text{opt}} = \frac{H_d}{\Delta S - R \ln \left(\frac{H_a}{H_d - H_a} \right)} \quad (\text{C.1})$$

where H_a [kJ mol⁻¹] is the activation energy, H_d [kJ mol⁻¹] is the deactivation energy, and ΔS [J mol⁻¹ K⁻¹] is the so-called entropy factor. Assuming H_d equal to 200 kJ mol⁻¹ [*Kattge and Knorr*, 2007; *Medlyn et al.*, 2002a] and inserting into Eq. C.1 mean values of H_a and ΔS as estimated by the 36 plant species analyzed by *Kattge and Knorr* [2007] (i.e., $H_a = 72$ kJ mol⁻¹ and $\Delta S = 649$ J mol⁻¹ K⁻¹), the optimal temperature for estimating V_{cmax} (and thus the one that corresponds to A_{mass}) is equal to 32.8 °C.

While it is widely known that the optimum temperature for photosynthesis varies with plant growth and temperature [i.e., acclimation effects; *Kattge and Knorr*, 2007; *Medlyn et al.*, 2002a, b], the purpose of our study is to generate realistic proxy plant species with coordinated variations of plant traits. Therefore, the assumption of uniform optimal temperature for photosynthesis, across the analyzed values of A_{mass} does not affect the final results.

Figure C.10 illustrates a theoretical relationship between maximum Rubisco capacity and photosynthetic capacity as obtained from the biochemical model of photosynthesis. More specifically, using this scheme, we obtain which is the value of V_{cmax} that yields the A_{mass} sampled from the GLOPNET database. It is worth mentioning that Rubisco activity is one, out of many factors limiting photosynthesis, therefore a plateau occurs when V_{cmax} increases leading to an upper bound in the yielded A_{mass} values. For the 100 generated proxy plant species, V_{cmax} was found to range from 11 to 177, 23 to 172, 32 to 241, with A_{mass} from 1.63 to 25.99, 3.48 to 25.26, 4.69 to 35.14, for evergreen, deciduous, and grass plant-life forms respectively. The coefficient of variation of V_{cmax} (A_{mass}) is in the same order of magnitude for the three examined plant-life forms, i.e., 55.7 (55.9), 40.5 (40.7), and 49.2 (48.7) % for evergreen, deciduous and grass plant-life forms respectively.

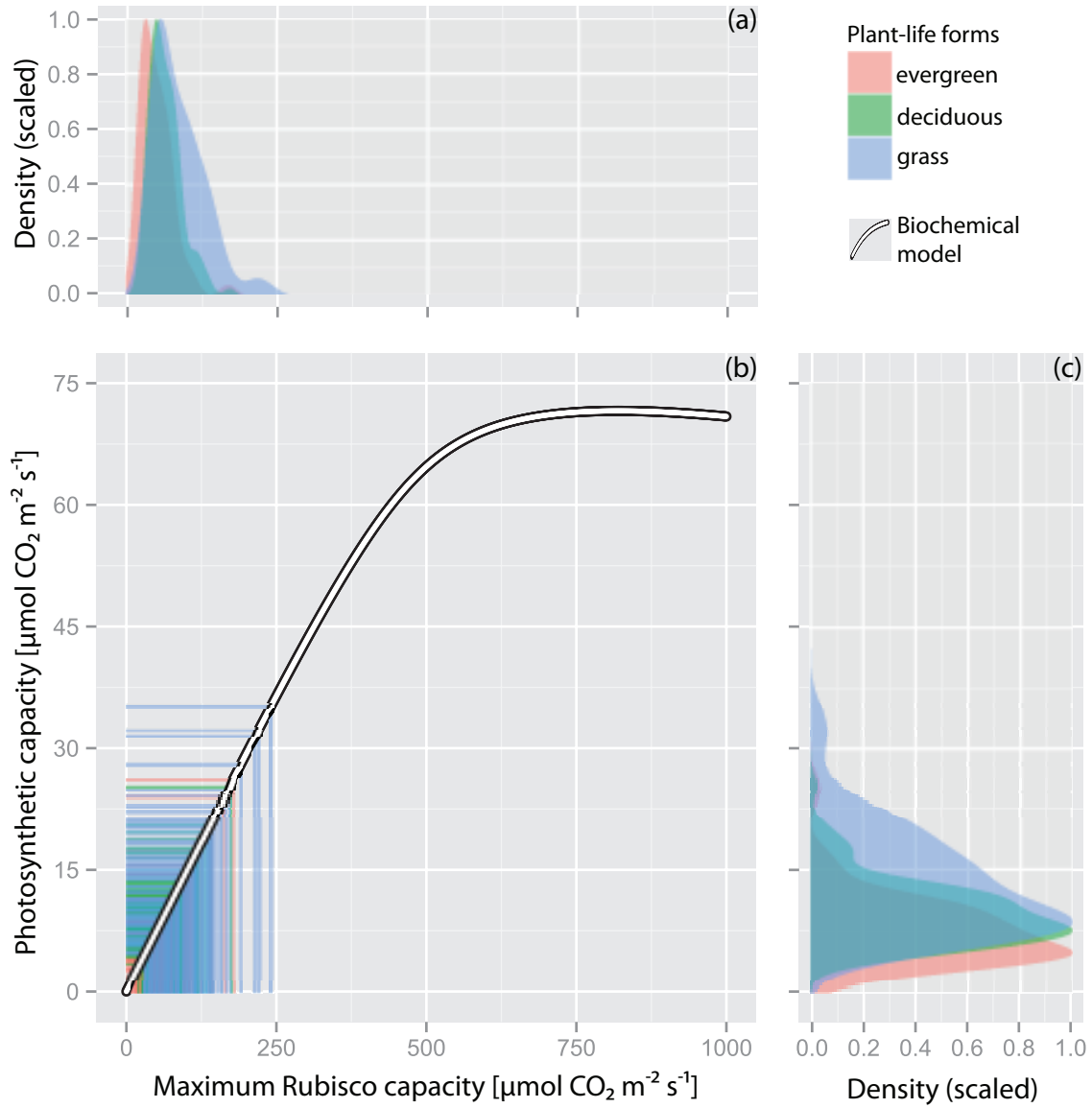


Figure C.10: Conversion function between photosynthetic capacity and maximum Rubisco capacity as obtained by a mechanistic biochemical model of photosynthesis. (a) Density of the yielded V_{cmax} , (b) theoretical curve as derived from the photosynthesis model, and (c) density of the originally sampled A_{mass} values for the three examined plant-life forms.

C.3 DATA DESCRIPTION

C.3.1 Eddy flux tower data

Data of photosynthetic activity (Gross Primary Productivity; GPP), estimated in five different eddy flux towers located in European Alps, are included in our analysis (Table C.6). Two sites with evergreen one with deciduous forest are

included as well as three grassland sites (Table C.6). A detailed description of the data (location, time period of coverage etc.) is summarized in Table C.6.

Table C.6: Sites (location and tower characteristics) with eddy covariance measurements used for the gross primary productivity (GPP) comparisons.

| Site | ID | Lon | Lat | Elevation [m] | PFT | Country | Period | Link |
|------------|--------|-------|-------|---------------|----------------------|-------------|-----------|---|
| Bayreuth | DE-Bay | 11.87 | 50.14 | 775 | Evergreen Needleleaf | Germany | 1996-1999 | http://fluxnet.ornl.gov/site/405 |
| Chamau | CH-Cha | 8.41 | 47.21 | 393 | Grass | Switzerland | 2006-2008 | http://fluxnet.ornl.gov/site/304 |
| Davos | CH-Dav | 9.86 | 46.82 | 1639 | Evergreen Needleleaf | Switzerland | 2000-2005 | http://fluxnet.ornl.gov/site/319 |
| Fruebuel | CH-Fru | 8.54 | 47.12 | 982 | Grass | Switzerland | 2006-2008 | http://fluxnet.ornl.gov/site/306 |
| Laegeren | CH-Lae | 8.37 | 47.48 | 689 | Deciduous Broadleaf | Switzerland | 2004-2009 | http://fluxnet.ornl.gov/site/308 |
| Oensingenl | CH-Oe1 | 7.73 | 47.29 | 450 | Grass | Switzerland | 2002-2003 | http://fluxnet.ornl.gov/site/313 |
| Renon | IT-Ren | 11.43 | 46.59 | 1730 | Evergreen Needleleaf | Italy | 1999-2009 | http://fluxnet.ornl.gov/site/530 |

c.3.2 MODIS data

MODIS estimates of GPP and LAI across the examined elevation gradients (representative of the European Alpine region) are based on the MODIS land product MOD17A2 (Version 005) and MOD15A2 (Version 005) for GPP and LAI respectively. The resolution of both products is $1 \times 1 \text{ km}^2$ with a eight-days regular time-step. Apart from the usual quality assurance layer of MODIS products, an additional analysis was conducted following the methodology presented by *Hwang et al.* [2011]. A detailed description of MODIS pre-processing for the Alpine region is provided in *Bogler* [2013] as well as in Section B.4.

c.3.3 Swiss National Forest Inventory

The Swiss National Forest Inventory (NFI; <http://www.lfi.ch>), a joint project of the Federal Office for the Environment (FOEN) and the Swiss Federal Institute for Forest, Snow and Landscape Research (WSL), records different vegetation variables related to the area, structure and status of forests in Switzerland. The NFI database consists so far of three surveys: the first was conducted for the period from 1983 to 1985 (NFI₁), the second from 1993 to 1995 (NFI₂), and the third from 2004 to 2006 (NFI₃). For more details on the Swiss NFI and its methods see *Brassel and Lischke* [2001] and www.lfi.ch as well as in Section B.5. In the present study, we are focusing on the changes in aboveground (woody) biomass (ΔAGB) across elevation gradients (data provided by *WSL* [2012]). This changes are estimated using the mean values (over the three consecutive inventories) of the annual increments of aboveground woody biomass of the survivor trees in the sampled plots. In order to convert tree biomass to carbon amounts, a fixed proportion of 50% C per kg of dry biomass was assumed. The identified species in the forest inventory plots are assigned to broad vegetation categories representing evergreen and deciduous woody plant-life forms. Evergreen plant-life

form corresponds to the following species: *Picea* sp. (Spruce), *Abies* sp. (Fir), *Pinus* sp. (Scots pine), and *Pinus cembra* (Arve); and deciduous plant-life form to: *Fagus sylvatica* (Beech), *Acer* sp. (Maple), *Fraxinus* sp. (Ash-tree), *Quercus* sp. (Oak), and *Castanea sativa* (Chestnut). Since the values from the forest inventories are reported per total area of the examined plot (not based on the relative coverage of each species), for a fair comparison with model results (presented per plant-life form in the main text), we keep only the plots where more than 80% of the total plot biomass is coming from only one of the examined plant-life forms. More details on the pre-processing of the NFI data can be found in Section [B.5](#).

REFERENCES

- Abbott, M., J. Bathurst, J. Cunge, and P. O'Connell, An introduction to the European Hydrological System - Système Hydrologique Européen, 'SHE', 1: History and philosophy of a physically-based, distributed modelling system, *Journal of Hydrology*, 87, 45–59, 1986a.
- Abbott, M. B., J. C. Bathurst, J. A. Cunge, P. E. O'Connell, and J. Rasmussen, An Introduction to the European Hydrological System - Système Hydrologique Européen, 'SHE', 2: Structure of a Physically-Based, Distributed Modelling System, *Journal of Hydrology*, 87(2), 61–77, 1986b.
- Ackerly, D., Community assembly, niche conservatism, and adaptive evolution in changing environments, *International Journal of Plant Sciences*, 164, 164–184, 2003.
- Adams, H., H. Barnard, and A. Loomis, Topography alters tree growth-climate relationships in a semi-arid forested catchment, *Ecosphere*, 5(11), 1–16, 2014.
- Ahlström, A., P. A. Miller, and B. Smith, Too early to infer a global NPP decline since 2000, *Geophysical Research Letters*, 39(15), 1–6, doi: 10.1029/2012GL052336, 2012.
- Albert, C. H., W. Thuiller, N. G. Yoccoz, R. Douzet, S. Aubert, and S. Lavorel, A multi-trait approach reveals the structure and the relative importance of intra- vs. interspecific variability in plant traits, *Functional Ecology*, 24(6), 1192–1201, doi: 10.1111/j.1365-2435.2010.01727.x, 2010a.
- Albert, C. H., W. Thuiller, N. G. Yoccoz, A. Soudant, F. Boucher, P. Saccone, and S. Lavorel, Intraspecific functional variability: extent, structure and sources of variation, *Journal of Ecology*, 98(3), 604–613, doi: 10.1111/j.1365-2745.2010.01651.x, 2010b.
- Albert, C. H., F. Grassein, F. M. Schurr, G. Vieilledent, and C. Violle, When and how should intraspecific variability be considered in trait-based plant ecology?, *Perspectives in Plant Ecology, Evolution and Systematics*, 13(3), 217–225, doi: 10.1016/j.ppees.2011.04.003, 2011.
- Altherr, E., P. Unfried, J. Hradetzky, and V. Hradetzky, Statistische Rindenbeziehungen als Hilfsmittel zur Ausformung und Aufmessung unentrindeten Stammholzes, *Tech. Rep. Teil IV*, Mitteilungen der Forstlichen Versuchs- und Forschungsanstalt Baden-Württemberg 90, 1978.

- Alton, P. B., L. Mercado, and P. North, A sensitivity analysis of the land-surface scheme JULES conducted for three forest biomes: Biophysical parameters, model processes, and meteorological driving data, *Global Biogeochemical Cycles*, 20(GB1008), 1–11, doi: 10.1029/2005GB002653, 2007.
- Ammann, C., C. R. Flechard, J. Leifeld, A. Neftel, and J. Fuhrer, The carbon budget of newly established temperate grassland depends on management intensity, *Agriculture, Ecosystems and Environment*, 121, 5–20, doi: 10.1016/j.agee.2006.12.002, 2007.
- Anderson, R. G., et al., Biophysical considerations in forestry for climate protection, *Frontiers in Ecology and the Environment*, 9(3), 174–182, doi: 10.1890/090179, 2011.
- Anderson-Teixeira, K. J., et al., CTFS-ForestGEO: a worldwide network monitoring forests in an era of global change, *Global Change Biology*, pp. n/a–n/a, doi: 10.1111/gcb.12712, 2014.
- Antonarakis, A., J. Munger, and P. Moorcroft, Imaging spectroscopy- and lidar-derived estimates of canopy composition and structure to improve predictions of forest carbon fluxes and ecosystem dynamics, *Geophysical Research Letters*, 41, 1–8, doi: 10.1002/2013GL058373, 2014.
- Araújo, M., and R. Costa-Pereira, Latitudinal gradients in intraspecific ecological diversity, *Biology Letters*, 9, 6–10, 2013.
- Archer, G., A. Saltelli, and I. Sobol', Sensitivity measures, ANOVA-like techniques and the use of bootstrap, *Journal of Statistical Computation and Simulation*, 58(2), 99–120, 1997.
- Arneth, A., et al., Terrestrial biogeochemical feedbacks in the climate system, *Nature Geoscience*, 3(8), 525–532, doi: 10.1038/ngeo0905, 2010.
- Arora, V., Modeling vegetation as a dynamic component in soil-vegetation-atmosphere transfer schemes and hydrological models, *Reviews of Geophysics*, 40(2), doi: 10.1029/2001RG000103, 2002.
- Arora, V., and G. J. Boer, Simulating Competition and Coexistence between Plant Functional Types in a Dynamic Vegetation Model, *Earth Interactions*, 10(10), 1–30, doi: 10.1175/EI170.1, 2006.
- Asbjornsen, H., et al., Ecohydrological advances and applications in plant-water relations research: a review, *Journal of Plant Ecology*, 4(1-2), 3–22, doi: 10.1093/jpe/rtro05, 2011.
- Assmann, E., *Waldertragskunde. Organische Produktion, Struktur, Zuwachs und Ertrag von Waldbeständen*, München, 1961.

- Auger, P., J. Poggiale, and E. Sánchez, A review on spatial aggregation methods involving several time scales, *Ecological Complexity*, 10, 12–25, doi: 10.1016/j.ecocom.2011.09.001, 2012.
- Bachelet, D., R. Neilson, T. Hickler, R. Drapek, J. Lenihan, M. T. Sykes, B. Smith, S. Sitch, and K. Thonicke, Simulating past and future dynamics of natural ecosystems in the United States, *Global Biogeochemical Cycles*, 17(2), 1045, doi: 10.1029/2001GB001508, 2003.
- Badeck, F., et al., Tree species composition in European pristine forests: comparison of stand data to model predictions, *Climatic Change*, 51(3), 307–347, doi: 10.1023/A:1012577612155.
- Bahn, M., M. Reichstein, J. Dukes, M. D. Smith, and N. G. McDowell, Climate-biosphere interactions in a more extreme world, *New Phytologist*, 2013.
- Baldocchi, D., An analytical solution for coupled leaf photosynthesis and stomatal conductance models, *Tree Physiology*, 14(7-8-9), 1069–1079, doi: 10.1093/treephys/14.7-8-9.1069, 1994.
- Baldocchi, D., Assessing the eddy covariance technique for evaluating carbon dioxide exchange rates of ecosystems: past, present and future, *Global Change Biology*, (9), 479–492, 2003.
- Baldocchi, D., and L. Xu, Carbon exchange of deciduous broadleaved forests in temperate and Mediterranean regions, in *Carbon Balance of Forest Biomes*, edited by P. Jarvis and H. Griffiths, chap. 9, pp. 187–216, BIOS Scientific Publishers Ltd, 2005.
- Baldocchi, D., T. Krebs, and M. Leclerc, "Wet/dry Daisyworld": a conceptual tool for quantifying the spatial scaling of heterogeneous landscapes and its impact on the subgrid variability of energy fluxes, *Tellus B*, 57B, 175–188, 2005.
- Baldocchi, D., et al., FLUXNET: a new tool to study the temporal and spatial variability of ecosystem-scale carbon dioxide, water vapor, and energy flux densities, *Bulletin of the American Meteorological Society*, 82(11), 2415–2434, doi: 10.1175/1520-0477(2001)082\$<\$2415:FANTTS\$>\$2.3.CO;2, 2001.
- Baldocchi, D. D., 'Breathing' of the terrestrial biosphere: lessons learned from a global network of carbon dioxide flux measurement systems, *Australian Journal of Botany*, 56(1), 1–26, doi: 10.1071/BTO7151, 2008.
- Baldocchi, D. D., and J. S. Amthor, *Canopy Photosynthesis: History, measurements and models*, chap. 2, pp. 9–31, Academic Press, doi: 10.1016/B978-012505290-0/50003-X, 2001.
- Baldocchi, D. D., and K. B. Wilson, Modeling CO₂ and water vapor exchange of a temperate broadleaved forest across hourly to decadal time scales, *Ecological Modelling*, 142(1-2), 155–184, doi: 10.1016/S0304-3800(01)00287-3, 2001.

- Baldocchi, D. D., K. B. Wilson, and L. Gu, How the environment, canopy structure and canopy physiological functioning influence carbon, water and energy fluxes of a temperate broad-leaved deciduous forest-an assessment with the biophysical model CANOAK, *Tree Physiology*, 22(15-16), 1065–1077, doi: 10.1093/treephys/22.15-16.1065, 2002.
- Barnes, B., and M. L. Roderick, An ecological framework linking scales across space and time based on self-thinning, *Theoretical Population Biology*, 66(2), 113–28, doi: 10.1016/j.tpb.2004.04.004, 2004.
- Bartelink, H. H., A model of dry matter partitioning in trees, *Tree Physiology*, 18(2), 91–101, doi: 10.1093/treephys/18.2.91, 1998.
- Bauerle, W. L., R. Oren, D. a. Way, S. S. Qian, P. C. Stoy, P. E. Thornton, J. D. Bowden, F. M. Hoffman, and R. F. Reynolds, Photoperiodic regulation of the seasonal pattern of photosynthetic capacity and the implications for carbon cycling., *Proceedings of the National Academy of Sciences of the United States of America*, 109(22), 8612–7, doi: 10.1073/pnas.1119131109, 2012.
- Beer, C., M. Reichstein, E. Tomelleri, P. Ciais, and M. Jung, Terrestrial Gross Carbon Dioxide Uptake: Global Distribution and Covariation with Climate, *Science*, 329(5993), 834–838, doi: 10.1126/science.1184984, 2010.
- Beven, K., How far can we go in distributed hydrological modelling?, *Hydrology and Earth System Sciences*, 5(1), 1–12, doi: 10.5194/hess-5-1-2001, 2001.
- Beven, K., Towards an alternative blueprint for a physically based digitally simulated hydrologic response modelling system, *Hydrological Processes*, 16(2), 189–206, doi: 10.1002/hyp.343, 2002.
- Beven, K. J., A manifesto for the equifinality thesis, *Journal of Hydrology*, 320(1-2), 18–36, doi: 10.1016/j.jhydrol.2005.07.007, 2006.
- Bird, R. E., and R. L. Hulstrom, *A Simplified Clear Sky Model for Direct and Diffuse Insolation on Horizontal Surfaces*, 38 pp., Solar Energy Research Institute, 1981.
- Bittner, S., N. Legner, F. Beese, and E. Priesack, Individual tree branch-level simulation of light attenuation and water flow of three *F. sylvatica* L. trees, *Journal of Geophysical Research*, 117(G1), doi: 10.1029/2011JG001780, 2012.
- Bogler, A., Analysis of Vegetation Changes in the Alpine Region using Satellite Imagery, Bs thesis, ETH Zurich, 2013.
- Bohrer, G., H. Mourad, T. a. Laursen, D. Drewry, R. Avissar, D. Poggi, R. Oren, and G. G. Katul, Finite element tree crown hydrodynamics model (FETCH) using porous media flow within branching elements: A new representation of tree hydrodynamics, *Water Resources Research*, 41(11), 1–17, doi: 10.1029/2005WR004181, 2005.

- Bolnick, D. I., et al., Why intraspecific trait variation matters in community ecology, *Trends in Ecology and Evolution*, 26(4), 183–92, doi: 10.1016/j.tree.2011.01.009, 2011.
- Bonan, G., *Ecological Climatology: Concepts and Applications*, Cambridge University Press, 2008a.
- Bonan, G. B., Forests and Climate Change: Forcings, Feedbacks, and the Climate Benefits of Forests, *Science*, 320(5882), 1444–1449, doi: 10.1126/science.1155121, 2008b.
- Bonan, G. B., D. Pollard, and L. Thompson, Effects of boreal forest vegetation on global climate, *Nature*, 359(6397), 716–718, doi: 10.1038/359716a0, 1992.
- Bonan, G. B., S. Levis, L. Kergoat, and K. W. Oleson, Landscapes as patches of plant functional types: An integrating concept for climate and ecosystem models, *Global Biogeochemical Cycles*, 16(2), doi: 10.1029/2000GB001360, 2002.
- Bonan, G. B., P. J. Lawrence, K. W. Oleson, S. Levis, M. Jung, M. Reichstein, D. M. Lawrence, and S. C. Swenson, Improving canopy processes in the Community Land Model version 4 (CLM4) using global flux fields empirically inferred from FLUXNET data, *Journal of Geophysical Research*, 116(G02014), 1–22, doi: 10.1029/2010JG001593, 2011.
- Bontemps, S., P. Defourny, E. V. Bogaert, O. Arino, V. Kalogirou, and J. R. Perez, GLOBCOVER: Products Description and Validation Report, *Tech. rep.*, 2009.
- Boone, a., et al., The Rhône-Aggregation Land Surface Scheme Intercomparison Project: An Overview, *Journal of Climate*, 17(1), 187–208, doi: 10.1175/1520-0442(2004)017<0187:TRLSSI>2.0.CO;2, 2004.
- Box, E. O., Plant functional types and climate at the global scale, *Journal of Vegetation Science*, 7(3), 309–320, doi: 10.2307/3236274, 1996.
- Brassel, P., and H. Lischke, *Swiss National Forest Inventory: Methods and Models of the Second Assessment*, Swiss Federal Research Institute WSL, Birmensdorf, 2001.
- Bratley, P., and B. Fox, Algorithm 659: Implementing Sobol’s quasirandom sequence generator, *ACM Transactions on Mathematical Software (TOMS)*, 14(1), 88–100, 1988.
- Bratley, P., B. Fox, and H. Niederreiter, Implementation and tests of low-discrepancy sequences, *ACM Transactions on Modeling and Computer Simulation (TOMACS)*, 2(3), 195–213, 1992.
- Buchmann, N., and E. Schulze, Net CO₂ and H₂O fluxes of terrestrial ecosystems, *Global Biogeochemical Cycles*, 13(3), 751–760, 1999.

- Bugmann, H., A review of forest gap models, *Climatic Change*, 51, 259–305, 2001.
- Bugmann, H., and A. Fischlin, Simulating forest dynamics in a complex topography using gridded climatic data, *Climatic Change*, 34, 201–211, 1996.
- Bugmann, H., X. Yan, M. T. Sykes, P. Martin, M. Lindner, P. Desanker, and S. Cumming, A comparison of forest gap models: model structure and behaviour, *Climatic Change*, 34(2), 289–313, 1996.
- Butler, D., Earth observation enters next phase, *Nature*, 508, 160–161, 2014.
- Cadotte, M. W., K. Carscadden, and N. Mirotchnick, Beyond species: functional diversity and the maintenance of ecological processes and services, *Journal of Applied Ecology*, 48(5), 1079–1087, doi: 10.1111/j.1365-2664.2011.02048.x, 2011.
- Campolongo, F., and R. Braddock, The use of graph theory in the sensitivity analysis of the model output: a second order screening method, *Reliability Engineering and System Safety*, 64(1), 1–12, doi: 10.1016/S0951-8320(98)00008-8, 1999.
- Campolongo, F., and A. Saltelli, Sensitivity analysis of an environmental model: an application of different analysis methods, *Reliability Engineering and System Safety*, 57(1), 49–69, 1997.
- Campolongo, F., S. Tarantola, and A. Saltelli, Tackling quantitatively large dimensionality problems, *Computer Physics Communications*, 117(1-2), 75–85, 1999.
- Campolongo, F., J. Cariboni, and A. Saltelli, An effective screening design for sensitivity analysis of large models, *Environmental Modelling & Software*, 22(10), 1509–1518, doi: 10.1016/j.envsoft.2006.10.004, 2007.
- Canadell, J., R. B. Jackson, J. B. Ehleringer, H. a. Mooney, O. E. Sala, and E.-D. Schulze, Maximum rooting depth of vegetation types at the global scale, *Oecologia*, 108(4), 583–595, doi: 10.1007/BF00329030, 1996.
- Cannell, M., and R. Dewar, Carbon allocation in trees: a review of concepts for modelling, *Advances in Ecological Research*, 25, 59–104, doi: 10.1016/S0065-2504(08)60213-5, 1994.
- Cannell, M., and J. Thornley, Temperature and CO₂ Responses of Leaf and Canopy Photosynthesis: a Clarification using the Non-rectangular Hyperbola Model of Photosynthesis, *Annals of Botany*, 82(6), 883–892, doi: 10.1006/anbo.1998.0777, 1998.
- Cariboni, J., D. Gatelli, R. Liska, and A. Saltelli, The role of sensitivity analysis in ecological modelling, *Ecological Modelling*, 203(1-2), 167–182, doi: 10.1016/j.ecolmodel.2005.10.045, 2007.

- Carvalhais, N., M. Reichstein, P. Ciais, G. J. Collatz, M. D. Mahecha, L. Montagnani, D. Papale, S. Rambal, and J. Seixas, Identification of vegetation and soil carbon pools out of equilibrium in a process model via eddy covariance and biometric constraints, *Global Change Biology*, 16(10), 2813–2829, doi: 10.1111/j.1365-2486.2010.02173.x, 2010.
- Carvalhais, N., et al., Implications of the carbon cycle steady state assumption for biogeochemical modeling performance and inverse parameter retrieval, *Global Biogeochemical Cycles*, 22(2), 1–16, doi: 10.1029/2007GB003033, 2008.
- Castanho, A. D. A., M. T. Coe, M. H. Costa, Y. Malhi, D. Galbraith, and C. A. Quesada, Improving simulated Amazon forest biomass and productivity by including spatial variation in biophysical parameters, *Biogeosciences*, 10(4), 2255–2272, doi: 10.5194/bg-10-2255-2013, 2013.
- Castelletti, A., S. Galelli, M. Ratto, R. Soncini-Sessa, and P. Young, A general framework for Dynamic Emulation Modelling in environmental problems, *Environmental Modelling and Software*, 34, 5–18, doi: 10.1016/j.envsoft.2012.01.002, 2012.
- Chan, K., A. Saltelli, and S. Tarantola, Sensitivity analysis of model output: variance-based methods make the difference, in *Proceedings of the 29th conference on Winter simulation*, pp. 261–268, IEEE Computer Society, 1997.
- Chan, K., A. Saltelli, and S. Tarantola, Winding stairs: a sampling tool to compute sensitivity indices, *Statistics and Computing*, 10(3), 187–196, doi: 10.1023/A:1008950625967, 2000.
- Chapin, F. S., J. T. Randerson, A. D. McGuire, J. A. Foley, and C. B. Field, Changing feedbacks in the climate-biosphere system, *Frontiers in Ecology and the Environment*, 6(6), 313–320, doi: 10.1890/080005, 2008.
- Chave, J., D. Coomes, S. Jansen, S. L. Lewis, N. G. Swenson, and A. E. Zanne, Towards a worldwide wood economics spectrum, *Ecology Letters*, 12(4), 351–66, doi: 10.1111/j.1461-0248.2009.01285.x, 2009.
- Chen, H., R. E. Dickinson, Y. Dai, and L. Zhou, Sensitivity of simulated terrestrial carbon assimilation and canopy transpiration to different stomatal conductance and carbon assimilation schemes, *Climate Dynamics*, 36(5), 1037–1054, doi: 10.1007/s00382-010-0741-2, 2011.
- Chen, W., R. Jin, and A. Sudjianto, Analytical Variance-Based Global Sensitivity Analysis in Simulation-Based Design Under Uncertainty, *Journal of Mechanical Design*, 127(5), 875–886, doi: 10.1115/1.1904642, 2005.
- Chesson, P., Scale transition theory: Its aims, motivations and predictions, *Ecological Complexity*, 10, 52–68, doi: 10.1016/j.ecocom.2011.11.002, 2012.

- Chopard, B., J. Borgdorff, and A. G. Hoekstra, A framework for multi-scale modelling, *Philosophical transactions of the Royal Society of London. Series A*, 372(June), 2014.
- Churkina, G., S. W. Running, A. Schloss, and The Participants Of The Potsdam NPP Model Intercomparison, Comparing global models of terrestrial net primary productivity (NPP): The importance of water availability, *Global Change Biology*, 5(S1), 46–55, doi: 10.1046/j.1365-2486.1999.00006.x, 1999.
- Ciais, P., et al., Carbon accumulation in European forests, *Nature*, 1, 425–429, 2008.
- Ciarapica, L., and E. Todini, TOPKAPI: a model for the representation of the rainfall-runoff process at different scales, *Hydrological Processes*, 16(2), 207–229, doi: 10.1002/hyp.342, 2002.
- Clark, J. S., Why environmental scientists are becoming Bayesians, *Ecology Letters*, 8(1), 2–14, doi: 10.1111/j.1461-0248.2004.00702.x, 2004.
- Clark, J. S., and A. E. Gelfand, A future for models and data in environmental science, *Trends in Ecology and Evolution*, 21(7), 375–80, doi: 10.1016/j.tree.2006.03.016, 2006.
- Coenders-Gerrits, A. M. J., R. J. van der Ent, T. A. Bogaard, L. Wang-Erlandsson, M. Hrachowitz, and H. H. G. Savenije, Uncertainties in transpiration estimates, *Nature*, 506(7487), E1–2, doi: 10.1038/nature12925, 2014.
- Collatz, G., J. Berry, G. Farquhar, and J. Pierce, The relationship between the Rubisco reaction mechanism and models of photosynthesis, *Plant, Cell & Environment*, 13(3), 219–225, doi: 10.1111/j.1365-3040.1990.tb01306.x, 1990.
- Collatz, G., J. Ball, C. Grivet, and J. Berry, Physiological and environmental regulation of stomatal conductance, photosynthesis and transpiration: a model that includes a laminar boundary layer, *Agricultural and Forest Meteorology*, 54(2-4), 107–136, doi: 10.1016/0168-1923(91)90002-8, 1991.
- Collatz, G., M. Ribas-Carbo, and J. A. Berry, Coupled photosynthesis-stomatal conductance model for leaves of C_4 plants, *Functional Plant Biology*, 19(5), 519–538, doi: 10.1071/PP9920519, 1992.
- Corripio, J., Vectorial algebra algorithms for calculating terrain parameters from DEMs and solar radiation modelling in mountainous terrain, *International Journal of Geographical Information Science*, 17(1), 1–23, doi: 10.1080/713811744, 2003.
- Costanza, R., and T. Maxwell, Resolution and predictability: An approach to the scaling problem, *Landscape Ecology*, 9(1), 47–57, doi: 10.1007/BF00135078, 1994.

- Cox, G., J. Gibbons, A. Wood, J. Craigon, S. Ramsden, and N. Crout, Towards the systematic simplification of mechanistic models, *Ecological Modelling*, 198(1-2), 240–246, doi: 10.1016/j.ecolmodel.2006.04.016, 2006.
- Cox, P., R. Betts, C. Jones, and S. Spall, Acceleration of global warming due to carbon-cycle feedbacks in a coupled climate model, *Nature*, 408(6809), 184–187, doi: 10.1038/35041539, 2000.
- Cox, P. M., D. Pearson, B. B. Booth, P. Friedlingstein, C. Huntingford, C. D. Jones, and C. M. Luke, Sensitivity of tropical carbon to climate change constrained by carbon dioxide variability, *Nature*, 494(7437), 341–4, doi: 10.1038/nature11882, 2013.
- Cramer, W., D. Kicklighter, A. Bondeau, B. Iii, G. Churkina, B. Nemry, A. Ruimy, A. Schloss, and The Participants Of The Potsdam NPP Model Intercomparison, Comparing global models of terrestrial net primary productivity (NPP): overview and key results, *Global change Biology*, 5(S1), 1–15, doi: 10.1046/j.1365-2486.1999.00009.x, 1999.
- Cramer, W., et al., Global response of terrestrial ecosystem structure and function to CO₂ and climate change: results from six dynamic global vegetation models, *Global Change Biology*, 7(4), 357–373, doi: 10.1046/j.1365-2486.2001.00383.x, 2001.
- Currie, D. J., Disentangling the roles of environment and space in ecology, *Journal of Biogeography*, 34(12), 2009–2011, doi: 10.1111/j.1365-2699.2007.01808.x, 2007.
- Dai, Y., R. Dickinson, and Y. Wang, A two-big-leaf model for canopy temperature, photosynthesis, and stomatal conductance, *Journal of Climate*, 17, 2281–2299, 2004.
- Daudet, F., A. Lacointe, J. Gaudillère, and P. Cruiziat, Generalized Münch coupling between sugar and water fluxes for modelling carbon allocation as affected by water status, *Journal of Theoretical Biology*, 214(3), 481–98, doi: 10.1006/jtbi.2001.2473, 2002.
- De Pury, D. G. G., and G. D. Faruhar, Simple scaling of photosynthesis from leaves to canopies without the errors of big-leaf models, *Plant, Cell & Environment*, 20(5), 537–557, doi: 10.1111/j.1365-3040.1997.00094.x, 1997.
- De Schepper, V., and K. Steppe, Tree girdling responses simulated by a water and carbon transport model, *Annals of Botany*, 108(6), 1147–1154, doi: 10.1093/aob/mcro68, 2011.
- Dewar, R. C., Maximum Entropy Production as an Inference Algorithm that Translates Physical Assumptions into Macroscopic Predictions: Don't Shoot the Messenger, *Entropy*, 11, 931–944, doi: 10.3390/e11040931, 2009.

- Dewar, R. C., Maximum entropy production and plant optimization theories, *Philosophical transactions of the Royal Society of London. Series B, Biological sciences*, 365(1545), 1429–35, doi: 10.1098/rstb.2009.0293, 2010.
- Dewar, R. C., and A. Porté, Statistical mechanics unifies different ecological patterns, *Journal of Theoretical Biology*, 251(3), 389–403, doi: 10.1016/j.jtbi.2007.12.007, 2008.
- Dewar, R. C., O. Franklin, A. Mäkelä, R. E. McMurtrie, and H. T. Valentine, Optimal Function Explains Forest Responses to Global Change, *BioScience*, 59(2), 127–139, doi: 10.1525/bio.2009.59.2.6, 2009.
- Díaz, S., M. Cabido, and F. Casanoves, Plant functional traits and environmental filters at a regional scale, *Journal of Vegetation*, 9(1981), 113–122, 1998.
- Díaz, S., J. Fargione, F. S. Chapin, and D. Tilman, Biodiversity loss threatens human well-being, *PLoS Biology*, 4(8), e277, doi: 10.1371/journal.pbio.0040277, 2006.
- Dietze, M. C., D. S. Lebauer, and R. Kooper, On improving the communication between models and data, *Plant, Cell and Environment*, 36(9), 1575–85, doi: 10.1111/pce.12043, 2013.
- Dietze, M. C., et al., Characterizing the performance of ecosystem models across time scales: A spectral analysis of the North American Carbon Program site-level synthesis, *Journal of Geophysical Research*, 116(G04029), doi: 10.1029/2011JG001661, 2011.
- Dirmeyer, P., G. Xiang, M. Zhao, G. Zhichang, T. Oki, and N. Hanasaki, GSWP-2: Multimodel analysis and implications for our perception of the land surface, *Bulletin of the American Meteorological Society*, 87(10), 1381–1397, doi: 10.1175/BAMS-87-10-1381, 2006.
- Dobzhansky, T., Nothing in biology makes sense except in the light of evolution, *American Biology Teacher*, 35, 1973.
- D’Odorico, P., F. Laio, A. Porporato, L. Ridolfi, A. Rinaldo, and I. Rodriguez-Iturbe, Ecohydrology of Terrestrial Ecosystems, *BioScience*, 60(11), 898–907, doi: 10.1525/bio.2010.60.11.6, 2010.
- Dolman, A. J., E. D. Schulze, and R. Valentini, Analyzing carbon flux measurements, *Science*, 301(5635), 916–7; author reply 916–7, doi: 10.1126/science.301.5635.916b, 2003.
- Dolman, A. J., D. G. Miralles, and R. A.M. de Jeu, Fifty years since Monteith’s 1965 seminal paper: the emergence of global ecohydrology, *Ecohydrology*, 7(3), 897–902, doi: 10.1002/eco.1505, 2014.

- Durrett, R., and S. Levin, The importance of being discrete (and spatial), *Theoretical Population Biology*, 46, 363–394, 1994.
- Dyke, J., and A. Kleidon, The Maximum Entropy Production Principle: Its Theoretical Foundations and Applications to the Earth System, *Entropy*, 12(3), 613–630, doi: 10.3390/e12030613, 2010.
- Eagleson, P., *Ecohydrology: Darwinian Expression of Vegetation Form and Function*, E-Libro, Cambridge University Press, 2002.
- Ebel, B. a., K. Loague, D. R. Montgomery, and W. E. Dietrich, Physics-based continuous simulation of long-term near-surface hydrologic response for the Coos Bay experimental catchment, *Water Resources Research*, 44(7), doi: 10.1029/2007WR006442, 2008.
- EC, Impact assessment guidelines, *Tech. Rep. 92*, SEC, 2009.
- Efron, B., Bootstrap Methods: Another Look at the Jackknife, *The Annals of Statistics*, 7, 1–26, 1979.
- Efron, B., Bayes' Theorem in the 21st century, *Science*, 50, doi: 10.1126/science.1236536, 2013.
- Efron, B., and R. J. Tibshirani, *An Introduction to the Bootstrap*, Chapman & Hall, New York, 1993.
- EPA, Guidance on the development, evaluation, and application of environmental models, *Tech. Rep. EPA/100/K-09/003*, Office of the Science Advisor, Council for Regulatory Environmental Modeling, 2009.
- Etzold, S., N. K. Ruehr, R. Zweifel, M. Dobbertin, A. Zingg, P. Pluess, R. Häsler, W. Eugster, and N. Buchmann, The Carbon Balance of Two Contrasting Mountain Forest Ecosystems in Switzerland: Similar Annual Trends, but Seasonal Differences, *Ecosystems*, 14(8), 1289–1309, doi: 10.1007/s10021-011-9481-3, 2011.
- Evans, M. R., Modelling ecological systems in a changing world, *Philosophical Transactions of the Royal Society B: Biological Sciences*, 367(1586), 181–190, doi: 10.1098/rstb.2011.0172, 2012.
- Evans, M. R., K. Norris, and T. Benton, Predictive ecology: systems approaches, *Philosophical Transactions of the Royal Society B: Biological Sciences*, 367(1586), 163–169, doi: 10.1098/rstb.2011.0191, 2012.
- Fang, H., S. Wei, C. Jiang, and K. Scipal, Theoretical uncertainty analysis of global MODIS, CYCLOPES, and GLOBCARBON LAI products using a triple collocation method, *Remote Sensing of Environment*, 124, 610–621, doi: 10.1016/j.rse.2012.06.013, 2012.

- Fang, H., et al., Characterization and intercomparison of global moderate resolution leaf area index (LAI) products: Analysis of climatologies and theoretical uncertainties, *Journal of Geophysical Research: Biogeosciences*, 118, doi: 10.1002/jgrg.20051, 2013.
- FAO, The Digitized Soil Map of the World, *Tech. Rep. (Release 1.0)*, Food and Agricultural Organisation), Rome, 1991.
- Farquhar, G., S. von Caemmerer, and J. Berry, A biochemical model of photosynthetic CO₂ assimilation in leaves of C₃ species, *Planta*, 149(1), 78–90, doi: 10.1007/BF00386231, 1980.
- Fatichi, S., and V. Ivanov, Interannual variability of evapotranspiration and vegetation productivity, *Water Resources Research*, 50, 3275–3294, doi: 10.1002/2013WR015044, Received, 2014.
- Fatichi, S., and S. Leuzinger, Reconciling observations with modeling: The fate of water and carbon allocation in a mature deciduous forest exposed to elevated CO₂, *Agricultural and Forest Meteorology*, 174–175, 144–157, doi: 10.1016/j.agrformet.2013.02.005, 2013.
- Fatichi, S., V. Y. Ivanov, and E. Caporali, Simulation of future climate scenarios with a weather generator, *Advances in Water Resources*, 34(4), 448–467, doi: 10.1016/j.advwatres.2010.12.013, 2011.
- Fatichi, S., V. Ivanov, and E. Caporali, A mechanistic ecohydrological model to investigate complex interactions in cold and warm water-controlled environments: 1. Theoretical framework and plot scale analysis, *Journal of Advances in Modeling Earth Systems*, 4(M05002), 2012a.
- Fatichi, S., V. Y. Ivanov, and E. Caporali, A mechanistic ecohydrological model to investigate complex interactions in cold and warm water-controlled environments. 2. Spatiotemporal analyses, *Journal of Advances in Modeling Earth Systems*, 4(M05002), 2012b.
- Fatichi, S., M. J. Zeeman, J. Fuhrer, and P. Burlando, Ecohydrological effects of management on subalpine grasslands: From local to catchment scale, *Water Resources Research*, 50, 148–164, doi: 10.1002/2013WR014535, 2014.
- Fernández-Martínez, M., et al., Nutrient availability as the key regulator of global forest carbon balance, *Nature Climate Change*, doi: 10.1038/NCLIMATE2177, 2014.
- Field, C. B., D. B. Lobell, H. A. Peters, and N. R. Chiariello, Feedbacks of Terrestrial Ecosystems to Climate Change, *Annual Review of Environment and Resources*, 32(1), 1–29, doi: 10.1146/annurev.energy.32.053006.141119, 2007.

- Fisher, J. I., G. C. Hurtt, R. Q. Thomas, and J. Q. Chambers, Clustered disturbances lead to bias in large-scale estimates based on forest sample plots, *Ecology Letters*, 11(6), 554–63, doi: 10.1111/j.1461-0248.2008.01169.x, 2008.
- Fisher, R., N. McDowell, D. Purves, P. Moorcroft, S. Sitch, P. Cox, C. Huntingford, P. Meir, and F. Ian Woodward, Assessing uncertainties in a second-generation dynamic vegetation model caused by ecological scale limitations, *New Phytologist*, 187(3), 666–681, doi: 10.1111/j.1469-8137.2010.03340.x, 2010.
- Foley, J., Net primary productivity in the terrestrial biosphere: The application of a global model, *Journal of Geophysical Research*, 99(D10), 20,773–20,783, doi: 10.1029/94JD01832, 1994.
- Foley, J., An equilibrium model of the terrestrial carbon budget, *Tellus B*, 47(3), 310–319, doi: 10.1034/j.1600-0889.47.issue3.3.x, 1995.
- Frank, D. C., J. Esper, C. C. Raible, U. Büntgen, V. Trouet, B. Stocker, and F. Joos, Ensemble reconstruction constraints on the global carbon cycle sensitivity to climate, *Nature*, 463(7280), 527–530, doi: 10.1038/nature08769, 2010.
- Franklin, O., J. Johansson, R. C. Dewar, U. Dieckmann, R. E. McMurtrie, A. Brännström, and R. Dybzinski, Modeling carbon allocation in trees: a search for principles, *Tree Physiology*, 32(6), 648–66, doi: 10.1093/treephys/tpr138, 2012.
- Frayer, W., and G. Furnival, Forest survey sampling designs-A history, *Journal of Forestry*, 12(1), 4–10, 1999.
- Freeze, R., and R. Harlan, Blueprint for a physically-based, digitally-simulated hydrologic response model, *Journal of Hydrology*, 9, 237–258, 1969.
- Frey, C., and S. Patil, Identification and Review of Sensitivity Analysis Methods, *Risk Analysis*, 22(3), 553–578, doi: 10.1111/0272-4332.00039, 2002.
- Friedlingstein, P., and I. Prentice, Carbon-climate feedbacks: a review of model and observation based estimates, *Current Opinion in Environmental Sustainability*, 2(4), 251–257, doi: 10.1016/j.cosust.2010.06.002, 2010.
- Friedlingstein, P., et al., Climate-carbon cycle feedback analysis: Results from the C⁴MIP model intercomparison, *Journal of Climate*, 19(14), 3337–3353, doi: 10.1175/JCLI3800.1, 2006.
- Friend, A. D., et al., Carbon residence time dominates uncertainty in terrestrial vegetation responses to future climate and atmospheric CO₂, *Proceedings of the National Academy of Sciences of the United States of America*, 111(9), 3280–5, doi: 10.1073/pnas.1222477110, 2014.
- Fulton, M., Adult recruitment as a function of juvenile growth rate in size-structured plant populations, *Oikos*, 62(1), 102–105, 1991.

- Fyllas, N., et al., Basin-wide variations in foliar properties of Amazonian forest: phylogeny, soils and climate, *Biogeosciences*, 6, 2677–2708, 2009.
- Gao, T., X. Yang, Y. Jin, H. Ma, J. Li, H. Yu, Q. Yu, X. Zheng, and B. Xu, Spatio-temporal variation in vegetation biomass and its relationships with climate factors in the Xilingol grasslands, Northern China, *PloS one*, 8(12), e83,824, doi: 10.1371/journal.pone.0083824, 2013.
- Gates, D., *Biophysical Ecology*, Biology and Medicine Series, Dover Publications, 2003.
- Gehrig-Fasel, J., A. Guisan, and N. E. Zimmermann, Tree line shifts in the Swiss Alps: Climate change or land abandonment?, *Journal of Vegetation Science*, 18, 571–582, 2007.
- GEOSTAT, Digitale Bodeneignungskarte der Schweiz, *Tech. rep.*, Swiss Federal Statistical Office, Bern, 2000.
- Gerten, D., S. Schaphoff, U. Haberlandt, W. Lucht, and S. Sitch, Terrestrial vegetation and water balance-hydrological evaluation of a dynamic global vegetation model, *Journal of Hydrology*, 286(1-4), 249–270, doi: 10.1016/j.jhydrol.2003.09.029, 2004.
- Gilgen, A. K., and N. Buchmann, Response of temperate grasslands at different altitudes to simulated summer drought differed but scaled with annual precipitation, *Biogeosciences*, 6(1), 2525–2539, 2009.
- Gimmi, U., A. Wolf, M. Bürgi, M. Scherstjanoi, and H. Bugmann, Quantifying disturbance effects on vegetation carbon pools in mountain forests based on historical data, *Regional Environmental Change*, 9(2), 121–130, doi: 10.1007/s10113-008-0071-7, 2008.
- Gimmi, U., B. Poulter, A. Wolf, H. Portner, P. Weber, and M. Bürgi, Soil carbon pools in Swiss forests show legacy effects from historic forest litter raking, *Landscape Ecology*, 28(5), 835–846, doi: 10.1007/s10980-012-9778-4, 2012.
- Giorgi, F., and R. Avissar, Representation of heterogeneity effects in earth system modeling: Experience from land surface modeling, *Reviews of Geophysics*, 34(4), 413–438, 1997.
- Gordon, W., J. Famiglietti, N. Fowler, T. G. F. Kittel, and K. A. Hibbard, Validation of simulated runoff from six terrestrial ecosystem models: results from VEMAP, *Ecological Applications*, 14(2), 527–545, doi: 10.1890/02-5287, 2004.
- Grace, J. B., et al., Does species diversity limit productivity in natural grassland communities?, *Ecology Letters*, 10(8), 680–9, doi: 10.1111/j.1461-0248.2007.01058.x, 2007.

- Granier, C., and D. Vile, Phenotyping and beyond: modelling the relationships between traits, *Current Opinion in Plant Biology*, 18C, 96–102, doi: 10.1016/j.pbi.2014.02.009, 2014.
- Graven, H. D., et al., Enhanced seasonal exchange of CO₂ by northern ecosystems since 1960, *Science*, 341(6150), 1085–9, doi: 10.1126/science.1239207, 2013.
- Grayson, R. B., I. D. Moore, and T. A. McMahon, Physically based hydrologic modeling: 1. A terrain-based model for investigative purposes, *Water Resources Research*, 28(10), 2639–2658, doi: 10.1029/92WR01258, 1992.
- Haddeland, I., et al., Multi-Model Estimate of the Global Terrestrial Water Balance: Setup and First Results, *Journal of Hydrometeorology*, 12(5), 869–884, doi: 10.1175/2011JHM1324.1, 2011.
- Hall, J. M., C. G. Staub, M. P. Marsik, R. Forrest, and M. Binford, Scaling categorical spatial data for earth systems models, *Global Change Biology*, 21, 1–3, doi: 10.1111/gcb.12708, 2015.
- Hallgren, W., and A. Pitman, The uncertainty in simulations by a Global Biome Model (BIOME3) to alternative parameter values, *Global Change Biology*, 6(5), 483–495, doi: 10.1046/j.1365-2486.2000.00325.x, 2000.
- Hamby, D., A review of techniques for parameter sensitivity analysis of environmental models, *Environmental Monitoring and Assessment*, 32(2), 135–154, doi: 10.1007/BF00547132, 1994.
- Hanan, N., P. Kabat, A. Dolman, and J. Elbers, Photosynthesis and carbon balance of a Sahelian fallow savanna, *Global Change Biology*, 4(5), 523–538, doi: 10.1046/j.1365-2486.1998.t01-1-00126.x, 1998.
- Harcombe, P., Tree life tables, *BioScience*, 37, 557–568, 1987.
- Hardiman, B., G. Bohrer, C. Gough, C. Vogel, and P. Curtis, The role of canopy structural complexity in wood net primary production of a maturing northern deciduous forest, *Ecology*, 92(9), 1818–1827, doi: 10.1890/10-2192.1, 2011.
- Harmon, M. E., Carbon sequestration in forest; addressing the scale question, *Journal of Forestry*, 99, 24–29, 2001.
- Harrison, S. P., I. Prentice, D. Barboni, K. E. Kohfeld, J. Ni, and J.-P. Sutra, Ecophysiological and bioclimatic foundations for a global plant functional classification, *Journal of Vegetation Science*, 21(2), 300–317, doi: 10.1111/j.1654-1103.2009.01144.x, 2010.
- Hartig, F., J. Dyke, T. Hickler, S. I. Higgins, R. B. O'Hara, S. Scheiter, and A. Huth, Connecting dynamic vegetation models to data - an inverse perspective, *Journal of Biogeography*, doi: 10.1111/j.1365-2699.2012.02745.x, 2012.

- Haxeltine, A., and I. Prentice, BIOME3: An equilibrium terrestrial biosphere model based on ecophysiological constraints, resource availability, and competition among plant functional types, *Global Biogeochemical Cycles*, 10(4), 693–709, doi: 10.1029/96GB02344, 1996a.
- Haxeltine, A., and I. Prentice, A general model for the light-use efficiency of primary production, *Functional Ecology*, 10(5), 551–561, 1996b.
- Haxeltine, A., I. Prentice, and I. Creswell, A coupled carbon and water flux model to predict vegetation structure, *Journal of Vegetation Science*, 7(5), 651–666, 1996.
- Hector, A., et al., Plant Diversity and Productivity Experiments in European Grasslands, *Science*, 286(5442), 1123–1127, doi: 10.1126/science.286.5442.1123, 1999.
- Heimann, M., and M. Reichstein, Terrestrial ecosystem carbon dynamics and climate feedbacks, *Nature*, 451(7176), 289–292, doi: 10.1038/nature06591, 2008.
- Heinsch, F., et al., Evaluation of remote sensing based terrestrial productivity from MODIS using regional tower eddy flux network observations, *IEEE Transactions on Geoscience and Remote Sensing*, 44(7), 1908–1925, doi: 10.1109/TGRS.2005.853936, 2006.
- Hély, C., L. Bremond, S. Alleaume, B. Smith, M. Sykes, and J. Guiot, Sensitivity of African biomes to changes in the precipitation regime, *Global Ecology and Biogeography*, 15(3), 258–270, doi: 10.1111/j.1466-822x.2006.00235.x, 2006.
- Hickler, T., B. Smith, M. T. Sykes, M. Davis, S. Sugita, and K. Walker, Using a generalized vegetation model to simulate vegetation dynamics in northeastern USA, *Ecology*, 85(2), 519–530, doi: 10.1890/02-0344, 2004.
- Hickler, T., et al., Projecting the future distribution of European potential natural vegetation zones with a generalized, tree species-based dynamic vegetation model, *Global Ecology and Biogeography*, 21(1), 50–63, doi: 10.1111/j.1466-8238.2010.00613.x, 2012.
- Higgins, S. I., L. Langan, and S. Scheiter, Progress in DGVMs: a comment on "Impacts of trait variation through observed trait-climate relationships on performance of an Earth system model: a conceptual analysis" by Verheijen et al. (2013), *Biogeosciences Discussions*, 11(3), 4483–4492, doi: 10.5194/bgd-11-4483-2014, 2014.
- Hoch, G., and C. Körner, Global patterns of mobile carbon stores in trees at the high-elevation tree line, *Global Ecology and Biogeography*, 21(8), 861–871, doi: 10.1111/j.1466-8238.2011.00731.x, 2012.

- Homma, T., and A. Saltelli, Importance measures in global sensitivity analysis of nonlinear models, *Reliability Engineering and System Safety*, 52(1), 1–17, doi: 10.1016/0951-8320(96)00002-6, 1996.
- Homolová, L., Z. Malenovský, J. G. Clevers, G. García-Santos, and M. E. Schaepman, Review of optical-based remote sensing for plant trait mapping, *Ecological Complexity*, 15, 1–16, doi: 10.1016/j.ecocom.2013.06.003, 2013.
- Hooper, D., et al., Effects of biodiversity on ecosystem functioning: a consensus of current knowledge, *Ecological Monographs*, 75(1), 3–35, 2005.
- House, J. I., I. Prentice, N. Ramankutty, R. A. Houghton, and M. Heimann, Reconciling apparent inconsistencies in estimates of terrestrial CO₂ sources and sinks, *Tellus B*, 55(2), 345–363, doi: 10.1034/j.1600-0889.2003.00037.x, 2003.
- Huang, S., S. J. Titus, and D. P. Wiens, Comparison of nonlinear height-diameter functions for major Alberta tree species, *Canadian Journal of Forest Research*, 22(9), 1297–1304, doi: 10.1139/x92-172, 1992.
- Huete, A., K. Didan, T. Miura, E. Rodriguez, X. Gao, and L. Ferreira, Overview of the radiometric and biophysical performance of the MODIS vegetation indices, *Remote Sensing of Environment*, 83(1-2), 195–213, doi: 10.1016/S0034-4257(02)00096-2, 2002.
- Hurlbert, A. H., and J. C. Stegen, When should species richness be energy limited, and how would we know?, *Ecology Letters*, 17(4), 401–13, doi: 10.1111/ele.12240, 2014.
- Hurt, G., R. Dubayah, J. Drake, P. R. Moorcroft, S. Pacala, J. Blair, and M. Fearon, Beyond potential vegetation: combining lidar data and a height-structured model for carbon studies, *Ecological Applications*, 14(3), 873–883, 2004.
- Hurt, G. C., P. R. Moorcroft, S. W. Pacala, and S. A. Levin, Terrestrial models and global change: challenges for the future, *Global Change Biology*, 4(5), 581–590, doi: 10.1046/j.1365-2486.1998.t01-1-00203.x, 1998.
- Hwang, T., L. Band, and T. C. Hales, Ecosystem processes at the watershed scale: Extending optimality theory from plot to catchment, *Water Resources Research*, 45(11), doi: 10.1029/2009WR007775, 2009.
- Hwang, T., C. Song, J. M. Vose, and L. E. Band, Topography-mediated controls on local vegetation phenology estimated from MODIS vegetation index, *Landscape Ecology*, 26(4), 541–556, doi: 10.1007/s10980-011-9580-8, 2011.
- IPCC, *Climate Change 2013: The Physical Science Basis. Contribution of Working Group I to the Fifth Assessment Report of the Intergovernmental Panel on Climate Change*, 1535 pp., Cambridge University Press, Cambridge, United Kingdom and New York, NY, USA, 2013.

- Iqbal, M., *An introduction to solar radiation*, 390 pp., Academic Press, 1983.
- Ishii, H., and S. Asano, The role of crown architecture, leaf phenology and photosynthetic activity in promoting complementary use of light among co-existing species in temperate forests, *Ecological Research*, 25(4), 715–722, doi: 10.1007/s11284-009-0668-4, 2010.
- Ito, A., and T. Sasai, A comparison of simulation results from two terrestrial carbon cycle models using three climate data sets, *Tellus B*, 58(5), 513–522, doi: 10.1111/j.1600-0889.2006.00208.x, 2006.
- Ivanov, V. Y., R. L. Bras, and D. C. Curtis, A weather generator for hydrological, ecological, and agricultural applications, *Water Resources Research*, 43(10), doi: 10.1029/2006WR005364, 2007.
- Ivanov, V. Y., R. L. Bras, and E. R. Vivoni, Vegetation-hydrology dynamics in complex terrain of semiarid areas: 1. A mechanistic approach to modeling dynamic feedbacks, *Water Resources Research*, 44(W03429), doi: 10.1029/2006WR005588, 2008a.
- Ivanov, V. Y., R. L. Bras, and E. R. Vivoni, Vegetation-hydrology dynamics in complex terrain of semiarid areas : 2 . Energy-water controls of vegetation spatiotemporal dynamics and topographic niches of favorability, *Water Resources Research*, 44(3), doi: 10.1029/2006WR005595, 2008b.
- Jackson, R., J. Canadell, J. Ehleringer, H. Mooney, O. E. Sala, and E. D. Schulze, A global analysis of root distributions for terrestrial biomes, *Oecologia*, 108(3), 389–411, doi: 10.1007/BF00333714, 1996.
- Jackson, R., H. Mooney, and E. Schulze, A global budget for fine root biomass, surface area, and nutrient contents, *Proceedings of the National Academy of Science*, 94(July), 7362–7366, 1997.
- Jakeman, A., R. Letcher, and J. Norton, Ten iterative steps in development and evaluation of environmental models, *Environmental Modelling & Software*, 21(5), 602–614, doi: 10.1016/j.envsoft.2006.01.004, 2006.
- Janott, M., S. Gayler, A. Gessler, M. Javaux, C. Klier, and E. Priesack, A one-dimensional model of water flow in soil-plant systems based on plant architecture, *Plant and Soil*, 341(1-2), 233–256, doi: 10.1007/s11104-010-0639-0, 2010.
- Jarvis, P. G., Scaling processes and problems, *Plant, Cell & Environment*, 18(10), 1079–1089, doi: 10.1111/j.1365-3040.1995.tb00620.x, 1995.
- Jasechko, S., Z. D. Sharp, J. J. Gibson, S. J. Birks, Y. Yi, and P. J. Fawcett, Terrestrial water fluxes dominated by transpiration, *Nature*, pp. 2–6, doi: 10.1038/nature11983, 2013.

- Jasienski, M., and F. Bazzaz, The fallacy of ratios and the testability of models in biology, *Oikos*, 84(2), 321–326, 1999.
- Jeltsch, F., K. a. Moloney, F. M. Schurr, M. Köchy, and M. Schwager, The state of plant population modelling in light of environmental change, *Perspectives in Plant Ecology, Evolution and Systematics*, 9(3-4), 171–189, doi: 10.1016/j.ppees.2007.11.004, 2008.
- Jenkinson, D., S. Andrew, J. Lynch, M. Goss, and P. Tinker, The Turnover of Organic Carbon and Nitrogen in Soil [and Discussion], *Philosophical Transactions of the Royal Society B: Biological Sciences*, 329(1255), 361–368, doi: 10.1098/rstb.1990.0177, 1990.
- Jennings, B. K., On the Nature of Science, *Physics in Canada*, 63(7), 1–26, 2007.
- Jensen, J., Sur les fonctions convexes et les inégalités entre les valeurs moyennes, *Acta Mathematica*, 30, 175–193, 1906.
- Johnson, F., H. Eyring, and R. Williams, The nature of enzyme inhibitions in bacterial luminescence: sulfanilamide, urethane, temperature and pressure, *Journal of Cellular and Comparative Physiology*, 20(3), 247–268, 1942.
- Johnson, I., and J. Thornley, A model of instantaneous and daily canopy photosynthesis, *Journal of Theoretical Biology*, 107(4), 531–545, doi: 10.1016/S0022-5193(84)80131-9, 1984.
- Jones, N., Climate assessments: 25 years of the IPCC, *Nature*, 501, 298–299, 2013.
- Jönsson, P., and L. Eklundh, Seasonality extraction by function fitting to time-series of satellite sensor data, *IEEE Transactions on Geoscience and Remote Sensing*, 40(8), 1824–1832, 2002.
- Jönsson, P., and L. Eklundh, TIMESAT - a program for analyzing time-series of satellite sensor data, *Computers and Geosciences*, 30(8), 833–845, doi: 10.1016/j.cageo.2004.05.006, 2004.
- Jung, M., G. Le Maire, S. Zaehle, S. Luyssaert, M. Vetter, G. Churkina, P. Ciais, N. Viovy, and M. Reichstein, Assessing the ability of three land ecosystem models to simulate gross carbon uptake of forests from boreal to Mediterranean climate in Europe, *Biogeosciences*, 4(4), 647–656, doi: 10.5194/bg-4-647-2007, 2007a.
- Jung, M., et al., Uncertainties of modeling gross primary productivity over Europe: A systematic study on the effects of using different drivers and terrestrial biosphere models, *Global Biogeochemical Cycles*, 21(GB4021), 1–12, doi: 10.1029/2006GB002915, 2007b.

- Kang, S., S. W. Running, M. Zhao, J. S. Kimball, and J. Glassy, Improving continuity of MODIS terrestrial photosynthesis products using an interpolation scheme for cloudy pixels, *International Journal of Remote Sensing*, 26(8), 1659–1676, doi: 10.1080/01431160512331326693, 2005.
- Kattge, J., and W. Knorr, Temperature acclimation in a biochemical model of photosynthesis: a reanalysis of data from 36 species, *Plant, Cell and Environment*, 30(9), 1176–90, doi: 10.1111/j.1365-3040.2007.01690.x, 2007.
- Kattge, J., W. Knorr, T. Raddatz, and C. Wirth, Quantifying photosynthetic capacity and its relationship to leaf nitrogen content for global-scale terrestrial biosphere models, *Global Change Biology*, 15(4), 976–991, doi: 10.1111/j.1365-2486.2008.01744.x, 2009.
- Kattge, J., et al., TRY - a global database of plant traits, *Global Change Biology*, 17(9), 2905–2935, doi: 10.1111/j.1365-2486.2011.02451.x, 2011.
- Katul, G., R. Oren, S. Manzoni, C. Higgins, and M. Parlange, Evapotranspiration: A process driving mass transport and energy exchange in the soil-plant-atmosphere-climate system, *Reviews of Geophysics*, 50(RG3002), doi: 10.1029/2011RG000366.1.INTRODUCTION, 2012.
- Kaufmann, E., Estimation of standing timber, growth and cut, in *Swiss National Forest Inventory: Methods and Models of the Second Assessment.*, edited by P. Bräsel and H. Lischke, pp. 162–196, Swiss Federal Research Institute WSL, Birmensdorf, 2001.
- Keeling, C., S. C. Piper, A. F. Bollenbacher, and J. S. Walker, Atmospheric CO₂ records from sites in the sio air sampling network, *Tech. rep.*, Carbon Dioxide Information Analysis Center, Oak Ridge National Laboratory, U.S. Department of Energy, Oak Ridge, Tenn., U.S.A., doi: 10.3334/CDIAC/atg.035, 2009.
- Keenan, T., S. Sabate, and C. Gracia, Soil water stress and coupled photosynthesis-conductance models: Bridging the gap between conflicting reports on the relative roles of stomatal, mesophyll conductance and biochemical limitations to photosynthesis, *Agricultural and Forest Meteorology*, 150(3), 443–453, doi: 10.1016/j.agrformet.2010.01.008, 2010.
- Keenan, T., M. S. Carbone, M. Reichstein, and A. D. Richardson, The model-data fusion pitfall: assuming certainty in an uncertain world, *Oecologia*, 167(3), 587–97, doi: 10.1007/s00442-011-2106-x, 2011a.
- Keenan, T., J. M. Serra, F. Lloret, M. Ninyerola, and S. Sabate, Predicting the future of forests in the Mediterranean under climate change, with niche- and process-based models: CO₂ matters!, *Global Change Biology*, 17(1), 565–579, doi: 10.1111/j.1365-2486.2010.02254.x, 2011b.

- Keenan, T., et al., Terrestrial biosphere model performance for inter-annual variability of land-atmosphere CO₂ exchange, *Global Change Biology*, 18(6), 1971–1987, doi: 10.1111/j.1365-2486.2012.02678.x, 2012.
- Keith, H., B. G. Mackey, and D. B. Lindenmayer, Re-evaluation of forest biomass carbon stocks and lessons from the world's most carbon-dense forests, *Proceedings of the National Academy of Science*, 106(28), 11,635–11,640, 2009.
- Kergoat, L., A model for hydrological equilibrium of leaf area index on a global scale, *Journal of Hydrology*, 212–213(0), 268–286, doi: 10.1016/S0022-1694(98)00211-X, 1998.
- Kerr, J. T., and M. Ostrovsky, From space to species: ecological applications for remote sensing, *Trends in Ecology and Evolution*, 18(6), 299–305, doi: 10.1016/S0169-5347(03)00071-5, 2003.
- Kichenin, E., D. A. Wardle, D. A. Peltzer, C. W. Morse, and G. T. Freschet, Contrasting effects of plant inter- and intraspecific variation on community-level trait measures along an environmental gradient, *Functional Ecology*, 27(5), 1254–1261, doi: 10.1111/1365-2435.12116, 2013.
- Kimmins, J., J. Blanco, B. Seely, C. Welham, and K. Scoullar, Complexity in modelling forest ecosystems: How much is enough?, *Forest Ecology and Management*, 256(10), 1646–1658, doi: 10.1016/j.foreco.2008.03.011, 2008.
- Kirchner, J. W., Getting the right answers for the right reasons: Linking measurements, analyses, and models to advance the science of hydrology, *Water Resources Research*, 42(3), 1–5, doi: 10.1029/2005WR004362, 2006.
- Kleidon, A., A basic introduction to the thermodynamics of the Earth system far from equilibrium and maximum entropy production, *Philosophical transactions of the Royal Society of London. Series B, Biological sciences*, 365(1545), 1303–15, doi: 10.1098/rstb.2009.0310, 2010.
- Kleidon, A., and H. Mooney, A global distribution of biodiversity inferred from climatic constraints: results from a process-based modelling study, *Global Change Biology*, 6, 507–523, 2000.
- Kleidon, A., K. Fraedrich, and C. Low, Multiple steady-states in the terrestrial atmosphere-biosphere system: a result of a discrete vegetation classification?, *Biogeosciences*, 4, 707–714, 2007.
- Kleidon, A., J. Adams, R. Pavlick, and B. Reu, Simulated geographic variations of plant species richness, evenness and abundance using climatic constraints on plant functional diversity, *Environmental Research Letters*, 4(1), 014,007, doi: 10.1088/1748-9326/4/1/014007, 2009.

- Knorr, W., Annual and interannual CO₂ exchanges of the terrestrial biosphere: Process based simulations and uncertainties, *Global Ecology and Biogeography*, 9(3), 225–252, doi: 10.1046/j.1365-2699.2000.00159.x, 2000.
- Kobayashi, H., D. D. Baldocchi, Y. Ryu, Q. Chen, S. Ma, J. L. Osuna, and S. L. Ustin, Modeling energy and carbon fluxes in a heterogeneous oak woodland: A three-dimensional approach, *Agricultural and Forest Meteorology*, 152, 83–100, doi: 10.1016/j.agrformet.2011.09.008, 2012.
- Koca, D., B. Smith, and M. T. Sykes, Modelling regional climate change effects on potential natural ecosystems in Sweden, *Climatic Change*, 78(2), 381–406, doi: 10.1007/s10584-005-9030-1, 2006.
- Körner, C., Why are there global gradients in species richness? Mountains might hold the answer, *Trends in Ecology and Evolution*, 15(12), 513–514, 2000.
- Körner, C., Carbon limitation in trees, *Journal of Ecology*, 91(1), 4–17, doi: 10.1046/j.1365-2745.2003.00742.x, 2003a.
- Körner, C., Atmospheric science. Slow in, rapid out—carbon flux studies and Kyoto targets, *Science*, 300(5623), 1242–3, doi: 10.1126/science.1084460, 2003b.
- Korner, C., *Alpine treelines*, 220 pp., Springer, 2012.
- Korzukhin, M., M. Ter-Mikaelian, and R. Wagner, Process versus empirical models: which approach for forest ecosystem management?, *Canadian Journal of Forest Research*, 26, 879–887, 1996.
- Krinner, G., N. Viovy, N. de Noblet-Ducoudré, J. Ogée, J. Polcher, P. Friedlingstein, P. Ciais, S. Sitch, and I. Prentice, A dynamic global vegetation model for studies of the coupled atmosphere-biosphere system, *Global Biogeochemical Cycles*, 19(GB1015), doi: 10.1029/2003GB002199, 2005.
- Kucharik, C. J., J. Foley, C. Delire, V. Fisher, M. Coe, J. Lenters, C. Young-Molling, and N. Ramankutty, Testing the performance of a dynamic global ecosystem model: Water balance, carbon balance, and vegetation structure, *Global Biogeochemical Cycles*, 14(3), 795–825, doi: 10.1029/1999GB001138, 2000.
- Kucharik, C. J., C. C. Barford, M. E. Maayar, S. C. Wofsy, R. K. Monson, and D. D. Baldocchi, A multiyear evaluation of a Dynamic Global Vegetation Model at three AmeriFlux forest sites: Vegetation structure, phenology, soil temperature, and CO₂ and H₂O vapor exchange, *Ecological Modelling*, 196(1–2), 1–31, doi: 10.1016/j.ecolmodel.2005.11.031, 2006.
- Kucherenko, S., and Y. Sytsko, Application of deterministic low-discrepancy sequences in global optimization, *Computational Optimization and Applications*, 30(3), 297–318, 2005.

- Kucherenko, S., B. Feil, N. Shah, and W. Mauntz, The identification of model effective dimensions using global sensitivity analysis, *Reliability Engineering and System Safety*, 96(4), 440–449, doi: 10.1016/j.ress.2010.11.003, 2011.
- Landsberg, J., Modelling forest ecosystems: state of the art, challenges, and future directions, *Canadian Journal of Forest Research*, 33, 385–397, doi: 10.1139/X02-129, 2003.
- Laughlin, D. C., and D. E. Laughlin, Advances in modeling trait-based plant community assembly, *Trends in Plant Science*, 18(10), 584–93, doi: 10.1016/j.tplants.2013.04.012, 2013.
- Laughlin, D. C., P. Z. Fulé, D. W. Huffman, J. Crouse, and E. Laliberté, Climatic constraints on trait-based forest assembly, *Journal of Ecology*, 99(6), 1489–1499, doi: 10.1111/j.1365-2745.2011.01885.x, 2011.
- Lavorel, S., and E. Garnier, Predicting changes in community composition and ecosystem functioning from plant traits: revisiting the Holy Grail, *Functional Ecology*, 16, 545–556, 2002.
- Lavorel, S., S. McIntyre, J. Landsberg, and T. Forbes, Plant functional classifications: from general groups to specific groups based on response to disturbance, *Trends in Ecology and Evolution*, 12(12), 1997.
- Lavorel, S., S. Díaz, J. H. C. Cornelissen, E. Garnier, S. P. Harrison, S. McIntyre, J. G. Pausas, N. P.-h. Catherine, and R. Carlos, Plant functional types: are we getting any closer to the Holy Grail?, in *Terrestrial ecosystems in a changing world*, edited by J. G. Canadell, D. E. Pataki, and L. F. Pitelka, i, chap. 13, Springer, Berlin, Heidelberg, 2007.
- Law, B., M. Williams, P. Anthoni, D. D. Baldocchi, and M. H. Unsworth, Measuring and modelling seasonal variation of carbon dioxide and water vapour exchange of a *Pinus ponderosa* forest subject to soil water deficit, *Global Change Biology*, 6(6), 613–630, doi: 10.1046/j.1365-2486.2000.00339.x, 2000.
- Lawlor, D. W., and W. Tezara, Causes of decreased photosynthetic rate and metabolic capacity in water-deficient leaf cells: a critical evaluation of mechanisms and integration of processes., *Annals of Botany*, 103(4), 561–79, doi: 10.1093/aob/mcn244, 2009.
- Lawrence, D. M., P. E. Thornton, K. W. Oleson, and G. B. Bonan, The Partitioning of Evapotranspiration into Transpiration, Soil Evaporation, and Canopy Evaporation in a GCM: Impacts on Land-Atmosphere Interaction, *Journal of Hydrometeorology*, 8(4), 862–880, doi: 10.1175/JHM596.1, 2007.
- Lawrie, J., and J. Hearne, Reducing model complexity via output sensitivity, *Ecological Modelling*, 207(2-4), 137–144, doi: 10.1016/j.ecolmodel.2007.04.013, 2007.

- Lazzarotto, P., P. Calanca, and J. Fuhrer, Dynamics of grass-clover mixtures: An analysis of the response to management with the PROductive GRASSland Simulator (PROGRASS), *Ecological Modelling*, 220(5), 703–724, doi: 10.1016/j.ecolmodel.2008.11.023, 2009.
- Le Quéré, C., et al., Trends in the sources and sinks of carbon dioxide, *Nature Geoscience*, 2(12), 831–836, doi: 10.1038/ngeo689, 2009.
- Le Quéré, C., et al., The global carbon budget 1959–2011, *Earth System Science Data*, 5, 165–185, doi: 10.3334/CDIAC/GCP, 2013.
- Le Roux, X., A. Lacointe, A. Escobar-Gutiérrez, and S. Le Dizès, Carbon-based models of individual tree growth: a critical appraisal, *Annals of Forest Science*, 58, 469–506, 2001.
- LeBauer, D., D. Wang, K. Richter, C. Davidson, and M. Dietze, Facilitating feedbacks between field measurements and ecosystem models, *Ecological Monographs*, 83(2), 133–154, 2013.
- Leuning, R., Modelling stomatal behaviour and photosynthesis of *Eucalyptus grandis*, *Australian Journal of Plant Physiology*, 17, 159–175, 1990.
- Leuning, R., A critical appraisal of a combined stomatal-photosynthesis model for C₃ plants, *Plant, Cell and Environment*, 18, 339–355, 1995.
- Leuzinger, S., C. Manusch, H. Bugmann, and A. Wolf, A sink limited growth model improves biomass estimation along boreal and alpine treelines, *Global Ecology and Biogeography*, in press, 2013.
- Leverenz, J. W., The effects of illumination sequence, CO₂ concentration, temperature and acclimation on the convexity of the photosynthetic light response curve, *Physiologia Plantarum*, 74(2), 332–341, doi: 10.1111/j.1399-3054.1988.tb00639.x, 1988.
- Levin, S., Dispersion and population interactions, *American Naturalist*, 108(960), 207–228, 1974.
- Levin, S., Population dynamic models in heterogeneous environments, *Annual Review of Ecology and Systematics*, 7(1976), 287–310, 1976.
- Levin, S., B. Grenfell, A. Hastings, and A. Perelson, Mathematical and computational challenges in population biology and ecosystems science, *Science*, 275(January), 1997.
- Levis, S., Modeling vegetation and land use in models of the Earth System, *Wiley Interdisciplinary Reviews: Climate Change*, 1(6), 840–856, doi: 10.1002/wcc.83, 2010.

- Li, H., M. S. Wigmosta, H. Wu, M. Huang, Y. Ke, A. M. Coleman, and L. R. Leung, A Physically Based Runoff Routing Model for Land Surface and Earth System Models, *Journal of Hydrometeorology*, 14(3), 808–828, doi: 10.1175/JHM-D-12-015.1, 2013.
- Lichstein, J. W., J. Dushoff, K. Ogle, A. Chen, D. W. Purves, J. P. Caspersen, and S. W. Pacala, Unlocking the forest inventory data: relating individual tree performance to unmeasured environmental factors, *Ecological Applications*, 20(3), 684–99, 2010.
- Link, P., K. Simonin, H. Maness, J. Oshun, T. Dawson, and I. Fung, Species differences in the seasonality of evergreen tree transpiration in a Mediterranean climate: Analysis of multiyear, half-hourly sap flow observations, *Water Resources Research*, 50, 1–26, doi: 10.1002/2013WR014023. Received, 2014.
- Lischke, H., and T. J. Löffler, Intra-specific density dependence is required to maintain species diversity in spatio-temporal forest simulations with reproduction, *Ecological Modelling*, 198(3-4), 341–361, doi: 10.1016/j.ecolmodel.2006.05.005, 2006.
- Liski, J., D. Perruchoud, and T. Karjalainen, Increasing carbon stocks in the forest soils of western Europe, *Forest Ecology and Management*, 169(1-2), 159–175, doi: 10.1016/S0378-1127(02)00306-7, 2002.
- Litton, C. M., J. W. Raich, and M. G. Ryan, Carbon allocation in forest ecosystems, *Global Change Biology*, 13(10), 2089–2109, doi: 10.1111/j.1365-2486.2007.01420.x, 2007.
- Liu, J., J. M. Chen, J. Cihlar, and W. Park, A process-based boreal ecosystem productivity simulator using remote sensing inputs, *Remote Sensing of Environment*, 62(2), 158–175, 1997.
- Liu, S., et al., Simulating the impacts of disturbances on forest carbon cycling in North America: Processes, data, models, and challenges, *Journal of Geophysical Research*, 116, G00K08, doi: 10.1029/2010JG001585, 2011.
- Liu, Z., and E. Todini, Towards a comprehensive physically-based rainfall-runoff model, *Hydrology and Earth System Sciences*, 6(5), 859–881, doi: 10.5194/hess-6-859-2002, 2002.
- Liu, Z., and E. Todini, Assessing the TOPKAPI non-linear reservoir cascade approximation by means of a characteristic lines solution, *Hydrological Processes*, 19(10), 1983–2006, doi: 10.1002/hyp.5662, 2005.
- Lloyd, J., J. Grace, A. Miranda, and P. Meir, A simple calibrated model of Amazon rainforest productivity based on leaf biochemical properties, *Plant, Cell & Environment*, 18(10), 1129–1145, doi: 10.1111/j.1365-3040.1995.tb00624.x, 1995.

- Lloyd, J., K. Bloomfield, T. Domingues, and G. D. Farquhar, Relevant foliar traits correlating better on a mass vs an area basis: of ecophysiological relevance or just a case of mathematical imperatives and statistical quicksand?, *New Phytologist*, 199(2004), 311–321, 2013.
- Lucas, N. S., and P. J. Curran, Forest ecosystem simulation modelling: the role of remote sensing, *Progress in Physical Geography*, 23(3), 391–423, doi: 10.1177/030913339902300304, 1999.
- Luo, Y., and E. Weng, Dynamic disequilibrium of the terrestrial carbon cycle under global change, *Trends in Ecology and Evolution*, 26(2), 96–104, doi: 10.1016/j.tree.2010.11.003, 2011.
- Luo, Y., et al., Modeled interactive effects of precipitation, temperature, and [CO₂] on ecosystem carbon and water dynamics in different climatic zones, *Global Change Biology*, 14(9), 1986–1999, doi: 10.1111/j.1365-2486.2008.01629.x, 2008.
- Luyssaert, S., E.-D. Schulze, A. Börner, A. Knohl, D. Hessenmöller, B. E. Law, P. Ciais, and J. Grace, Old-growth forests as global carbon sinks, *Nature*, 455(7210), 213–215, doi: 10.1038/nature07276, 2008.
- Luyssaert, S., et al., The European carbon balance. Part 3: forests, *Global Change Biology*, 16(5), 1429–1450, doi: 10.1111/j.1365-2486.2009.02056.x, 2010.
- MacArthur, R., and R. Levins, The limiting similarity, convergence, and divergence of coexisting species, *American Naturalist*, 101(921), 377–385, 1967.
- Magnani, F., S. Leonardi, R. Tognetti, J. Grace, and M. Borghetti, Modelling the surface conductance of a broad-leaf canopy: effects of partial decoupling from the atmosphere, *Plant, Cell & Environment*, 21(8), 867–879, doi: 10.1046/j.1365-3040.1998.00328.x, 1998.
- Maire, V., P. Martre, J. Kattge, F. Gastal, G. Esser, S. Fontaine, and J.-F. Soussana, The coordination of leaf photosynthesis links C and N fluxes in C₃ plant species, *PloS one*, 7(6), e38345, doi: 10.1371/journal.pone.0038345, 2012.
- Mäkelä, A., On guiding principles for carbon allocation in eco-physiological growth models, *Tree Physiology*, 32(6), 644–7, doi: 10.1093/treephys/tps033, 2012.
- Mäkelä, A., J. Landsberg, A. R. Ek, T. E. Burk, M. Ter-Mikaelian, G. I. Agren, C. D. Oliver, and P. Puttonen, Process-based models for forest ecosystem management: current state of the art and challenges for practical implementation, *Tree Physiology*, 20(5-6), 289–298, 2000.
- Mäkelä, A., T. J. Givnish, F. Berninger, T. N. Buckley, G. D. Farquhar, and P. Hari, Challenges and Opportunities of the Optimality Approach in Plant Ecology, *Silva Fennica*, 36(3), 605–614, 2002.

- Manson, S., Simplifying complexity: a review of complexity theory, *Geoforum*, 32(3), 405–414, doi: doi:10.1016/S0016-7185(00)00035-X, 2001.
- Manzoni, S., G. Vico, A. Porporato, and G. Katul, Biological constraints on water transport in the soil-plant-atmosphere system, *Advances in Water Resources*, 51, 292–304, doi: 10.1016/j.advwatres.2012.03.016, 2013.
- Martin, P., Vegetation responses and feedbacks to climate: a review of models and processes, *Climate Dynamics*, 8, 201–210, 1993.
- Matsumoto, M., and T. Nishimura, Mersenne twister: a 623-dimensionally equidistributed uniform pseudo-random number generator, *ACM Transactions on Modeling and Computer Simulation (TOMACS)*, 8(1), 3–30, doi: 10.1145/272991.272995, 1998.
- Matthews, H. D., M. Eby, T. Ewen, P. Friedlingstein, and B. J. Hawkins, What determines the magnitude of carbon cycle-climate feedbacks?, *Global Biogeochemical Cycles*, 21(2), 1–12, doi: 10.1029/2006GB002733, 2007.
- Maxwell, R. M., et al., Surface-subsurface model intercomparison: A first set of benchmark results to diagnose integrated hydrology and feedbacks, *Water Resources Research*, 50(2), 1531–1549, doi: 10.1002/2013WR013725. Received, 2014.
- McCann, K. S., The diversity-stability debate, *Nature*, 405(6783), 228–33, doi: 10.1038/35012234, 2000.
- McDowell, N. G., Mechanisms linking drought, hydraulics, carbon metabolism, and vegetation mortality., *Plant Physiology*, 155(3), 1051–1059, doi: 10.1104/pp.110.170704, 2011.
- McGill, B. J., B. J. Enquist, E. Weiher, and M. Westoby, Rebuilding community ecology from functional traits, *Trends in Ecology and Evolution*, 21(4), 178–85, doi: 10.1016/j.tree.2006.02.002, 2006.
- McMahon, S. M., et al., Improving assessment and modelling of climate change impacts on global terrestrial biodiversity, *Trends in Ecology and Evolution*, 26(5), 249–59, doi: 10.1016/j.tree.2011.02.012, 2011.
- Medlyn, B. E., E. Dreyer, D. Ellsworth, M. Forstreuter, P. C. Harley, M. U. F. Kirschbaum, and X. L. E. Roux, Temperature response of parameters of a biochemically based model of photosynthesis. II. A review of experimental data, *Plant, Cell and Environment*, 61(0), 1167–1179, 2002a.
- Medlyn, B. E., D. Loustau, and S. Delzon, Temperature response of parameters of a biochemically based model of photosynthesis. I. Seasonal changes in mature maritime pine (*Pinus pinaster* Ait.), *Plant, Cell and Environment*, 25(9), 1155–1165, doi: 10.1046/j.1365-3040.2002.00890.x, 2002b.

- Medlyn, B. E., A. P. Robinson, R. Clement, and R. E. McMurtrie, On the validation of models of forest CO₂ exchange using eddy covariance data: some perils and pitfalls, *Tree Physiology*, 25(7), 839–57, doi: 10.1093/treephys/25.7.839, 2005.
- Medlyn, B. E., R. a. Duursma, and M. J. B. Zeppel, Forest productivity under climate change: a checklist for evaluating model studies, *Wiley Interdisciplinary Reviews: Climate Change*, 2(3), 332–355, doi: 10.1002/wcc.108, 2011.
- Medlyn, B. E., et al., Effects of elevated [CO₂] on photosynthesis in European forest species: a meta-analysis of model parameters, *Plant, Cell and Environment*, 10, 1475–1495, 1999.
- Medvigy, D., and P. R. Moorcroft, Predicting ecosystem dynamics at regional scales: an evaluation of a terrestrial biosphere model for the forests of north-eastern North America, *Philosophical Transactions of the Royal Society B: Biological Sciences*, 367(1586), 222–35, doi: 10.1098/rstb.2011.0253, 2012.
- Medvigy, D., S. C. Wofsy, J. W. Munger, D. Y. Hollinger, and P. R. Moorcroft, Mechanistic scaling of ecosystem function and dynamics in space and time: Ecosystem Demography model version 2, *Journal of Geophysical Research*, 114(G1), 1–21, doi: 10.1029/2008JG000812, 2009.
- Medvigy, D., S.-j. Jeong, K. L. Clark, N. S. Skowronski, and K. V. R. Schäfer, Effects of seasonal variation of photosynthetic capacity on the carbon fluxes of a temperate deciduous forest, *Journal of Geophysical Research: Biogeosciences*, 118, 1–12, doi: 10.1002/2013JG002421, 2013.
- Meentemeyer, V., Macroclimate and lignin control of litter decomposition rates, *Ecology*, 59(3), 465–472, 1978.
- Melillo, J., A. McGuire, D. Kicklighter, B. Moore, C. Vorosmarty, and A. Schloss, Global climate change and terrestrial net primary production, *Nature*, 363, 234–240, doi: 10.1038/363234a0, 1993.
- Melillo, J. M., et al., Soil warming and carbon-cycle feedbacks to the climate system., *Science*, 298(5601), 2173–6, doi: 10.1126/science.1074153, 2002.
- Melton, J. R., and V. K. Arora, Sub-grid scale representation of vegetation in global land surface schemes: implications for estimation of the terrestrial carbon sink, *Biogeosciences*, 11(4), 1021–1036, doi: 10.5194/bg-11-1021-2014, 2014.
- Messier, J., B. J. McGill, and M. J. Lechowicz, How do traits vary across ecological scales? A case for trait-based ecology, *Ecology Letters*, 13(7), 838–48, doi: 10.1111/j.1461-0248.2010.01476.x, 2010.
- Miller, J., Basic concepts of kinematic-wave models, *Tech. rep.*, U. S. Geological Survey professional paper 1320, Washington, 1984.

- Miller, P. A., T. Giesecke, T. Hickler, R. H. W. Bradshaw, B. Smith, H. Seppä, P. J. Valdes, and M. T. Sykes, Exploring climatic and biotic controls on Holocene vegetation change in Fennoscandia, *Journal of Ecology*, 96(2), 247–259, doi: 10.1111/j.1365-2745.2007.01342.x, 2008.
- Miralles, D. G., R. a. M. De Jeu, J. H. Gash, T. R. H. Holmes, and a. J. Dolman, Magnitude and variability of land evaporation and its components at the global scale, *Hydrology and Earth System Sciences*, 15(3), 967–981, doi: 10.5194/hess-15-967-2011, 2011.
- Moles, A. T., D. D. Ackerly, C. O. Webb, J. C. Tweddle, J. B. Dickie, A. J. Pitman, and M. Westoby, Factors that shape seed mass evolution, *Proceedings of the National Academy of Sciences of the United States of America*, 102(30), 10,540–4, doi: 10.1073/pnas.0501473102, 2005a.
- Moles, A. T., D. D. Ackerly, C. O. Webb, J. C. Tweddle, J. B. Dickie, and M. Westoby, A brief history of seed size, *Science*, 307(5709), 576–80, doi: 10.1126/science.1104863, 2005b.
- Monteith, J., Accommodation between transpiring vegetation and the convective boundary layer, *Journal of Hydrology*, 166(3), 251–263, doi: 10.1016/0022-1694(94)05086-D, 1995.
- Moorcroft, P., How close are we to a predictive science of the biosphere?, *Trends in Ecology and Evolution*, 21(7), 400–407, doi: 10.1016/j.tree.2006.04.009, 2006.
- Moorcroft, P., G. Hurtt, and S. Pacala, A method for scaling vegetation dynamics: the ecosystem demography model (ED), *Ecological Monographs*, 71(4), 557–585, 2001.
- Moorcroft, P. R., Recent advances in ecosystem-atmosphere interactions: an ecological perspective, *Proceedings of the Royal Society B: Biological sciences*, 270(1521), 1215–27, doi: 10.1098/rspb.2002.2251, 2003.
- Morales, P., T. Hickler, D. P. Rowell, B. Smith, and M. T. Sykes, Changes in European ecosystem productivity and carbon balance driven by regional climate model output, *Global Change Biology*, 13(1), 108–122, doi: 10.1111/j.1365-2486.2006.01289.x, 2007.
- Morales, P., et al., Comparing and evaluating process-based ecosystem model predictions of carbon and water fluxes in major European forest biomes, *Global Change Biology*, 11(12), 2211–2233, doi: 10.1111/j.1365-2486.2005.01036.x, 2005.
- Morin, X., L. Fahse, M. Scherer-Lorenzen, and H. Bugmann, Tree species richness promotes productivity in temperate forests through strong complementarity between species, *Ecology Letters*, 14(12), 1211–9, doi: 10.1111/j.1461-0248.2011.01691.x, 2011.

- Morokoff, W., and R. Caflisch, Quasi-random sequences and their discrepancies, *SIAM Journal on Scientific Computing*, 15(6), 1251–1279, 1994.
- Morris, M., Factorial sampling plans for preliminary computational experiments, *Technometrics*, 33(2), 161 – 174, doi: 10.2307/1269043, 1991.
- Muller, B., F. Pantin, M. Génard, O. Turc, S. Freixes, M. Piques, and Y. Gibon, Water deficits uncouple growth from photosynthesis, increase C content, and modify the relationships between C and growth in sink organs, *Journal of Experimental Botany*, 62(6), 1715–29, doi: 10.1093/jxb/erq438, 2011.
- Mutke, J., and W. Barthlott, Patterns of vascular plant diversity at continental to global scales, *Biologische skrifter*, 55, 521–531, 2005.
- Myneni, R., et al., Global products of vegetation leaf area and fraction absorbed PAR from year one of MODIS data, *Remote Sensing of Environment*, 83, 214–231, 2002.
- Naeem, S., and S. Li, Biodiversity enhances ecosystem reliability, *Nature*, 390(December), 507–509, 1997.
- Neelin, J. D., A. Bracco, H. Luo, J. C. McWilliams, and J. E. Meyerson, Considerations for parameter optimization and sensitivity in climate models., *Proceedings of the National Academy of Sciences of the United States of America*, 107(50), 21,349–54, doi: 10.1073/pnas.1015473107, 2010.
- Neilson, R., A model for predicting continental-scale vegetation distribution and water balance, *Ecological Applications*, 5(2), 362–385, doi: 10.2307/1942028, 1995.
- Niederreiter, H., Quasi-Monte Carlo methods and pseudo-random numbers, *Bulletin of the American Mathematical Society*, 84(6), 957–1041, 1978.
- Niederreiter, H., *Random Number Generation and Quasi-Monte Carlo Methods*, Cbms-Nsf Regional Conference Series in Applied Mathematics, Society for Industrial and Applied Mathematics, 1992.
- Niederreiter, H., *Quasi-Monte Carlo Methods*, John Wiley & Sons, Ltd, doi: 10.1002/9780470061602.eqf13019, 2010.
- Nightingale, J., S. Phinn, and A. Held, Ecosystem process models at multiple scales for mapping tropical forest productivity, *Progress in Physical Geography*, 28(2), 241–281, doi: 10.1191/0309133304pp411ra, 2004.
- Niu, S., et al., Thermal optimality of net ecosystem exchange of carbon dioxide and underlying mechanisms., *New Phytologist*, 194(3), 775–83, doi: 10.1111/j.1469-8137.2012.04095.x, 2012.

- Norberg, J., M. C. Urban, M. Vellend, C. a. Klausmeier, and N. Loeuille, Eco-evolutionary responses of biodiversity to climate change, *Nature Climate Change*, 2(10), 747–751, doi: 10.1038/nclimate1588, 2012.
- Norman, J., Scaling processes between leaf and canopy levels, in *Scaling Physiological Processes: Leaf to Globe*, edited by J. Ehleringer and C. Field, chap. 4, pp. 41–76, Academic Press, New York, 1993.
- Novick, K., R. Oren, P. Stoy, J.-Y. Juang, M. Siqueira, and G. Katul, The relationship between reference canopy conductance and simplified hydraulic architecture, *Advances in Water Resources*, 32(6), 809–819, doi: 10.1016/j.advwatres.2009.02.004, 2009.
- Nuttle, W., Eco-hydrology's past and future in focus, *EOS Transactions*, 83(May), 205, 2002.
- Oberhuber, W., I. Swidrak, D. Pirkebner, and A. Gruber, Temporal dynamics of non-structural carbohydrates and xylem growth in *Pinus sylvestris* exposed to drought, *Canadian Journal of Forest Research*, 41, 1590–1597, doi: 10.1139/X11-084, 2011.
- Oki, T., and S. Kanae, Global hydrological cycles and world water resources, *Science*, 313(5790), 1068–72, doi: 10.1126/science.1128845, 2006.
- Ordoñez, J. C., P. M. van Bodegom, J.-P. M. Witte, I. J. Wright, P. B. Reich, and R. Aerts, A global study of relationships between leaf traits, climate and soil measures of nutrient fertility, *Global Ecology and Biogeography*, 18(2), 137–149, doi: 10.1111/j.1466-8238.2008.00441.x, 2009.
- Oreskes, N., K. Shrader-Frechette, and K. Belitz, Verification, validation, and confirmation of numerical models in the earth sciences, *Science*, 263(5147), 641, doi: 10.1126/science.263.5147.641, 1994.
- Osnas, J., J. Lichstein, P. Reich, and S. Pacala, Global Leaf Trait Relationships: Mass, Area, and the Leaf Economics Spectrum, *Science*, 340, 741–744, doi: 10.1126/science.1231574, 2013.
- Ostle, N. J., et al., Integrating plant-soil interactions into global carbon cycle models, *Journal of Ecology*, 97(5), 851–863, doi: 10.1111/j.1365-2745.2009.01547.x, 2009.
- Pacala, S., and D. Deutschman, Details that matter: the spatial distribution of individual trees maintains forest ecosystem function, *Oikos*, 74, 357–365, 1995.
- Pacala, S., C. Canham, and J. J. Silander, Forest models defined by field measurements. I: The design of a northeastern forest simulator, *Canadian Journal of Forest Research*, 23, 1980–1988, 1993.

- Pan, Y., R. Birdsey, J. Hom, M. K. and K. Clark, Improved estimates of net primary productivity from MODIS satellite data at regional and local scales, *Ecological Applications*, 16(1), 125–132, 2006.
- Pan, Y., R. a. Birdsey, O. L. Phillips, and R. B. Jackson, The Structure, Distribution, and Biomass of the World's Forests, *Annual Review of Ecology, Evolution, and Systematics*, 44(1), 593–622, doi: 10.1146/annurev-ecolsys-110512-135914, 2013.
- Papageorgiou, A., Fast convergence of quasi-Monte Carlo for a class of isotropic integrals, *Mathematics of Computation*, 70(233), 297–306, 2000.
- Papoulis, A., *Probability, random variables, and stochastic processes*, McGraw-Hill series in systems science, McGraw-Hill, 1965.
- Pappas, C., S. Fatichi, S. Rimkus, P. Burlando, and M. Huber, The role of local scale heterogeneities in terrestrial ecosystem modeling, *Journal of Geophysical Research: Biogeosciences*, under review-a.
- Pappas, C., S. Fatichi, and P. Burlando, Modeling terrestrial carbon and water dynamics across climatic gradients: does plant diversity matter?, *New Phytologist*, under review-b.
- Pappas, C., S. Fatichi, S. Leuzinger, A. Wolf, and P. Burlando, Sensitivity analysis of a process-based ecosystem model: Pinpointing parameterization and structural issues, *Journal of Geophysical Research: Biogeosciences*, 118(2), 505–528, doi: 10.1002/jgrg.20035, 2013.
- Paruelo, J. M., W. K. Lauenroth, I. C. Burke, and O. E. Sala, Grassland Precipitation-Use Efficiency Varies Across a Resource Gradient, *Ecosystems*, 2(1), 64–68, doi: 10.1007/s100219900058, 1999.
- Paschalis, A., S. Fatichi, P. Molnar, S. Rimkus, and P. Burlando, On the effects of small scale space-time variability of rainfall on basin flood response, *Journal of Hydrology*, 514, 313–327, doi: 10.1016/j.jhydrol.2014.04.014, 2014.
- Paskov, S., and J. Traub, Faster valuation of financial derivatives, *The Journal of Portfolio Management*, 22(1), 113–123, 1995.
- Pavlick, R., D. T. Drewry, K. Bohn, B. Reu, and a. Kleidon, The Jena Diversity-Dynamic Global Vegetation Model (JeDi-DGVM): a diverse approach to representing terrestrial biogeography and biogeochemistry based on plant functional trade-offs, *Biogeosciences*, 10(6), 4137–4177, doi: 10.5194/bg-10-4137-2013, 2013.
- Peng, C., From static biogeographical model to dynamic global vegetation model: a global perspective on modelling vegetation dynamics, *Ecological Modelling*, 135(1), 33–54, doi: 10.1016/S0304-3800(00)00348-3, 2000.

- Perruchoud, D., F. Kienast, E. Kaufmann, and O. Bräker, 20th century carbon budget of forest soils in the Alps, *Ecosystems*, 2, 320–337, 1999.
- Perry, G. L., and N. J. Enright, Spatial modelling of vegetation change in dynamic landscapes: a review of methods and applications, *Progress in Physical Geography*, 30(1), 47–72, doi: 10.1191/0309133306pp469ra, 2006.
- Peterson, G., C. Allen, and C. Holling, Ecological resilience, biodiversity, and scale, *Ecosystems*, (1), 6–18, 1998.
- Pfisterer, A. B., and B. Schmid, Diversity-dependent production can decrease the stability of ecosystem functioning, *Nature*, 416(6876), 84–6, doi: 10.1038/416084a, 2002.
- Piao, S., et al., Evaluation of terrestrial carbon cycle models for their response to climate variability and to CO₂ trends, *Global Change Biology*, 19(7), 2117–32, doi: 10.1111/gcb.12187, 2013.
- Pielke, R., Influence of the spatial distribution of vegetation and soils on the prediction of cumulus convective rainfall, *Reviews of Geophysics*, 39(1999), 2001.
- Pielke, R., R. Avissar, M. Raupach, D. AJ, X. Zeng, and A. S. Denning, Interactions between the atmosphere and terrestrial ecosystems: influence on weather and climate, *Global Change Biology*, 4, 461–475, 1998.
- Pielke, R. A., et al., Land use/land cover changes and climate: modeling analysis and observational evidence, *Wiley Interdisciplinary Reviews: Climate Change*, 2(6), 828–850, doi: 10.1002/wcc.144, 2011.
- Pietsch, S., and H. Hasenauer, Evaluating the self-initialization procedure for large-scale ecosystem models, *Global Change Biology*, 12(9), 1658–1669, doi: 10.1111/j.1365-2486.2006.01211.x, 2006.
- Pitman, A., The evolution of, and revolution in, land surface schemes designed for climate models, *International Journal of Climatology*, 23(5), 479–510, doi: 10.1002/joc.893, 2003.
- Pitman, A., A. Henderson-Sellers, and Z.-L. Yang, Sensitivity of regional climates to localized precipitation in global models, *Nature*, 346, doi: 10.1038/346734a0, 1990.
- Poorter, H., H. Lambers, and J. Evans, Trait correlation networks: a whole-plant perspective on the recently criticized leaf economic spectrum, *New Phytologist*, 2014.
- Porporato, A., and I. Rodriguez-Iturbe, Ecohydrology-a challenging multidisciplinary research perspective, *Hydrological Sciences Journal*, 47(5), 2002.

- Porporato, A., and I. Rodriguez-Iturbe, From random variability to ordered structures: a search for general synthesis in ecohydrology, *Ecohydrology*, 6(3), 333–342, doi: 10.1002/eco.1400, 2013.
- Potter, K. A., H. Arthur Woods, and S. Pincebourde, Microclimatic challenges in global change biology, *Global Change Biology*, 19(10), 2932–9, doi: 10.1111/gcb.12257, 2013.
- Prentice, C., M. Heimann, and S. Sitch, The carbon balance of the terrestrial biosphere: Ecosystem models and atmospheric observations, *Ecological Applications*, 10(6), 1553–1573, 2000.
- Prentice, I., and H. Helmisaari, Silvics of north European trees: Compilation, comparisons and implications for forest succession modelling, *Forest Ecology and Management*, 42(1-2), 79–93, doi: 10.1016/0378-1127(91)90066-5, 1991.
- Prentice, I., W. Cramer, S. Harrison, R. Leemans, R. Monserud, and A. Solomon, A global biome model based on plant physiology and dominance, soil properties and climate, *Journal of Biogeography*, 19(2), 117–134, 1992.
- Prentice, I., M. T. Sykes, and W. Cramer, A simulation model for the transient effects of climate change on forest landscapes, *Ecological Modelling*, 65(1-2), 51–70, doi: 10.1016/0304-3800(93)90126-D, 1993.
- Prentice, I. C., A. Bondeau, W. Cramer, S. P. Harrison, T. Hickler, W. Lucht, S. Sitch, B. Smith, and M. T. Sykes, Dynamic global vegetation modeling: quantifying terrestrial ecosystem responses to large-scale environmental change, in *Terrestrial ecosystems in a changing world*, edited by J. G. Canadell, D. E. Pataki, and L. F. Pitelka, chap. 15, Springer, Berlin, Heidelberg, 2007.
- Prentice, I. C., N. Dong, S. M. Gleason, V. Maire, and I. J. Wright, Balancing the costs of carbon gain and water transport: testing a new theoretical framework for plant functional ecology, *Ecology Letters*, 17(1), 82–91, doi: 10.1111/ele.12211, 2014.
- Press, W. H., *Numerical recipes: the art of scientific computing*, 3 ed., Cambridge University Press, 2007.
- Prinn, R., Development and application of earth system models, *Proceedings of the National Academy of Science*, 110, 3673–3680, doi: 10.1073/pnas.1107470109, 2012.
- Pujol, G., B. Iooss, and A. Janon, *sensitivity: Sensitivity Analysis*, r package version 1.6-1, 2012.
- Purves, D., and S. Pacala, Predictive models of forest dynamics, *Science*, 320(5882), 1452–1453, doi: 10.1126/science.1155359, 2008a.

- Purves, D., and S. Pacala, Predictive models of forest dynamics, *Science*, 527(1986), 15–16, 2008b.
- Quillet, A., C. Peng, and M. Garneau, Toward dynamic global vegetation models for simulating vegetation-climate interactions and feedbacks: recent developments, limitations, and future challenges, *Environmental Reviews*, 18(1), 333–353, doi: 10.1139/A10-016, 2010.
- Radtke, P. J., T. E. Burk, and P. V. Bolstad, Estimates of the distributions of forest ecosystem model inputs for deciduous forests of eastern North America, *Tree physiology*, 21(8), 505–12, 2001.
- Rafsgaard, J., Terminology, modelling protocol and classification of hydrological model codes, in *Distributed Hydrological Modelling*, edited by J. Abbott, M.B. and Refsgaard, pp. 17–39, Springer, 1996.
- Rastetter, E. B., A. W. King, B. J. Cosby, G. M. Hornberger, R. V. O'Neill, and J. E. Hobbie, Aggregating Fine-Scale Ecological Knowledge to Model Coarser-Scale Attributes of Ecosystems, *Ecological Applications*, 2(1), 55, doi: 10.2307/1941889, 1992.
- Raupach, M. R., P. J. Rayner, D. J. Barrett, R. S. DeFries, M. Heimann, D. S. Ojima, S. Quegan, and C. C. Schmullius, Model-data synthesis in terrestrial carbon observation: methods, data requirements and data uncertainty specifications, *Global Change Biology*, 11(3), 378–397, doi: 10.1111/j.1365-2486.2005.00917.x, 2005.
- RCoreTeam, R: A Language and Environment for Statistical Computing, *Tech. rep.*, R Foundation for Statistical Computing, Vienna, Austria, 2012.
- Read, J., R. Hill, and G. Hope, Contrasting responses to water deficits of *Nothofagus* species from tropical New Guinea and high latitude temperate forests: can rainfall regimes constrain latitudinal range?, *Journal of Biogeography*, 37(10), 1962–1976, doi: 10.1111/j.1365-2699.2010.02346.x, 2010.
- Reed, S., V. Koren, M. Smith, Z. Zhang, F. Moreda, D.-J. Seo, , and DMIP Participants, Overall distributed model intercomparison project results, *Journal of Hydrology*, 298(1-4), 27–60, doi: 10.1016/j.jhydrol.2004.03.031, 2004.
- Regnier, P., et al., Anthropogenic perturbation of the carbon fluxes from land to ocean, *Nature Geoscience*, (June), doi: 10.1038/ngeo1830, 2013.
- Reich, P., The world-wide 'fast-slow' plant economics spectrum: a traits manifesto, *Journal of Ecology*, 102, 275–301, doi: 10.1111/1365-2745.12211, 2014.
- Reich, P. B., and J. Oleksyn, Global patterns of plant leaf N and P in relation to temperature and latitude, *Proceedings of the National Academy of Sciences of the United States of America*, 101(30), 11,001–6, doi: 10.1073/pnas.0403588101, 2004.

- Reich, P. B., M. B. Walters, and D. S. Ellsworth, From tropics to tundra: global convergence in plant functioning., *Proceedings of the National Academy of Sciences of the United States of America*, 94(25), 13,730–4, 1997.
- Reich, P. B., I. J. Wright, and C. H. Lusk, Predicting leaf physiology from simple plant and climate attributes: a global GLOPNET analysis, *Ecological Applications*, 17(7), 1982–8, 2007.
- Reichstein, M., et al., Reduction of ecosystem productivity and respiration during the European summer 2003 climate anomaly: a joint flux tower, remote sensing and modelling analysis, *Global Change Biology*, 13(3), 634–651, doi: 10.1111/j.1365-2486.2006.01224.x, 2007.
- Reichstein, M., et al., Climate extremes and the carbon cycle, *Nature*, 500(7462), 287–295, doi: 10.1038/nature12350, 2013.
- Reu, B., R. Proulx, K. Bohn, J. G. Dyke, A. Kleidon, R. Pavlick, and S. Schmidlein, The role of climate and plant functional trade-offs in shaping global biome and biodiversity patterns, *Global Ecology and Biogeography*, 20(4), 570–581, doi: 10.1111/j.1466-8238.2010.00621.x, 2011.
- Reynolds, J. F., H. Bugmann, and L. Pitelka, How Much Physiology is Needed in Forest Gap Models for Simulating Long-Term Vegetation Response to Global Change?, *Climatic Change*, 51, 541–557, 2001.
- Richardson, A. D., et al., Terrestrial biosphere models need better representation of vegetation phenology: Results from the North American Carbon Program Site Synthesis, *Global Change Biology*, 18(2), 566–584, doi: 10.1111/j.1365-2486.2011.02562.x, 2011.
- Rodriguez-Iturbe, I., Ecohydrology: A hydrologic perspective of climate-soil-vegetation dynamics, *Water Resources Research*, 36(1), 3, doi: 10.1029/1999WR900210, 2000.
- Rodriguez-Iturbe, I., A. Porporato, F. Laio, and L. Ridolfi, Intensive or extensive use of soil moisture: plant strategies to cope with stochastic water availability, *Geophysical Research Letters*, 28(23), 4495–4497, 2001.
- Rogers, A., The use and misuse of $V_{c,max}$ in Earth System Models, *Photosynthesis Research*, 119(1-2), 15–29, doi: 10.1007/s11120-013-9818-1, 2014.
- Roxburgh, S., et al., A critical overview of model estimates of net primary productivity for the Australian continent, *Functional Plant Biology*, 31(11), 1043–1059, doi: 10.1071/FP04100, 2004.
- Sack, L., C. Scoffoni, G. P. John, H. Poorter, C. M. Mason, R. Mendez-Alonzo, and L. a. Donovan, How do leaf veins influence the worldwide leaf economic spectrum? Review and synthesis, *Journal of Experimental Botany*, 64(13), 4053–80, doi: 10.1093/jxb/ert316, 2013.

- SAEFL/WSL, Forest Report 2005: Facts and Figures about the Condition of Swiss Forest, *Tech. rep.*, Berne: Swiss Federal Agency for the Environment, Forest and Landscape; Birmensdorf: Swiss Federal Research Institute WSL, 2005.
- Sala, A., D. R. Woodruff, and F. C. Meinzer, Carbon dynamics in trees: feast or famine?, *Tree Physiology*, 32(6), 764–775, doi: 10.1093/treephys/tpr143, 2012.
- Saltelli, A., Sensitivity analysis: Could better methods be used?, *Journal of Geophysical Research*, 104(D3), 3789–3793, doi: 10.1029/1998JD100042, 1999.
- Saltelli, A., Making best use of model evaluations to compute sensitivity indices, *Computer Physics Communications*, 145(2), 280–297, doi: 10.1016/S0010-4655(02)00280-1, 2002.
- Saltelli, A., and P. Annoni, How to avoid a perfunctory sensitivity analysis, *Environmental Modelling & Software*, 25(12), 1508–1517, doi: 10.1016/j.envsoft.2010.04.012, 2010.
- Saltelli, A., and M. Scott, Guest editorial: The role of sensitivity analysis in the corroboration of models and its link to model structural and parametric uncertainty, *Reliability Engineering and System Safety*, 57(1), 1–4, doi: 10.1016/S0951-8320(97)00022-7, 1997.
- Saltelli, A., K. Chan, and E. Scott, *Sensitivity analysis*, Wiley series in probability and statistics, Wiley, 2000a.
- Saltelli, A., S. Tarantola, and F. Campolongo, Sensitivity analysis as an ingredient of modeling, *Statistical Science*, 15(4), 377–395, doi: 10.1214/ss/1009213004, 2000b.
- Saltelli, A., S. Tarantola, F. Campolongo, and M. Ratto, *Sensitivity analysis in practice: a guide to assessing scientific models*, Wiley, 2004.
- Saltelli, A., M. Ratto, S. Tarantola, and F. Campolongo, Sensitivity analysis practices: Strategies for model-based inference, *Reliability Engineering and System Safety*, 91(10–11), 1109–1125, doi: 10.1016/j.res.2005.11.014, 2006.
- Saltelli, A., M. Ratto, T. Andres, F. Campolongo, J. Cariboni, D. Gatelli, M. Saisana, and S. Tarantola, *Global Sensitivity Analysis: The Primer*, Wiley-Blackwell, 2008.
- Saltelli, A., P. Annoni, I. Azzini, F. Campolongo, M. Ratto, and S. Tarantola, Variance based sensitivity analysis of model output. Design and estimator for the total sensitivity index, *Computer Physics Communications*, 181(2), 259–270, doi: 10.1016/j.cpc.2009.09.018, 2010.

- Sato, H., A. Ito, and T. Kohyama, SEIB-DGVM: A new Dynamic Global Vegetation Model using a spatially explicit individual-based approach, *Ecological Modelling*, 200(3-4), 279–307, doi: 10.1016/j.ecolmodel.2006.09.006, 2007.
- Savage, V. M., C. T. Webb, and J. Norberg, A general multi-trait-based framework for studying the effects of biodiversity on ecosystem functioning, *Journal of Theoretical Biology*, 247(2), 213–29, doi: 10.1016/j.jtbi.2007.03.007, 2007.
- Saxton, K. E., and W. J. Rawls, Soil Water Characteristic Estimates by Texture and Organic Matter for Hydrologic Solutions, *Soil Science Society of America Journal*, 70(5), 1569, doi: 10.2136/sssaj2005.0117, 2006.
- Schaefer, K., et al., A model-data comparison of gross primary productivity: Results from the North American Carbon Program site synthesis, *Journal of Geophysical Research*, 117(G3), G03,010, doi: 10.1029/2012JG001960, 2012.
- Scheiter, S., L. Langan, and S. I. Higgins, Next-generation dynamic global vegetation models: learning from community ecology, *New Phytologist*, 198(3), 957–969, doi: 10.1111/nph.12210, 2013.
- Schellnhuber, H., 'Earth system' analysis and the second Copernican revolution, *Nature*, 402(December), 1999.
- Schenk, H., and R. Jackson, The global biogeography of roots, *Ecological Monographs*, 72(3), 311–328, 2002a.
- Schenk, H. J., and R. B. Jackson, Rooting depths, lateral root spreads and below-ground/above-ground allometries of plants in water-limited ecosystems, *Journal of Ecology*, 90(3), 480–494, doi: 10.1046/j.1365-2745.2002.00682.x, 2002b.
- Scherrer, D., and C. Körner, Infra-red thermometry of alpine landscapes challenges climatic warming projections, *Global Change Biology*, 16, 2602–2613, doi: 10.1111/j.1365-2486.2009.02122.x, 2009.
- Schlaepfer, D., B. Ewers, B. Shuman, D. Williams, J. Frank, W. Massaman, and W. K. Lauenroth, Terrestrial water fluxes dominated by transpiration: Comment, *Ecosphere*, 5(5), 1–9, 2014.
- Schlesinger, W. H., and S. Jasechko, Transpiration in the global water cycle, *Agricultural and Forest Meteorology*, 189–190, 115–117, doi: 10.1016/j.agrformet.2014.01.011, 2014.
- Schwalm, C. R., et al., A model-data intercomparison of CO₂ exchange across North America: Results from the North American Carbon Program site synthesis, *Journal of Geophysical Research*, 115(G00H05), doi: 10.1029/2009JG001229, 2010.

- Schwarb, M., The Alpine precipitation climate: Evaluation of a high-resolution analysis scheme using comprehensive rain-gauge data, Ph.D. thesis, ETH Zurich, Switzerland, 2000.
- Schymanski, S. J., A. Kleidon, M. Stieglitz, and J. Narula, Maximum entropy production allows a simple representation of heterogeneity in semiarid ecosystems., *Philosophical transactions of the Royal Society of London. Series B, Biological sciences*, 365(1545), 1449–55, doi: 10.1098/rstb.2009.0309, 2010.
- Sears, M. W., E. Raskin, and M. J. Angilletta, The world is not flat: defining relevant thermal landscapes in the context of climate change., *Integrative and comparative Biology*, 51(5), 666–75, doi: 10.1093/icb/ucr111, 2011.
- Sellers, P., Y. Mintz, Y. C. Sud, and A. Dalcher, A simple biosphere model (SiB) for use within general circulation models, *Journal of the Atmospheric Sciences*, 43(6), 505–531, 1986.
- Seneviratne, S. I., T. Corti, E. L. Davin, M. Hirschi, E. B. Jaeger, I. Lehner, B. Orlowsky, and A. J. Teuling, Investigating soil moisture-climate interactions in a changing climate: A review, *Earth-Science Reviews*, 99(3–4), 125–161, doi: 10.1016/j.earscirev.2010.02.004, 2010.
- Sheng, G., M. Elzas, T. Oren, and B. Cronhjort, Model validation: a systemic and systematic approach, *Reliability Engineering and System Safety*, 42(2–3), 247–259, doi: 10.1016/0951-8320(93)90092-D, 1993.
- Shinozaki, K., K. Yoda, K. Hozumi, and T. Kira, A quantitative analysis of plant form-the pipe model theory: I. Basic Analyses, *Japanese Journal of Ecology*, 14(3), 97–105, 1964.
- Shugart, H. H., S. Saatchi, and F. G. Hall, Importance of structure and its measurement in quantifying function of forest ecosystems, *Journal of Geophysical Research*, 115(May), G00E13, doi: 10.1029/2009JG000993, 2010.
- Singsaas, E. L., D. R. Ort, and E. H. DeLucia, Variation in measured values of photosynthetic quantum yield in ecophysiological studies, *Oecologia*, 128(1), 15–23, doi: 10.1007/s004420000624, 2001.
- Sitch, S., et al., Evaluation of ecosystem dynamics, plant geography and terrestrial carbon cycling in the LPJ dynamic global vegetation model, *Global Change Biology*, 9(2), 161–185, doi: 10.1046/j.1365-2486.2003.00569.x, 2003.
- Sitch, S., et al., Evaluation of the terrestrial carbon cycle, future plant geography and climate-carbon cycle feedbacks using five Dynamic Global Vegetation Models (DGVMs), *Global Change Biology*, 14(9), 2015–2039, doi: 10.1111/j.1365-2486.2008.01626.x, 2008.

- Smith, B., I. Prentice, and M. T. Sykes, Representation of vegetation dynamics in the modelling of terrestrial ecosystems: comparing two contrasting approaches within European climate space, *Global Ecology and Biogeography*, 10(6), 621–637, 2001.
- Smith, B., W. Knorr, J.-L. Widlowski, B. Pinty, and N. Gobron, Combining remote sensing data with process modelling to monitor boreal conifer forest carbon balances, *Forest Ecology and Management*, 255(12), 3985–3994, doi: 10.1016/j.foreco.2008.03.056, 2008.
- Smith, P., Do grasslands act as a perpetual sink for carbon?, *Global change biology*, pp. 1–4, doi: 10.1111/gcb.12561, 2014.
- Sobol', I., On the distribution of points in a cube and the approximate evaluation of integrals, *Computational Mathematics and Mathematical Physics*, 7(4), 86–112, 1967.
- Sobol', I., Uniformly distributed sequences with an additional uniform property, *USSR Computational Mathematics and Mathematical Physics*, 16(5), 236 – 242, doi: 10.1016/0041-5553(76)90154-3, 1976.
- Sobol', I., Sensitivity analysis for nonlinear mathematical models, *Mathematical Modeling and Computational Experiment*, 1(4), 407–414, 1993.
- Sobol', I., *A primer for the Monte Carlo method*, 128 pp., CRC Press, Florida, 1994.
- Sobol', I., On quasi-Monte Carlo integrations, *Mathematics and Computers in Simulation*, 47(2-5), 103–112, doi: 10.1016/S0378-4754(98)00096-2, 1998.
- Sobol', I., and S. Kucherenko, On global sensitivity analysis of quasi-Monte Carlo algorithms, *Monte Carlo Methods and Applications*, 11(1), 83–92, doi: 10.1515/1569396054027274, 2005.
- Solomatine, D., and T. Wagener, Hydrological Modeling, in *Treatise on Water Science*, edited by P. Wilderer and S. Uhlenbrook, chap. 2.16, pp. 435–457, Academic Press, Oxford, 2011.
- Sperry, J. S., Hydraulic constraints on plant gas exchange, *Agricultural and Forest Meteorology*, 104(1), 13–23, doi: 10.1016/S0168-1923(00)00144-1, 2000.
- Sprugel, D., Disturbance, equilibrium, and environmental variability: what is 'natural' vegetation in a changing environment?, *Biological Conservation*, 58, 1–18, 1991.
- Stephens, G. L., et al., An update on Earth's energy balance in light of the latest global observations, *Nature Geoscience*, 5(10), 691–696, doi: 10.1038/ngeo01580, 2012.

- Stewart, J., and L. Gay, Preliminary modelling of transpiration from the FIFE site in Kansas, *Agricultural and Forest Meteorology*, 48(3-4), 305–315, 1989.
- Stoy, P. C., A. M. Trowbridge, and W. L. Bauerle, Controls on seasonal patterns of maximum ecosystem carbon uptake and canopy-scale photosynthetic light response: contributions from both temperature and photoperiod, *Photosynthesis Research*, doi: 10.1007/s11120-013-9799-0, 2013.
- Strigul, N., D. Pristinski, D. Purves, J. Dushoff, and S. Pacala, Scaling from trees to forests: tractable macroscopic equations for forest dynamics, *Ecological Monographs*, 78(4), 523–545, 2008.
- Sugiura, D., and M. Tateno, Optimal leaf-to-root ratio and leaf nitrogen content determined by light and nitrogen availabilities., *PloS one*, 6(7), e22236, doi: 10.1371/journal.pone.0022236, 2011.
- Sumner, D. M., and J. M. Jacobs, Utility of Penman-Monteith, Priestley-Taylor, reference evapotranspiration, and pan evaporation methods to estimate pasture evapotranspiration, *Journal of Hydrology*, 308(1-4), 81–104, doi: 10.1016/j.jhydrol.2004.10.023, 2005.
- Tague, C., and L. Band, RHESSys: regional hydro-ecologic simulation system-an object-oriented approach to spatially distributed modeling of carbon, water, and nutrient cycling, *Earth Interactions*, 8(19), 1–42, 2004.
- Tague, C. L., N. G. McDowell, and C. D. Allen, An integrated model of environmental effects on growth, carbohydrate balance, and mortality of *Pinus ponderosa* forests in the southern Rocky Mountains, *PloS one*, 8(11), e80286, doi: 10.1371/journal.pone.0080286, 2013.
- Tang, G., and P. J. Bartlein, Simulating the climatic effects on vegetation: approaches, issues and challenges, *Progress in Physical Geography*, 32(5), 543–556, doi: 10.1177/0309133308100443, 2008.
- Tang, G., and P. J. Bartlein, Modifying a dynamic global vegetation model for simulating large spatial scale land surface water balances, *Hydrology and Earth System Sciences*, 16(8), 2547–2565, doi: 10.5194/hess-16-2547-2012, 2012.
- Tang, G., B. Beckage, and B. Smith, The potential transient dynamics of forests in New England under historical and projected future climate change, *Climatic Change*, doi: 10.1007/s10584-012-0404-x, 2012.
- Tang, G., T. Hwang, and S. M. Pradhanang, Does consideration of water routing affect simulated water and carbon dynamics in terrestrial ecosystems?, *Hydrology and Earth System Sciences*, 18(4), 1423–1437, doi: 10.5194/hess-18-1423-2014, 2014a.

- Tang, J., P. Pilesjö, P. A. Miller, A. Persson, Z. Yang, E. Hanna, and T. V. Callaghan, Incorporating topographic indices into dynamic ecosystem modelling using LPJ-GUESS, *Ecohydrology*, 7(4), 1147–1162, doi: 10.1002/eco.1446, 2014b.
- Tardieu, F., C. Granier, and B. Muller, Water deficit and growth. Co-ordinating processes without an orchestrator?, *Current Opinion in Plant Biology*, 14(3), 283–289, doi: 10.1016/j.pbi.2011.02.002, 2011.
- Tezara, W., V. Mitchell, S. Driscoll, and D. Lawlor, Water stress inhibits plant photosynthesis by decreasing coupling factor and ATP, *Nature*, 401(6756), 914–917, doi: 10.1038/4484, 1999.
- Thomas, S. C., Photosynthetic capacity peaks at intermediate size in temperate deciduous trees, *Tree Physiology*, 30(5), 555–73, doi: 10.1093/treephys/tpq005, 2010.
- Thompson, S. E., C. J. Harman, P. A. Troch, P. D. Brooks, and M. Sivapalan, Spatial scale dependence of ecohydrologically mediated water balance partitioning: A synthesis framework for catchment ecohydrology, *Water Resources Research*, 47, 1–20, doi: 10.1029/2010WR009998, 2011.
- Thuiller, W., et al., Predicting global change impacts on plant species' distributions: Future challenges, *Perspectives in Plant Ecology, Evolution and Systematics*, 9(3-4), 137–152, doi: 10.1016/j.ppees.2007.09.004, 2008.
- Tian, Y., et al., Multiscale analysis and validation of the MODIS LAI product: I. Uncertainty assessment, *Remote Sensing of Environment*, 83, 414–430, 2002.
- Tilman, D., Diversity and production in European grasslands, *Science*, 286, 1099–1100, 1999.
- Tilman, D., J. Knops, D. Wedin, P. Reich, M. Ritchie, and E. Siemann, The influence of functional diversity and composition on ecosystem processes, *Science*, 277(5330), 1300–1302, doi: 10.1126/science.277.5330.1300, 1997.
- Tilman, D., P. B. Reich, and J. M. H. Knops, Biodiversity and ecosystem stability in a decade-long grassland experiment, *Nature*, 441(7093), 629–32, doi: 10.1038/nature04742, 2006.
- Todini, E., The ARNO rainfall-runoff model, *Journal of Hydrology*, 175(1-4), 339–382, doi: 10.1016/S0022-1694(96)80016-3, 1996.
- Trivedi, M. R., P. M. Berry, M. D. Morecroft, and T. P. Dawson, Spatial scale affects bioclimate model projections of climate change impacts on mountain plants, *Global Change Biology*, 14(5), 1089–1103, doi: 10.1111/j.1365-2486.2008.01553.x, 2008.

- Turner, D. P., S. V. Ollinger, and J. S. Kimball, Integrating Remote Sensing and Ecosystem Process Models for Landscape- to Regional-Scale Analysis of the Carbon Cycle, *BioScience*, 54(6), 573, doi: 10.1641/0006-3568(2004)054[0573:IRSAEP]2.0.CO;2, 2004.
- Tuzet, A., A. Perrier, and R. Leuning, A coupled model of stomatal conductance, photosynthesis and transpiration, *Plant, Cell & Environment*, 26(7), 1097–1116, doi: 10.1046/j.1365-3040.2003.01035.x, 2003.
- Van Bodegom, P. M., J. C. Douma, J. P. M. Witte, J. C. Ordoñez, R. P. Bartholomeus, and R. Aerts, Going beyond limitations of plant functional types when predicting global ecosystem-atmosphere fluxes: exploring the merits of traits-based approaches, *Global Ecology and Biogeography*, 21(6), 625–636, doi: 10.1111/j.1466-8238.2011.00717.x, 2012.
- van der Molen, M. K., et al., Drought and ecosystem carbon cycling, *Agricultural and Forest Meteorology*, 151(7), 765–773, doi: 10.1016/j.agrformet.2011.01.018, 2011.
- Verheijen, L. M., V. Brovkin, R. Aerts, G. Bönisch, J. H. C. Cornelissen, J. Kattge, P. B. Reich, I. J. Wright, and P. M. van Bodegom, Impacts of trait variation through observed trait-climate relationships on performance of an Earth system model: a conceptual analysis, *Biogeosciences*, 10(8), 5497–5515, doi: 10.5194/bg-10-5497-2013, 2013.
- Vico, G., and A. Porporato, Modelling C₃ and C₄ photosynthesis under water-stressed conditions, *Plant Soil*, 313(1-2), 187–203, doi: 10.1007/s11104-008-9691-4, 2008.
- Violle, C., M.-L. Navas, D. Vile, E. Kazakou, C. Fortunel, I. Hummel, and E. Garnier, Let the concept of trait be functional!, *Oikos*, 116(5), 882–892, doi: 10.1111/j.2007.0030-1299.15559.x, 2007.
- Violle, C., B. J. Enquist, B. J. McGill, L. Jiang, C. H. Albert, C. Hulshof, V. Jung, and J. Messier, The return of the variance: intraspecific variability in community ecology, *Trends in Ecology and Evolution*, 27(4), 244–52, doi: 10.1016/j.tree.2011.11.014, 2012.
- von Caemmerer, S., *Biochemical models of leaf photosynthesis*, Techniques in plant sciences, CSIRO Pub., 2000.
- Wagner, H. M., *Principles of operations research: With applications to managerial decisions*, N.J: Prentice-Hall, Englewood Cliffs, 1969.
- Wallach, D., and M. Genard, Effect of uncertainty in input and parameter values on model prediction error, *Ecological Modelling*, 105(2-3), 337–345, doi: 10.1016/S0304-3800(97)00180-4, 1998.

- Wang, K., and R. E. Dickinson, A Review of Global Terrestrial Evapotranspiration: Observation, Modeling, Climatology, and Climatic Variability, *Reviews of Geophysics*, 50(RG2005), doi: 10.1029/2011RG000373, 2012.
- Wang, Y. P., X. J. Lu, I. J. Wright, Y. J. Dai, P. J. Rayner, and P. B. Reich, Correlations among leaf traits provide a significant constraint on the estimate of global gross primary production, *Geophysical Research Letters*, 39(19), 1–7, doi: 10.1029/2012GL053461, 2012.
- Wang, Z., et al., Evaluating weather effects on interannual variation in net ecosystem productivity of a coastal temperate forest landscape: A model inter-comparison, *Ecological Modelling*, 222(17), 3236–3249, doi: 10.1016/j.ecolmodel.2011.06.005, 2011.
- Waring, R., and P. Schroeder, Application of the pipe model theory to predict canopy leaf area, *Canadian Journal of Forest*, 12(3), 556–560, doi: 10.1139/x82-086, 1982.
- Wattenbach, M., F. Hattermann, R. Weng, F. Wechsung, V. Krysanova, and F. Badeck, A simplified approach to implement forest eco-hydrological properties in regional hydrological modelling, *Ecological Modelling*, 187, 40–59, doi: 10.1016/j.ecolmodel.2005.01.026, 2005.
- Webb, C. T., J. a. Hoeting, G. M. Ames, M. I. Pyne, and N. LeRoy Poff, A structured and dynamic framework to advance traits-based theory and prediction in ecology, *Ecology Letters*, 13(3), 267–83, doi: 10.1111/j.1461-0248.2010.01444.x, 2010.
- Weisberg, M., Who is a Modeler?, *The British Journal for the Philosophy of Science*, 58(2), 207–233, doi: 10.1093/bjps/axm011, 2007.
- Welsh, A., A. Peterson, and S. Altmann, The fallacy of averages, *American Naturalist*, 132(2), 277–288, 1988.
- Weng, E., and Y. Luo, Relative information contributions of model vs. data to short- and long-term forecasts of forest carbon dynamics, *Ecological Applications*, 21(5), 1490–505, 2011.
- Westoby, M., D. S. Falster, A. T. Moles, P. A. Vesk, and I. J. Wright, PLANT ECOLOGICAL STRATEGIES: Some Leading Dimensions of Variation Between Species, *Annual Review of Ecology and Systematics*, 33(1), 125–159, doi: 10.1146/annurev.ecolsys.33.010802.150452, 2002.
- Westoby, M., P. Reich, and I. Wright, Understanding ecological variation across species: area-based vs mass-based expression of leaf traits, *New Phytologist*, pp. 322–323, 2013.

- Whitehead, D., F. Kelliher, C. Frampton, and M. Godfrey, Seasonal development of leaf area in a young, widely spaced *Pinus radiata* D. Don stand, *Tree Physiology*, 14(7-8-9), 1019–1038, doi: 10.1093/treephys/14.7-8-9.1019, 1994.
- Whitfield, J., Survival of the likeliest?, *PLoS biology*, 5(5), e142, doi: 10.1371/journal.pbio.0050142, 2007.
- Wickham, H., *ggplot2: elegant graphics for data analysis*, Springer New York, 2009.
- Williams, M., et al., Improving land surface models with FLUXNET data, *Biogeosciences*, 6(7), 1341–1359, doi: 10.5194/bg-6-1341-2009, 2009.
- Wilson, K. B., D. D. Baldocchi, and P. J. Hanson, Spatial and seasonal variability of photosynthetic parameters and their relationship to leaf nitrogen in a deciduous forest, *Tree Physiology*, 20(9), 565–578, 2000.
- Wohlfahrt, G., M. Bahn, E. Haubner, I. Horak, W. Michaeler, K. Rottmar, U. Tappeiner, and A. Cernusca, Inter-specific variation of the biochemical limitation to photosynthesis and related leaf traits of 30 species from mountain grassland ecosystems under different land use, *Plant, Cell & Environment*, 22(10), 1281–1296, doi: 10.1046/j.1365-3040.1999.00479.x, 1999.
- Wolf, A., E. Blyth, R. Harding, D. Jacob, E. Keup-Thiel, H. Goettel, and T. Callaghan, Sensitivity of an ecosystem model to hydrology and temperature, *Climatic Change*, 87(1), 75–89, doi: 10.1007/s10584-007-9339-z, 2008.
- Wolf, A., P. Ciais, V. Bellassen, N. Delbart, C. B. Field, and J. A. Berry, Forest biomass allometry in global land surface models, *Global Biogeochemical Cycles*, 25(GB3015), 1–16, doi: 10.1029/2010GB003917, 2011.
- Wood, E. F., et al., Hyperresolution global land surface modeling: Meeting a grand challenge for monitoring Earth's terrestrial water, *Water Resources Research*, 47(5), 1–10, doi: 10.1029/2010WR010090, 2011.
- Woodward, F., Predicting plant responses to global environmental change, *New Phytologist*, 122(41), 239–251, 1992.
- Wramneby, A., B. Smith, S. Zaehle, and M. T. Sykes, Parameter uncertainties in the modelling of vegetation dynamics-Effects on tree community structure and ecosystem functioning in European forest biomes, *Ecological Modelling*, 216(3-4), 277–290, doi: 10.1016/j.ecolmodel.2008.04.013, 2008.
- Wright, I. J., et al., The worldwide leaf economics spectrum, *Nature*, 428(6985), 821–7, doi: 10.1038/nature02403, 2004.
- Wright, I. J., et al., Modulation of leaf economic traits and trait relationships by climate, *Global Ecology and Biogeography*, 14(5), 411–421, doi: 10.1111/j.1466-822x.2005.00172.x, 2005.

- Wright, J. P., and A. Sutton-Grier, Does the leaf economic spectrum hold within local species pools across varying environmental conditions?, *Functional Ecology*, 26(6), 1390–1398, doi: 10.1111/1365-2435.12001, 2012.
- WSL, WSL, 2012: Schweizerisches Landesforstinventar LFI, 2012.
- Wuertz, D., many others, and see the SOURCE file, *fOptions: Basics of Option Valuation*, r package version 2140.79, 2011.
- Wüest, M., C. Frei, A. Altenhoff, M. Hagen, M. Litschi, and C. Schär, A gridded hourly precipitation dataset for Switzerland using rain-gauge analysis and radar-based disaggregation, *International Journal of Climatology*, 30(10), 1764–1775, doi: 10.1002/joc.2025, 2010.
- Wullschleger, S., Biochemical Limitations to Carbon Assimilation in C₃ Plants—A Retrospective Analysis of the A/C_i Curves from 109 Species, *Journal of Experimental Botany*, 44(262), 907–920, 1993.
- Wullschleger, S. D., et al., Plant functional types in Earth system models: past experiences and future directions for application of dynamic vegetation models in high-latitude ecosystems, *Annals of Botany*, 114(1), 1–16, doi: 10.1093/aob/mcu077, 2014.
- Würth, M. K. R., K. Winter, and C. Körner, Leaf carbohydrate responses to CO₂ enrichment at the top of a tropical forest, *Oecologia*, 116(1-2), 18–25, doi: 10.1007/PL00013821, 1998.
- Yang, W., et al., MODIS leaf area index products: from validation to algorithm improvement, *IEEE Transactions on Geoscience and Remote Sensing*, 44(7), 1885–1898, doi: 10.1109/TGRS.2006.871215, 2006.
- Zaehle, S., S. Sitch, B. Smith, and F. Hatterman, Effects of parameter uncertainties on the modeling of terrestrial biosphere dynamics, *Global Biogeochemical Cycles*, 19(GB3020), doi: 10.1029/2004GB002395, 2005.
- Zaehle, S., et al., Projected Changes in Terrestrial Carbon Storage in Europe under Climate and Land-use Change, 1990–2100, *Ecosystems*, 10(3), 380–401, doi: 10.1007/s10021-007-9028-9, 2007.
- Zaremba, S., The mathematical basis of Monte Carlo and quasi-Monte Carlo methods, *SIAM review*, 10(3), 303–314, 1968.
- Zeeman, M. J., R. Hiller, A. K. Gilgen, P. Michna, P. Plüss, N. Buchmann, and W. Eugster, Management and climate impacts on net CO₂ fluxes and carbon budgets of three grasslands along an elevational gradient in Switzerland, *Agricultural and Forest Meteorology*, 150(4), 519–530, doi: 10.1016/j.agrformet.2010.01.011, 2010.
- Zeide, B., Primary unit of the tree crown, *Ecology*, 74(5), 1598–1602, 1993.

- Zhao, M., S. W. Running, and R. R. Nemani, Sensitivity of Moderate Resolution Imaging Spectroradiometer (MODIS) terrestrial primary production to the accuracy of meteorological reanalyses, *Journal of Geophysical Research*, 111(G1), G01,002, doi: 10.1029/2004JG000004, 2006.
- Zhao, S., and S. Liu, Scale criticality in estimating ecosystem carbon dynamics, *Global change biology*, 20, 2240–2251, doi: 10.1111/gcb.12496, 2014.
- Ziehn, T., M. Scholze, and W. Knorr, On the capability of Monte Carlo and adjoint inversion techniques to derive posterior parameter uncertainties in terrestrial ecosystem models, *Global Biogeochemical Cycles*, 26(3), 1–13, doi: 10.1029/2011GB004185, 2012.
- Zweifel, R., L. Zimmermann, F. Zeugin, and D. M. Newbery, Intra-annual radial growth and water relations of trees: implications towards a growth mechanism, *Journal of Experimental Botany*, 57(6), 1445–1459, doi: 10.1093/jxb/erj125, 2006.
- Zweifel, R., K. Steppe, and F. J. Sterck, Stomatal regulation by microclimate and tree water relations: interpreting ecophysiological field data with a hydraulic plant model, *Journal of Experimental Botany*, 58(8), 2113–31, doi: 10.1093/jxb/erm050, 2007.